VOLUME 37 MARCH 1959 NUMBER 3

Canadian Journal of Chemistry

Published by THE NATIONAL RESEARCH COUNCIL
OTTAWA CANADA

Canadian Journal of Chemistry

Under the authority of the Chairman of the Committee of the Privy Council on Scientific and Industrial Research, the National Research Council issues THE CANADIAN JOURNAL OF CHEMISTRY and five other journals devoted to the publication, in English or French, of the results of original scientific research. Matters of general policy concerning these journals are the responsibility of a joint Editorial Board consisting of: members representing the National Research Council of Canada; the Editors of the Journals; and members representing the Royal Society of Canada and four other scientific societies.

The Chemical Institute of Canada has chosen the Canadian Journal of Chemistry as its medium of publication for scientific papers.

Manuscripts for publication should be submitted to Dr. Léo Marion, Editor-in-Chief, Canadian Journal of Chemistry, National Research Council, Ottawa 2, Canada.
(For instructions on preparation of copy, see **Notes to Contributors** (inside back cover).)

Proof, correspondence concerning proof, and orders for reprints should be sent to the Manager, Editorial Office (Research Journals), Division of Administration and Awards, National Research Council, Ottawa 2, Canada.

Subscriptions, renewals, requests for single or back numbers, and all remittances should be sent to Division of Administration and Awards, National Research Council, Ottawa 2, Canada. Remittances should be made payable to the Receiver General of Canada, credit National Research Council.

The journals published, frequency of publication, and prices are:

Canadian Journal of Biochemistry and Physiology	Monthly	$9.00 a year
Canadian Journal of Botany	Bimonthly	$6.00 a year
Canadian Journal of Chemistry	Monthly	$12.00 a year
Canadian Journal of Microbiology	Bimonthly	$6.00 a year
Canadian Journal of Physics	Monthly	$9.00 a year
Canadian Journal of Zoology	Bimonthly	$5.00 a year

The price of regular single numbers of all journals is $2.00.

Canadian Journal of Chemistry

Issued by THE NATIONAL RESEARCH COUNCIL OF CANADA

VOLUME 37 MARCH 1959 NUMBER 3

A PROPOSED STRUCTURE FOR CHLOROPHYLL *d*[1]

A. S. HOLT AND H. V. MORLEY[2]

ABSTRACT

Treatment of chlorophyll *a* or methyl chlorophyllide *a* with potassium permanganate effected oxidation of the 2-vinyl group without concomitant oxidation of the cyclopentanone ring. One of the products obtained was of especial interest because its visible absorption spectrum was identical with that of a previously known, but chemically uncharacterized, pigment—chlorophyll *d*. The preparation and identification of this oxidation product as 2-desvinyl-2-formyl-chlorophyll-*a* is given and its probable identity with chlorophyll *d* is discussed in detail.

Chlorophyll *d* is a pigment which has been reported to occur in a number of species of the Rhodophyceae, a group which contains chlorophyll *a* but, at most, only traces of chlorophyll *b* (1, 2). It was first isolated and described by Manning and Strain in 1943 (2). Recently Smith and Benitez (3) obtained chromatographically pure samples and calculated the specific absorption curve by determining the magnesium content and by assuming the molecular weight to be that of chlorophyll *a* (see Fig. 1). To date its chemical constitution has not been determined nor has any useful function been ascribed to it, although there have been speculations that it may be responsible for the anomalous action spectra of photosynthesis and chlorophyll fluorescence in red algae (1).

The present work arose from some observations made in connection with studies on the allomerization of chlorophyll *a*. When the phase test intermediate of chlorophyll *a*, in acetone containing base, was treated with dilute permanganate, it was oxidized immediately. Examination with a visual spectroscope showed a "red" absorption maximum at about 675 mμ, which was characteristic of Mg-purpurin-18 (4). However, when base was omitted a gradual but different spectral change occurred; two new "red" maxima appeared at about 650 and 685 mμ. When the mixture was chromatographed, there were, besides a minor zone of unchanged chlorophyll *a*, three new zones. The pigments were designated as fractions A, B, and C, in the relative order of their position on the column, fraction C being uppermost. Each fraction gave a positive phase test which indicated that allomerization had not occurred. Most interesting was fraction A which had visible absorption spectra in methanol and in ether which were identical with those published for chlorophyll *d* (2, 3). The present communication describes fraction A and evidence to indicate that it is similar to and probably identical with chlorophyll *d*. Fractions B and C will be discussed in a subsequent communication.

The change in spectrum obtained when fraction A in isopropanol was treated with methanolic magnesium methoxide (4) is given in Fig. 2. Enhanced absorption in the

[1]*Manuscript received November 14, 1958.*
Contribution from the Division of Applied Biology, National Research Council, Ottawa, Canada.
Issued as N.R.C No. 5038.
[2]*N.R.C. Postdoctorate Fellow, 1957–58.*

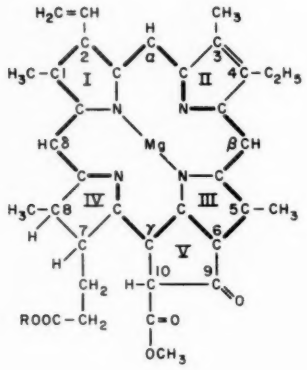

COMPOUND	R	Mg
CHLOROPHYLLIDE	H	+
PHEOPHORBIDE	H	−
CHLOROPHYLL	$C_{20}H_{39}$	+
PHEOPHYTIN	$C_{20}H_{39}$	−
METHYL CHLOROPHYLLIDE	CH_3	+
METHYL PHEOPHORBIDE	CH_3	−

b COMPOUNDS: $3-CH_3$ IS REPLACED BY CHO
"PYRO" COMPOUNDS: $10-CO_2CH_3$ IS REPLACED BY H
"MESO" COMPOUNDS: $2-CH=CH_2$ IS REPLACED BY C_2H_5
CHLORIN E_6 – TRIMETHYL ESTER: R=CH_3, RING V
IS REPLACED BY $\gamma-CH_2CO_2CH_3$ AND $6-CO_2CH_3$

FIG. 1. Structure of chlorophyll *a* and its derivatives.

"green" and decreased absorption in the "red" are characteristic of phase-test-positive pigment (5). When aqueous or methanolic KOH was added to a pyridine or dimethylformamide solution, the intermediate was more strikingly reddish to the eye than when magnesium methoxide was added, but was far less stable.

The positive phase test indicated that ring V of this product was intact. Thus, the remaining likely sites of oxidation were the vinyl group of ring I and the hydrogen atoms at positions 7 and 8 of ring IV. The appearance of an infrared absorption band at 1675 cm^{-1} in the spectrum of the magnesium-free derivative indicated that oxidation of the vinyl group had probably occurred (Fig. 3, curve 2). On comparing the infrared spectrum with that of pheophytin *b*, it seemed likely that the extra band was due to a conjugated aldehyde group (6). Treatment with small quantities of sodium borohydride (7) yielded a product whose spectrum no longer contained the band at 1675 cm^{-1} (Fig. 3, curve 4). This compound gave a positive phase test, and possessed a visible absorption spectrum which was, for all practical purposes, identical with that of meso-methyl pheophorbide *a* (8). Such a result was consistent only with the assumption that oxidation of the hydrogen atoms at positions 7 and 8 had not occurred, since replacement of these

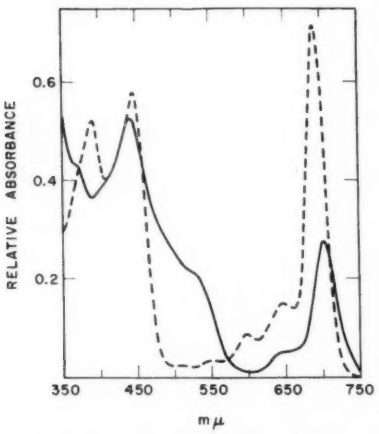

FIG. 2. Visible absorption spectra of fraction A in isopropanol plus and minus methanolic $Mg(OCH_3)_2$. Dashes: isopropanol alone. Solid line: an equal concentration of pigment in a 1:5 mixture of methanolic $Mg(OCH_3)_2$ (*ca.* 20 mg of Mg per milliliter of stock solution) in isopropanol. Air atmosphere.

in meso-methyl pyropheophorbide *a* by hydroxyl groups causes the "red" maximum to shift from 658 to 667 mμ (9).

Previously, Fischer and Walter (10) had carried out studies on the oxidation of the vinyl group of magnesium-free derivatives of chlorophyll *a* using permanganate in aqueous pyridine. These workers stated that owing to the activating influence of the 10-carbomethoxy group, oxidation yielded purpurins and left the vinyl group intact. To avoid this they chose chlorin-e_6-trimethyl ester and methyl pyropheophorbide *a* as starting materials. The 2-desvinyl-2-formyl derivatives were the only compounds isolated which possessed a conjugated carbonyl group. The 2-desvinyl-2-formyl structure of fraction A and its methyl derivative (prepared from methyl chlorophyllide *a*) was confirmed when their chlorin-e_6-trimethyl esters were shown to be identical with the known compound 2-desvinyl-2-formyl-chlorin-e_6-trimethyl ester (10). The absorption of this compound in the double bond stretching region is given in Fig. 3, curve 3, and clearly shows the ester (1725 cm^{-1}) and formyl (1673 cm^{-1}) bands. The oxime was also prepared and its spectrum was found to be identical with that reported earlier (10).

The formation of the 2-desvinyl-2-formyl derivative under the conditions described was in disagreement with the results of Fischer and Walter. These workers found only the 7,8-dihydroxy derivative when aqueous acetone was used as the solvent. Another disagreement was that while the spectrum of the magnesium-free derivative of fraction A agreed well with that given for 2-desvinyl-2-formyl-methyl pheophorbide *a* (prepared by ring closure of the 2-desvinyl-2-formyl-chlorin-e_6-trimethyl ester), that of the product obtained by introducing magnesium into the pheophorbide did not agree with the spectrum of fraction A. It was reported, however, that when magnesium was removed the resulting spectrum was shifted to the "blue" relative to that of the original pheophorbide. It was thought that this product may have resulted from a secondary reaction at the 2-position.

Having shown that fraction A was a 2-desvinyl-2-formyl derivative of chlorophyll *a*, it remained to show its relationship to chlorophyll *d*. Excellent agreement of the visible absorption spectra of fraction A and its magnesium-free derivative with those of chlorophyll *d* and pheophytin *d* in ether (3) are shown in Figs. 4 and 5. Fraction A

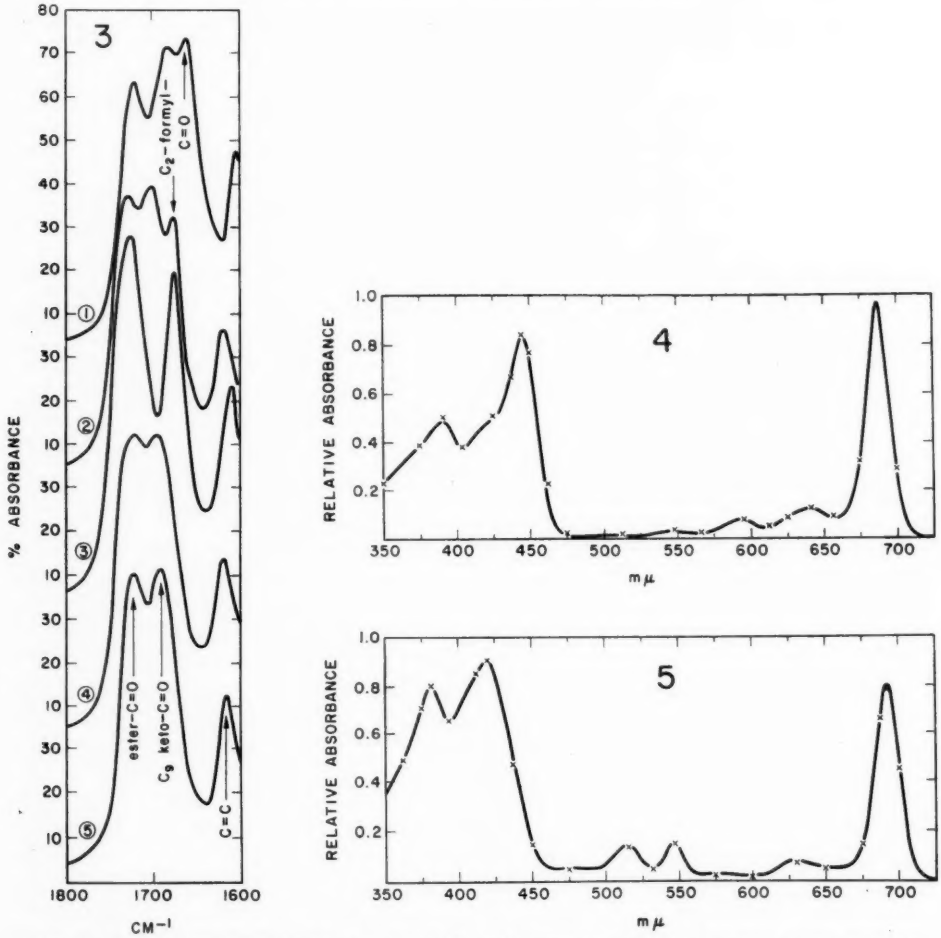

FIG. 3. Double bond stretching region of the infrared absorption spectra of fraction A and its derivatives in chloroform. (1) Fraction A or 2-desvinyl-2-formyl-chlorophyll-*a*. (2) 2-Desvinyl-2-formyl-pheophytin-*a*. (3) 2-Desvinyl-2-formyl-chlorin-e_6-trimethyl ester. (4) 2-Desvinyl-2-hydroxymethyl-pheophytin-*a*. (5) 2-Desvinyl-2-formyl-pheophytin-*a*-2-dimethyl acetal. Concentration *ca.* 5% (w/v).

FIG. 4. Visible absorption spectrum of 2-desvinyl-2-formyl-chlorophyll-*a* in ether (solid line) compared with published spectrum of chlorophyll *d* (3) (indicated by crosses). The spectra were adjusted to make "blue" maxima equal.

FIG. 5. Visible absorption spectrum of 2-desvinyl-2-formyl-pheophytin-*a* in ether (solid line) compared with published spectrum for pheophytin *d* (3) (indicated by crosses). The spectra were adjusted to make the "blue" maxima equal.

appeared to be identical with chlorophyll *d* in all respects. The most significant similarity was the ready interconversion of the magnesium-free derivative and a product whose properties corresponded to those of a so-called isomer of pheophytin *d*, namely, isopheophytin *d*. This product has now been shown to be the dimethyl acetal derivative; it was formed readily in the presence of methanolic hydrogen chloride, the reagent used by Manning and Strain (2) to convert chlorophyll *d* into pheophytin *d*. Total conversion back to the 2-formyl compound is effected by extracting the acetal from ether into aqueous HCl, as shown in Fig. 6. Formation of the acetal of fraction A was

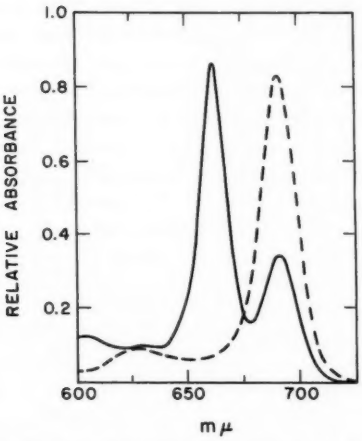

FIG. 6. Visible absorption curve of a mixture of 2-desvinyl-2-formyl-pheophorbide-*a* methyl ester in ether and its dimethyl acetal derivative. Solid line: after 1 minute exposure of the 2-formyl compound to 4.9% (w/w) methanolic HCl. Dashes: after extraction of the pigment into 20% (w/w) aqueous HCl and its transfer back into ether.

followed spectrophotometrically in methanol containing ammonium chloride (11) and resulted in an equilibrium mixture. Since the acetal of the 2-formyl-chlorin-e_6 derivative was always present in the mother liquor after crystallization, it would appear that it was formed in methanol, even in the absence of hydrochloric acid. From these findings it seems that absorption curves of 2-formyl derivatives of chlorophyll *a* should be measured in non-hydroxylic solvents, e.g. ether, to ensure that no contamination with the acetal occurs. Figure 3, curve 5, shows the double bond stretching region of the infrared absorption curve of the acetal. The carbonyl absorption band of the 2-formyl group is missing.

Although formation of the acetal of methyl pheophorbide *b* has been observed using orthoformic ester (12), it was not formed in detectable quantities in methanolic hydrogen chloride even after 24 hours. This difference in the behavior of the formyl groups at positions 2 and 3 is but one example of the non-equivalence of these positions in the phorbide nucleus. Other examples, still involving the formyl group, are as follows: (1) the carbonyl absorption band of the 2-formyl group of fraction A in chloroform absorbs at 1662 cm^{-1} (Fig. 3, curve 1), whereas that of chlorophyll *b* absorbs at 1655 cm^{-1} (6); and (2) introduction of a formyl group at position 2 of meso-methyl pheophorbide *a* causes a "red" shift and has little effect on the hydrochloric acid number, whereas its introduction at position 3 causes a "blue" shift and an increase of five in the acid number (8, 13). (The hydrochloric acid number is the percentage strength acid (w/w) which extracts about two-thirds of the pigment from an equal volume of ether solution (14).)

The probable effect of permanganate on the double bond of the phytol chain has not been mentioned. Oxidation at this point would not have affected the visible absorption spectrum but would have altered the chromatographic behavior. The product(s) formed would have been expected to be strongly adsorbed at the top of a sugar column. To test the effect of the presence of one hydroxyl group in the molecule the 2-hydroxymethyl derivative was prepared and co-chromatographed with a mixture of fraction A and chlorophylls *b* and *b'*, using the method described by Manning and Strain (2). Five zones were observed, the topmost being the firmly bound 2-hydroxy compound; further

down the column was the band of chlorophyll *b*, followed closely by fraction A and chlorophyll *b'*. The lowest band was well separated and was probably fraction A' (the "red" maximum in ether was at 687 mμ, as compared with 686 mμ for fraction A). The chromatographic properties of fraction A were identical with those described for chlorophyll *d* (2) making it likely that the phytol group was intact, and that fraction A and chlorophyll *d* are identical. Further support for this view is the fact that the specific absorption coefficient of the "red" absorption maximum was found to be in reasonable agreement with the value given by Smith and Benitez (3).

Unfortunately chlorophyll *d* was apparently absent from the three species of red algae which were made available to us. This was not unexpected, since conclusive demonstration of the occurrence of chlorophyll *d* in all 18 species tested by Manning and Strain (2) is lacking. *Chondrus crispus* and *Gigartina stellata* were collected fresh in the vicinity of Halifax, Nova Scotia, and were shipped immediately via air mail in iced containers. Upon their delivery, which was about eight to twelve hours later, the samples were extracted using published methods. *Rhodocorton rothii* was collected on the coast of Ireland and was delivered, in a moist condition, several days after its collection. No special storage conditions were maintained during transit. A further check upon the presence of chlorophyll *d* was the treatment of all chlorophyll pigment with aqueous hydrochloric acid to decompose any of the dimethyl acetal derivative which might have been formed from the use of methanol during extraction. It seems improbable that the condition of the first two species of red algae could have deteriorated during shipment to the extent that chlorophyll *d* was destroyed *in vivo* prior to their arrival. It is believed, however, that the successful re-isolation of chlorophyll *d*, perhaps from the original sources which were collected on the Pacific Coast of the United States of America (2, 3), will show this pigment to be a 2-desvinyl-2-formyl derivative of chlorophyll *a*.

EXPERIMENTAL

All solvents were reagent grade and were, with the exception of acetone, used without further purification. Acetone was refluxed with a slight excess of $KMnO_4$ and distilled over anhydrous K_2CO_3. Chlorophyll *a* and methyl chlorophyllide *a* were prepared as given previously (15, 16). Chlorin-e_6-trimethyl ester was prepared from chlorophyll *a* by mild hydrolysis in boiling 2% (w/v) methanolic KOH for 15 minutes, and subsequent isolation and treatment according to previous methods (17). Visible absorption spectra were measured on a Cary Recording Spectrophotometer, Model 11M; infrared absorption spectra were measured on a Perkin–Elmer Model 21, Double Beam Recording Infrared Spectrophotometer.

2-Desvinyl-2-formyl-chlorophyll-a

Chlorophyll *a* (1 g) dissolved in purified acetone (300 ml) was oxidized with freshly prepared aqueous potassium permanganate (3% w/v). About 18 ml were added in 3-ml portions with stirring during 1 hour. Samples were removed at 10-minute intervals and transferred into ether, and the course of the reaction followed spectrophotometrically. When the ratio of absorbance at 650 mμ to that at 687 mμ reached *ca.* 2.5, the mixture was poured into a large volume of ether and the manganese dioxide was removed by filtration. The filtrate was well washed with water and extracted three times with aqueous potassium hydroxide (0.5 *N*), which removed a small quantity of acidic products. After several washes with distilled water, the ether solution was evaporated to dryness under vacuum. The pigment was adsorbed on a powdered sucrose column from 1 l. of 50% (v/v) ether – petroleum ether (b.p. 30–60° C). Five hundred milliliters of 10% ether plus 5% isopropanol in petroleum ether removed unchanged chlorophyll *a* and fraction A

together, and left fractions B and C adhering to the column. Chlorophyll *a* and fraction A were separated later using 0.5% isopropanol in petroleum ether. Chlorophyll *a* passed into the suction flask ahead of fraction A. Fraction A was re-chromatographed and traces of impurities were removed by successive treatments with 50, 75, and 90% benzene in petroleum ether, followed by 0.5 and 1.0% isopropanol – petroleum ether mixtures. The yield was about 100 mg.

Prolonging the oxidation increased the yield of acidic products with concomitant decrease in the yields of fractions A, B, and C. No significant decrease in the ratio of absorbance at 687 to 650 mμ was noted, however.

2-Desvinyl-2-formyl-chlorophyllide-a Methyl Ester

Methyl chlorophyllide *a* (170 mg) was oxidized, and fractions corresponding to those designated above were isolated as follows: A and B were separated from C by passing the pigment dissolved in 60% $CHCl_3$ – petroleum ether mixture through a sugar column. A and B and a small amount of methyl chlorophyllide *a* passed into the suction flask. The mixture was dried and adsorbed on a fresh column from 25% $CHCl_3$ in petroleum ether and treated with 3.5% isopropanol in petroleum ether. Fraction A passed into the flask after methyl chlorophyllide *a*. It was then re-chromatographed and treated with 0.75% isopropanol plus 20% $CHCl_3$ in petroleum ether. The acid number of the magnesium-free derivative was 16.5.

2-Desvinyl-2-formyl-chlorin-e_6-trimethyl Ester

This was prepared as a reference compound by oxidation of chlorin-e_6-trimethyl ester using the method given for chlorophyll *a*. The product was isolated by the method of Fischer and Walter (10). It was also prepared by oxidation of chlorophyll *a* (0.7 g), and subsequent hydrolysis in methanolic KOH. After the transfer of the pigment mixture into ether, 15% HCl (w/v) was used to extract all pigment no longer containing phytol. This acid-extractable fraction was then esterified with diazomethane in ether. Extraction of the ether solution with 2% HCl removed the chlorin-e_6-trimethyl ester derivative of fraction C, while 5% HCl removed most of that of fraction B. The pigment remaining in the ether was evaporated to dryness and adsorbed on a powdered sugar column from 15% chloroform in petroleum ether, and treated with 10% $CHCl_3$ plus 0.7% isopropanol in petroleum ether. The sugar column was extruded and the main zone of pigment was isolated and extracted with ether. The ether solution was well washed with distilled water and evaporated to dryness. The product was crystallized from methanol containing a trace of acetone. The precipitate was removed and washed well with pentane. Two further crystallizations yielded long needles, m.p. 222–223° C. Found: C, 67.5; H, 6.15. Calculated for $C_{36}H_{40}O_7N_4$: C, 67.5; H, 6.25%.

The same compound was prepared by oxidation of methyl chlorophyllide *a* using appropriate variations of the above procedure. A mixed melting point of the products obtained from the three starting materials showed no depression. The visible absorption spectra were identical. Absorption maxima in ether: I, 691; II, 632; III, 575; IV, 545; V, 509; VI, *ca.* 480; VII, 414 mμ. Relative absorbancies: VII > I > V > IV > II > VI > III.

The oxime derivative was prepared as given by Fischer and Walter (10). Absorption maxima in ether: I, 671; II, 617; III, 564; IV, 534; V, 501; VI, 403 mμ. Relative absorbancies: VI > I > V > IV > II > III.

2-Desvinyl-2-formyl-pheophorbide-a Dimethyl Acetal Methyl Ester

The methyl ester of fraction A was dissolved in a small volume of 5% (w/w) methanolic

HCl. After 1 minute, the pigment was transferred into ether by dilution with distilled water. The pigment was evaporated to dryness after removal of acid, and adsorbed on a sucrose column from 1% pyridine in petroleum ether. The column was developed by 0.5% isopropanol in petroleum ether, and the main zone of pigment was removed after extrusion of the sugar. Absorption maxima in ether: I, 664; II, 634; III, 607; IV, 558; V, 534; VI, 505; VII, 471; VIII, 406 mμ. Relative absorbancies: VIII > I > VI = V > III > II > IV > VII.

2-Desvinyl-2-hydroxymethyl-pheophytin-a

2-Desvinyl-2-formyl-chlorophyll-*a* (5 mg) in methanol (20 ml) was treated with sodium borohydride (5 mg). After 2 minutes the "red" absorption maximum shifted from about 690 mμ to about 660 mμ. The mixture was poured into ether and was well shaken with aqueous 0.5% potassium acid phosphate, and with distilled water. The solution was evaporated to dryness and the pigment was adsorbed on sucrose from 100% benzene. The column was developed with 2% isopropanol in petroleum ether. Pigment in the main zone was isolated and magnesium was removed by dilute aqueous HCl in acetone. Absorption maxima in ether: I, 660; II, 630; III, 603; IV, 556; V, 533; VI, 503; VII, 490 mμ. Relative absorbancies: I > VI > V > III > VII > II > IV.

Determination of Magnesium Content of Fraction A

The magnesium content in 50 ml of an ether solution was determined by the method of Smith and Benitez (3). Absorbance per cm at 687 mμ: 6.60. Slope of the calibration curve at 540 mμ: 0.266 absorbance units per cm per 0.108 mg of magnesium. Absorbance of unknown at 540 mμ: 0.185, equivalent to 0.076 mg of magnesium. Weight of fraction A per 50 ml calculated using the specific absorption coefficient of Smith and Benitez: 2.99 mg. Weight calculated from magnesium determination assuming molecular weight of 895: 2.81 mg. Calculated extinction coefficient: 117.8; Smith and Benitez: 110.4 for chlorophyll *d*.

ACKNOWLEDGMENTS

The authors are very grateful to Miss C. I. MacFarlane of the Nova Scotia Research Foundation for having sent the samples of *Chondrus* and *Gigartina*, and to Dr. M. B. Allen of the Kaiser Foundation, Berkeley, California, for having sent the sample of *Rhodocorton*. Infrared absorption spectra were measured by Mr. F. Rollin. Technical assistance was provided by Mr. E. Versteeg.

REFERENCES

1. Rabinowitch, E. I. Photosynthesis. Vol. II. Pt. 2. Interscience Publishers, Inc., New York. 1956.
2. Manning, W. M. and Strain, H. H. J. Biol. Chem. **151**, 1 (1943).
3. Smith, J. H. C. and Benitez, A. Modern methods of plant analysis. Vol. IV. Springer-Verlag, Berlin. 1955. pp. 142–196.
4. Holt, A. S. Can. J. Biochem. Physiol. **36**, 439 (1958).
5. Weller, A. J. Am. Chem. Soc. **76**, 5819 (1954).
6. Holt, A. S. and Jacobs, E. E. Plant Physiol. **30**, 553 (1955).
7. Holt, A. S. To be published.
8. Fischer, H. and Lakatos, E. Ann. **506**, 123 (1933).
9. Fischer, H. and Lautsch, W. Ann. **528**, 247 (1937).
10. Fischer, H. and Walter, H. Ann. **549**, 44 (1941).
11. Haworth, R. D. and Lapworth, A. J. Chem. Soc. 79 (1922).
12. Fischer, H., Breitner, S., Hendschel, A., and Nüssler, L. Ann. **503**, 1 (1933).
13. Fischer, H., Lakatos, E., and Schnell, J. Ann. **509**, 201 (1934).
14. Willstätter, R. and Stoll, A. Untersuchungen über Chlorophyll. J. Springer, Berlin. 1913.
15. Holt, A. S. and Jacobs, E. E. Am. J. Botany, **41**, 710 (1954).
16. Jacobs, E. E., Vatter, A., and Holt, A. S. Arch. Biochem. and Biophys. **53**, 228 (1954).
17. Fischer, H. and Orth, H. Chemie des pyrroles. Vol. II. Pt. 2. Leipzig. 1940.

A MASS SPECTROMETER WITH A LOW-TEMPERATURE IONIZATION CHAMBER

TO STUDY HETEROGENEOUS REACTIONS OF ATOMS AND FREE RADICALS: EXAMPLE, IODINE ATOMS[1]

L. P. BLANCHARD[2] AND P. LE GOFF

ABSTRACT

The main features of a mass spectrometer in which the ionization chamber can be cooled in a controlled way to the temperature of liquid nitrogen are given. Atoms or free radicals, formed in a heterogeneous quartz reactor that can be heated to 1000° C, effuse through a small hole in the wall of this reactor and enter directly into the ionization chamber. With this instrument it is possible to study the various ways in which unstable particles disappear during collisions on a metallic surface maintained at low and controlled temperatures.

The collision efficiency "b" of iodine atoms to form iodine molecules was found to vary between 1.7×10^{-3} and 4×10^{-3} on a surface at a temperature between +40° C and −25° C. Between −25° C and −60° C, the atoms are condensed at the same time as the iodine molecules; at lower temperatures, they are more "volatile" than iodine molecules, most of them colliding on the molecules of condensed iodine without reacting.

INTRODUCTION

In recent years an increasing number of workers have been focusing their attention on the study of atoms and free radicals trapped on surfaces maintained at liquid nitrogen or helium temperatures, but little attention has been paid to the trapping process itself.

A special mass spectrometer was designed and constructed in Nancy to study the primary process that takes place when a free radical collides with a surface at a controlled low temperature. Four possibilities must be considered in this process:

(1) that the radicals are adsorbed and trapped in the free state without undergoing any transformation;

(2) that the radicals are adsorbed on the surface but interreact to form stable molecules which immediately freeze to the surface;

(3) that the radicals are adsorbed and react as in (2) but form volatile products that leave the surface;

(4) that the radicals undergo elastic collisions with the cooled surface, while stable products are formed elsewhere by secondary reactions.

It has been reported that when the temperature of a surface on which radicals have been trapped is allowed to rise slowly, a point is reached where the radicals regain sufficient mobility to react and form stable molecules, giving off heat and sometimes light. The instrument mentioned above has been designed to study the mechanism of such reactions, since with it, it is possible to analyze directly the unstable as well as the stable products formed during the recombination–desorption process.

Operating Principle of the Instrument (See Fig. 1)

The ionization chamber of the mass spectrometer was machined out of a block of non-magnetic stainless steel that is mounted in such a way that its temperature can be lowered in a controlled manner to that of liquid nitrogen. The particles contained in a molecular jet coming from a nearby reactor are admitted to the ionization chamber through a slit "A_2" cut in one of the side walls. The present reactor is a quartz tube,

[1]*Manuscript received November 7, 1958.*
Contribution from l'École Nationale Supérieure des Industries Chimiques, Université de Nancy, France.
[2]*Postdoctorate Fellow of the National Research Council of Canada. Present address: Département de Génie Chimique, Université Laval, Quebec, Canada.*

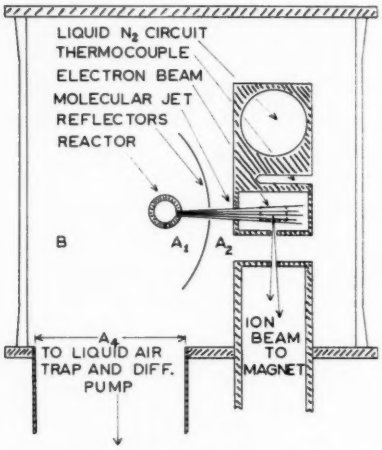

FIG. 1. Schematic diagram of the ion source. The ion source unit and the reactor are shown at a scale six times that of the bell jar enclosure.

3 mm i.d., that can be heated to 1000° C. This tube located 8 mm away from the ionization chamber contains a small orifice "A_1" through which effuse the gases of the molecular jet. The ion source and reactor assembly are located within a large bell jar, which is evacuated by a 600-liter-per-second mercury diffusion pump, and liquid-nitrogen trap.

The metallic block which contains the ionization chamber has no physical contact with the neighboring parts of the ion source: the filament (made of 0.258 mm carbon rod) is mounted on one of the pole pieces of the source magnet, while the other pole piece serves as the electron trap. Contrary to usual mass spectrometer technique, the ion source is grounded through the copper tubes of the liquid nitrogen circuit and the ion acceleration potential is applied to the magnet analyzer tube. Electrical insulation of the tube from the rest of the vacuum envelope is maintained by mineral-free synthetic rubber *o*-rings at the vacuum seals and teflon sheet elsewhere.

After deviation in the magnetic field the ion beam falls on the first copper–beryllium dynode of a 12-stage Allen-type ion–electron multiplier. The outcoming signal is fed to the vertical amplifier of a cathode ray oscilloscope. Fast scanning of the mass spectrum can be carried out by modulation of the magnet current (10 sweeps/second) or the ion acceleration potential (100 sweeps/second).

Flow and Pressure of Gases in the Ionization Chamber

A fraction of the molecular stream leaving the reactor enters directly into the ionization chamber while the complementary fraction diffuses into the bell jar.

Under usual operating conditions the following pressures are observed in the instrument: 1×10^{-2} mm Hg in the reactor, 1.1×10^{-4} mm Hg in the ionization chamber, and 1.6×10^{-5} mm Hg in the bell jar. Using the method previously described (2) for the statistical study of the fate of every molecule, an expression was found for the molecular concentration in that region of the chamber where the ionizing electron beam crosses the molecular stream. In the case of a condensable gas, with the reactor and the ion source both at room temperature, this expression is composed of two terms: one (amounting to 14% of the total concentration) which represents the "equivalent jet concentration", i.e. the molecules that have come directly from the reactor and have *not yet*

collided with the chamber walls; the second (the remaining 86%) which corresponds to the molecules homogeneously distributed throughout the chamber and undergoing an average number of 102 collisions with the walls before leaving by a "collision" with one of the four slits.

If "b" is the probability that the particle will disappear at every collision with the walls, then the concentration C in the ionizing region is given by the following expression:

$$\frac{C}{C_0} = 0.14+0.86\left(\frac{T_r}{T_e}\right)^{\frac{1}{2}} \frac{(1-b)}{(1+101b)}$$

where T_r and T_e are respectively the temperatures of the reactor and of the ionization chamber and C_0 is the concentration in the case where $T_r = T_e$ and $b = 0$.

EXPERIMENTAL RESULTS

Experiments were carried out using mixtures of iodine vapor and argon, the argon serving as internal standard.

1. Spectrum of Iodine at Low Temperatures

When iodine vapor is introduced at a constant flow rate into the source through the reactor maintained at room temperature, i.e. +40° C, and the chamber is progressively cooled to lower temperatures, the following results are observed:

(*a*) *Between +40° C and −45° C* the reading of an ionization gauge located in the bell jar is constant; the I_2^+ peak decreases from 5.7 to 2.2 while the I^+ peak remains essentially constant at 1.4.* This is in fact the variation with temperature of the cracking pattern of iodine molecules.

(*b*) *Between −45° C and −70° C* the vapor pressure of iodine passes from 1×10^{-4} to approximately 1×10^{-6} mm Hg. Effectively the reading from the ionization gauge decreases and the I_2^+ and I^+ peaks fall to about 6% of their values at room temperature. It must be concluded that the condensation probability of iodine molecules on the walls varies gradually from zero to one in this temperature range.

(*c*) *Below −70° C* the condensation probability is equal to one. The remaining ionic intensities are constant and correspond to the molecules arriving in the jet directly from the reactor.

2. Dissociation of Iodine into Atoms

When the reactor is heated to 697° C, the ionization chamber being maintained at +40° C, the I_2^+ peak is observed to fall to 32% of its initial value, while the intensity of the I^+ peak remains constant. From thermodynamic data it can be assumed that the iodine molecules passing through the reactor are totally dissociated into atoms. Thus the iodine molecules observed would come solely from recombination reactions on the walls. The probability of recombination of an iodine atom at every collision has been calculated to be: 1.7×10^{-3}.

3. Freezing Experiments with Iodine Atoms and Molecules

When the ionization chamber is slowly cooled, the reactor being maintained at 697° C, the I_2^+ and I^+ peak intensities vary in a manner completely different from that observed when the reactor is at 40° C.

At first, the I_2^+ peak decreases slowly from 1.8 at +40° C to 1.6 at −40° C, then sharply to 0.3 at −70° C. The I^+ peak, on the other hand, increases from 1.2 to 1.5

*I_2^+ *and* I^+ *peak intensities are expressed as the ratio of the peak height to that of argon at each temperature.*

then decreases slowly to a value of 0.6. The fundamental difference from the first case resides in the fact that the I^+ peak maintains an appreciable intensity below $-70°$ C.

A detailed analysis of the various low temperature mass spectra has been given elsewhere (1), however the essential points of the method are as follows:

(1) The mass spectrometric sensitivity and cracking pattern of iodine having been obtained in the first experiment, the concentration of molecules at each temperature of the present case can be evaluated.

(2) By subtracting from the total I^+ peak measured that part due to the dissociative ionization of iodine molecules, the intensity of the I^+ peak due to iodine atoms is thus obtained at each temperature.

(3) By means of an iodine material balance in the ionization chamber and the assumption that the mass spectrometric sensitivity for I^+ coming from iodine atoms is constant, the concentration of these atoms in the ionization chamber at every temperature is obtained.

The experimental results are as follows (refer to Fig. 2):

(1) When the temperature drops from $+40°$ C to $-30°$ C, the iodine atom concentration decreases slowly, the collision efficiency for the recombination of iodine atoms increasing from 1.7×10^{-3} to about 4×10^{-3}.

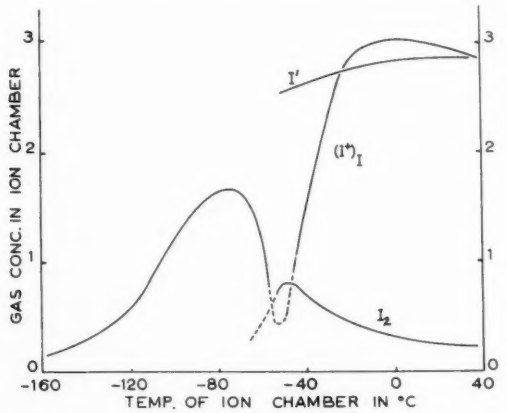

FIG. 2. Concentration variations of atomic and molecular iodine in the ionization chamber when this chamber is being cooled. Reactor at 697° C. The unit of concentration used on this graph corresponds to a pressure of 5×10^{-4} mm Hg at $+40°$ C.

(2) From $-30°$ C, the iodine atom concentration decreases sharply: iodine atoms disappear readily when they collide with the walls, *without* giving molecules which would desorb from the surface. However, it is not possible to distinguish whether the atoms are condensed in a free state within the matrix of the molecules condensing simultaneously, or whether the atoms recombine beforehand to form molecules that are immediately frozen out.

(3) When the temperature is lowered further, the iodine atom concentration presents a new maximum between $-70°$ C and $-80°$ C which would indicate that the majority of these atoms rebound from the layer of condensed iodine molecules without recombining or condensing.

4. Defrosting Experiments

A film of iodine was condensed on the walls of the chamber:

(1) by cooling the chamber gradually, and later

(2) by introducing the vapor into a precooled source at $-195°$ C.

Defrosting experiments showed no particular characteristics; iodine molecules alone were desorbed at the same rate and at the same temperature regardless of the reactor temperature during the freezing process.

The work described here was carried out in the laboratories of Professor M. Letort, to whom the authors are indebted for the facilities placed at their disposal. One of us (L.P.B.) wishes to thank the National Research Council of Canada for a Postdoctorate Overseas Fellowship.

REFERENCES

1. Conference on Mass Spectrometry in London, England, September, 1958.
2. Le Goff, P. J. chim. phys. **53**, 359 (1956).

THE DEHYDRATION OF UREA, BENZAMIDE, AND PHENYLUREA BY THIONYL CHLORIDE IN THE PRESENCE OF AMMONIA[1]

PAUL E. GAGNON, JEAN L. BOIVIN,[2] AND JOHN H. DICKSON[3]

ABSTRACT

The decomposition of thionyl chloride in the presence of ammonia was found to give sulphur, ammonium sulphate, and ammonium sulphamate besides ammonium chloride. Heating urea and the reaction products of thionyl chloride and ammonia under pressure yielded guanidine hydrochloride and melamine, under different conditions of temperature, time, and pressure. Under similar conditions, benzamide was transformed into benzonitrile, and phenylurea into aniline or aniline black and diphenylurea, guanidine being absent.

INTRODUCTION

Guanidine has been synthesized from urea using various dehydrating agents, such as sulphur trioxide (1), sulphur dioxide (2), ammonium sulphamate (1), aluminum metal, or aluminum chloride (3) in the presence of ammonia or ammonium salts. In all cases, the highest yields of guanidine were obtained when the reaction was carried out under pressure (4). Since thionyl chloride is a good dehydrating agent, which reacts with water giving sulphur dioxide and hydrochloric acid, it is of interest to study its potentiality with respect to the dehydration of urea, benzamide, and phenylurea.

As the formation of guanidine is considered as an ammoniation of cyanamide, which in turn is produced by dehydration of urea:

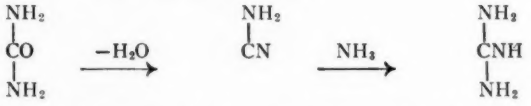

there is an indication that guanidine would be unstable if thionyl chloride reacted alone with urea. It is known that ammonium salts or ammonia under pressure stabilize the molecule, and the effect of both will be necessary at high temperatures to prevent its decomposition into melamine (5).

Preliminary experiments carried out by heating, in a pressure vessel, urea, thionyl chloride, and ammonia which had been frozen separately in liquid air proved to be hazardous and unreliable. Therefore, to study the dehydrating properties of thionyl chloride with respect to urea and benzamide, a solution of thionyl chloride in anhydrous benzene was treated with an excess of ammonia. The yellow solid was collected and dried over calcium chloride and used without further purification. It will be called a thionyl chloride – ammonia complex since it is an ill-defined material (6, 7, 8, 9).

Thermal Stability of the Thionyl Chloride – Ammonia Complex

Since the synthesis of guanidine is best carried out under pressure, the thermal stability of the thionyl chloride – ammonia complex was studied under various conditions of temperature and pressure. It was observed that sulphur, ammonium sulphate, and ammonium sulphamate were the reaction products obtained, besides the normally

[1]*Manuscript received June 4, 1958.*

Contribution from the Department of Chemistry, Laval University, Quebec, Que., with financial assistance from the Defence Research Board of Canada. This paper constitutes part of a thesis submitted to the Graduate School, Laval University, in partial fulfillment of the requirements for the degree of Doctor of Science.

[2]*Defence Research Board, C.A.R.D.E., Valcartier, Que.*

[3]*Graduate student, holder of a Shell Oil Co. of Canada Ltd. Scholarship in 1957–58, Laval University, Quebec, Que.*

present ammonium chloride under different conditions. At atmospheric pressure over a range of temperature of 150–325° C, the yield of sulphur was nearly constant to 7.5% and there was an increase of ammonium sulphate from 0.9% at 150° C to 7.5% at 300° C and a decrease to 5.2% at 325° C, as shown in Table I. Ammonium sulphamate was obtained in maximum yield at 250° C, which decreased from 12.6 to 3.1% at 325° C.

Under an ammonia pressure of 100 and 300 p.s.i., the results were similar, but it was observed that ammonium sulphate was present in larger quantities from 275 until 350° C.

TABLE I

Decomposition products of the thionyl chloride – ammonia complex at atmospheric pressure

Temp., °C	% Composition of solid products			
	S	NH_4Cl	$(NH_4)_2SO_4$	$NH_2SO_3NH_4$
150	7.2	65.7	0.9	8.2
175	7.2	64.4	1.3	9.2
200	7.3	64.7	1.1	10.8
225	7.8	65.2	1.3	11.9
250	7.8	64.1	2.1	12.6
275	7.8	65.7	3.9	11.9
300	7.5	61.8	7.5	4.2
325	7.3	62.4	5.2	3.1

Guanidine from Urea and Thionyl Chloride – Ammonia Complex

As ammonium sulphamate is present in the decomposition products of the complex, it is expected that it could transform urea into guanidine (1). The reaction of the thionyl chloride – ammonia complex with urea was studied under various conditions of temperature, pressure, time, and ratio of reactants.

The method used consisted of mixing thoroughly urea with the dry thionyl chloride – ammonia complex and heating the mixture under normal pressure or under ammonia pressure in the autoclave. The reaction products were analyzed for sulphur, ammonium sulphate, ammonium sulphamate, guanidine, and melamine. Results are given in Table II for the reaction under 300 p.s.i. for a 30-minute period of heating.

TABLE II

Guanidine formation at 300 p.s.i. pressure for a 30-minute period of heating

Temp., °C	% Composition of reaction products				
	S	$(NH_4)_2SO_4$	$NH_2SO_3NH_4$	$H_2NC(NH)NH_2$	$C_3H_6N_6$
150	6.8	2.0	4.9	—	—
175	6.9	0.6	6.4	—	—
200	7.2	1.2	4.7	—	—
225	7.6	3.8	4.5	—	—
250	7.6	28.6	3.5	19.4	2.8
275	6.9	38.0	2.3	33.8	3.9
300	5.8	38.5	2.5	35.1	4.1
325	5.7	23.5	2.1	31.2	4.5
350	5.6	7.5	1.3	17.5	3.7

At atmospheric pressure, urea was transformed into guanidine between 225° C and 250° C. The conversion of urea into guanidine reached a maximum at 275° C and then fell off sharply at higher temperatures so that no guanidine was found when the experiment was carried out above 325° C. The fact that melamine was found in place of

guanidine at the higher temperatures indicates that the guanidine decomposed into cyanamide which trimerized into melamine. Ammonia pressure had a stabilizing effect, and the yield of guanidine was increased from 17 to 35% at 275–300° C when the pressure was either 100 or 300 p.s.i.

In the solid products, sulphur was present to a practically constant proportion of about 7.0% which, however, decreased with increasing temperatures to 5.6%. Ammonium sulphate increased proportionally with the amount of guanidine formed while the ammonium sulphamate content decreased.

With different ratios of urea at a temperature of 275° C and an ammonia pressure of 300 p.s.i., the yield of sulphur was practically constant and the production of ammonium sulphate varied directly with increasing quantity of urea used, whereas the yield of ammonium sulphamate varied inversely with the urea. When the reaction time was limited to 30 minutes, the yield of sulphur was about 7%. Between 60 and 150 minutes, it fell to 5%, but with longer periods of heating it decreased sharply and was less than 1% after 210 minutes. The proportion of ammonium sulphate in the reaction products remained constant for heating periods longer than 60 minutes. Although ammonium sulphate decomposed at temperatures above 300° C (10) during a reaction time of 30 minutes, it was quite stable at 275° C, even when heated for periods up to $3\frac{1}{2}$ hours. Only traces of ammonium sulphamate were found in the reaction products under these conditions.

Guanidine and ammonium sulphate increased continuously with the reaction time up to a maximum yield of about 44%, and further heating had no apparent effect. The increase in the reaction time was unfavorable for the formation of melamine and the yield was reduced from 14.4% after 60 minutes to 10.5% after 210 minutes.

Benzonitrile from the Thionyl Chloride – Ammonia Complex and Benzamide

Since the thionyl chloride – ammonia complex was a dehydrating agent by way of the formation, on heating, of ammonium sulphamate, amides should be converted into the corresponding nitriles (11, 12). By heating the thionyl chloride – ammonia complex and benzamide under pressure, benzonitrile was obtained in only 5% yield at 175° C and more was formed as the temperature was increased until a maximum yield of 57.4% was reached at 325° C. The production of ammonium sulphate increased to a maximum of about 30% at 275° C and then decreased with increasing temperatures. A maximum yield of ammonium sulphamate was obtained at 150° C, but decreased continuously with the increase in temperature.

Products of the Reaction of Phenylurea with the Thionyl Chloride – Ammonia Complex

The reaction of the thionyl chloride – ammonia complex with phenylurea at different pressures led to a mixture of salts where aniline was present at the lower temperatures and aniline black at temperatures above 250° C. When the experiments were performed at atmospheric pressure, the highest yield of ammonium sulphate obtained was about 4% whereas the quantity of ammonium sulphamate for temperatures above 200° C was much lower. The yield of aniline, constant up to a temperature of 275° C, increased slightly at higher temperatures and was accompanied by an increase in the pressure.

An ammonia pressure of 100 p.s.i. gave rise to larger amounts of ammonium sulphamate at 150° C which decreased as the temperature was raised. Again fairly large amounts of aniline black were present up to 300° C. The ammonia pressure caused an increase in the yield of ammonium sulphate and a much higher yield of aniline which, however, decreased from 63.3% at 150° C to 22.0% at 325° C, while that of ammonium sulphate increased from 0.2% at 150° C to 7.9% at 325° C.

A higher ammonia pressure of 300 p.s.i. favored the production of larger quantities of ammonium sulphate, the maximum yields being obtained at 200° and 275° C. Higher temperatures led to reduced yields. Ammonium sulphamate production was highest at the lower temperatures although the amount was a good deal lower. The maximum yield of aniline, 63.3%, was also obtained at the lower temperatures. Ammonia pressure stabilized aniline particularly at the higher temperatures where the minimum yield was found to be about 37%.

Also diphenylurea was obtained between 150 and 250° C at 300 p.s.i., in yields varying from 0.1 to 4.0%, depending on the temperature used. At pressure lower than 300 p.s.i., diphenylurea could not be isolated.

DISCUSSION OF RESULTS

The ill-defined thionyl chloride – ammonia complex was decomposed at ordinary pressure or under an ammonia pressure into sulphur, ammonium sulphate, and ammonium sulphamate. While it is difficult to account specifically for all these products, this behavior should be similar to that of sulphur dioxide and ammonia which give, by heating under pressure, ammonium sulphamate and sulphur and no ammonium sulphate (2). The fact that ammonium sulphate is present indicates that a similar oxidoreduction has taken place where ammonia reduced the chloro derivative of sulphur dioxide into sulphur giving water, which then hydrolyzed part of ammonium sulphamate into ammonium sulphate.

When urea is present, the mechanism of formation of the products sulphur, ammonium sulphate, ammonium sulphamate, guanidine, and melamine is easily explained by reactions similar to the synthesis of guanidine from urea, sulphur dioxide, and ammonia (2). In this case, urea is dehydrated into cyanamide and ammonolyzed into guanidine. Guanidine is present in the actual synthesis as the hydrochloride because of the greater solubility of this salt in liquid ammonia than the sulphamate salt, whereas guanidine sulphate is completely insoluble (5).

When monophenylurea was heated with ammonium sulphamate, aniline, guanidine, and cyanuric acid were produced (12). On heating thionyl chloride and ammonia with monophenylurea, ammonium chloride, sulphate, sulphamate, aniline, aniline black, and diphenylurea were formed. It was assumed that monophenylurea underwent ammonolysis to give urea and aniline, and also diphenylurea. It is well known that aniline, in the presence of an oxidizing agent, forms a polymer, or better a variety of polymers, grouped together under the generic name of aniline blacks, the exact constitution of which is still unknown; since free sulphur was absent, it was concluded that it had oxidized the aniline to form aniline black, sulphur being transformed into hydrogen sulphide.

The absence of urea or guanidine derivatives in the reaction products was explained by the inhibition of hydrogen sulphide to form ammonium sulphamate from the chloro derivative of sulphur dioxide.

EXPERIMENTAL

Thionyl Chloride – Ammonia Complex

Thionyl chloride (20.0 g) was added to a 1-l. flask containing anhydrous benzene (400 ml), and anhydrous ammonia was bubbled through the solution until there was no further evolution of heat. The light yellow solid which precipitated out was separated by filtration on a Büchner funnel, washed with anhydrous benzene, and dried in a vacuum desiccator over calcium chloride (yield, 30.4 g).

The dried yellow starting material (8.0 g) was added to the removable Pyrex glass

liner of a pressure vessel which had a volume of 183 ml without the liner, and 108 ml with the liner in place. The liner was fitted with a glass wool plug, and air was displaced by the evaporation of several drops of liquid ammonia in the autoclave. The reaction vessel was then heated at the desired temperature for 30 minutes, removed from the heating jacket, and cooled rapidly.

The solid products were analyzed for sulphur, ammonium chloride, sulphate, and sulphamate (2). Ammonium sulphamate was extracted from the mixture by means of absolute alcohol in which it is slightly soluble and recrystallized to give a melting point of 131° C, which was not depressed by admixing an authentic sample.

Since it would be impracticable to give all the results obtained, the data were omitted.

Thionyl Chloride – Ammonia Complex and Urea

The yellow starting material (5.5 g), made from thionyl chloride and ammonia, and urea (3.0 g, 0.05 mole) were intimately mixed and heated as in the above method. The products were analyzed for sulphur, ammonium sulphate, ammonium sulphamate, guanidine hydrochloride, and melamine (2). Guanidine hydrochloride was isolated by absolute ethanol extraction of the dried products and recrystallized from a mixture of alcohol and acetone. It had a melting point of 184–185° C, which was not depressed by mixing with an authentic sample.

Reaction with Benzamide

The yellow starting material (5.5 g) was added to a glass liner containing benzamide (6.1 g, 0.06 mole, m.p. 130° C) which had been recrystallized. The two solid compounds were then thoroughly mixed and heated in the autoclave and cooled overnight. Caution was exercised in reducing the internal pressure to atmospheric pressure since benzonitrile could be entrained out.

Benzonitrile was determined by extraction with ether and weighing the residue. It boiled at 188–191° C and gave benzoic acid, m.p. 121° C, by hydrolysis with alcoholic sodium hydroxide. The residue which was insoluble in ether was analyzed for ammonium sulphate and sulphamate (2).

Reaction with Monophenylurea

The yellow starting material (5.5 g) and monophenylurea (6.8 g, 0.05 mole) were placed in a Pyrex liner, thoroughly mixed together, and heated in the autoclave. The solid products were analyzed for aniline, ammonium sulphate, ammonium sulphamate, and diphenylurea by extraction or precipitation with barium chloride (2).

REFERENCES

1. MACKAY, J. S. U.S. Pat. No. 2,515,244. July 18, 1950.
2. BOIVIN, J. L. Can. J. Chem. **34**, 827 (1956).
3. SANDER, F. Ger. Pat. No. 527,237. Jan. 1, 1928.
4. BLAIR, J. S. J. Am. Chem. Soc. **48**, 87 (1926).
5. BOIVIN, J. L. Can. J. Chem. **33**, 1467 (1955).
6. SCHIFF, H. Ann. 102 (1857).
7. MICHAELIS, A. Z. Chem. (2), **6**, 460 (1870).
8. EPHRAIM, F. and PIATROWSKI, H. Ber. **44**, 379 (1911).
9. SCHENK, P. W. Ber. **75**, 94 (1942).
10. SMITH, W. J. Soc. Chem. Ind. (London), **14**, 629 (1895); **15**, 3 (1896).
11. BOIVIN, J. L. Can. J. Chem. **28**, 671 (1950).
12. GAGNON, P. E., BOIVIN, J. L., and HAGGART, C. Can. J. Chem. **34**, 1662 (1956).

DIALKYL PHOSPHOROISOTHIOCYANATIDATES[1]

MARSHALL KULKA

ABSTRACT

An improved method for the preparation of dialkyl phosphoroisothiocyanatidates (II) is given. These compounds (II) are labile and decompose under the influence of heat and catalysts to the corresponding alkyl thiocyanates (III). In the presence of water they hydrolyze to dialkyl hydrogenphosphates (VI) in high yield. A series of thiourea derivatives (VII) has been prepared from II and amines.

Some discrepancies have appeared in the literature regarding diethyl phosphoroisothiocyanatidate (1). The compound is referred to as a thiocyanate by some workers (2, 3, 4), and isothiocyanate by others (5, 6). There has also been a lack of harmony in regard to its properties and preparation. Saunders *et al.* (2) first reported that when diethyl phosphorochloridate (I) was heated under gentle reflux with potassium thiocyanate, diethyl phosphorothiocyanatidate boiling at 40° (13 mm) was obtained. Kosolapoff (7) pointed out that this boiling point was too low and when the English workers (3) re-examined the reaction, they found that it proceeded at room temperature to form diethyl phosphorothiocyanatidate in 50% yield boiling at 80–82° (1 mm). Other workers have employed acetone (5) and methyl ethyl ketone (4) as solvent but without improvement in yield.

Recently (5, 6) it was pointed out that the higher-boiling reaction product of I and potassium thiocyanate reacted readily with amines to form thiourea derivatives. This indicated that the product is diethyl phosphoroisothiocyanatidate (II) and not a thiocyanate. It can be assumed that II arises through a thiocyanate–isothiocyanate rearrangement which in phosphorus compounds would be expected to take place with ease.

Dialkyl phosphoroisothiocyanatidates (II) were required as intermediates in connection with a synthetic program of insecticides. For this reason a study of the preparation and properties of II was undertaken. It was found that the compound (II) could be readily prepared and in excellent yield by merely stirring a solution of I in dry benzene with ammonium thiocyanate at 20°, followed by washing with cold brine solution, drying, and cautiously distilling.

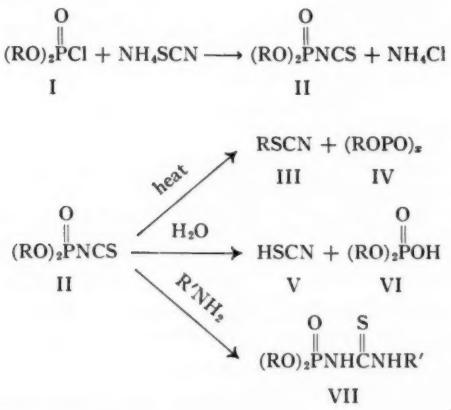

[1]*Manuscript received November 10, 1958.*
Contribution from the Dominion Rubber Company Limited, Research Laboratories, Guelph, Ontario.

Diethyl phosphoroisothiocyanatidate (II) is a labile compound. Under the influence of heat it decomposed to a low-boiling material which appeared to be the same as that obtained by the original workers (2) and mistaken for II. The decomposition occurred very rapidly at 150°, more slowly in refluxing benzene or methyl ethyl ketone, and was catalyzed by traces of ammonium or potassium thiocyanate. The low-boiling phosphorus-free decomposition product did not react with amines but on heating with aqueous alcoholic alkali yielded diethyl disulphide and sodium cyanide, a reaction which is characteristic of alkyl thiocyanates. After an examination of the physical properties it was concluded that the decomposition product of II was ethyl thiocyanate (III, R = ethyl). In the same way di-*n*-butyl phosphoroisothiocyanatidate (II, R = *n*-butyl) on heating alone or in the presence of ammonium thiocyanate decomposed to butyl thiocyanate III, (R = *n*-butyl) and presumably butyl metaphosphate (IV).

It will be seen that II is both an anhydride and an isothiocyanate presenting at least two sites for attack. With warm water II did not react like a typical isothiocyanate. Instead hydrolysis occurred to form thiocyanic acid (V) and dialkyl hydrogenphosphate (VI) in high yield. This makes an excellent preparative method for VI. Primary amines attacked II at the isothiocyanate site to form dialkyl phosphorylthioureas shown in Tables I and II.

TABLE I

N¹-Diethylphosphoryl-N²-substituted thioureas

$$(C_2H_5O)_2\overset{O}{\overset{\|}{P}}NHC\overset{S}{\overset{\|}{N}}HR$$

R =	Prepared from:	M.p., °C	Method of prep.	Yield, %	Analyses, N Calc.	Found
Phenyl (5)	Aniline	107–108	A	77	9.70	9.63
p-Chlorophenyl	*p*-Chloroaniline	129–130	B	91	8.68	9.14
3,4-Dimethoxyphenyl	3,4-Dimethoxyaniline	124–125	B	52	8.04	8.08
β-Naphthyl	β-Naphthylamine	117–118	B	60	8.28	8.50
2,4-Dichlorobenzyl	2,4-Dichlorobenzylamine	133–134	A	86	7.55	7.45
Cyclohexyl	Cyclohexylamine	84–85	A	90	9.52	9.67
Phenylethyl	Phenethylamine	80–81	A	48	8.86	8.57
β-Pentachloroanilinoethyl	N-2-Aminoethylpentachloroaniline	134–135	B	55	C, 30.99 H, 3.37	C, 30.59 H, 3.57
β-*p*-Chlorophenylmercaptoethyl	*p*-Chlorophenyl 2-aminoethyl sulphide	85–86	A	45	7.32	7.56
3-Indolylethyl	Tryptamine	134–136	C	37	11.83	11.65
Octadecyl	Stearylamine	62–63	A	57	6.04	5.84

TABLE II

Bis(dialkylphosphorylthioureas)

$$(C_2H_5O)_2\overset{O}{\overset{\|}{P}}NHC\overset{S}{\overset{\|}{N}}H - X - NHC\overset{S}{\overset{\|}{N}}HP\overset{O}{\overset{\|}{(}}OC_2H_5)_2$$

X =	Prepared from:	M.p., °C	Method of prep.	Yield, %	Analyses, N Calc.	Found
1,2-Ethylene	Ethylenediamine	149–150	A	50	C, 32.00 H, 6.22	C, 32.50 H, 6.47
p-Phenylene	*p*-Phenylenediamine	144–145 decomp.	C	85	11.25	11.42
o-Phenylene	*o*-Phenylenediamine	137–138 decomp.	C	55	11.25	11.18
4-Methyl-1,3-phenylene	4-Methyl-1,3-phenylenediamine	145–146	C	62	10.92	10.79
4,4′-Diphenylmethane	4,4′-Diaminodiphenylmethane	142–143	C	50	9.50	9.82
1,5-Naphthalene	1,5-Diaminonaphthalene	163–166 decomp.	C	48	10.22	10.15

EXPERIMENTAL

Diethyl Phosphoroisothiocyanatidate (II, R = Ethyl)

To a stirred and cooled solution of diethyl phosphorochloridate (150 g) in dry benzene (100 ml) was added ammonium thiocyanate (75 g), and the reaction mixture was stirred at 15–20° for 5 hours. Then benzene (300 ml) was added and the reaction mixture quickly washed with cold dilute sodium chloride solution until the washings were no more acid to litmus. The benzene solution was dried over sodium sulphate, the solvent removed under slightly reduced pressure, and the colorless residual liquid distilled applying only steam heat, b.p. (1 mm) = 88°, $n_D^{23} = 1.4772$. The yield of the colorless liquid was 155 g or 91%. The pure product also distilled at 112–113° (12 mm). In a cool dark place it could be kept for several months.

Di-n-butyl Phosphoroisothiocyanatidate (II, R = Butyl)

This was prepared from di-*n*-butyl phosphorochloridate (I, R = butyl) and ammonium thiocyanate in 65% yield according to the procedure described above. The colorless liquid boiled at 104–105° (0.1 mm) and the pure product distilled at 153–155° (12 mm) with only slight decomposition, $n_D^{20} = 1.4728$. An attempt to analyze this compound for carbon and hydrogen gave erratic results as is usually the experience with phosphorus compounds.

n-Butyl Thiocyanate (III, R = Butyl)

(*a*) *From di-n-butyl phosphorochloridate.*—A reaction mixture of di-*n*-butyl phosphorochloridate (50 g), ammonium thiocyanate (30 g), and dry benzene (50 ml) was stirred and heated under reflux for 5 hours. The cooled reaction mixture was washed with water, the solvent removed, and the residue distilled, b.p. (12 mm) = 64°, $n_D^{20} = 1.4640$. The yield was 26 g. On redistillation this liquid boiled at 184–185°. These properties are identical with those of butyl thiocyanate reported in the literature (8). Anal. Calc. for C_5H_9NS: C, 52.17; H, 7.82. Found: C, 52.15; H, 7.95. The colorless odoriferous liquid contained nitrogen and sulphur but no phosphorus or chlorine, and when boiled with aqueous alcoholic potassium hydroxide yielded dibutyl disulphide and sodium cyanide.

(*b*) *Directly from di-n-butyl phosphoroisothiocyanatidate.*—A reaction mixture of di-*n*-butyl phosphoroisothiocyanatidate (14 g), dry benzene (50 ml), and ammonium thiocyanate (1 g) was heated under reflux for 3 hours, cooled, and filtered. The solvent was removed from the filtrate and the residue distilled. There was obtained two fractions, one consisting of butyl thiocyanate (5 g) and the other unchanged starting material (4 g).

Ethyl Thiocyanate

This compound boiling at 140–143° with $n_D^{25} = 1.4615$ was obtained in 85% yield as a colorless odoriferous liquid from diethyl phosphorochloridate in a manner similar to that described in section (*a*) for butyl thiocyanate and also directly from diethyl phosphoroisothiocyanatidate. The properties of this compound were identical with those of ethyl thiocyanate reported in the literature (9).

Diethyl Hydrogenphosphate (VI, R = Ethyl)

A mixture of diethyl phosphoroisothiocyanatidate (II, R = ethyl) (70 g) and water (350 ml) was heated on the steam bath with occasional swirling for 15 minutes. The aqueous thiocyanic acid was removed under slightly reduced pressure from the resulting clear solution and the residual liquid distilled, b.p. (0.2 mm) = 130–135°, $n_D^{24} = 1.4162$. These properties agree with those of diethyl hydrogenphosphate reported in the literature (10). The yield was 49 g or 89%.

A small portion of the diethyl hydrogenphosphate in alcohol solution when treated with a strong aqueous solution of lead acetate yielded white needles of the lead salt of VI (R = ethyl) which melted at 183–184°; lit. m.p. 180° (7).

Preparation of the N^1-Dialkylphosphoryl-N^2-substituted Thioureas

Method A.—Diethyl phosphoroisothiocyanatidate (II) (1 mole) was added dropwise with cooling and stirring to the amine (1 mole), the temperature being kept below 50°. The reaction product which solidified was crystallized from methanol or aqueous methanol.

Method B.—This method was essentially the same as method A except that dry benzene was used as solvent for the amine and the product usually crystallized from the benzene solution on cooling.

Method C.—This method was essentially the same as method A except that acetone was employed as solvent for the amine and the product usually crystallized from the acetone solution on cooling.

N^1-Di-n-butylphosphoryl-N^2-p-chlorophenylthiourea (VII, R = *n*-Butyl, R′ = *p*-Chlorophenyl)

This was prepared in 58% yield from di-*n*-butyl phosphoroisothiocyanatidate and *p*-chloroaniline by method B. It melted at 65–66° after crystallization from aqueous methanol. Anal. Calc. for $C_{15}H_{24}N_2O_3ClPS$: N, 7.39. Found: N, 6.94, 6.85.

$N^1,N^{1\prime}$-(1,4-Phenylene)-$N^2,N^{2\prime}$-bis(di-n-butylphosphorylthiourea)

This was prepared in 72% yield by method C from *p*-phenylenediamine and di-*n*-butyl phosphoroisothiocyanatidate. The white solid melted at 149–150°. Anal. Calc. for $C_{24}H_{44}N_4O_6P_2S_2$: N, 9.18. Found: N, 8.85.

N^1-Diethylphosphoryl-N^2,N^2-diethylthiourea

This was prepared in 65% yield by method A from diethyl phosphoroisothiocyanatidate and diethylamine. The white product when crystallized by dissolving in acetone and cooling in dry ice melted at 70–72°. When exposed to moist air it liquefied to an acidic product. Anal. Calc. for $C_9H_{21}N_2O_3PS$: N, 10.45. Found: N, 10.19, 10.56.

REFERENCES

1. American Chemical Society Official Reports. Chem. Eng. News, **30**, 4515 (1952).
2. Saunders, B. C., Stacey, G. J., Wild, F., and Wilding, I. G. E. J. Chem. Soc. 699 (1948).
3. Cook, H. G., Ilett, J. D., Saunders, B. C., Stacey, G. J., Watson, H. G., Wilding, I. G. E., and Woodcock, S. J. J. Chem. Soc. 2921 (1949).
4. McIvor, R. A., McCarthy, G. D., and Grant, G. A. Can. J. Chem. **34**, 1819 (1956).
5. Levchenko, E. S. and Zhmurova, I. N. Ukrain. Khim. Zhur. **22**, 623 (1956); Chem. Abstr. **51**, 5719 (1957).
6. Michalski, J. and Wieczorkowski, J. Roczniki Chem. **31**, 585 (1957); Chem. Abstr. **52**, 5283 (1958).
7. Kosolapoff, G. M. Organophosphorus compounds. John Wiley & Sons, Inc., New York. 1950. p. 242.
8. Kaufman, R. J. and Adams, R. J. Am. Chem. Soc. **45**, 1744 (1923).
9. Hawthorne, J. J. Chem. Soc. **89**, 563 (1906).
10. Toy, A. D. P. J. Am. Chem. Soc. **70**, 3882 (1948).

REACTIONS OF OXYGEN ACTIVATED BY ELECTRICAL DISCHARGE WITH BUTENE-1

J. M. S. Jarvie and R. J. Cvetanović

ABSTRACT

Reactions of oxygen activated by electrical discharge with butene-1 have been studied in a "spherical diffusion" reaction zone. When small concentrations of oxygen are passed through the discharge tube in helium as the carrier gas, and the concentration of butene-1 in the reaction zone is sufficiently high, the observed products are entirely explainable by an interaction of the ground-state oxygen atoms with butene-1. With large deviations from these conditions considerable complexities arise, and under some conditions α-butylene ozonide and its decomposition products become important and the products are then explainable without any significant participation of oxygen atoms in the process.

INTRODUCTION

The number of methods available for the production of oxygen atoms in the laboratory is limited. One of the earliest methods employed for the production of oxygen atoms was the gaseous electrical discharge in oxygen molecules (1). The other methods frequently used are the mercury-photosensitized decomposition of nitrous oxide and the photodecomposition of nitrogen dioxide, and both these methods have been used extensively in this laboratory to study reactions of oxygen atoms. With the use of the nitrous oxide technique the main features of the reactions of oxygen atoms with olefins have now been established (2). In the present work one of the olefin reactions with oxygen atoms produced by electrical discharge was studied in order to compare this method for producing oxygen atoms with the nitrous oxide and the nitrogen dioxide methods. The relatively simple reaction of oxygen atoms with butene-1 was chosen for this purpose. An experimental arrangement incorporating the usual features of a "diffusion flame technique" (3, 4) was adopted in order to minimize any tendency for the occurrence of surface reactions, and to find out at the same time whether the application of the Garvin–Kistiakowsky "Temperature Pattern Method" (5) for the determination of rate constants is suitable for this reaction.

In the reaction of oxygen atoms with butene-1, two principal products are formed, α-butylene oxide and *n*-butyraldehyde, together with smaller amounts of methyl ethyl ketone and traces of some other compounds (2). The addition products possess excess energy when formed because of the high heats of reaction and decompose if not deactivated collisionally. This fragmentation is essentially suppressed at a pressure of about 10 mm (6) and the course of the reaction is then relatively simple. In the present work, on the other hand, considerable complexities are observed, especially under certain conditions. At the same time the electrical discharge technique is widely used to generate oxygen atoms and study their reactions. It is therefore essential to emphasize its potentially complex character. The latter is due to several factors. The technique is restricted to relatively quite low pressures, and as a result the concentration of the primary reactant is also low so that secondary attacks by oxygen atoms on the products may and indeed very frequently do take place. Also, when "hot" products are formed in the primary step, as is the case in the addition of oxygen atoms to olefins, they will tend to decompose

[1]*Manuscript received September 29, 1958.*
Contribution from the Division of Applied Chemistry, National Research Council, Ottawa, Canada.
Issued as N.R.C. No. 5035.
[2]*National Research Council Postdoctorate Fellow 1956–57. Present address: Jackson Laboratory, Organic Chemicals Department, E. I. du Pont de Nemours and Company, Wilmington, Delaware, U.S.A.*

into free radicals at the low pressures, leading thus to further secondary reactions. An additional potential disadvantage of the low pressures is the difficulty of establishing whether any surface reactions occur. (In the present work any surface reactions in the reaction zone have been disregarded: it is likely that at least under some experimental conditions employed they are unimportant.) Another factor contributing to the observed complexities is the frequent presence, in addition to oxygen atoms, of other reactive or potentially reactive species, including here excess molecular oxygen when present. The object of the present work is to illustrate on the example of a reaction, the mechanism of which has been previously established by more convenient methods, some of the complexities which may be encountered in the application of the electrical discharge technique. The discussion of the obtained results is consequently more extensive than would be otherwise justifiable in view of its largely qualitative character.

EXPERIMENTAL

Apparatus

The apparatus used was an all-glass flow system. The gas flows were controlled by capillaries and needle valves (Edwards and Co.) with a constant pressure head. The pressure in the reactor was varied by means of internal capillaries of various dimensions. Helium and oxygen were passed through a liquid nitrogen trap before the discharge to remove any grease or mercury vapor in the gases, as these gave inconsistent results due to coating of the surface of the discharge tube (a quartz tube, 10 mm i.d.). An electrodeless discharge was used at microwave frequencies, supplied from a Raytheon Diatherm unit with the use of a 90% power output. The two probes were of copper wire, each a $\frac{1}{4}$ wavelength. These were placed at a distance of 22 cm from the nozzle through which the gases were discharged into a wide pyrex tube in which the reaction was carried out. The nozzle projected some distance into the reaction zone and had an orifice 0.5 mm in diameter. Butene-1 was introduced directly into the wide tube, but at a point below the nozzle to assure uniform distribution before the reaction zone was reached.

The products were frozen out in two liquid nitrogen traps and were transferred to a LeRoy still (7) at $-120°$ C and fractionated to obtain the products free of unreacted butene-1 and of any products of equal or greater volatility.

Attempts were made to measure the concentration of oxygen atoms at the nozzle by measuring the heat of recombination on a hot platinum wire, on a hot platinum wire coated with either silver or cobalt, and a silver-plated glass tip probe. It was found that all these methods gave inconsistent results so the direct measurement of the oxygen atom concentration was abandoned.

Materials

Research grade butene-1 (Phillips Petroleum Co.) was transferred to a storage volume at liquid nitrogen temperature and degassed at dry ice temperature. This was repeated several times until a pressure of 10^{-5} mm Hg was obtained.

Oxygen (People's Gas Co., Ottawa) was used without further purification. In some of the experiments extra-dry and pure oxygen (Matheson Co.) was used and it was found that the results obtained were identical with those obtained with the ordinary cylinder oxygen.

Helium (Air Reduction Co.) was passed through a liquid nitrogen trap to remove any water and was used without any further purification.

Analysis of Products

The products of the reaction after the removal of the unreacted butene-1 and of any products of equal or greater volatility in the low-temperature fractionation still

were passed through a gas–liquid chromotographic (GLC) column. The GLC apparatus used was modelled on that used by Callear and Cvetanović (8). The column consisted of 7.5-ft glass tubing (4 mm i.d.) packed with glass spheres passing 270 mesh with dinonyl phthalate as the liquid phase (4 g of dinonyl phthalate per 100 g of glass spheres). The column was maintained at room temperature. For some analyses a high resolution 50-ft column of $\frac{1}{4}$-in. copper tubing was used. It contained, as the stationary phase, 40 g of tricresyl phosphate per 100 g of firebrick (30–60 mesh). The products eluted from the column could be collected at liquid nitrogen temperature, and thus analyzed also by infrared and mass spectrometer.

The products of the reaction identified by these means were propionaldehyde, acetaldehyde, methyl alcohol, ethyl alcohol, *n*-butyraldehyde, α-butylene oxide, methyl ethyl ketone, and α-butylene ozonide. A sample of α-butylene ozonide was kindly prepared by Dr. T. Vrbaški using the method of Harries (9, 10).

RESULTS

The reaction of butene-1 with oxygen atoms produced by microwave discharge was found to be more complex than the corresponding reaction with oxygen atoms formed by mercury-photosensitized decomposition of nitrous oxide (2) or by photolysis of nitrogen dioxide (6). In the last two reactions *n*-butyraldehyde, α-butylene oxide, and small amounts of methyl ethyl ketone, acetaldehyde, and propionaldehyde are formed. In the present case, in addition to these compounds, ethanol and methanol and under certain conditions α-butylene ozonide and formaldehyde are also produced, and propionaldehyde is frequently formed in large amounts.

In order to obtain some insight into the mechanism of formation of these products, the pressure of butene-1, oxygen, and helium and the total pressure were varied.

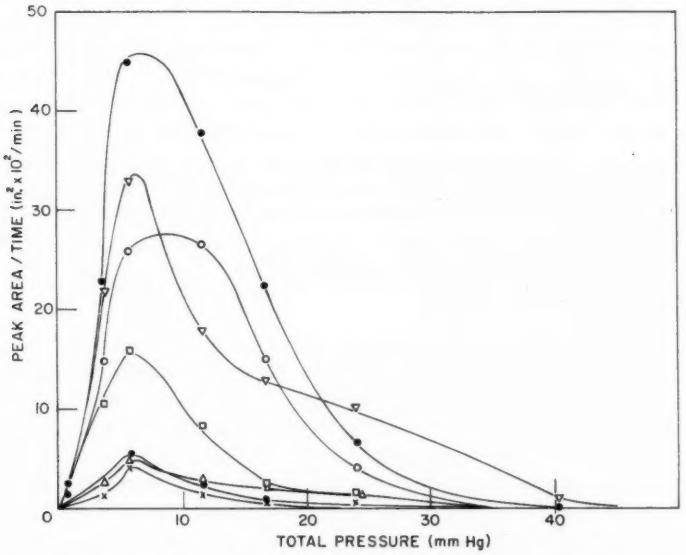

FIG. 1. Variation in the amounts of products formed per unit time with total pressure at low butene-1 flow. Oxygen flow 2.54 ml/min, helium flow 54.0 ml/min, butene-1 flow 0.75 ml/min: × methanol, △ methyl ethyl ketone, ⊕ acetaldehyde, □ ethanol, ○ *n*-butyraldehyde, ▽ propionaldehyde, ● α-butylene oxide.

Variation of Total Pressure

The total pressure was varied from 0 to 40 mm for both high and low butene-1 flows, using constant flows of the reactants in each case. In Fig. 1, the results obtained for the amounts of the products formed (measured as peak area per unit time from the GLC data) as a function of total pressure are shown for low butene-1 flow (0.75 ml/min). The main products are α–butylene oxide, propionaldehyde, ethanol, and *n*-butyraldehyde with smaller amounts of methyl ethyl ketone, acetaldehyde, and methanol. All the products show maxima at around 6.5 mm. It is understandable that there would be, at low pressure, a decrease in the amounts of the products formed due to recombination of the oxygen atoms on the walls of the discharge tube. However, at high pressure there was a gradual decrease in the amounts of products until at 40 mm there were essentially no products detectable on GLC. It was noted that during this gradual decrease the light intensity of the discharge appeared to decrease also. The light intensity of the discharge was therefore measured as a function of the pressure and it was found that the photocell readings showed a similar decrease to that observed above. Since the light intensity probably parallels in an approximate and qualitative manner the amount of dissociation of the molecules into atoms, it would appear that as the pressure is increased the energy available for dissociation of the molecules is reduced.

The experiments with high butene-1 flow (40 ml/min) showed the same general trends as found for low butene-1 flow and the maxima in the amounts of products were again at around 6 mm (Fig. 2). There was, however, an important difference: the amount of propanal formed remained in this case quite small, while it is one of the major products at low butene-1 flow.

Variation of Oxygen: Helium Ratio

The ratio of oxygen to helium was varied at constant pressure (3.5 mm) and constant butene-1 flow (0.75 ml/min). A plot of percentage oxygen against peak area of the products per unit time is shown in Fig. 3. The results obtained showed the same trends as before, with α-butylene oxide, propionaldehyde, *n*-butyraldehyde, and ethanol as the main products and smaller amounts of acetaldehyde, methyl ethyl ketone, and methanol. Up to about 7% oxygen there was an increase in the peak areas of each of the products, but as the percentage oxygen was still further increased (and at the same time the percentage of helium was correspondingly decreased) there was a general decrease in the amounts of the products. Since this is observed with all the products, it would appear that this effect is concerned with the initial formation of the oxygen atoms in the discharge. A possible explanation of this effect is that the efficiency of oxygen for the capture of electrons is less than that of helium, so that at high oxygen percentages the concentration of oxygen atoms is reduced.

Variation of Oxygen in the Absence of Helium

The flow of oxygen was varied from 0.80 ml/min to 25.6 ml/min in the absence of helium at a constant butene-1 flow (0.75 ml/min). The total pressure for this range of oxygen flows varied from 0.19 mm to 2.60 mm. Since the butene-1 flow was small compared to the oxygen flow, the total pressure was essentially the partial pressure of oxygen. Under these conditions it was found that the results were not reproducible. However, it was possible to note certain trends in the results. As the pressure of oxygen increased, there was an increase in the amounts of α-butylene oxide, propionaldehyde, and a small increase in the amount of acetaldehyde and methyl ethyl ketone, while amounts of ethanol and methanol decreased. Under these conditions, however, *n*-butyraldehyde was not found in the products.

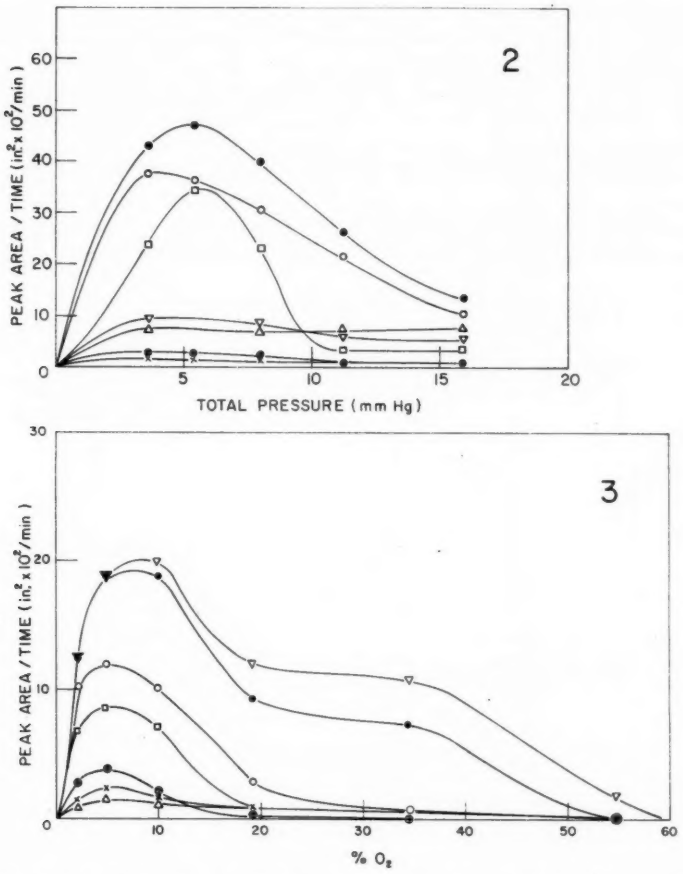

FIG. 2. Variation in the amounts of products formed per unit time with total pressure at high butene-1 flow. Oxygen flow 2.54 ml/min, helium flow 54.0 ml/min, butene-1 flow 40.1 ml/min: × methanol, △ methyl ethyl ketone, ⊗ acetaldehyde, □ ethanol, ○ *n*-butyraldehyde, ▽ propionaldehyde, ● α-butylene oxide.

FIG. 3. Plot of per cent oxygen in discharge gas against the amount of product formed per unit time. Total pressure 3.4 mm, butene flow 0.75 ml/min: × methanol, △ methyl ethyl ketone, ⊕ acetaldehyde, □ ethanol, ○ *n*-butyraldehyde, ▽ propionaldehyde, ● α-butylene oxide.

In all these experiments it was noted that a large diffuse GLC peak appeared at an elution time of about 200 minutes. This peak was collected and analyzed by infrared and mass spectra. It was found to be identical with a synthetic sample of α-butylene ozonide. Some observations on the stability and the manner of decomposition of a synthetic sample of α-butylene ozonide suggested that this compound was probably the main initial product in these experiments. It was probably formed directly from ozone and butene-1 while α-butylene oxide, acetaldehyde, and methyl ethyl ketone were formed in the course of the same reaction or together with propionaldehyde in the subsequent decomposition of the α-butylene ozonide. The absence of *n*-butyraldehyde suggested that a reaction of oxygen atoms with butene-1 was unimportant under these conditions.

Variation of Oxygen in the Presence of Helium

The partial pressure of oxygen was varied at constant total pressure (3.5 mm), constant helium flow (54.0 ml/min), and constant butene-1 flow (0.75 ml/min). The results obtained have been plotted in Fig. 4. Below 0.05 mm it was not possible to observe any products, perhaps because the small amounts of oxygen atoms formed recombined before they reached the nozzle. Above this pressure there was a steep increase in the amount of products to a maximum, and at higher partial pressures of oxygen there was a gradual decline in the amount of products formed. As was found above, propionaldehyde, α-butylene oxide, *n*-butyraldehyde, and ethanol were the main products with smaller amounts of acetaldehyde, methanol, and methyl ethyl ketone.

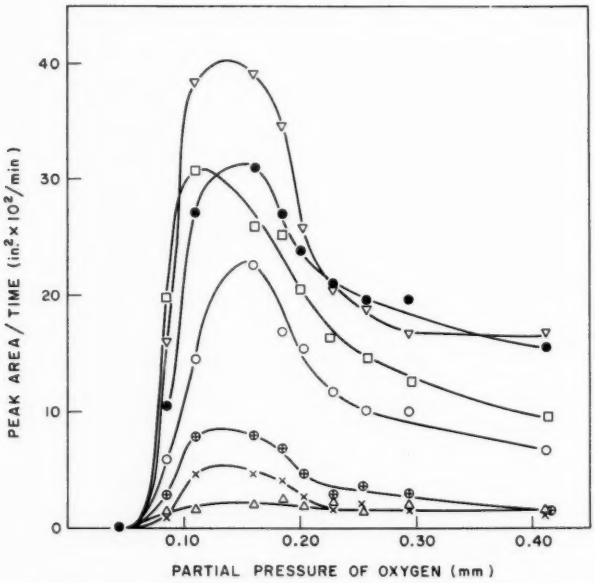

FIG. 4. Plot of oxygen pressure against the amount of products formed per unit time. Butene-1 flow 0.75 ml/min, helium flow 54.0 ml/min, total pressure 3.5 mm: × methanol, △ methyl ethyl ketone, ⊕ acetaldehyde, □ ethanol, ○ *n*-butyraldehyde, ▽ propionaldehyde, ● α-butylene oxide.

Variation of Butene-1

The flow rate of butene-1 was varied from 0.56 ml/min to 40 ml/min at constant flows of helium (54.0 ml/min) and oxygen (2.54 ml/min) and constant pressure (3.5 mm). A plot of the partial pressure of butene-1 against the GLC peak area per unit time is shown in Fig. 5. It is apparent from this graph that the compounds formed fall into two classes. The first class of compounds (α-butylene oxide, *n*-butyraldehyde, ethanol, and methyl ethyl ketone) show a steady rise in the amount formed at lower partial pressures of butene-1 and finally reach a constant value, while with the second class (propionaldehyde, acetaldehyde, and methanol) after an initial sharp increase in the amounts formed there is a gradual decrease to constant values. In order to determine whether these effects were due to a change in the discharge intensity, photocell readings were taken of the light intensities of the discharge and it was found that these remained

constant. Thus, under these conditions the change in the amount of product formed is directly connected with the partial pressure of butene-1. At very low butene-1 flow (0.56 ml/min) a relatively large amount of water was formed, probably due to secondary attack on the compounds initially formed by excess oxygen atoms. This effect was not noted at higher concentrations of butene-1.

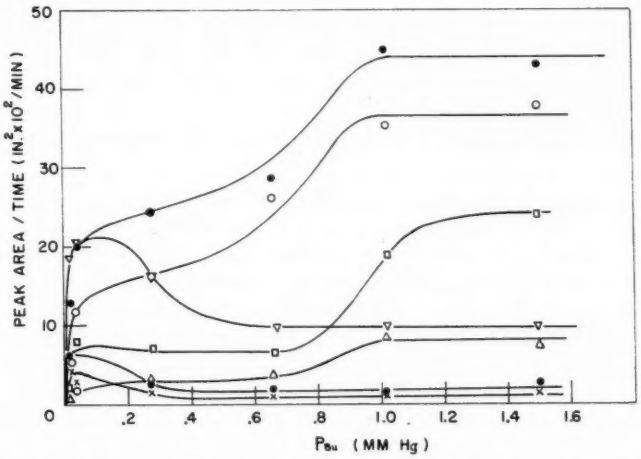

FIG. 5. Plot of butene-1 pressure against the amount of products formed per unit time. Total pressure 3.5 mm, oxygen flow 2.54 ml/min, helium flow 54 ml/min: × methanol, △ methyl ethyl ketone, ⊗ acetaldehyde, □ ethanol, ○ *n*-butyraldehyde, ▽ propionaldehyde, ● α-butylene oxide.

DISCUSSION

Since discharge is passed through oxygen and helium some distance from the nozzle, it is convenient to treat the reactions occurring in the discharge tube separately from those occurring at the nozzle, i.e. in the reaction zone where butene-1 is present as well.

The proposed reactions which are likely to occur in the discharge tube are the following:

$$\mathrm{He} + e \rightarrow \mathrm{He}^* \qquad [\phi_1]$$

$$\mathrm{O_2} + e \rightarrow 2\mathrm{O} \qquad [\phi_2]$$

$$\mathrm{O_2} + e \rightarrow \mathrm{O_2}^* \qquad [\phi_3]$$

$$\mathrm{He}^* + \mathrm{O_2} \rightarrow 2\mathrm{O} + \mathrm{He} \qquad [\mathrm{I}]$$

$$\mathrm{He}^* + \mathrm{O_2} \rightarrow \mathrm{O_2}^* + \mathrm{He} \qquad [\mathrm{II}]$$

$$\mathrm{He}^* + \mathrm{He} \rightarrow 2\mathrm{He} \qquad [\mathrm{III}a]$$

$$\mathrm{O_2}^* + \mathrm{He} \rightarrow \mathrm{O_2} + \mathrm{He} \qquad [\mathrm{III}b]$$

$$\mathrm{O} + \mathrm{O} + \mathrm{W} \rightarrow \mathrm{O_2} + \mathrm{W} \qquad [\mathrm{IV}]$$

$$\mathrm{O} + \mathrm{O} + \mathrm{M} \rightarrow \mathrm{O_2}^* + \mathrm{M} \qquad [\mathrm{V}]$$

$$\mathrm{O} + \mathrm{O_2}^* + \mathrm{M} \rightarrow \mathrm{O_3} + \mathrm{M} \qquad [\mathrm{VI}]$$

$$\mathrm{O} + \mathrm{O_2} + \mathrm{M} \rightarrow \mathrm{O_3} + \mathrm{M} \qquad [\mathrm{VII}]$$

$$\mathrm{O} + \mathrm{O_3} \rightarrow 2\mathrm{O_2}. \qquad [\mathrm{VIII}]$$

Reaction [ϕ_1] is probably the initiation reaction in the discharge since the efficiency for electron capture is greater in the case of helium than oxygen. When no helium is

present, reactions [ϕ_2] and [ϕ_3] take place giving oxygen atoms and excited oxygen molecules. Reactions [I] and [II] form oxygen atoms and excited oxygen molecules by transfer of energy from the excited helium. The quenching of the excited helium and excited oxygen are shown in reactions [III*a*] and [III*b*]. Reactions [IV] and [V] recombine oxygen molecules by third-body collision with the wall and other molecules, respectively. To account for the formation of ozone, reactions [VI] and [VII] are proposed. Reaction [VIII] re-forms oxygen molecules by the attack of oxygen atoms on ozone.

Of the products formed in the discharge tube the only ones which may reach the nozzle and eventually react with butene-1 in the reaction zone are: oxygen atoms, ozone, and excited oxygen molecules.

The general mechanism of reaction of oxygen atoms with butene-1 is as follows (2):

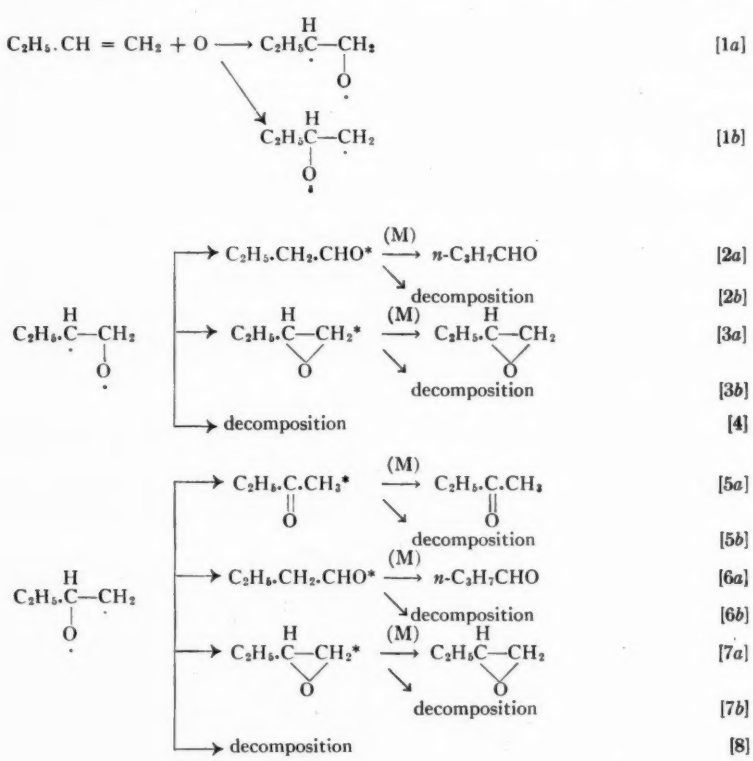

where [1*a*], addition to the less substituted carbon atom of the double bond, largely predominates over [1*b*] so that considerably more n-C_3H_7CHO is formed than $C_2H_5.CO.CH_3$. There is reason to believe that pressure-independent decomposition processes, reactions [4] and [8], are not very important in this reaction (2). At pressures higher than about 10 to 30 mm the collisional deactivations in [2*a*], [3*a*], [5*a*], [6*a*], and [7*a*] are essentially complete, so that the main products are α-butene oxide, n-butyraldehyde, and a smaller amount of methyl ethyl ketone. In addition to these, even at the higher pressures, very small amounts of acetaldehyde and propionaldehyde are also

formed (2, 6) and the mechanism of their formation is not yet known, although they may be due then to some pressure-independent fragmentation. At lower pressures the pressure-independent fragmentation processes begin to be of importance, especially so below about 10 mm. This leads to an increase in the amounts of acetaldehyde and propionaldehyde and to a decrease in the addition products (α-butene oxide, n-butyraldehyde, and methyl ethyl ketone) (6).

Disregarding for the moment methanol and ethanol, which are observed in the present work in addition to the above compounds, it is evident that under conditions of the experiments plotted in Fig. 5 (total pressure 3.5 mm, helium to oxygen ratio approximately 20) and when the partial pressure of butene-1 is sufficiently high the products formed are within the limits of experimental accuracy, quantitatively, such as would be expected to be formed in the reaction of the ground state oxygen atoms with butene-1 at the actual total pressure (3.5 mm). At such a low total pressure the pressure-dependent fragmentation is quite important and appreciable amounts of free C_2H_5 radicals and smaller amounts of free CH_3 radicals could be expected to be produced. The formation of ethanol and methanol is then explained by the interaction of these free radicals with the molecular oxygen present, as is frequently observed. Thus, in the reaction of butene-2 with oxygen atoms from the mercury-photosensitized decomposition of N_2O, the relatively large amounts of free CH_3 radicals form large amounts of methanol when some molecular oxygen is added (2). The same reaction with oxygen atoms from photolysis of NO_2 gives large amounts of CH_3NO_3 and CH_3NO_2 instead (11), because of the presence of excess NO_2. In the reaction of butene-1 with oxygen atoms from NO_2 photolysis some $C_2H_5NO_3$ has indeed been identified, suggesting the presence of free C_2H_5 radicals (the elution time of $C_2H_5NO_2$ is considerably larger than that of $C_2H_5NO_3$ and $C_2H_5NO_2$ would, therefore, not be observed in small amounts at the GLC column temperature used) (6). Similarly in the isobutene reaction very small amounts of CH_3NO_3 and CH_3NO_2 are found, suggesting formation of some free CH_3 radicals, as would be expected in this case. All this supports the proposed explanation for the formation of ethanol and methanol in the present work. The absence of these two compounds in the same reaction with oxygen atoms formed from N_2O, even when molecular oxygen is present (2), is explained by the much higher total pressures used and the consequent suppression of the pressure dependent fragmentation. In the NO_2 work, the excess NO_2 acted as free radical scavenger as already indicated, so that even at low pressures no alcohols were detected.

As the butene-1 pressure is decreased in Fig. 5, ethanol and the direct oxygen atom addition products, α-butene oxide, n-butyraldehyde, and methyl ethyl ketone, begin to decrease while propionaldehyde, acetaldehyde, and methanol increase. This suggests that under conditions of these experiments butene-1 pressure has to be relatively quite high before secondary processes are suppressed and that propionaldehyde, acetaldehyde, and methanol result at least to a large extent from secondary processes, especially so propionaldehyde. The trend in ethanol is consistent with the mechanism of its formation suggested in the preceding paragraph. It shows at the same time that the effect of decreasing butene pressure is not due (at least not predominantly so) to a decreasing efficiency of the gaseous mixture for collisional deactivation as butene concentration is lowered, since the trend in ethanol would be expected then to be the same as that of propionaldehyde, acetaldehyde, and methanol.

The foregoing explanations are supported by the difference in the composition of the

products at various pressures for a low and a high butene flow as shown in Figs. 1 and 2, respectively. In this case again, propionaldehyde, acetaldehyde, and methanol are much smaller, especially so propionaldehyde, at the high butene flow.

Relatively high butene-1 pressures necessary to suppress secondary processes even when the partial pressure of oxygen is small, as in Fig. 5, would seem to preclude quantitative use of the Garvin–Kistiakowsky's Temperature Pattern Method for this reaction, at least under conditions of the present experiments. At small butene-1 pressures, such as would be anticipated to be necessary in order not to confine the reaction to a very small region around the nozzle, considerable complexities arise. The results of the experiments at such low partial pressures of butene are shown in Figs. 1, 3, and 4. The observed complexities are difficult to explain in detail, but are likely to be of general occurrence under certain experimental conditions and may seriously affect both quantitative and qualitative studies of oxygen atom reactions. For this reason a discussion of these results may be in order.

The reasons for the general trend in the amounts of products formed with varying pressure, as shown in Fig. 1, have already been discussed. The gaseous mixture in these experiments consisted mainly of helium which is probably not too efficient as a collisional deactivator and there are no drastic changes in the character of the products formed. At higher pressure the relative increase in propionaldehyde is conspicuous. This is probably due to the simultaneous increase in the partial pressure of oxygen (the composition of the gases was kept constant while the pressure was varied). The effect of the increasing concentration of oxygen is shown better in Figs. 3 and 4. Here again the reasons for the general decline in the amounts of products formed as oxygen concentration is increased have already been discussed. Attention should now be focussed on the variation in the relative amounts of the products, and it is evident that at higher percentages of oxygen in the mixture propionaldehyde becomes relatively more important while *n*-butanal and ethanol tend to be suppressed. Roughly similar trend was observed when oxygen pressure was varied in the absence of helium. As the oxygen pressure was increased from 0.2 to 2.6 mm the amounts of α-butylene oxide and propionaldehyde increased, ethanol decreased, and *n*-butyraldehyde was not found in the products under these conditions. In these last experiments, however, the reproducibility was poor and also α-butylene ozonide was identified as an important product. This compound is unstable and the lack of reproducibility was almost certainly largely due to the varying extent of its decomposition.

The formation of α-butylene ozonide suggests an important participation of ozone in the process under these conditions. When ozone reacts at room temperature with butene-1 in the gas phase (in the presence of excess oxygen) propionaldehyde and formaldehyde appear to be the main products (12). The largely increased formation of propionaldehyde at low butene-1 and larger oxygen concentrations is probably due to this reaction. In agreement with this, under these conditions large amounts of polymerized formaldehyde were found in the liquid nitrogen trap for the collection of the products, from where samples of the polymer were directly withdrawn for qualitative identification.

The manner in which ozone is formed is uncertain. There are two general possibilities: it may be formed in and after the discharge but predominantly before the gases reach the nozzle, or it may result from the reactions which take place after the stream of gas containing oxygen atoms meets butene-1 in the reaction zone. The first possibility depends on the efficiency of reaction [VII] which competes with [VIII] and with the reverse

of [VII]. Depending on the pressure of the gas and its efficiency as the "third body", a certain steady-state concentration of ozone should establish itself. It is not possible at present to predict with certainty whether this concentration should in a particular case be negligible compared with the concentration of oxygen atoms. The problem has been recently discussed by Herron and Schiff (13), who could not detect ozone mass spectrometrically in oxygen subjected to electrical discharge, although calculations based on literature values of rate constants of the above reactions (but for a different "third body") suggested detectable steady-state concentrations of ozone. Such calculated steady-state concentrations of ozone would be of the correct order of magnitude to be of importance under conditions of some of the present experiments.

The established formation of α-butylene ozonide cannot be regarded as a proof that ozone results directly from the discharge, since it may be, perhaps, equally well formed in the reaction zone. It is well known that under certain conditions in the atmosphere (and these conditions were simulated in the laboratory) ozone is formed in a chain reaction following an initial interaction of oxygen atoms with hydrocarbons (14). The detailed mechanism of this chain process is not known, although it appears reasonably certain that it involves initially an interaction of free radicals with molecular oxygen to form a hydroperoxy free radical. The latter, perhaps, reacts with another molecule of oxygen to give ozone. In agreement with these views it was possible to initiate ozone formation by generating free radicals in an oxygen atmosphere (14). Similar conditions can be readily envisaged in some of the experiments in the present work. Hydroperoxy radicals appear to be able also to react in some instances directly with olefins to form epoxides (15). It is evident then that explanations can be suggested for the results of some experiments in the present work, in particular to explain the formation of the ozonide, propanal, and the epoxide and the significant absence of *n*-butanal, as outlined before, without assuming any significant participation of oxygen atoms in the process (except, perhaps, in the initiation stage). Further substantial progress has to be made in this general field before a more reliable and quantitative discussion can be undertaken.

Substantial quantities of excited molecules of oxygen have been detected (13) mass spectrometrically in oxygen subjected to electrical discharge, the excited state being probably the $^1\Delta_g$ electronic state. What effect, if any, such molecules would have on butene-1 is not known. The increased formation of propanal at lower butene-1 concentrations, as shown in Fig. 5, cannot be due to excited molecules of oxygen since in this case no suppression with increasing butene-1 pressure would be expected. Under conditions of these experiments (low oxygen concentration in helium) no evidence was detected for any significant reaction of eventually present excited oxygen molecules with butene-1. Whether such molecules play a role in the experiments in which the concentration of oxygen in the discharge tube is large cannot be said at present because it is not possible to treat the results in a quantitative manner.

In conclusion, it ought to be stressed that the present work shows that under appropriate conditions oxygen atoms produced from molecular oxygen by electrical discharge lead to the same type of reaction as obtained with ground state oxygen atoms produced by mercury-photosensitized decomposition of nitrous oxide or by photolysis of nitrogen dioxide. The observed differences are understandable in view of the low over-all pressures and the excess molecular oxygen present. At the same time, considerable caution has to be exercised in the choice of the appropriate conditions when this technique is employed in order to avoid secondary processes which can sometimes completely mask the primary reactions of the oxygen atoms.

ACKNOWLEDGMENTS

The authors wish to acknowledge the assistance of Dr. A. W. Tickner for mass spectrometer analyses, Mr. J. Waterman for the building of the electronic equipment, and Dr. T. Vrbaški for the preparation of α-butylene ozonide.

REFERENCES

1. HARTECK, P. and KOPSCH, U. Z. physik. Chem. B, **12**, 327 (1937).
2. CVETANOVIĆ, R. J. J. Chem. Phys. **25**, 376 (1956); Can. J. Chem. **36**, 623 (1958).
3. HARTEL, H. V. and POLYANI, M. Z. physik. Chem. B, **11**, 97 (1930).
4. HELLER, W. Trans. Faraday Soc. **33**, 1556 (1937).
5. GARVIN, D. and KISTIAKOWSKY, G. B. J. Chem. Phys. **20**, 105 (1952).
6. SATO, S. and CVETANOVIĆ, R. J. Can. J. Chem. **36**, 970 (1958).
7. LE ROY, D. J. Can. J. Research, B, **28**, 492 (1950).
8. CALLEAR, A. B. and CVETANOVIĆ, R. J. Can. J. Chem. **33**, 1256 (1955).
9. HARRIES, C. and HAEFFNER, K. Ber. **41**, 3098 (1908).
10. HARRIES, C. and KOETSCHAU, R. Ber. **42**, 3305 (1909).
11. SATO, S. and CVETANOVIĆ, R. J. Can. J. Chem. **36**, 1668 (1958).
12. VRBAŠKI, T. and CVETANOVIĆ, R. J. Preliminary results.
13. HERRON, J. T. and SCHIFF, H. I. Can. J. Chem. **36**, 1159 (1958).
14. HAAGEN-SMIT, A. J. and FOX, M. M. Ind. Eng. Chem. **48**, 1484 (1956). HAAGEN-SMIT, A. J., BRADLEY, C. E., and FOX, M. M. Proceedings of the Second National Air Pollution Symposium. Pasadena, Calif. 1952. p. 54.
15. MAYO, F. R. J. Am. Chem. Soc. **80**, 2465 (1958).

PREPARATION OF 1,5-DIPHENYLNAPHTHALENE[1]

A. S. BAILEY[2]

ABSTRACT

The transformation of 1,5-dioxodecalin into 1,5-diphenylnaphthalene is described.

1-Phenylnaphthalene does not form solid complexes with the usual complexing agents (1) but has been found to form a complex with benzotrifuroxan (2). It was of interest, therefore, to prepare 1,5-diphenylnaphthalene and examine its complex-forming abilities. After this work was completed a synthesis of the hydrocarbon was reported in the literature (3).

It is stated (3) that treatment of 1,5-dioxodecalin (I, mixture of isomers) with phenylmagnesium bromide gives the glycol (III, m.p. 233–249°) in 33% yield. Under these conditions and using the pure *trans*-diketone (I) the only crystalline material isolated

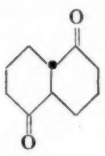

I

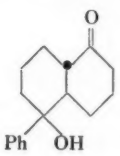

II

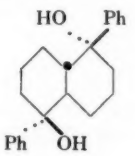

III

IV

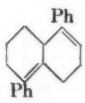

V

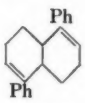

VI

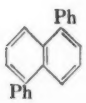

VII

R.CH=CH.CH=CH.R

VIII

was the monoadduct (II, yield 45%), none of the glycol being formed. However, treatment of the diketone (I) with lithium phenyl gave an excellent yield of 1,5-dihydroxy-1,5-diphenyldecahydronaphthalene (III, m.p. 275–277°). The material appeared to be homogeneous and it most probably has structure (III) with the two phenyl groups equatorial. This is the most stable isomer, having the larger groups equatorial, and its formation is likely to be favored by "steric approach control" (4).

Buchta and co-workers dehydrated the glycol (m.p. 233–249°) with potassium hydrogen sulphate, affording an olefin (m.p. 117–119°, 22% yield) to which structure (IV, R = Ph) was assigned without any supporting evidence (3). By dehydrating the pure glycol (III) with formic acid, an olefin (m.p. 179–182°) has now been obtained which may have structure (IV, R = Ph), (V), or (VI); the ultraviolet spectrum of the olefin

[1]*Manuscript received October 7, 1958.*
Contribution from the Dyson Perrins Laboratory, South Parks Road, Oxford, England.
[2]*Address during 1958–59, Royal Military College, Kingston, Ontario.*

showed λ_{max} 235 mμ (ϵ 19,300); λ_{inflex} 284 mμ (ϵ 6020); the absorption then steadily decreased (at 310 mμ, ϵ = 2400). Styrene has two absorption bands (λ_{max} 244 mμ, ϵ 12,000 and λ_{max} 282 mμ, ϵ 450) and the ultraviolet spectrum of 1-phenylcyclohexene contains only a single band (λ_{max} 247 mμ, ϵ 12,940) (5). Compounds having structures (V) or (VI) would be expected to show absorption of this type, the value of ϵ being smaller than 24,000 because of the non-coplanarity of the phenyl and reduced napththalene rings (6). This evidence suggests that the olefin obtained in this work is the conjugated diene (IV, R = Ph). The ultraviolet spectrum of (IV, R = Ph) indicates that the benzene and hexahydronaphthalene rings in this compound must be non-coplanar, since 1,4-diphenylbutadiene (VIII, R = Ph) has λ_{max} 328 mμ, ϵ 41,000 (5).

The corresponding diketone (IV, R = CO.CH_3) (7) has an absorption band at 295 mμ whose intensity (ϵ = 9020) is only one third of that of the open-chain analogue (VIII, R = $COCH_3$) which has λ_{max} 272 mμ (ϵ 31,000) and λ_{max} 279 mμ (ϵ 32,000) (8).

Dehydrogenation of the hexahydro compound using palladium–charcoal gave 1,5-diphenylnaphthalene (VII) in 80% yield as compared with the 20% obtained using sulphur (3). The ultraviolet spectra of 1-phenylnaphthalene and 1,5-diphenylnaphthalene are very similar, indicating non-coplanarity of the benzene and naphthalene rings.

EXPERIMENTAL

Ultraviolet spectra were determined in ethanol solution; infrared spectra measured in Nujol mulls unless otherwise indicated. All melting points are uncorrected.

1-Hydroxy-5-oxo-1-phenyldecahydronaphthalene (II)

To a solution of phenylmagnesium bromide (magnesium 3 g, bromobenzene 20 cc) in ether (50 cc) was added *trans*-1,5-dioxodecalin (5 g, m.p. 160°) (9) in benzene (100 cc) and the mixture refluxed and stirred for 5 hours. Next day water and saturated ammonium chloride solution were added, the aqueous layer extracted with benzene, the combined organic layers dried (magnesium sulphate), and the solvents removed. The semisolid residue was triturated with petroleum ether (10 cc, b.p. 60–80°) and then crystallized from benzene (25 cc) giving a solid (3.3 g, 45%) of m.p. 150–155°. Crystallization from benzene and then from methanol gave 1-hydroxy-5-oxo-1-phenyldecahydronaphthalene, colorless plates, m.p. 163–164° (mixed m.p. with starting material, 130–145°). Found: C, 78.4; H, 8.1%. Calc. for $C_{16}H_{20}O_2$: C, 78.7; H, 8.2%. Ultraviolet spectrum: λ_{max} 205 mμ (ϵ 9620); λ_{max} 251 mμ (ϵ 205); λ_{max} 257 mμ (ϵ 246); λ_{max} 263 mμ (ϵ 204); λ_{max} 266 mμ (ϵ 161). Infrared spectrum contained bands at 3390 cm^{-1} (OH); 1686 cm^{-1} (CO); 1600 cm^{-1} (ar. CC). The *2,4-dinitrophenylhydrazone* formed orange-colored needles (from acetic acid), m.p. 207–209°. Found: C, 62.2; H, 5.6; N, 13.4%. Calc. for $C_{22}H_{24}O_5N_4$: C, 62.3; H, 5.7; N, 13.2%. The *semicarbazone* crystallized from 2-methoxyethanol as colorless prisms, m.p. 253–255°. Found: C, 67.2; H, 7.9; N, 13.3%. Calc. for $C_{17}H_{23}N_3O_2$: C, 67.7; H, 7.7; N, 13.9%. A solution of the carbinol (1 g) in formic acid (10 cc) was refluxed for 30 minutes, the solution cooled, diluted with water, and the mixture extracted with ether. The ethereal extracts were washed with sodium carbonate solution, dried (magnesium sulphate), and the solvent removed, giving an oil whose ultraviolet absorption λ_{max} 240 mμ (ϵ 11,100) indicated that the double bond formed was conjugated with the benzene nucleus; but the infrared spectrum of the oil (natural film) contained two carbonyl bands (1710 and 1665 cm^{-1}) indicating the presence of some $\alpha\beta$-unsaturated ketone. The benzene mother liquors from the Grignard reaction were evaporated giving an oil which did not crystallize and whose infrared spectrum contained bands at 3370

cm^{-1}, 1692 cm^{-1}, and 1595 cm^{-1}. A portion of this oil was dehydrated with formic acid, the product isolated in the usual way and distilled up to 250° (oil bath) at 0.01 mm. The infrared spectrum of the resulting glass contained intense carbonyl bands (1715 and 1645 cm^{-1}) indicating absence of the glycol (III) in the original preparation. Ultraviolet spectrum of the glass: λ_{max} 237 mμ (ϵ 11,100).

1,5-Dihydroxy-1,5-diphenyldecahydronaphthalene (III)

Trans-1,5-dioxodecalin (5 g) in warm benzene (70 cc) was added dropwise to a solution of lithium phenyl prepared from lithium (1.7 g), bromobenzene (19 g), and ether (50 cc). The mixture was then stirred and boiled under nitrogen for 10 hours. Next day water and ammonium chloride solution were added, the suspension stirred for 2 hours, the solid collected, washed well with water, and dried (8.4 g, 87%), m.p. 250–255°. The glycol crystallized from 2-ethoxyethanol as colorless, hexagonal plates, m.p. 275–277°. Found: C, 81.7; H, 7.8%. Calc. for $C_{22}H_{26}O_2$: C, 82.0; H, 8.1%. Ultraviolet spectrum: λ_{max} 207 mμ (ϵ 21,080), λ_{max} 252 mμ (ϵ 417), λ_{max} 257 mμ (ϵ 487), λ_{max} 260 mμ (ϵ 417), λ_{max} 263 mμ (ϵ 368), λ_{max} 266 mμ (ϵ 278). The infrared spectrum contained bands at 3472 cm^{-1} (OH) and 1605 cm^{-1} (ar. CC).

1,5-Diphenylnaphthalene (VII)

The finely powdered glycol (2 g) was added to formic acid (25 cc) and the suspension heated under reflux (oil bath, 140°) for 30 minutes. Hot dimethylformamide (25 cc) was added, the solution boiled for 5 minutes, allowed to cool, the solid which separated collected, and washed with a little ethanol (1.3 g, 73%). After crystallization from acetic acid the product had m.p. 167–172°; crystallization from benzene gave a specimen of m.p. 179–182°. Found: C, 92.2; H, 7.3. Calc. for $C_{22}H_{22}$: C, 92.3; H, 7.7%. Ultraviolet spectrum: λ_{max} 235 mμ (ϵ 19,300), λ_{inflex} 284 mμ (ϵ 6020). Infrared spectrum 1597 cm^{-1} (ar. CC). The 1,5-diphenylhexahydronaphthalene (1.2 g) was mixed with 30% palladium–charcoal (0.2 g) (10) and heated (metal bath) at 240° for 30 minutes, the temperature of the bath was then raised to 300° (30 minutes), and finally to 330° (30 minutes), a slow stream of hydrogen being passed through the apparatus. The cold solid was extracted exhaustively with chloroform, the extracts evaporated, and the residue crystallized from benzene (0.94 g, 80%, m.p. 220–223°). 1,5-Diphenylnaphthalene formed colorless needles (from benzene) m.p. 223–224°, reported (3) m.p. 220–222°. Found: C, 94.2; H, 5.55. Calc. for $C_{22}H_{16}$: C, 94.3; H, 5.7%. Ultraviolet spectrum: λ_{max} 228 mμ (ϵ 48,200), λ_{max} 297 mμ (ϵ 14,200). The hydrocarbon did not give a solid complex with either 2,4,7-trinitrofluorenone or with benzotrifuroxan.

REFERENCES

1. Friedel, R. A., Orchin, M., and Reggel, L. J. Am. Chem. Soc. **70**, 199 (1948). Orchin, M. and Friedel, R. A. J. Am. Chem. Soc. **71**, 3002 (1949).
2. Bailey, A. S. and Case, J. R. Tetrahedron, **3**, 113 (1958).
3. Buchta, E., Vates, H., and Knopp, H. Chem. Ber. **91**, 228 (1958).
4. Dauben, W. G., Blanz, E. J., Jr., Jiu, J., and Micheli, R. A. J. Am. Chem. Soc. **78**, 3752 (1956).
5. Braude, E. A. Ann. Repts. on Progr. Chem. (Chem. Soc. London), **42**, 105 (1945). Eliel, E. L., McCoy, J. W., and Price, C. C. J. Org. Chem. **22**, 1533 (1957). Mixer, R. Y. and Young, W. G. J. Am. Chem. Soc. **78**, 3379 (1956).
6. Braude, E. A. and Nachod, F. C. Determination of organic structures by physical methods. Academic Press, Inc., New York. 1955. Chap. 4. Klyne, W. Progress in stereochemistry I. Butterworth Scientific Publications, London. 1954. p. 126.
7. Inhoffen, H. H. and Kath, J. Chem. Ber. **87**, 1589 (1954).
8. Ahmad, R., Sondheimer, F., Weedon, B. C. L., and Woods, R. J. J. Chem. Soc. 4089 (1952).
9. Johnson, W. S., Gutsche, C. D., and Banerjee, D. K. J. Am. Chem. Soc. **73**, 5464 (1951).
10. Linstead, R. P. and Thomas, S. L. S. J. Chem. Soc. 1127 (1940).

THE ADSORPTION OF HYDROGEN ON RUTHENIUM–ALUMINA[1]

M. J. D. Low and H. A. Taylor

ABSTRACT

The rate of adsorption of hydrogen on Ru–Al_2O_3 has been studied at four temperatures from 100 to 257° C at pressures from 15 to 80 cm DBP. The Elovich parameters α and a for these data have been calculated and their temperature and pressure dependencies found. It is shown that, regardless of temperature, the amount adsorbed at a given time and the parameters α and log $a\alpha$ show a dependence on the initial pressure which is different above and below 25 cm DBP indicating different types of adsorption. The temperature dependencies yield an energy of activation for the initial rate of the high pressure chemisorption of 17.7 kcal mole^{-1} which is independent of the pressure. Similar E values below 25 cm increase with a decrease in pressure. Four runs showed a very slow nitrogen adsorption on the same surface, raising the question of an enhancement of the adsorption of one gas by traces of another.

The elementary state of our knowledge of chemisorption and the lack of complete correlation with such physical factors as surface geometry or work function suggests that more attention be given to the chemical factors involved, such as the chemical reactions which may occur at surfaces contributing to chemisorption. It is obvious that, since the classical treatment of experimental data has not provided this information, new treatments and new techniques are necessary. The authors (1) have recently attempted this in a study of the chemisorption of hydrogen on nickel–kieselguhr. A variation, not hitherto observed, in the type of adsorption dependent on the initial gas pressure, independent of temperature, was discovered. That this effect is not peculiar to the nickel–hydrogen system is shown in the present study and in others which will be reported later. The accounting for the effect was given in the earlier paper. No repetition, here, is necessary, since the results presented speak for themselves.

EXPERIMENTAL

The adsorbent used was a commercial Ru·Al_2O_3 hydrogenation catalyst weighing 15.82 g.[2] It consisted of 1.25 cm extruded Al_2O_3 pellets with 0.5% Ru on the surface and was placed in a Vycor tube in the constant-volume adsorption system described previously, in which the pressure changes during adsorption were read on a dibutyl phthalate (DBP) manometer. After 10 hours of evacuation at 500° C the pressure in the system was below 10^{-6} mm, the catalyst maintaining its original black color. Pure hydrogen was introduced and remained for 10 minutes at 500° C and 60 cm DBP pressure, followed by evacuation at the same temperature for 2 hours. This procedure was repeated six times. After the first treatment the catalyst turned grey and remained so until exposure to air occurred at the end of all the experiments, when it resumed its original color. A final treatment with hydrogen at 500° C and 30 cm Hg pressure was made for 2 hours. It was found that, after this treatment and after subsequent experiments, a pressure of less than 10^{-6} mm Hg could be attained by evacuating at 500° C for about 6 hours. A standard evacuation time of 10 hours at 500° C was adopted. The hydrogen was purified by diffusion through heated palladium thimbles. The catalyst was maintained at constant temperature by means of vapor baths.

The chemisorption rate data were treated using the Elovich equation (2),

$$dq/dt = a \exp(-\alpha q),$$

[1]*Manuscript received November 6, 1958.*
Contribution from the Nichols Laboratory, New York University, New York 53, New York, U.S.A.
[2]*Purchased from Baker and Co. Inc., Lot No. 1979. The support is* γ–Al_2O_3.

where q is the amount adsorbed in time t, a is the initial rate, and α, a constant. For large values of $a\alpha$ the integrated equation has the form (3),

$$q_{nt}-q_{mt} = (2.3/\alpha)\log(n/m),$$

where q_{nt} and q_{mt} are the volumes of gas at n.t.p. adsorbed at times nt and mt, n and m being integers. When, as in the present study, the values of $a\alpha$ are large, the closeness of approach to constancy of $(q_{nt}-q_{mt})$ for successive values of mt serves as a much more satisfactory test of the applicability of the Elovich equation than is ever possible by a linearity of a $q-\log t$ plot. Values of α are then readily obtained from the differences $(q_{nt}-q_{mt})$, and a can be calculated from the Elovich equation and the experimental points.

RESULTS

The experimental conditions of pressure and temperature and the calculated constant of the rate equations for the runs performed are summarized in Table I. The experiments were performed in the order shown in column 1. The temperature of the adsorbent T and the calculated initial pressure P_i are shown in columns 2 and 3. Column 4 lists the mean α value calculated as mentioned, and in column 5 are the average deviations in per cent of the α values found during the run. Column 6 lists the values of $\log a\alpha$ with their average deviation in per cent in column 7. Column 8 shows the initial rates, a, and column 9 the values of q_1, the calculated amount adsorbed at $t = 1$ minute.

Plots of q against $\log t$ were linear in all cases. The precision with which the Elovich constants can reproduce the experimental data is shown in Table II for two typical runs by a comparison of q_{obs} with q_{calc} calculated from the relation: $q = (2.3/\alpha)\log(1+a\alpha t)$.

TABLE I

Run	T, °C	P_i, cm DBP	α	% dev.	$\log a\alpha$	% dev.	$a = x \cdot 10^n$		q_1
							x	n	
1103	100	78.4	6.4	9	8.03	0.2	1.7	7	2.87
1104	100	65.1	7.5	7	8.85	0.5	9.4	7	2.71
1105	100	48.8	8.2	2	9.81	0.2	7.9	8	2.77
1107	257	79.9	12.5	8	15.10	0.3	1.0	14	2.78
1108	257	33.1	14.5	5	15.40	0.2	1.7	14	2.45
1109	257	66.1	13.7	4	15.76	0.3	4.2	14	2.65
1110	257	49.4	14.6	4	16.10	0.8	8.6	15	2.54
1111	257	16.4	23.3	4	21.72	0.2	2.3	20	2.15
1112	257	32.7	15.0	3	15.91	0.1	5.4	14	2.43
1113	257	24.2	17.7	2	17.84	0.1	3.9	16	2.32
1114	100	31.8	8.4	5	8.84	0.4	9.0	7	2.44
1115	100	24.2	10.1	6	10.48	0.5	3.0	9	2.39
1116	100	16.1	10.6	11	10.04	0.7	1.0	9	2.18
1117	100	16.2	10.6	12	9.97	0.6	8.9	8	2.16
1118	100	65.8	7.3	6	8.84	0.3	9.5	7	2.78
1119	200	17.6	20.4	2	20.09	0.05	6.0	18	2.27
1120	200	66.3	12.2	5	14.20	0.1	1.3	13	2.67
1121	200	49.5	12.8	3	14.67	0.2	3.7	13	2.63
1123	200	78.8	12.2	4	14.49	0.1	2.5	13	2.74
1125	200	33.0	14.3	8	15.35	0.3	1.6	14	2.47
1127	200	24.5	14.8	6	15.74	0.3	3.7	14	2.44
1128	147	79.0	8.9	4	10.83	0.2	7.6	9	2.80
1132	147	48.8	10.2	3	11.52	0.2	3.3	10	2.60
1134	147	79.0	9.5	6	11.22	0.2	1.8	10	2.73
1136	147	16.0	14.7	12	13.89	0.6	5.3	12	2.17
1137	147	32.2	10.5	6	11.15	0.4	1.3	10	2.45
1138	147	24.5	11.5	7	11.76	0.6	5.0	10	2.35

TABLE II
Comparison of q_{obs} and q_{calc}

Min.	Run 1103, $T = 100°$ C, $P_i = 78.4$ cm DBP			Run 1108, $T = 257°$ C, $P_i = 33.1$ cm DBP		
	P	q_{obs}	q_{calc}	P	q_{obs}	q_{calc}
0	93.03	0	0	39.05	0	0
0.5	64.50	2.70	2.77	—	—	—
1.0	63.72	2.85	2.88	19.50	2.45	2.45
1.5	63.35	2.92	2.94	—	—	—
2.0	63.03	2.99	2.98	19.20	2.51	2.50
2.5	62.83	3.02	3.01	—	—	—
3.0	62.67	3.05	3.02	19.08	2.53	2.52
3.5	62.55	3.07	3.07	—	—	—
4.0	62.45	3.10	3.09	18.95	2.55	2.54
4.5	62.35	3.12	3.11	—	—	—
5.0	62.26	3.13	3.13	18.90	2.56	2.56
6.0	—	—	—	18.84	2.57	2.57
7.0	—	—	—	18.79	2.58	2.58
7.5	61.94	3.19	3.19	—	—	—
8.0	—	—	—	18.74	2.59	2.59
9.0	—	—	—	18.70	2.60	2.60
10	61.70	3.24	3.23	18.68	2.60	2.61
15	61.40	3.30	3.30	18.50	2.63	2.64
20	61.18	3.34	3.34	18.41	2.65	2.66
25	61.01	3.38	3.36	18.30	2.67	2.67
30	60.87	3.40	3.38	18.24	2.68	2.68
35	60.75	3.42	3.43	18.15	2.70	2.69
40	60.66	3.44	3.45	18.10	2.70	2.70
50	60.52	3.47	3.48	18.01	2.72	2.72
60	60.38	3.49	3.51	17.95	2.73	2.73
70	—	—	—	17.87	2.75	2.74
80	60.19	3.51	3.56	17.81	2.76	2.75
90	—	—	—	17.80	2.76	2.76
100	60.00	3.55	3.59	17.73	2.77	2.77

Temperature and Pressure Dependencies of a and α

Inspection of Table I shows that a variety of initial pressures were used at each of four temperatures. Although these initial pressures were not identical at all temperatures they are close enough for comparative purposes. Each group of runs at nearly identical initial pressures could be used to determine the temperature dependence of a parameter, while from each group of runs at the same temperature a pressure dependence could be derived.

α–T, P Relations

Figure 1 shows plots of α values against $1/T$ for the five pressures approximating 15, 25, 30, 50, 65, and 80 cm DBP. The linearity of these plots suggested the representation of the α–T relation in the form $\alpha = u + w/T$. Since the slopes of the plots are not equivalent, the parameters u and w must be functions of the initial pressure. Plotting the values of u and w as a function of P_i as in Fig. 2, it becomes apparent that a change of slope occurs in the pressure range 25–27 cm DBP. This has been taken as a dividing mark and points at pressures above 25 cm have been taken in one group, points below 25 cm in another group, a linear dependence of u and w on P_i being assumed. In the high pressure range these dependencies are given numerically by the equations:

$$u = 33.26 - 0.0678\,P_i$$
$$w = -8710 + 10.02\,P_i$$

while at low pressures:

$$u = 90.40 - 2.322\,P_i$$
$$w = -29018 + 823.3\,P_i$$

using a least-squares method where justified by the number of points involved.

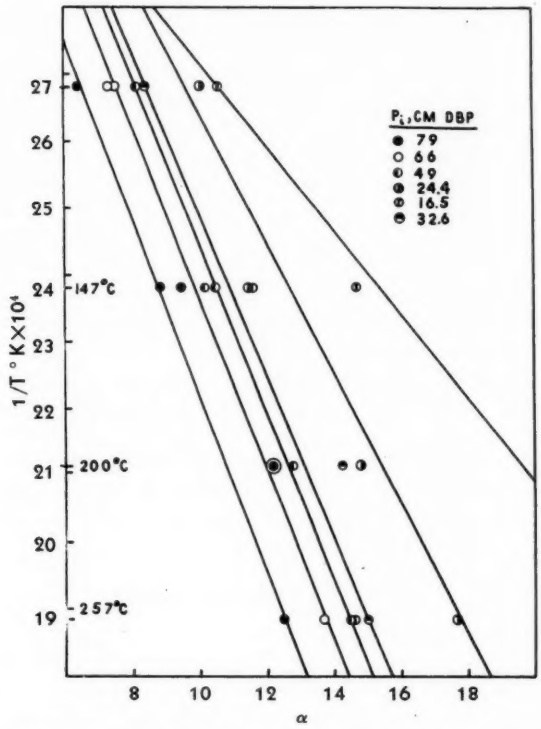

FIG. 1. Variation of α with temperature at different pressures.

log $a\alpha$–T, P Relation

In a similar manner log $a\alpha$ is found to be linear in $1/T$ and is expressible by the equation:

$$\log a\alpha = r + s/T.$$

The terms r and s are found to be pressure dependent and show a similar linear dependence above and below 30 cm to that found for α. The following equations give the numerical dependencies:

$$\begin{aligned} \text{high pressure:} \quad r &= 35.05 - 0.0456\, P_t \\ -s &= 9513 - 10.52\, P_t \\ \text{low pressure:} \quad r &= 85.96 - 2.03\, P_t \\ -s &= 28421 - 7585\, P_t. \end{aligned}$$

The change in the pressure dependence of both α and log $a\alpha$ in the neighborhood of 25 cm is also reflected in the actual volumes of gas adsorbed at a given time q_t, when considered as a function of the initial pressure, P_t. Figure 3 illustrates this at 257° C where q_t values for 2, 10, and 100 minutes are plotted as a function of P_t. In each case there is an abrupt change of slope around 25 cm. Plots at the other temperatures show a similar effect at the same pressure irrespective of the temperature. Again, it was shown previously (1) that the energy of activation E as conventionally calculated may be related to the quantities represented here as w and s by the relation, $E = Rwq - sR$,

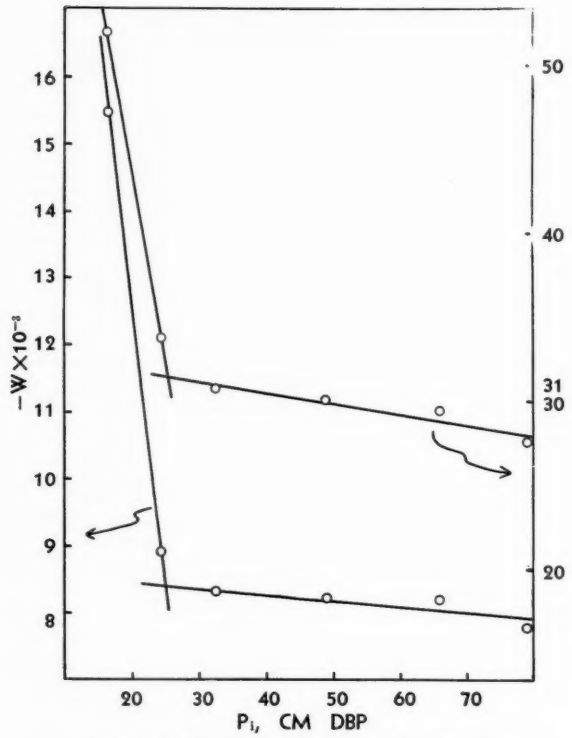

FIG. 2. Variation of w and u with initial pressure.

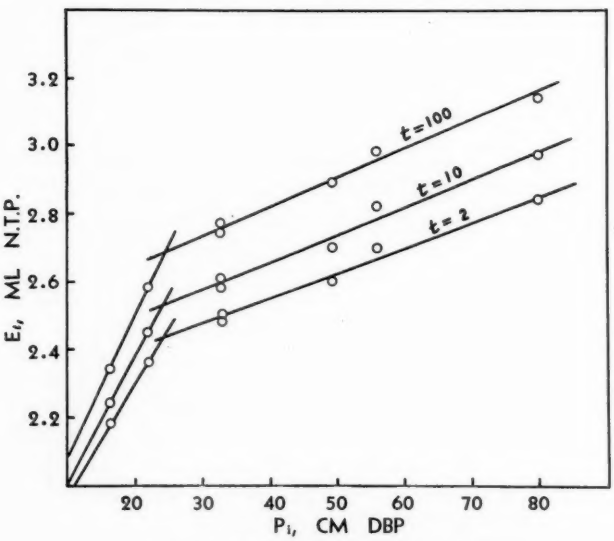

FIG. 3. Variation of q_t with initial pressure.

where R is the gas constant. Table III presents these various values in kcal/mole for the several initial pressures. Figure 4 shows the variation of $(-sR)$ as a function of the initial pressure. Although there is some scatter to the points there is distinct evidence of a change in pressure dependence around 25 cm. From the previous relation it is seen that $(-sR)$ is a measure of the energy of activation, E, at $q = 0$. It is essentially an extrapolated value for E at the beginning of the slow adsorption. In Fig. 5 are plotted values of J as a function of the initial pressure, derived by expressing the temperature dependence of the initial rates, a, by the relation, $\ln a = I+J/T$. If the initial rate of the slow adsorption, a, is Arrhenian, its energy of activation, E_a, should be given by $E_a = -JR$, where R is the gas constant. The similarity of Figs. 4 and 5 showing the change in slope at the same pressure, with an apparent independence of pressure above the break, becomes quantitative in the high pressure range. From Fig. 4 the high pressure value of $E_{q=0}$ is 17.7 kcal/mole. From Fig. 5 the high pressure value of J is -8800 yielding E_a as 17.6 kcal/mole. The agreement of these two values of E is, of course, necessary and only indicates consistency in the alternative treatments, on the one hand of a alone, on the other, of α and $a\alpha$. The agreement, nevertheless, provides some confirmation of the form of the temperature dependencies of α and $a\alpha$ used. The independence of initial pressure on the part of $E_{q=0}$ above 25 cm DBP contrasts with the marked dependence below 25 cm. This in itself is significant that two different adsorption processes are involved.

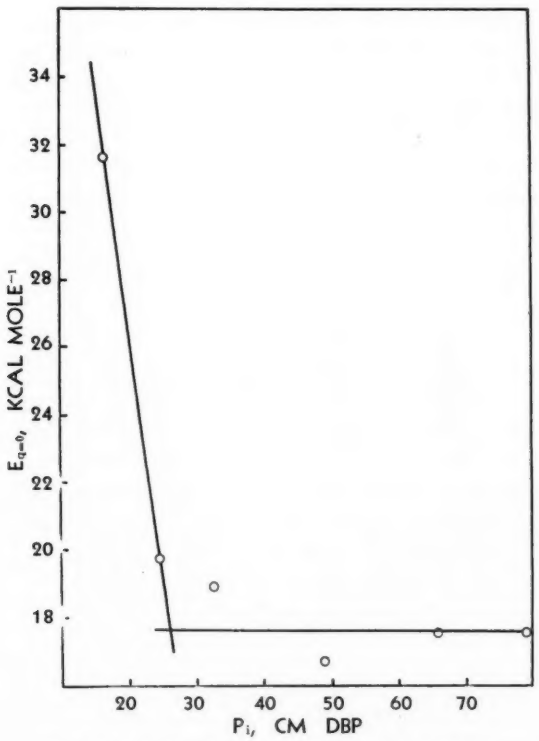

FIG. 4. Variation of activation energy with initial pressure.

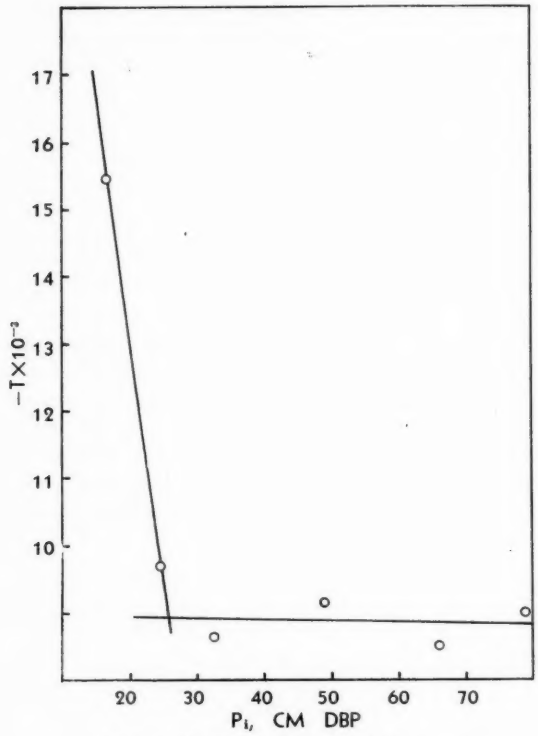

FIG. 5. Variation of J with initial pressure.

TABLE III

Data for activation energy

P_i	$-w$	$-s$	$-Rw$	$-sR$	$s/w = q_{E=0}$
79	7789	8836	15.48	17.56	1.13
66	8220	8880	16.33	17.64	1.08
49	8234	8432	16.36	16.75	1.02
32.6	8325	9518	16.54	18.91	1.14
24.4	8929	9914	17.74	19.70	1.11
16.5	15433	15906	30.67	31.61	1.03

Although E is positive for $q = 0$, it may be seen from Table III that as adsorption proceeds, E will rapidly become negative. As pointed out previously, therefore, E has no significance when calculated from values taken during the course of adsorption and its apparent variation during adsorption is no valid argument for "surface heterogeneity". It should be pointed out that in the present study, as in the earlier study on nickel, the temperature range covered corresponds to a decreasing total adsorption with increasing temperature. This may be seen from Fig. 6, which plots the amounts adsorbed after 100 minutes for the different temperatures and initial pressures. Although these are not strictly saturation values for the surface, so very little more gas is adsorbed after 100 minutes that they approximate saturation values. Thus in run 1134, 3.23 ml

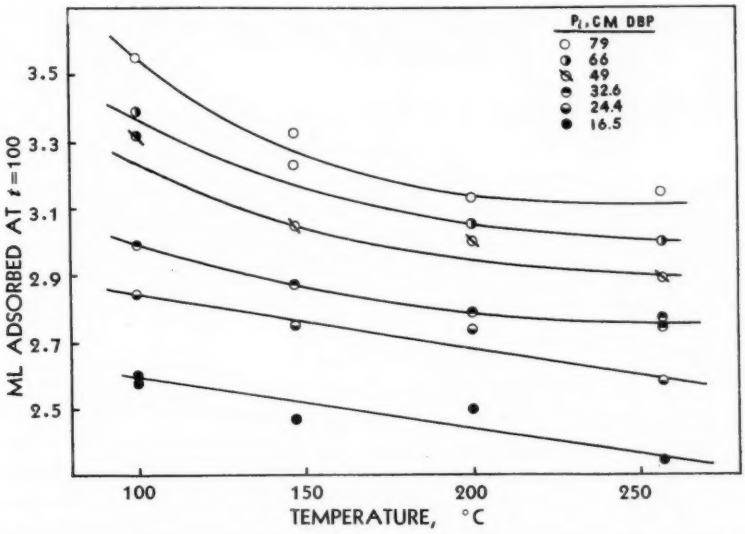

FIG. 6. Variation of the amounts adsorbed after 100 minutes with temperature at different initial pressures.

are adsorbed at 100 minutes, and 3.35 ml at 975 minutes. In run 1136 whereas 2.47 ml are adsorbed at 100 minutes only 2.60 ml are adsorbed at 1710 minutes. There is every indication at each pressure studied that the total adsorption is diminishing with increasing temperature. This contrasts with the classical studies of the variation of energy of activation of adsorption with coverage wherein the temperature range studied was restricted to regions in which the isobars increased with increasing temperature. It is not inconceivable that the well-known variation of the equilibrium amount adsorbed as a function of temperature, initially high at low temperature, decreasing to a minimum, rising to a maximum, and decreasing steadily thereafter as the temperature is increased, may simply reflect changes in the values of α associated with changes in the adsorption process.

Nitrogen Adsorption

At the conclusion of the experiments with hydrogen four exploratory runs were made using nitrogen. At 100° C and 257° C a definite but very slow adsorption of nitrogen was found to occur. The data are shown graphically in Fig. 7. Owing to the slow adsorption, the precision of the experiments was very poor and further investigation was abandoned. The results obtained, nevertheless, appear to confirm the views expressed by Amano and Taylor (4) that ruthenium should be included in group A of Trapnell's (5) classification as capable of adsorbing nitrogen. However, Trapnell's classification was intended for the pure metal films and may not apply to commercial catalyst preparations. Amano and Taylor found that in each initial run with each catalyst where there had been no previous contact with ammonia there was an anomaly in the rate of ammonia decomposition. Further, "between individual runs the catalyst was reduced for 2 hours at 450° C in hydrogen. After each such reduction the rate of decomposition rose gradually." The parallel situation in the present work with ruthenium after long use for hydrogen adsorption and possibly containing traces of unremoved hydrogen with

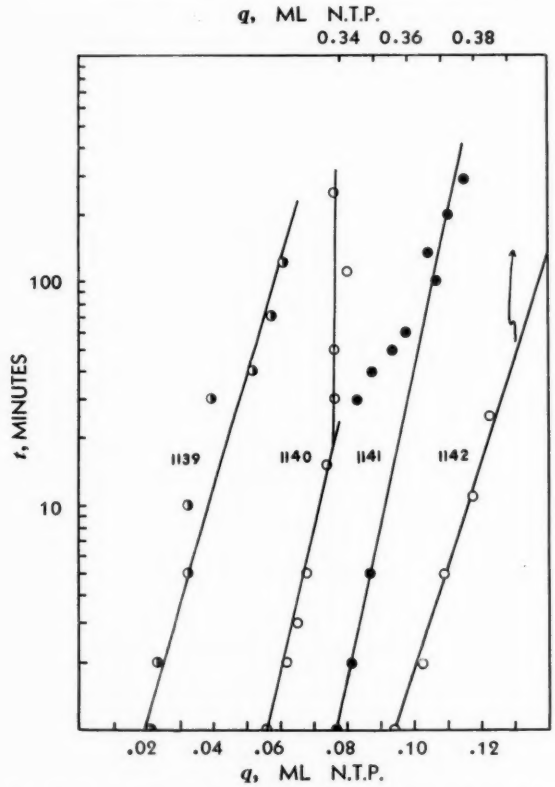

FIG. 7. Adsorption of nitrogen. 1139: P_i = 59.8 cm; 257° C; 1140: P_i = 73.1 cm; 257° C (displaced by +0.02 ml); 1141: P_i = 35.7 cm; 257° C (displaced by +0.04 ml); 1142: P_i = 59.4 cm; 100° C.

that of Amano and Taylor with a purposeful hydrogen treatment is obvious. It suggests that the small nitrogen adsorption may be facilitated by the presence of hydrogen. A similar effect was found by Gundry (6), who observed no nitrogen adsorption on clean nickel films but a small nitrogen adsorption in the presence of traces of hydrogen. The conclusion is obvious that the presence of hydrogen can create sites for nitrogen adsorption that are not already present on the clean metal or which nitrogen cannot make for itself. Considerable further study of the effects of traces of one gas on the adsorption of another, not alone from the point of view of poisoning but particularly for the possibility of enhancement of adsorption, is necessary for a complete understanding of the functions of the gas and the surface in chemisorption.

REFERENCES

1. LEIBOWITZ, L., LOW, M. J. D., and TAYLOR, H. A. J. Phys. Chem. **62**, 471 (1958).
2. TAYLOR, H. A. and THON, N. J. Am. Chem. Soc. **74**, 4169 (1952).
3. SARMOUSAKIS, J. N. and LOW, M. J. D. J. Chem. Phys. **25**, 178 (1956).
4. AMANO, A. and TAYLOR, H. J. Am. Chem. Soc. **76**, 4201 (1954).
5. TRAPNELL, B. M. W. Proc. Roy. Soc. A, **218**, 566 (1953).
6. GUNDRY, P. M. Private communication.

VIBRATIONAL SPECTRA OF NAPHTHALENE-d_0, -α-d_4, AND -d_8 MOLECULES[1]

S. S. MITRA[2] AND H. J. BERNSTEIN

ABSTRACT

The infrared and Raman spectra of the naphthalene-α-d_4 molecule have been obtained. The spectra of the d_0 molecule have also been repeated and for the most part previous measurements have been confirmed. Together with the literature data for the naphthalene-d_8 molecule, a complete assignment has been presented for all three molecules. It is recognized that the assignment is not definitive, although satisfactory agreement with the requirements of the band polarizations and contours, as well as product and sum rules, has been obtained. The calculated and observed values for the heat capacity and entropy are also in good agreement.

1. INTRODUCTION

A large amount of experimental work has been reported on the vibrational spectra of naphthalene and naphthalene-d_8 molecules. The present position has been summarized in three recent communications (1, 2, 3) (henceforth referred to as I, II, and III respectively), along with the presentation of three independent sets of assignments. Manneback (4) has given a theoretical discussion of the planar skeletal vibrations of the molecule. Calculations of vibrational frequencies using force constants transferred from benzene have been given by Brandmüller and Schmid (5) for the symmetrical A_g class, and by Scully and Whiffen (6) for the out-of-plane vibrations, A_u, B_{1u}, B_{2g}, and B_{3g}.

In the present investigation we have obtained the infrared[3] and Raman spectra of the intermediate α-d_4 compound, and along with the data on the d_0 and d_8 molecules, a complete assignment for all the three molecules has been attempted. Additional bands not used as fundamentals have been explained as combination tones.

2. EXPERIMENTAL

The photoelectrically recorded spectra of naphthalene and α-naphthalene-d_4[4] were obtained using a White Raman grating spectrometer (8). Mass spectrometric analysis of the d_4 sample gives its composition as 0.8, 10.6, 8.4, 70.4, 8.9, and 1.0%, respectively, for the 1D, 2D, 3D, 4D, 5D, and 6D molecules. The Raman spectra are shown in Figs. 1 and 2.

The infrared spectra of the two compounds were measured on a Perkin–Elmer Model 12C double pass spectrometer equipped with CsBr, NaCl, and LiF optics. The infrared spectra were recorded for solutions in CS_2 and CCl_4 (about 1 M by volume). Comparison with a spectrum of a less pure sample of the α-d_4 compound enabled us to eliminate some of the bands not belonging to the d_4 molecule. The infrared spectra are shown in Figs. 3 and 4. The experimental data are tabulated in Table I.

The Raman and infrared data of Lippincott and O'Reilly (1) and Luther *et al.* (3) were used for the d_8 compound, except for the CsBr region where the spectrum has been carefully re-examined for reasons given in Section 4.

[1]*Manuscript received November 21, 1958.*
Contribution from the Division of Pure Chemistry, National Research Council, Ottawa, Canada.
Issued as N.R.C. No. 5050.
[2]*N.R.C. Postdoctorate Research Fellow 1957–.*
[3]*Bayer and O'Reilly (7) have reported a few infrared bands of the α-d_4 compound in the region 700 cm^{-1} to 900 cm^{-1}, which are in agreement with our observations.*
[4]*We are greatly indebted to Dr. L. Leitch, who prepared this compound.*

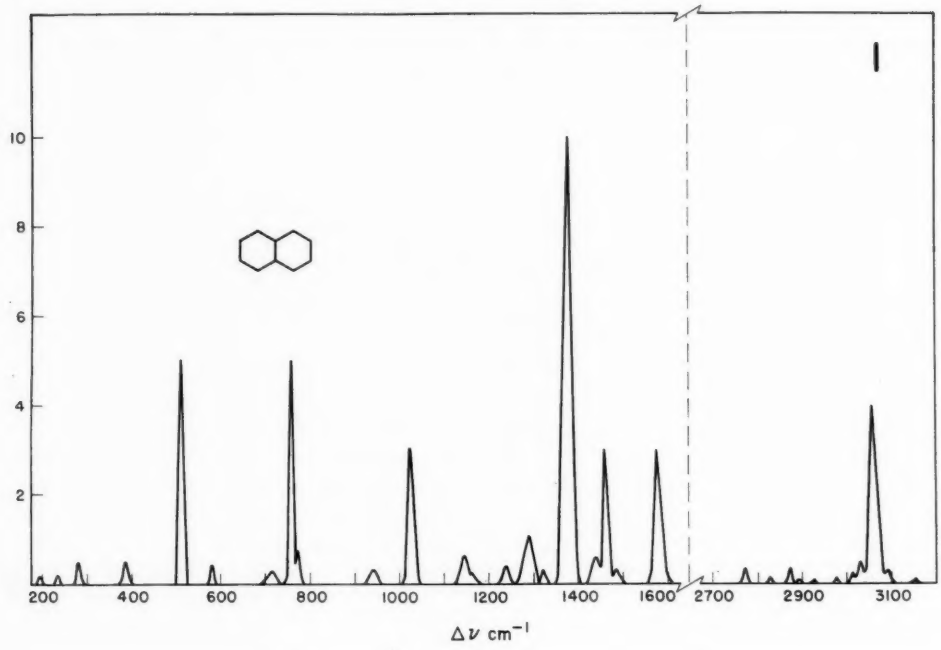

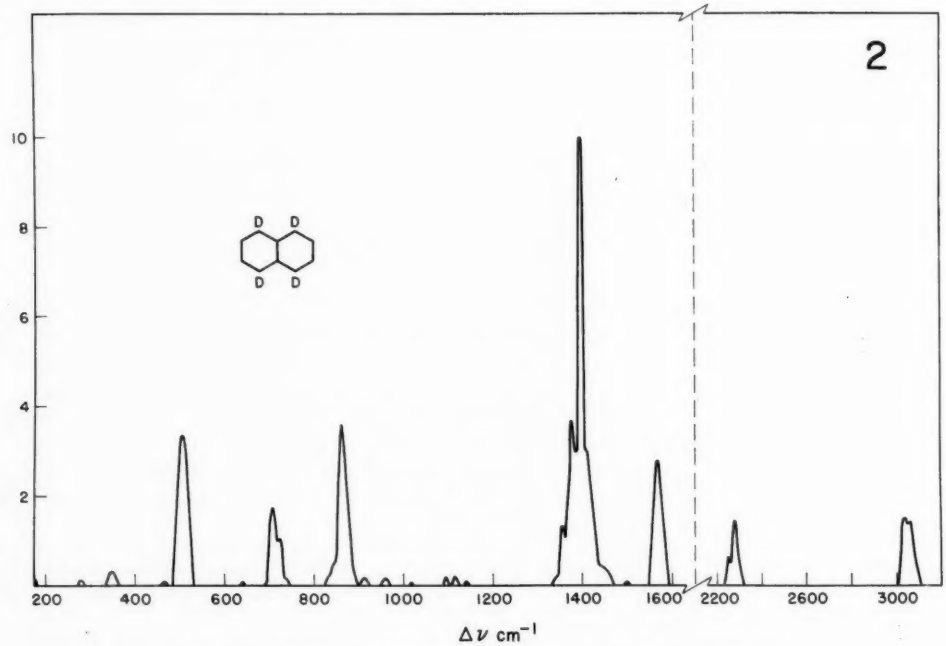

FIG. 1. Raman spectrum of naphthalene (liquid, *ca.* 90° C).
FIG. 2. Raman spectrum of naphthalene-α-d_4 (liquid, *ca.* 90° C).

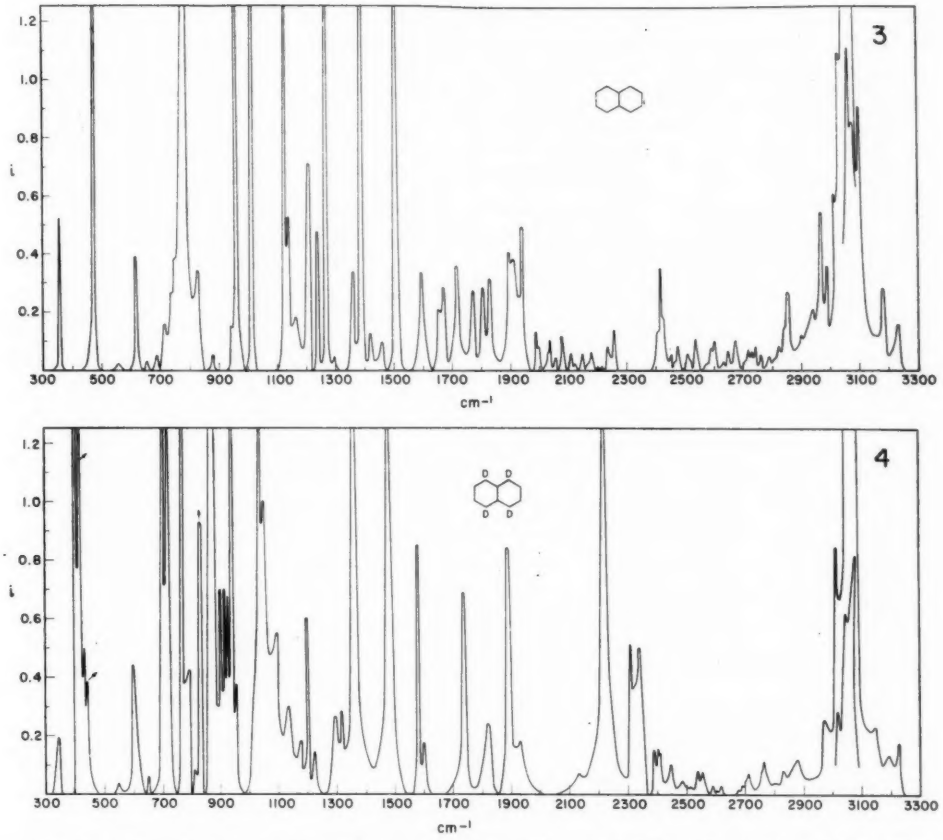

FIG. 3. Infrared spectrum of naphthalene in solution. 300 cm^{-1} to 700 cm^{-1}: solution in CCl_4 (CsBr prism); 700 cm^{-1} to 850 cm^{-1}: solution in CS_2 (NaCl prism); 850 cm^{-1} to 2000 cm^{-1}: solution in CCl_4 (NaCl prism); 2000 cm^{-1} to 3300 cm^{-1}: solution in CCl_4 (LiF prism). Intensities have been calculated for a 1 M solution and 1 mm path length except for the region 2000 cm^{-1} to 3300 cm^{-1} where the path length is 2.7 mm.

FIG. 4. Infrared spectrum of naphthalene-α-d_4 in solution. Conditions are the same as in Fig. 3. Intensities are calculated for a 1 M solution and 1 mm path length as usual, except for the region 2300 cm^{-1} to 3300 cm^{-1} where the path length is 2.7 mm. The arrows indicate bands due to the presence of other isotopically substituted species.

3. DISCUSSION

All three molecules belong to the D_{2h} point group. Each has 48 fundamental modes of vibration, of which 24 are Raman active, 20 infrared active, and 4 are completely inactive. Since the center of symmetry is a symmetry element of the D_{2h} point group, the mutual exclusion principle holds. In assigning the fundamentals the following points have been kept in mind.

(i) The frequencies of a particular mode in the three molecules should be in the order $d_0 > d_4 > d_8$.

(ii) The frequencies should lie in the spectral regions characteristic of the different types of vibrations, and should be consistent with the isotope ratio (R) associated with the type of vibration (1).

TABLE I

Infrared and Raman frequencies of naphthalene-d_0, -α-d_4, and -d_8 in cm^{-1}

Naphthalene		Naphthalene-α-d_4		Naphthalene-d_8	Naphthalene		Naphthalene-α-d_4		Naphthalene-d_8
Infrared	Raman*	Infrared	Raman*	infrared†	Infrared	Raman*	Infrared	Raman*	infrared†
359(1)	195(0.5)	338(0.5)	183(0.5)	328(0.5)	1458(0)	2978(0.5)	1318(0.5)	1569(6)d?	
476(3)	285(1)d	407(8)	280(0.5)	404(5)	1506(4)	3012(0.5)	1362(5)	2252(3)	
562(0)	386(1)d	435(1)	350(1)	542(0)	1592(0.7)	3031(1)	1480(4)	2276(5)	
618(1)	512(10)p	557(0)	467(0)	594(2)	1652(0)	3060(8)p	1581(2)	3045(5)	
655(0)	585(1)d	602(1)	505(7)p	626(10)	1669(0.5)	3092(0.5)	1601(0.5)	3063(5)	
689(0)	717(0.5)	654(0)	639(0)		1715(0.7)	3154(0)	1738(1)		
717(0)	758(10)p	710(5)	710(5)p		1770(0.5)		1822(0.5)		
739(0)	770(1.5)	729(7)	721(1)p		1804(0.5)		1888(1.5)		
753(0)	943(0.5)	775(4)	737(0.5)		1830(0.5)		1931(0.5)		
782(20)	1025(6)p	793(1)	828(0.5)		1896(0.8)		2132(0)		
825(0.5)	1145(1)d	823(0)	844(1)d		1908(0.8)		2217(2)		
877(0)	1158(0.5)	874(20)	864(7)p		1939(1)		2260(4)		
943(0)	1239(1)	905(1.5)	908(0.5)p		2256(0)		2268(1)		
958(5)	1320(0.5)	917(1.5)	958(0.5)d		2414(0.5)		2278(1)		
1011(5)	1376(20)p	929(1.5)	1020(0?)		2851(0.5)		2295(0)		
1128(4)	1438(1)d	942(4)	1095(0.5)		2968(1)		2308(0.5)		
1138(1)	1460(6)p	957(0.5)	1114(0.5)		2987(0.8)		2338(0)		
1163(0)	1483(0.5)d	1038(3)	1140(0?)		3010(0.5)		3014(1)		
1210(1.5)	1577(6)p	1051(0.5)	1341(0.5)		3027(1)		3046(4)		
1238(1)	1624(0)	1098(0.5)	1355(1)d		3060(10)		3076(5)		
1267(4)	2774(0.5)	1137(0.5)	1379(3)d?		3076(4)				
1295(0)	2828(0)	1178(0.5)	1397(20)p		3098(1)				
1361(0.5)	2874(0.5)	1199(1)	1410(1)d?		3180(0.5)				
1387(4)	2894(0)	1214(0.5)	1451(1)d		3230(0.5)				
1419(0)	2928(0)	1296(0.5)	1497(0)						

*p = polarized, d = depolarized.
†For rest of the infrared and Raman data on naphthalene-d_8 see ref. 1.

(iii) The Teller–Redlich product rule should be obeyed.

(iv) The frequency sum rules (9, 10) should be obeyed. In this particular case the application of these rules means for a particular symmetry class

$$\Sigma\nu(d_4) = (\Sigma\nu(d_0)+\Sigma\nu(d_8))/2$$

and

$$\Sigma\nu^2(d_4) = (\Sigma\nu^2(d_0)+\Sigma\nu^2(d_8))/2.$$

The assignment should be consistent with:

(v) the polarization of the Raman lines in the molten phase, and with the polarization of the infrared bands of single crystal samples (for this point see refs. 1, 2, 3; and also Person, Pimentel, and Schnepp (11); and Pimentel, McClellan, Person, and Schnepp (12));

(vi) the contours of the infrared bands in the gaseous phase (3, 11);

(vii) the intensity of the bands;

(viii) the calculations of Brandmüller and Schmid (5), and Scully and Whiffen (6);

(ix) the trends calculated by Manneback (4) for the skeletal modes; that is, the frequencies should be in the following increasing order:

$$A_gB_{3u}A_gB_{3u}\ldots.$$

$$B_{2u}B_{3u}B_{2u}B_{3u}\ldots$$

$$A_gB_{1g}A_gB_{1g}\ldots.$$

$$B_{2u}B_{1g}B_{2u}B_{1g}\ldots;$$

(x) the experimental values of the heat capacity and entropy of gaseous naphthalene.

As we do not possess any single crystal or gas phase infrared spectra of the d_4 compound, for assigning the infrared modes of this molecule, criteria (v) in part and (vi) could not be used. Criterion (x) could be used only for the d_0 compound, since no experimental data on the thermodynamic properties of the d_4 and d_8 compounds exist.

4. INFRARED ASSIGNMENT

The band polarization measurements in the solids, and band contours in the gas phase spectra, decide unambiguously the species of many bands. The intensity and position aid in identifying the bands with particular vibrations. Our infrared assignments do not differ very much from those of McClellan and Pimentel (2). The bands for the intermediate d_4 molecule have been selected chiefly from intensity considerations and requirements of the product rule ratio and sum rules.

B_{1u} Class

McClellan and Pimentel's assignment of the four B_{1u} fundamentals for the d_0 and d_8 compounds is in complete agreement with Scully and Whiffen's predictions. We have accepted this assignment and have tried to choose four reasonable intermediate frequencies for the d_4 compound. From intensity considerations the band at 874 cm^{-1} is the only possibility for ν_{22}. In the case of ν_{23}, there are three strong bands of the d_4 molecule with frequencies intermediate between 782 cm^{-1} (d_0) and 626 cm^{-1} (d_8). A Fermi resonance has been assumed to occur between the pair at 729 cm^{-1} and 775 cm^{-1}, and the band at 710 cm^{-1} is considered to be a combination. A rough center-of-gravity calculation predicts the position of the unperturbed bands at 740 cm^{-1}. One of these is assigned as ν_{23} and the other a combination band of species B_{1u}. As the band at 407 cm^{-1} of the d_4 molecule is the strongest in that vicinity, it had to be selected as ν_{24}. However, if one accepts the reported (1) value of 408 cm^{-1} for the fundamental of the d_8 molecule, the criterion (i) of Section 3 is obviously violated. This suggested that a re-examination of the d_8 spectrum in this region would be worthwhile, and indeed, the position was measured at 404 cm^{-1} instead of 408 cm^{-1}. As no data below 300 cm^{-1} are available for the d_4 and d_8 compounds, values of 172 cm^{-1} and 163 cm^{-1} are estimated for the ν_{25} fundamental in these molecules.

B_{2u} Class

For the B_{2u} species our choice of ν_{31} (CC stretch) for the d_8 molecule is different from that in II. The chief criticism of the choice of the 1440 cm^{-1} band in II is that it is not observed in solution spectra of d_8, whereas the corresponding 1592 cm^{-1} band of the d_0 compound is a relatively strong band. Instead, we have chosen the fairly strong 1540 cm^{-1} band as ν_{31} in the d_8 compound. In I, the band at 1540 cm^{-1} has also been used instead of 1440 cm^{-1}. With reasonable choices for the CH and CD valence modes, the complete B_{2u} assignment is consistent with product and sum rules.

B_{3u} Class

Our assignment for the B_{3u} class differs from that of II only in two places, ν_{45} and ν_{47}. Instead of their 1143, 905 cm^{-1} pair for the ν_{45} mode in the d_0 and d_8 molecules we have preferred the 1210, 946 cm^{-1} pair. The chief reason is that the 1210 cm^{-1} band is stronger than the band in the 1140 cm^{-1} region of our spectrum of the d_0 compound in solution. For the ν_{47} mode we have chosen the 877, 756 cm^{-1} pair instead of the pair 742, 680 cm^{-1} adopted in II. Although both the 877 cm^{-1} and 742 cm^{-1} bands are observed in

solution, only the former is observed in the gas phase. Moreover, according to Person, Pimental, and Schnepp (11) the best choice of symmetry class for the 877 cm^{-1} band is unambiguously B_{3u}, whereas that for the 742 cm^{-1} band is either B_{1u} or B_{3u}. Further the 680 cm^{-1} band is not observed in solution spectra of the d_8 compound but the band at 756 cm^{-1} is. This assignment thus coincides with I. Our assignments of the CH and CD valence modes are essentially similar to those of II.

5. ASSIGNMENT OF RAMAN FREQUENCIES

A_g Class

For assigning the Raman active A_g modes Brandmüller and Schmid's theoretical calculations are a good guide. All the intense and polarized bands observed in the Raman spectra are included in this class. Our assignment does not differ essentially from II. Corresponding strong and polarized bands of the d_4 compound could be identified and were assigned to the A_g species. Instead of the 1240, 1006 cm^{-1} pair we have preferred that at 1158, 929 cm^{-1} for one of the CH and CD bending modes in the d_0 and d_8 molecules. As neither of the bands (1240 or 1158 cm^{-1}) are polarized, one cannot have an unambiguous choice. Lippincott and O'Reilly's argument in favor of Fermi resonance between the two strong bands at 1379 cm^{-1} and 1460 cm^{-1} in the d_0 molecule has been accepted. Our estimated position for the unperturbed band, however, is 1405 cm^{-1} instead of their value of 1393 cm^{-1}, because the corresponding band of the d_4 compound is situated at 1397 cm^{-1}. Moreover, a rough center-of-gravity calculation with the observed intensities of the two bands in question also requires a higher value.

B_{1g} Class

Following II, the 1624, 1573 cm^{-1} pair has been assigned to the CC stretching frequency ν_{16}; but as we have not observed any corresponding line in the d_4 molecule, a value of 1610 cm^{-1} has been estimated for this mode in the intermediate compound. Since in our Raman spectrum of the d_0 compound no line has been observed at 1586 cm^{-1}, it has not been included in the present assignment. Instead, the 1483, 1451, 1408 cm^{-1} system has been chosen as the ν_{17} CC stretching mode in the d_0, d_4, and d_8 molecules respectively. Moreover, the 1451 cm^{-1} band of the d_4 compound clearly shows depolarization. Of the two CH in-plane deformation modes ν_{18} and ν_{20}, ν_{18} has been assigned as in II. A corresponding line at 1410 cm^{-1} was observed for the intermediate compound, which appears to be depolarized. In the case of ν_{20}, the 1145 cm^{-1} line of the d_0 molecule (being clearly a depolarized line) has been retained in the B_{1g} symmetry class as in II, but for its counterpart in the d_8 molecule we have used 829 cm^{-1} instead of 929 cm^{-1}, since the latter has already been included in our A_g symmetry class. The former choice has also been adopted in I. For the ν_{20} band of the intermediate compound, the 844 cm^{-1} band has been selected, which is depolarized and also has an isotope ratio value (R) of the right order. For the two in-plane distortion modes (ν_{19} and ν_{21}) there is no specific criterion for selection, excepting for Manneback's rule $A_g < B_{1g}$ for all skeletal modes. For the ν_{21} vibration, the 585 cm^{-1} line has been preferred to 611 cm^{-1} as chosen by II, because the latter was not observed in this work for the d_0 molecule; furthermore, the 585 cm^{-1} line is clearly depolarized. As we have not been able to detect any corresponding line in the d_4 molecule, an estimated value of 582 cm^{-1} has been used. The 569 cm^{-1} band seems to be the corresponding frequency in the d_8 molecule. Thus the assignment for the ν_{21} mode completely agrees with that of I. We have also adopted their selection of a rather high frequency for the ν_{19} mode. Thus for this mode the line at 1320 cm^{-1} has been chosen for the d_0 molecule, with its counterpart at 1295 cm^{-1} in d_8. As no line has

been observed in the d_4 molecule in this region, a frequency of 1309 cm^{-1} has been estimated. After the selection of the CH and CD valence modes for the A_g class, the rest of the observed bands in these regions have been used in the B_{1g} class. As we do not have enough CD stretching lines in the d_8 molecule, an estimated frequency of 2220 cm^{-1} was used instead of using the 2257 cm^{-1} line twice (once in A_g and once in B_{1g}, as done in II).

Out-of-plane Modes (Raman)

For the out-of-plane deformation modes, calculations of vibration frequencies have been made by Scully and Whiffen (6). On the basis of their calculations for the d_0 and d_8 molecules it is not difficult to select the intermediate d_4 frequencies having proper intensity and obeying the sum and product rules. The major discrepancy of such an assignment is that the calculated thermodynamic functions for the d_0 compound show large deviations from the observed ones. On the other hand, McClellan and Pimentel's (II) assignment gives very good agreement between the calculated and experimental values of the thermodynamic properties, but is completely inconsistent with Scully and Whiffen's calculations. We have tried to present an assignment which gives reasonable agreement with the thermodynamic properties, and at the same time does not violate grossly Scully and Whiffen's predictions.

Agreement of calculated values of thermodynamic functions with the observed ones requires a low frequency line (preferably 195 cm^{-1}) to be included among the fundamentals. This has been done by II. In addition to this, a skeletal normal co-ordinate treatment requires that the lowest out-of-plane frequencies have the order $B_{1u} < B_{2g}$

TABLE II

The fundamental vibration frequencies for naphthalene-d_0, -α-d_4, and -d_8; (assignment A)

Species	Freq. No.	Type of vibration	$C_{10}H_8$, cm^{-1}	$C_{10}H_4D_4$ (1-4-5-8), cm^{-1}	$C_{10}D_8$, cm^{-1}
A_g (∥)	1	CH stretching	3060	3045	2268
	2	CH stretching	3031	2276	2257
	3	CC stretching	1577	1569	1548
	4	CC stretching	1405*	1397	1380
	5	CH bending	1158	1095	929
	6	CC stretching	1025	908	862
	7	CH bending	943	864	777
	8	Skeletal breathing	758	710	694
	9	Skeletal distortion	512	505	491
A_u (⊥)	10	CH bending	915		
	11	CH bending	730		
	12	Skeletal distortion	698?		
	13	Skeletal distortion	400e		
B_{1g} (∥)	14	CH stretching	3092	3063	2302
	15	CH stretching	2978	2252	2220e
	16	CC stretching	1624	1610e	1573
	17	CC stretching	1483	1451	1408
	18	CH bending	1438	1410	1170
	19	Skeletal distortion	1320	1309e	1295
	20	CH bending	1145	844	829
	21	Skeletal distortion	585	582e	569
B_{1u} (⊥)	22	CH bending	958	874	791
	23	CH bending	782	740*	626
	24	Skeletal bending	476	407	404
B_{2g} (⊥)	25	Wing-wagging	176	172e	163e
	26	CH bending	1239	1114	1006
	27	CH bending	717	639	541
	28	Skeletal bending	195	183	180
B_{2u} (∥)	29	CH stretching	3060	3046	2299
	30	CH stretching	3027	2260	2259
	31	CC stretching	1592	1581	1540
	32	CC stretching	1387	1362	1260
	33	CH bending	1267	1199	1039
	34	CH bending	1128	929	886
	35	Skeletal distortion	618	602	594
	36	Skeletal distortion	359	338	328
B_{3g} (⊥)	37	CH bending	1099	958	875
	38	CH bending	874	828	752
	39	Skeletal bending	770	737	671
	40	Skeletal bending	285	280	270
B_{3u} (∥)	41	CH stretching	3076	3076	2323†
	42	CH stretching	2987	2278	2278
	43	CC stretching	1715	1601	1562
	44	CC stretching	1506	1480	1403
	45	CH bending	1210	1038	946
	46	CH bending	1011	942	831
	47	Skeletal distortion	877	823	756
	48	Skeletal distortion	562	557	542

*Denotes the estimated unperturbed position of a fundamental that is affected by Fermi resonance.
e Estimated value.
†Band observed in solid phase only.

$< B_{3g}$. Thus the present assignment of the non-planar deformation frequencies (B_{2g} and B_{3g}) has been chiefly based on the following facts: (1) inclusion of the 195 cm^{-1} band as a fundamental, (2) consistency with the trend indicated by Scully and Whiffen's calculations, (3) consistency with the inequality $B_{1u} < B_{2g} < B_{3g}$ for the lowest frequencies, and finally, (4) utilization of those few Raman bands left over, i.e. not used as A_g or B_{1g} modes. Final assignments given in Table II satisfy product and sum rule requirements also. One weak point of this assignment is that it has included two frequencies 874 cm^{-1} and 1099 cm^{-1} for the d_0 molecule, which we have not observed. As we are not left with any other bands to be used for this purpose we have used the data of Lippincott and O'Reilly (I) and Luther *et al.* (III). For the d_4 molecule all the lines have been recorded by us. And for the d_8 molecule, as usual, we have used the data of I.

6. A_u MODES

Finally we are left with the selection of four A_u fundamentals, which are inactive in both infrared and Raman. Very little basis exists for their selection. The bands which have been observed in the infrared spectra of the solid but not in gas or solution can be chosen for this species because, presumably, the selection rules for a free molecule could break down in the crystal field. In II, this procedure has also been followed, but as all frequencies chosen are greater than those calculated by Scully and Whiffen, we preferred to make a new choice, not inconsistent with the trends indicated by the calculations. Lines at 915 cm^{-1} and 730 cm^{-1} have been selected on the above basis (i.e., observed in solid phase only). The line at 698 cm^{-1} has been reported for solid naphthalene by Person, Pimentel, and Schnepp (11), and not in solution, but as it has also been observed by them in the gas phase, there is some doubt as to its assignment as an A_u mode. Luther *et al.*, however, have not observed this band in the gas phase. The last frequency selected at 400 cm^{-1} is just a guess, made by all the previous workers (I, II, and III) also. No attempt has been made to assign the A_u modes of the other two molecules.

The assignment of all the fundamentals is presented in Table II. The observed and calculated product rule ratios and $\Sigma\nu$ and $\Sigma\nu^2$ values are recorded in Table III.

TABLE III

Product rule ratio and $\Sigma\nu$ and $\Sigma\nu^2$ values for the naphthalene-d_0, -α-d_4, and -d_8 molecules

	$\Pi\frac{\nu(d_4)}{\nu(d_0)}$		$\Pi\frac{\nu(d_8)}{\nu(d_0)}$		$\Sigma\nu(d_4)\times10^{-3}$ cm^{-1}		$\Sigma\nu^2(d_4)\times10^{-6}$ cm^{-2}	
Species	Obs.	Calc.	Obs.	Calc.	Obs.	Calc.	Obs.	Calc.
A_g	0.524	0.500	0.260	0.250	12.369	12.338	22.395	22.300
A_u		0.707		0.500				
B_{1g}	0.518	0.514	0.287	0.268	12.521	12.516	23.904	23.735
B_{1u}	0.721	0.718	0.519	0.515	2.193	2.188	1.507	1.497
B_{2g}	0.751	0.712	0.566	0.531	1.936	1.939	1.683	1.712
B_{2u}	0.518	0.508	0.278	0.258	11.317	11.321	21.518	21.523
B_{3g}	0.781	0.760	0.568	0.546	2.803	2.798	2.225	2.250
B_{3u}	0.518	0.508	0.261	0.258	11.795	11.793	22.357	22.305

7. THERMODYNAMIC PROPERTIES

The heat capacity and entropy of naphthalene-d_0 have been calculated at 451.0° K and 522.7° K using the above assignments. The formulas and physical constants published by the A.P.I. Research Project 44 (13) have been used in these calculations. The calculated values are compared with the experimental ones due to Barrow and

McClellan (14) in Table IV. The agreement is not significant however, due to the uncertainty in the value of the lowest A_u frequency.

TABLE IV

Comparison of the experimental and calculated values of the heat capacity and entropy of naphthalene

Temp., °K	$C_p°$, cal/deg-mole			$S°$, cal/deg-mole		
	Expt.	Calc. assign. A	Calc. assign. B	Expt.	Calc. assign. A	Calc. assign. B
451.0	48.18±0.48	48.23	48.02	96.85±0.44	96.88	96.75
522.7	54.17±0.54	54.36	54.15	104.41±0.44	104.45	104.28

TABLE V

Combination bands

Infrared, cm^{-1}	Assignment	Raman, cm^{-1}	Assignment
	Naphthalene-d_8		
655	$\nu_{34}+\nu_{39}=671\ (B_{1u})$	386	$2\nu_{28}=390\ (A_g)$
689	$\nu_9+\nu_{35}=688\ (B_{1u})$	2774	$\nu_{16}+\nu_5=2782\ (B_{1g})$
717	?	2828	$(\nu_{39}+\nu_{31})+\nu_{21}=2838\ (A_g)$
739 B_{1u} or B_{3u}	$\nu_{37}-\nu_{36}=740\ (B_{1u})$	2874	$\nu_4+\nu_{17}=2888\ (B_{1g})$
753 B_{1u}	$\nu_{43}+\nu_{39}=757\ (B_{1u})$	2894	$\nu_3+\nu_{19}=2897\ (B_{1g})$
825 B_{1u}	?	2928	$(\nu_{39}+\nu_6)+\nu_{34}=2935\ (B_{2g})$
943	$\nu_{31}+\nu_{36}=944\ (B_{3u})$	3012	$2\nu_{44}=3012\ (A_g)$
1138 B_{3u}	$\nu_{32}+\nu_{39}=1153\ (B_{3u})$	3154	$2\nu_3=3154\ (A_g)$
1163	$\nu_{39}+\nu_{19}=1170\ (B_{3u})$		
1238 B_{2u}	$\nu_{39}+\nu_{34}=1246\ (B_{2u})$		
1295	$\nu_{32}+\nu_9=1294\ (B_{1u})$		
1361 B_{3u}	$\nu_{47}+\nu_9=1389\ (B_{3u})$		
1419	$\nu_7+\nu_{24}=1419\ (B_{1u})$		
1458	$\nu_{22}+\nu_9=1470\ (B_{1u})$		
1652	$\nu_{33}+\nu_{32}=1656\ (B_{2u})$		
1669	$\nu_{19}+\nu_{36}=1679\ (B_{3u})$		
1770	$\nu_{38}+\nu_9=1779\ (B_{2u})$		
1804	$\nu_{39}+\nu_6=1807\ (B_{1u})$		
1830	$\nu_{17}+\nu_{35}=1842\ (B_{3u})$		
1896	$\nu_9+\nu_{32}=1899\ (B_{2u})$		
1908	$\nu_{18}+\nu_{24}=1914\ (B_{2u})$		
1939	$\nu_{33}+\nu_5=1940\ (B_{1u})$		
2256	$\nu_3+\nu_{44}=2264\ (B_{3u})$		
2414	$\nu_{46}+\nu_4=2416\ (B_{3u})$		
2851	$\nu_{30}+\nu_{43}=2860\ (B_{2u})$		
2968	$(\nu_{33}+\nu_{39})+\nu_{19}=2976\ (B_{3u})$		
3010	$\nu_{32}+\nu_{19}=3011\ (B_{3u})$		
3098	$(\nu_{33}+\nu_8)+\nu_8=3098\ (B_{1u})$		
3180	$2\nu_{44}+\nu_{35}=3188\ (B_{1u})$		
3230	$\nu_1+\nu_{35}=3236\ (B_{1u})$		
	Naphthalene-α-d_4		
435	Impurity ?	350	$2\nu_{25}=366\ (A_g)$
654	$\nu_{36}-\nu_{35}=656\ (B_{2u})$	467	$\nu_{39}+\nu_{43}=463\ (B_{1g})$
710	$\nu_{19}-\nu_{33}=$? (B_{2u}); Impurity ?	721	$\nu_{43}+\nu_{35}=729\ (B_{2g})$
740*	$\nu_{43}+\nu_{25}=740\ (B_{1u})$	1020	$\nu_{39}+\nu_{25}=1027\ (B_{2g})$
793	$\nu_4-\nu_{35}=795\ (B_{2u})$	1140	$\nu_{27}+\nu_9=1144\ (B_{2g})$
905	$\nu_{39}+\nu_{25}=909\ (B_{2u})$	1341	$\nu_{27}+\nu_6=1349\ (B_{2g})$
917	$\nu_{21}+\nu_{36}=920\ (B_{3u})$	1355	$\nu_{40}+\nu_5=1375\ (B_{2g})$?
957	Impurity ?	1379	$\nu_{43}+\nu_{47}=1380\ (A_g)$
1051	$\nu_9+\nu_{43}=1062\ (B_{2u})$	1497	$\nu_7+\nu_{37}=1503\ (B_{2g})$

Infared, cm^{-1}	Assignment	Raman, cm^{-1}	Assignment
	Naphthalene-α-d_4 (*continued*)		
1098	$\nu_{43}-\nu_9=1096\ (B_{2u})$		
1137	$\nu_{43}+\nu_{21}=1139\ (B_{2u})$		
1178	$\nu_{39}+\nu_{36}=1182\ (B_{3u})$		
1214	$\nu_{34}+\nu_{40}=1219\ (B_{1u})$		
1296	$\nu_{36}+\nu_{37}=1296\ (B_{1u})$		
1318	$\nu_9+\nu_{47}=1328\ (B_{3u})$		
1738	$\nu_7+\nu_{22}=1738\ (B_{1u})$		
1822	$\nu_{37}+\nu_{22}=1832\ (B_{2u})$		
1888	$\nu_{37}+\nu_{24}=1887\ (B_{1u})$		
1931	$\nu_{39}+\nu_{33}=1936\ (B_{1u})$		
2132	$\nu_{45}+\nu_5=2133\ (B_{2u})$		
2217	$\nu_7+\nu_{33}=2226\ (B_{2u})$		
2268	$\nu_{33}+\nu_4=2271\ (B_{1u})$		
2295	$(\nu_{30}+\nu_{36})+\nu_{35}=2296\ (B_{1u})$		
2308	$\nu_{43}+\nu_3=2311\ (B_{2u})$		
2338	$\nu_7+\nu_{44}=2344\ (B_{3u})$		
3014	$\nu_{18}+\nu_{43}=3011\ (B_{2u})$		
	Naphthalene-d_8†		
721	$\nu_{33}+\nu_{48}=722\ (B_{1u})$	346‡	$2\nu_{28}=354\ (A_g)$
738 B_{3u}	?	1120	$\nu_{19}-\nu_{33}=1115\ (B_{1g})$
819 B_{1u} or B_{3u}	?	1219	$\nu_{39}+\nu_{35}=1220\ (B_{1g})$
837 B_{3u} ?	$\nu_4-\nu_{48}=838\ (B_{2u})$	1437	$\nu_{37}+\nu_{21}=1444\ (B_{1g})$
879 B_{2u} ?	$\nu_{33}-\nu_{40}=896\ (B_{2u})$	2780	$\nu_{17}+\nu_4=2788\ (B_{1g})$
905	$\nu_{38}+\nu_{25}=915\ (B_{2u})$		
1087	$\nu_5+\nu_{35}=1092\ (B_{1u})$		
1172	$\nu_7+\nu_{34}=1181\ (B_{1u})$		
1193 B_{2u}	$\nu_6+\nu_{36}=1190\ (B_{2u})$		
1214 B_{2u}, 1228 B_{2u}	$\nu_3-\nu_{36}=1220\ (B_{2u})$		
1292	$\nu_{39}+\nu_{33}=1297\ (B_{2u})$		
1311 B_{2u}	$\nu_{21}+\nu_{43}=1325\ (B_{2u})$		
1330	$\nu_5+\nu_{24}=1333\ (B_{1u})$		
1418 B_{2u}	?		
1626 B_{2u}	$(\nu_{35}+\nu_{33})+\nu_{24}=1624\ (B_{2u})$		
2101	$\nu_{37}+\nu_{43}=2103\ (B_{1u})$		
2149	$(\nu_{19}-\nu_{35})+\nu_{33}=2154\ (B_{1u})$		
2431	$\nu_3+\nu_{34}=2434\ (B_{2u})$		
2861	$\nu_{39}+\nu_{21}=2868\ (B_{3u})$		
3152	$\nu_1+\nu_{34}=3154\ (B_{2u})$		

*Denotes the estimated unperturbed position of a fundamental that is affected by Fermi resonance.

†Data from ref. 1.

‡From ref. 3.

8. COMBINATION BANDS

Most of the infrared and Raman bands of the three compounds not used as fundamentals have been explained as combination bands. The assignment is consistent with the known symmetry established in some cases from the infrared solid data (11). The assignments are presented in Table V.

9. AN ALTERNATIVE ASSIGNMENT (B)

An alternative assignment of fundamentals is possible, which obeys all the necessary criteria mentioned above. This assignment differs from that given above (assignment A) only in a few respects. These are pointed out in Table VI. The essential difference is the inclusion of the 386, 350, 339 cm^{-1} system as an out-of-plane Raman mode and assigning the 195, 183, 180 cm^{-1} system to the A_u species. The calculated thermodynamic properties using this alternative assignment (B) are also included in Table IV.

TABLE VI
Alternative assignment (B) of some of the fundamentals

Species	Freq. No.	$C_{10}H_8$, cm^{-1}	$C_{10}H_4D_4$ (1-4-5-8), cm^{-1}	$C_{10}D_8$, cm^{-1}
A_g	ν_5	1239	1140	1006
A_u	ν_{10}	1094		
	ν_{11}	842		
	ν_{12}	730		
	ν_{13}	195		
B_{2g}	ν_{26}	1158	958	875
	ν_{28}	285	280	270
B_{3g}	ν_{37}	1099	1020	929
	ν_{40}	386	350	339

The chief drawbacks of this assignment are: firstly, the vibration frequency at 195 cm^{-1} has to be used as an A_u mode, although it is observed in the Raman spectrum. It is quite unlikely that an A_u mode will become Raman active in the molten state in violation of the selection rule, although Scully and Whiffen (6) in their assignment of the A_u class have assumed such violation. Secondly, two of the d_4 Raman bands at 1020 cm^{-1} and 1140 cm^{-1} used here, are very weak and rather doubtful. The only advantage of this assignment over the previous one (A) presented in this communication is that the numerical deviations from Scully and Whiffen's calculated frequencies for the out-of-plane modes are reduced.

REFERENCES

1. Lippincott, E. R. and O'Reilly, E. J. J. Chem. Phys. **23**, 238 (1955).
2. McClellan, A. L. and Pimentel, G. C. J. Chem. Phys. **23**, 245 (1955).
3. Luther, H., Feldmann, K., and Hampel, B. Z. Elektrochem. **59**, 1008 (1955). Luther, H., Brandes, G., Günzler, H., and Hampel, B. Z. Elektrochem. **59**, 1012 (1955).
4. Manneback, C. J. chim. phys. **46**, 49 (1949).
5. Brandmüller, J. and Schmid, E. Z. Physik, **144**, 428 (1956).
6. Scully, D. B. and Whiffen, D. H. J. Mol. Spectroscopy, **1**, 257 (1957).
7. Bayer, R. W. and O'Reilly, E. J. J. Phys. Chem. **62**, 504 (1958).
8. White, J. U., Alpert, N., and DeBell, A. G. J. Opt. Soc. Am. **45**, 154 (1955).
9. Bernstein, H. J. and Pullin, A. D. E. J. Chem. Phys. **21**, 2188 (1953).
10. Decius, J. C. and Wilson, E. B. J. Chem. Phys. **19**, 1409 (1951). Sverdlov, L. M. Doklady Akad. Nauk S.S.S.R. **78**, 1115 (1951).
11. Person, W. B., Pimentel, G. C., and Schnepp, O. J. Chem. Phys. **23**, 230 (1955).
12. Pimentel, G. C., McClellan, A. L., Person, W. B., and Schnepp, O. J. Chem. Phys. **23**, 234 (1955).
13. Selected Values of Properties of Hydrocarbons. Circular of the National Bureau of Standards. C461. U.S. Govt. Printing Office, Washington, D.C. 1947.
14. Barrow, G. M. and McClellan, A. L. J. Am. Chem. Soc. **73**, 573 (1951).

ULTRAVIOLET ABSORPTION SPECTRA AND ACIDITIES OF ISOMERIC THIATRIAZOLE AND TETRAZOLE DERIVATIVES[1]

EUGENE LIEBER,[2] J. RAMACHANDRAN, C. N. R. RAO, AND C. N. PILLAI

ABSTRACT

The ultraviolet absorption spectra of 5-(substituted)amino-1,2,3,4-thiatriazoles and the corresponding isomeric 1-substituted-tetrazoline-5-thiones have been studied. The spectra and the dipole moments of the 5-(substituted)amino-1,2,3,4-thiatriazoles eliminate the possibility of meso-ionic structures for these compounds. The dipole moments of 5-amino-, 5-methylamino-, and 5-dimethylamino-1,2,3,4-thiatriazole were all high but approximately of the same value (5.77 to 5.84 D). This suggests that the amino thiatriazoles are best represented by conventional covalent structures with significant ionic resonance contributions. The thiatriazole ring system exhibits a characteristic absorption maximum at 250–255 mμ and an electron-withdrawing effect approximately equal to the tetrazolyl ring system. The tetrazolinethionolyl ring system is similarly electron-withdrawing. The relative acidities of the 1-substituted-tetrazoline-5-thiones and the 5-alkylmercaptotetrazoles have also been studied and the results support the observations made on the basis of their ultraviolet absorption spectra.

INTRODUCTION

In recent communications, Lieber and co-workers (1, 2) reported upon the formation and chemistry of 5-(substituted)amino-1,2,3,4-thiatriazoles, I, and the corresponding isomeric 1-substituted-tetrazoline-5-thiones, II (R^2 = H). 5-Amino-1,2,3,4-thiatriazole[3]

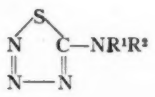

I

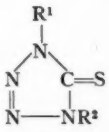

II

(1, 3, 4) (I, R^1 = R^2 = H) has a high melting point (128–130°, decomp.), a well-defined crystalline character, and is easily soluble in water. In general, the crystalline character and relatively high melting points extend to the 5-(substituted)amino-1,2,3,4-thiatriazoles (I, R^1 = (substituted)aryl; R^2 = H) and the corresponding isomeric 1-substituted-tetrazoline-5-thiones (II, R^1 = (substituted)aryl; R^2 = H) (1). This behavior has been explained by the proposal (1) that compounds of structure I (R^2 = H) exist as a tautomeric mixture probably in zwitterion form, the latter being best expressed as a meso-ionic structure,[4] III (R^3 = H):

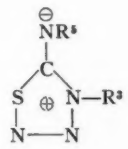

III

[1]*Manuscript received August 26, 1958.*
Contribution from the Department of Chemistry of De Paul University, Chicago, Illinois.
[2]*To whom all requests for reprints and additional information should be addressed.*
[3]*Nomenclature and ring number system from A. M. Patterson and L. T. Cappel, The ring index, Reinhold Publishing Corp., New York. 1940.*
[4]*A study of all the possible tautomeric structures, charged and uncharged, shows that the proton of 5-(substituted)-amino-1,2,3,4-thiatrazoles,* I (R^1 = *alkyl, aryl, or hydrogen,* R^2 = H), *could appear on all the nitrogen atoms present. It is represented on the nitrogen in position 3 in order to bring out its analogy to other meso-ionic structures.*

The 5-(substituted)arylamino-1,2,3,4-thiatriazoles (I, R^1 = substituted aryl; R^2 = H) undergo a facile isomerization in basic media to tetrazole derivatives which are found to be moderately strong acids (1). These latter compounds are also capable of tautomerism, of which structure IV (R^2 = H) is of principal interest due to the formation of the thiol-grouping. Recently, Lieber and co-workers (5) have demonstrated by a study of their infrared absorption spectra that the substances are thiones of structures II and V. The 5-(substituted)mercapto-tetrazoles (IV, R^1 = H; R^2 = alkyl, alkaryl, or aryl) are also of considerable interest in that they are isomeric with structures I and II. Two members of IV, namely, 5-methylmercaptotetrazole (IV, R^1 = H; R^2 = CH_3)

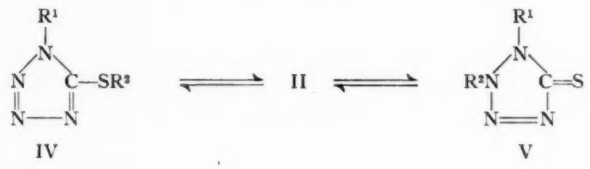

and 5-benzylmercaptotetrazole (IV, R^1 = H; R^2 = $C_6H_5CH_2$), are included in the present investigation. These derivatives are also acids. The present communication reports on the ultraviolet absorption spectra of the isomeric structures I, II, and IV and also the comparative acidities in order to gain an insight into the structural problems pointed out above.

EXPERIMENTAL

Compounds.—The 5-(substituted)amino-1,2,3,4-thiatriazoles (I, R^1 = H or CH_3; R^2 = substituent) and the 1-substituted-tetrazolinethiones (II, R^2 = H) were prepared by methods described elsewhere (1, 2, 3). 5-Methylmercaptotetrazole, IV (R^1 = H; R^2 = CH_3), m.p. 152° (uncorr.), was prepared by the method of Freund and Paradies (6). 5-Benzylmercaptotetrazole, IV (R^1 = H; R^2 = $C_6H_5CH_2$), m.p. 138–138.5° (uncorr.); anal. calc. for $C_8H_8N_4S$: S, 16.68; found: S, 16.75; this compound was prepared by essentially the same procedure by diazotization of S-benzyl isothiosemicarbazide hydrochloride and recrystallization from aqueous ethanol.

Spectroscopy.—A Beckman, Model DU, spectrophotometer and a Cary recording spectrophotometer were used for all the measurements. The wavelengths are recorded in mμ and the intensities in terms of logarithms of the molar extinction coefficients.

Comparative acidities.—The apparent dissociation constants of II (R^2 = H) and IV (R^2 = CH_3 and $C_6H_5CH_2$ respectively) were determined by potentiometric titration in 50% ethanol using a precalibrated photovolt pH meter. Standardization of the apparatus was accomplished with a series of substituted benzoic acids having reported pK_a's in the range encountered in the present investigation. It was found that differences in apparent dissociation constants as low as 0.1 pK_a units were reproducible.

Dielectric constant measurements.—The dielectric constant measurements were made in purified dioxan essentially as described in the literature (7).

RESULTS AND DISCUSSION

5-(Substituted)amino-1,2,3,4-thiatriazoles

The ultraviolet absorption data are summarized in Table I with a few typical absorption spectral curves shown in Fig. 1. 5-Amino-1,2,3,4-thiatriazole (I, R^1 = R^2 = H) shows

a strong absorption band at 267 mμ and the introduction of a saturated substituent causes a prominent bathochromic shift. Baker and co-workers (8, 9) during their investigation of cyclic meso-ionic compounds found that sydnones which contained no

TABLE I

Ultraviolet absorption spectra of 5-(substituted)amino-1,2,3,4-thiatriazoles[b] (I)

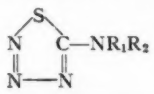

R_1	R_2	log ε		log ε		log ε	
		λ_{max}	max	λ_{max}	max	λ_{max}	max
H	H	250[a]	3.51	267	3.68	—	—
CH_3	H	255[a]	—	274	—	—	—
n-C_4H_9	H	255[a]	3.65	276	3.84	—	—
n-C_7H_{15}	H	255[a]	3.68	277	3.99	—	—
$C_6H_5CH_2$	H	255[a]	3.62	275	3.85	—	—
CH_3	CH_3	255[a]	3.40	279	3.79	—	—
C_6H_5	H	241	3.91	285[a]	3.91	302	4.03
4-$CH_3C_6H_4$	H	242	3.96	290[a]	3.97	305	4.03
4-ClC_6H_4	H	246	3.98	293	4.07	306[a]	4.03
4-$CH_3OC_6H_4$	H	243	3.98	298	4.04	311[a]	3.99
4-$N(CH_3)_2C_6H_4$	H	261.5	4.18	—	—	322.5	4.06
4-$NO_2C_6H_4$	H	222	—	—	—	335	—

[a]Appears as a shoulder.
[b]All measurements in ethanolic solution of pH 7.5.

other conjugated system showed a well-defined absorption maximum around 292 mμ in the ultraviolet region. They explained this by the suggestion that the sydnone ring possessed aromatic character and was a hybrid of a large number of contributing forms. Henry, Finnegan, and Lieber (10) found that 1,3-dialkyl-5-aminotetrazoles, VI, have a characteristic absorption band between 254 and 258 mμ, whereas the usual substituted tetrazoles containing no other conjugated system have been reported to show only end absorption (11, 12). On this basis a structure of the type VI was proposed. Baker and Ollis (9) have suggested that meso-ionic structures be represented so that the sydnone ring becomes positively charged so as to emphasize its aromatic nature. This is shown by structure VII, which does not imply that a complete negative charge is resident

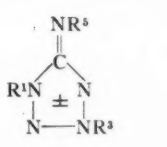

VI

VII

$R^5 = H$
$R^1 = R^3 =$ alkyl

upon the exocyclic nitrogen atom. The difficulty of representing such structures is recognized (9), although the attempted exclusion of structures which can be represented satisfactorily[5] by any one covalent or polar structure might exclude compounds which

[5]*This was recognized by Baker and Ollis (9), who pointed out that "the inevitable ambiguity here is the word satisfactory".*

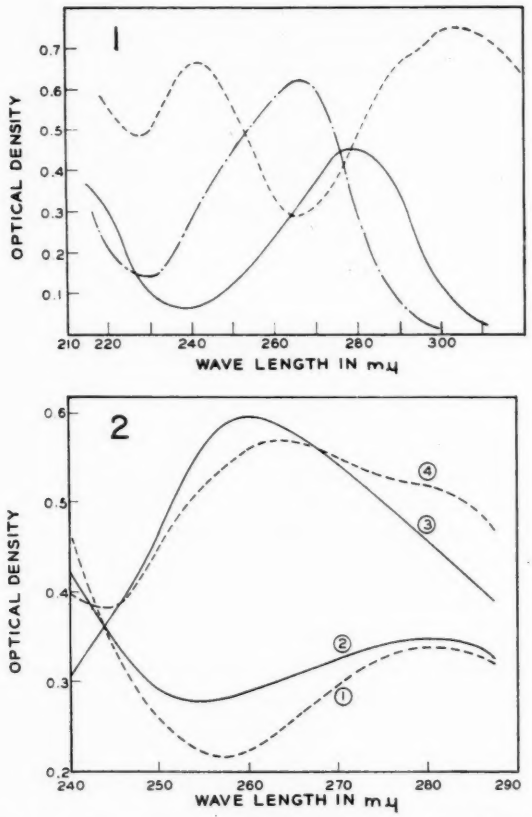

FIG. 1. Ultraviolet absorption spectra of 5-(substituted)amino-1,2,3,4-thiatriazoles:
– – – – – 5-*p*-tolylamino;
– · – · – · 5-amino;
———— 5-dimethylamino.

FIG. 2. Ultraviolet absorption spectra of 1-phenyl tetrazoline-5-thione (II, $R^2 = H$; $R^1 = C_6H_5$) in solvents of varying pH:
(1) 0.1 *N* NaOH;
(2) pH 7.5;
(3) 0.1 *N* HCl;
(4) 95% ethanol.

are, indeed, meso-ionic. Thus, Henry, Finnegan, and Lieber (10) found that, surprisingly, 2-methyl-5-alkylaminotetrazoles, VIII, which have been considered to possess the tetrazole ring system with normal covalent bonds, appear to exist principally in meso-ionic form, IX, since their ultraviolet absorption spectra are very similar to those for the 1,3-dialkyl-5-iminotetrazoles (structures VI or VII). The introduction of a methyl group

VIII IX

into the 5-amino position of either 1- or 2-methyl-5-aminotetrazole effects a bathochromic shift in the absorption maximum (10). The above ideas have been supported by the X-ray analysis of the hydrobromide of 1,3-dimethyl-5-iminotetrazole (13), and a modified 3-dimensional Fourier synthesis (14) has demonstrated unambiguously that the structures are cyclic meso-ionic. In their survey of known meso-ionic compounds Baker and Ollis (9) present structures which bear a close analogy to that of structure III proposed in this communication. Two such structures X and XI are shown below in comparison with structure III (*vide ut supra*).[6] Accordingly, the ultraviolet absorption data (Table I) and the analogies discussed above may appear to support a meso-ionic structure for the

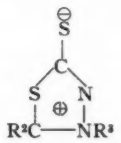

X

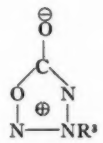

XI

5-(substituted)amino-1,2,3,4-thiatriazoles (III).

Baker and Ollis (9) have defined a meso-ionic compound as a 5- or possibly 6-membered heterocyclic compound which cannot be satisfactorily represented by any one covalent or polar structure and possesses a sextet of electrons in association with all the atoms comprising the ring. The ring bears a fractional positive charge balanced by a corresponding negative charge located on a covalently attached atom or group of atoms. The 5-(substituted)amino-1,2,3,4-thiatriazoles can be represented as meso-ionic structures III (R^3 = H). However, a conclusive assignment of meso-ionic structure in these compounds is not possible on the basis of the ultraviolet spectra, since the dimethylamino derivative (I, $R^1 = R^2 = CH_3$) *in which no tautomerism is possible* also shows the same characteristic absorptions. For this reason the dipole moments of 5-amino- (I, $R^1 = R^2$ = H); 5-methylamino- (I, R^1 = H; $R^2 = CH_3$); and 5-dimethylamino-1,2,3,4-thiatriazole (I, $R^1 = R^2 = CH_3$), respectively, were determined. Although it has been demonstrated by Kaufman and co-workers (7) that this measurement does not provide a sound basis for the assignment of meso-ionic structures, it was felt that it could contribute to a clearer picture of the thiatriazole ring system. Further, if structures I (R^1 = H) are meso-ionic there would be a significant difference in the dipole moments of the 5-(monosubstituted)amino- and 5-(disubstituted)amino-1,2,3,4-thiatriazoles. The dipole moments obtained are summarized below:

Compound I		
R^1	R^2	μ (Debye units)
H	H	5.77
H	CH_3	5.72
CH_3	CH_3	5.84

While the dipole moments are large they are all approximately the same. It is therefore suggested that 5-amino-1,2,3,4-thiatriazole and its derivatives are best represented by

[6]*Recent investigations (15, 16) in progress in this laboratory have revealed that substances formerly considered to be derivatives of azidodithiocarbonic acid,* $N_3C(S)SH$, *are in reality derivatives of 1,2,3,4-thiatriazoline-5-thione, the simplest members of which has a relatively high decomposition point and is nicely crystalline. Its structure should be closely related to* XI (R^3 = H) *replacing the oxygens by sulphur.*

conventional covalent structures and that the ultraviolet absorption spectral characteristics are due to the interaction of the thiatriazole nucleus with the substituent in the 5-position. Unfortunately, the dipole moment data do not provide the direction of the moment in these compounds.[7] The thiatriazole ring contains three nitrogen atoms (positions 2, 3, and 4) which are sp^2 hybridized and which should induce a large concentration of negative charge away from the ring and the substituent in the 5-position. The ultraviolet absorption data supports this suggestion.

From the data in Table I, it can be seen that all of the 5-alkyl substituted derivatives exhibit a shoulder at 255 mμ and an absorption band around 275 mμ. Since the unsubstituted compound (I, $R^1 = R^2 = H$) also exhibits a shoulder at 250 mμ, it is considered that this 250–255 mμ absorption is characteristic of the 1,2,3,4-thiatriazole ring system:

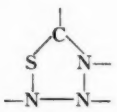

The major absorption bands at the longer wavelength are caused by the interaction of the amino or the substituted group with the heterocyclic nucleus. It will also be noted from Table I that there is very little change in the position of this maximum with different alkyl substituents including the benzyl group in the 5-amino position. Table I also shows that all of the 5-arylamino-1,2,3,4-thiatriazoles studied (I, $R^1 = H$; R^2 = aryl) show a distinct peak in the vicinity of 242 mμ, probably due to the thiatriazole nucleus. Also indicated are a shoulder and a peak at longer wavelengths probably due to the interaction of the aromatic ring with the heterocyclic nucleus. Analogies with the ultraviolet absorption spectra of 5-(substituted)amino tetrazoles (17) and substituted amino-1,2,3-triazoles (18) can be made. The 5-arylamino-1,2,3,4-thiatriazoles (I, $R^1 = H$; R^2 = aryl) may also be considered as substituted benzenes, XII. The position of the absorption maxima of the compounds represented by structure XII depends markedly

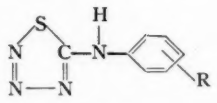

XII

on the nature of the substituent R on the aromatic ring, the λ_{max} increasing approximately in proportion to the electron-donating power of the substituent. This proportionality indicates that the grouping XIII is an electron-withdrawing group, capable of appreciable resonance interaction. Recently, Rao (19) has correlated the ultraviolet absorption spectra of meta- and para-disubstituted benzenes with reactivities and resonance parameters (20). The correlation of the wavelength displacements with the reactivities and

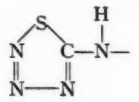

XIII

[7] *An investigation on an extended series of appropriate structures* I ($R^1 = H$; R^2 = *substituted aryl*) *to determine the direction of this moment is in progress and will be reported upon in a separate communication.*

resonance parameters indicate that the electron-withdrawing ability of XIII by resonance interaction is of the same order of magnitude as that of the 5-aminotetrazolyl group:

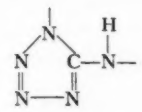

This is surprising in view of the somewhat smaller electronegativity value for sulphur over that of nitrogen (21).

Accordingly, from the above discussion it is concluded that the ultraviolet absorption data and the dipole moments reported are due to hybridization effects (22) and the contribution of ionic resonance structures XIV and XV. The case here is similar to that reported by Kaufman and co-workers (7) for 1-ethyltetrazole, XVI, which has a higher moment (5.46 D) than the meso-ionic compound 1,3-dimethyl-5-iminotetrazole (4.02 D) (VI, $R^5 = H$; $R^1 = R^3 = CH_3$). In the case of XVI the moment is directed with the

XIV XV

XVI XVII

negative pole away from the carbon atom in the ring, the high dipole moment probably due to the hybridization effects of the 2, 3, and 4 ring nitrogens and resonance contributions of ionic structures (7). In the case of 1,3-dimethyl-5-imino-tetrazole (VI, $R^5 = H$; $R^1 = R^3 = CH_3$; XVII), the moment is directed with the negative pole towards the exocyclic nitrogen at the 5-position, the lower value of the moment being the results of the hybridization effect of the nitrogen in position-2 in the ring of XVII, which results in a concentration of negative charge away from the exocyclic nitrogen atom and the ring.

1-Substituted Tetrazoline-5-thiones

The ultraviolet absorption spectral data obtained with the 1-(substituted)phenyl-tetrazoline-5-thiones (II, $R^2 = H$; $R^1 = aryl$) are summarized in Table II. Considering these compounds as substituted benzene, represented by the structure XVIII, it will be noted (Table II) that the compounds display primary absorption bands in the region 217–254 mμ, which can be ascribed to the primary bands of the substituted benzene (19).

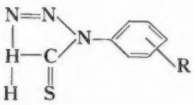

XVIII

This primary absorption maximum varies in proportion to the electron-donating power of the substituents on the 1-phenyl group. Thus, a bathochromic shift in the absorption maximum is observed with substitution by groups capable of donating electrons by resonance interaction. This effect is appreciable in the case of the *p*-dimethylamino derivative (XVIII, R = 4-$(CH_3)_2N$) which exhibits the primary band at 254 mμ. From the

TABLE II

Ultraviolet absorption spectra of 1-substituted tetrazoline-5-thiones

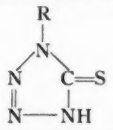

R	λ_{max}	log ϵ_{max}	λ_{max}	log ϵ_{max}	λ_{max}	log ϵ_{max}	In 0.1 *N* NaOH in 95% ethanol λ_{max}
C_6H_5	217.5	4.19	262	3.85	280[a]	3.81	280
2-$CH_3C_6H_4$	—	—	253	3.98	271[a]	3.71	—
2-$CH_3OC_6H_4$	217	4.53	254	4.43	274[a]	4.23	—
4-FC_6H_4	219	4.12	262	3.91	282[a]	3.79	—
4-$CH_3C_6H_4$	220	4.50	262.5	4.18	282[a]	4.10	278
4-$CH_3OC_6H_4$	229	4.14	264	3.98	280[a]	3.91	274
4-ClC_6H_4	226	4.22	263.5	3.77	288[a]	3.79	—
2,4-$Cl_2C_6H_3$	222[a]	4.27	250[a]	3.96	281[a]	3.61	—
4-$(CH_3)_2NC_6H_4$	254	4.31	295	4.22	—	—	308[a]
4-$NO_2C_6H_4$	—	—	252	4.32	332.5	3.91	—
$C_6H_5CH_2$	—	—	248	4.09	—	—	—
CH_3	—	—	245	4.13	—	—	245

[a]Appears as a shoulder.

correlation of Rao (19), it is found that the 1-tetrazoline thionyl group, XIX, is electron withdrawing in nature of about the same order of magnitude as the 5-amino-tetrazolyl group and the 5-amino-1,2,3,4-thiatriazole group (XIII).

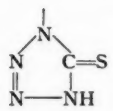

XIX

In addition to the primary band of the substituted benzene, the 1-aryl-tetrazoline-5-thiones (XVIII), in general, exhibit another absorption maximum between 252 and 295 mμ and a shoulder between 270 and 288 mμ (Table II). The absorption maximum is considered to be due to the acid XVIII and the shoulder as being due to the anion XX. No definite assignments seem to be possible in the case of the 1-(*p*-nitro)phenyl derivative (XVIII, R = 4-O_2N—C_6H_4), probably due to the absorption of the nitro group itself.

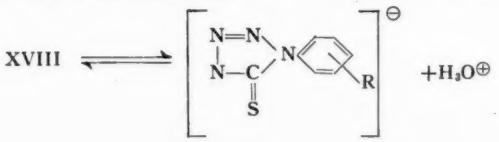

XX

In Fig. 2 are shown the absorption spectra of 1-phenyl-tetrazoline-5-thione (II, $R^2 = H$; $R^1 = C_6H_5$) in solvents of different pH. In 95% ethanol, the bands due to the undissociated acid and the anion are observed at 262 and 280 mμ respectively. In 0.1 *N* hydrochloric acid, however, the 262 mμ band appears as a strong peak and the shoulder at 280 mμ disappears. In 0.1 *N* sodium hydroxide solution, the shoulder at 280 mμ assigned to the anion becomes a peak and the 262 mμ band is absent. From Fig. 2 it can be seen that the compound is almost completely dissociated even in a buffer of pH 7.5. The absorption spectra further indicates that the anion is considerably resonance stabilized, since the anions absorb at higher wavelengths than the undissociated acids. Table II also lists the absorption maxima of some of the 1-substituted tetrazoline-5-thiones (II, $R^2 = H$) in 0.1 *N* sodium hydroxide in 95% ethanol. From the data in Table II it is seen that the 1-alkyl-derivatives exhibit only one absorption maximum at lower wavelengths than the 1-alkyl-derivatives. Further, the anion of 1-methyltetrazoline-5-thione (II, $R^2 = H$; $R^1 = CH_3$) absorbs at the same wavelength as the undissociated acid. This suggests that there is little or negligible extra resonance stabilization of the anion in the alkyl derivatives.

A study of the apparent dissociation constants of the 1-substituted tetrazoline-5-thiones (II, $R^2 = H$) summarized in Table III seems to support the observations based on the ultraviolet spectra regarding the electrical effects of the substituents in this system (R in XVIII). A plot of the pK_a values of the 1-substituted phenyltetrazoline-5-thiones

TABLE III

Apparent dissociation constants of 1-substituted tetrazoline-5-thiones (Temperature, 25±2° C)

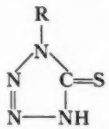

R	pK_a[a]
4-$NO_2C_6H_4$	3.36
2,4-$Cl_2C_6H_3$	3.41
4-FC_6H_4	3.61
4-ClC_6H_4	3.62
2-$CH_3C_6H_4$	3.62
C_6H_5	3.65
2-$CH_3OC_6H_4$	3.74
4-$CH_3C_6H_4$	3.75
4-$CH_3OC_6H_4$	3.78
$C_6H_5CH_2$	3.80
C_2H_5	3.85
CH_2	3.86
CH_2=CH—CH_2	3.91
4-$(CH_3)_2N$—C_6H_4	4.09

[a]Mean of three independent determinations.

(XVIII) against the Hammett sigma (σ) values for groups (23) is reasonably linear as shown in Fig. 3. The slope of this line, the rho value (ρ), is smaller than the rho values for the 5-(substituted)phenylamino-4-phenyl-1,2,3-triazoles and the 5-(substituted)-phenylaminotetrazoles (24, 25). This indicates a smaller magnitude of the electrical effects of the substituents in the tetrazolinethione system (XIX). It is, however, interesting to note (Table III) that while the pK_a of the aryl derivatives varies between 3.36

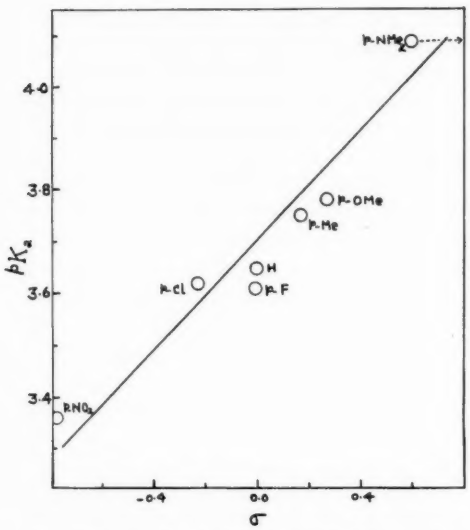

FIG. 3. pK_a of 1-substituted tetrazoline-5-thiones versus Hammet sigma (σ) values for groups.

and 4.09, the alkyl derivatives possess pK_a values between 3.80 and 3.91. In 1-(*p*-dimethylamino)phenyltetrazoline-5-thione (XVIII, R = 4-$(CH_3)_2N$) where there is strong complimentary substitution, the displacement of the primary benzene band in the ultraviolet spectrum is greatest as is also the effect on the acidity. The 2-methyl, 2-methoxy, and 2,4-dichlorophenyl derivatives exhibit the ultraviolet absorption bands (Table II) at wavelengths lower than the corresponding para isomers. The ortho derivatives also show slight increase in acidity from the para derivatives (Table III). Such behavior may be due to steric effects of the ortho substituents (26, 28). The possibility of intramolecular hydrogen bonding cannot be excluded in the case of the ortho-anisyl derivative (XVIII, R = 2-$CH_3OC_6H_4$). The band displacement exhibited by the *p*-fluorophenyl derivative (XVIII, R = 4-FC_6H_4) is too small to be accounted for on the basis of the proposed resonance parameter of -0.44 (20) for the *p*-fluoro group. A lower resonance parameter of the order of -0.10 seems more reasonable (26, 27).

TABLE IV

Apparent dissociation constants of 5-(substituted)mercapto tetrazoles
(Temperature, 25±2° C)

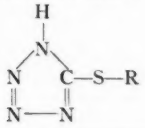

R	pK_a[a]
CH_3	4.07
$C_6H_5CH_2$	3.94

[a]Mean of three independent measurements.

The 5-alkyl mercaptotetrazoles (IV, $R^1 = H$; R^2 = alkyl)[8] are weaker acids (Table IV) compared to the corresponding 1-substituted tetrazoline-5-thiones (II, $R^2 = H$). The ultraviolet absorption of 5-alkyl mercaptotetrazoles (Table V) are similar to the derivatives of tetrazole (17) rather than those of the tetrazoline-5-thiones. Since there is no conjugating group in the 5-position, these mercapto derivatives absorb at lower wavelengths. Further, the ultraviolet absorption spectrum of the 5-methylmercapto derivative (IV, $R^1 = H$; $R^2 = CH_3$) in alkaline solution shows little extra resonance stabilization of the anion.

TABLE V

Ultraviolet absorption spectra of 5-substituted mercapto tetrazoles

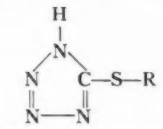

			In 0.1 *N* sodium hydroxide in 95% ethanol
R	λ_{max}	log ϵ	λ_{max}
CH_3	230[a]	3.52	235[a]
$C_6H_5CH_2$	220[a]	4.05	—

[a]Appears as a shoulder.

ACKNOWLEDGMENT

The authors gratefully acknowledge grants-in-aid from the Frederick Gardner Cottrell Program of the Research Corporation, New York, N.Y., and the Lilly Research Laboratories, Eli Lilly and Company, Indianapolis, Indiana, which made this study possible.

REFERENCES

1. LIEBER, E., PILLAI, C. N., and HITES, R. D. Can. J. Chem. **35**, 832 (1957).
2. LIEBER, E. and RAMACHANDRAN, J. Can. J. Chem. **37**, 101 (1959).
3. LIEBER, E., OFTEDAHL, E., PILLAI, C. N., and HITES, R. D. J. Org. Chem. **22**, 441 (1957).
4. FREUND, M. and SCHANDER, A. Ber. **29**, 2500 (1896).
5. LIEBER, E., RAO, C. N. R., PILLAI, C. N., RAMACHANDRAN, J., and HITES, R. D. Can. J. Chem. **36**, 801 (1958).
6. FREUND, M. and PARADIES, T. Ber. **34**, 3110 (1910).
7. KAUFMAN, M. H., ERNSBERGER, F. M., and MCEWEN, W. S. J. Am. Chem. Soc. **78**, 4197 (1956).
8. BAKER, W., OLLIS, W. D., and POOLE, V. D. J. Chem. Soc. 307 (1949).
9. BAKER, W. and OLLIS, W. D. Quart. Revs. **11**, 15 (1957).
10. HENRY, R. A., FINNEGAN, W. G., and LIEBER, E. J. Am. Chem. Soc. **76**, 2894 (1954).
11. ELPERN, B. and NACHOLD F. C. J. Am. Chem. Soc. **72**, 3379 (1950).
12. ELPERN, B. J. Am Chem. Soc. **75**, 661 (1953).
13. BRYDEN, J. H., HENRY, R. A., FINNEGAN, W G., BOSCHAN, R. H., MCEWAN, W. S., and VAN DOLAH, R. W. J. Am. Chem. Soc. **75**, 4863 (1953).
14. BRYDEN, J. H. Acta Cryst. **8**, 211 (1955); **9**, 874 (1956); **10**, 148 (1958).
15. LIEBER, E., PILLAI, C. N., RAMACHANDRAN, J., and HITES, R. D. J. Org. Chem. **22**, 1750 (1957).
16. LIEBER, E., OFTEDAHL, E., GRENDA, S., and HITES, R. D. Chem. & Ind. 893 (1958).
17. LIEBER, E., RAO, C. N. R., and PILLAI, C. N. Current Sci. (India), **26**, 167 (1957).
18. LIEBER, E., RAO, C. N. R., and CHAO, T. S. Spectrochim. Acta, **10**, 250 (1958).
19. RAO, C. N. R. Chem. & Ind. 666 (1957); 1239 (1957).
20. TAFT, R. W., JR. *In* Steric effects in organic chemistry. *Edited by* M. S. Newman. John Wiley & Son, Inc., New York. 1956. Chap. 13.
21. HINE, J. Physical organic chemistry. McGraw-Hill Book Company, New York. 1956. p. 7.

[8]*The* C=S *and the* —N—C=S *frequencies are not apparent in these compounds as in the 1-substituted-tetrazoline-5-thiones,* II ($R^2 = H$), *(5).*

22. COULSON, C. A. Valence. Oxford University Press. 1952.
23. JAFFE, H. H. Chem. Revs. **53**, 191 (1953).
24. LIEBER, E., RAO, C. N. R., CHAO, T. S., and RAMACHANDRAN, J. J. Org. Chem. (1959).
25. HENRY, R. A., FINNEGAN, W. G., and LIEBER, E. J. Am. Chem. Soc. **76**, 88 (1954).
26. JONES, R. N., FORBES, W. F., and MUELLER, W. A. Can. J. Chem. **35**, 504 (1957).
27. RAO, C. N. R. J. Sci. Ind. Research (India), **17** (In press) (1958).
28. HERBST, R. M. and WILSON, K. R. J. Org. Chem. **22**, 1142 (1957).

THE CHARACTERIZATION OF TRI-*O*-TOSYL SUCROSE[1]

P. D. Bragg and J. K. N. Jones

ABSTRACT

Tri-*O*-tosyl sucrose was synthesized by the action of *p*-tolylsulphonyl chloride upon sucrose in pyridine, and the tosyl groups were shown by methylation to be mainly (84%) located on the three primary hydroxyl groups.

INTRODUCTION

Hockett and Zief (1) prepared sulphonyl esters of sucrose by reaction with methane sulphonyl (mesyl) chloride or *p*-tolyl-sulphonyl (tosyl) chloride in pyridine solution. Although none of the products were isolated in crystalline form, analytical values were recorded for the tri-*O*- and octa-*O*-mesyl and tosyl sucrose derivatives. Tosyl and mesyl compounds undergo a large number of important reactions (2) so thorough characterization of the trisubstituted sucrose was considered to be desirable.

Tri-*O*-tosyl sucrose was prepared by Hockett and Zief's method (1). Complete methylation to tri-*O*-tosyl-penta-*O*-methyl sucrose was obtained by a single treatment with methyl iodide and silver oxide in dimethylformamide solution (3). Detosylation and subsequent hydrolysis gave a mixture of tri-*O*-methyl glucose, di-*O*-methyl fructose, and di-*O*-methyl glucose. A small amount (5%) of tri-*O*-methyl fructose was also present.

The methyl ethers of glucose were characterized by conversion to 2,3,4-tri-*O*-methyl-*N*-phenyl-D-glucosylamine and 2,4-di-*O*-methyl-*N*-*p*-nitrophenyl-D-glucosylamine respectively.

The di-*O*-methyl fructose was chromatographically identical with 3,4-di-*O*-methyl fructose. The measured rotation was lower than the quoted value (4) but this was probably due to the presence of an optically inactive impurity derived from the filter paper on which the sugar was fractionated. The identity of the fructose methyl ether was confirmed as 3,4-di-*O*-methyl-D-fructofuranose by periodic acid oxidation followed by bromine oxidation to dimethylsuccinic acid and the isolation of crystalline (−)-D-dimethoxysuccinamide formed by the action of ammonia on the methyl ester (5).

The isolation of 2,4-di-*O*-methyl-D-glucose from the hydrolysis mixture suggests that some undermethylation had occurred. In glucose the hydroxyl group at $C_{(3)}$ is less reactive than that at $C_{(2)}$, $C_{(4)}$, or $C_{(6)}$ (9), and 2,4-di-*O*-methyl glucose would result from undermethylation.

This sugar might arise through the formation of a 3,6-anhydro ring on the glucose residue of sucrose during methylation. But no 2,4-di-*O*-methyl-D-glucose was formed from methyl 2,4-di-*O*-methyl-3,6-anhydro α-D-glucoside when the latter was submitted to the conditions of hydrolysis used for the methylated sucrose derivative. The infrared spectrum of the methylated sucrose showed that hydroxyl groups were absent. However, it has been observed in these laboratories that incompletely methylated polysaccharides which had been submitted to the Kuhn methylation procedure in dimethylformamide (3) gave an infrared spectrum without hydroxyl peaks, and yet gave amounts of sugars which indicated that methylation was incomplete. This phenomenon is as yet unexplained.

The tri-*O*-tosyl sucrose consisted mainly therefore of 6,1[1],6[1]-tri-*O*-tosyl sucrose. This

[1]*Manuscript received November 10, 1958.*
Contribution from the Department of Chemistry, Queen's University, Kingston, Ontario.

result is in agreement with the results of Lemieux and Barrette (6), who found that the trianhydro sucrose derived from the above compound was different from that obtained from 4,1^1,6^1-tri-*O*-tosyl sucrose, which had been prepared from 2,3,6,3^1,4^1-penta-*O*-acetyl sucrose (7). This structure is also supported by the isolation of a sirupy di-iodo-di-deoxy-mono-*O*-tosyl sucrose pentaacetate from the action of sodium iodide (8) on tri-*O*-tosyl sucrose pentaacetate. The iodine atoms are probably located on the $C_{(6)}$ of both fructose and glucose moieties, the tosyl group on fructose-$C_{(1)}$ remaining unsubstituted. In agreement with this, Lemieux and Barrette (6) obtained only a mono-iodo derivative from 4,1^1,6^1-tri-*O*-tosyl sucrose.

It is probable that the tri-*O*-tosyl sucrose is not pure. However the high yield (89%) of di-iodo-di-deoxy-mono-*O*-tosyl sucrose pentaacetate (analysis indicates 94% purity) that was prepared from it shows that at least 84% of the preparation must have tosyl groups on $C_{(6)}$ and $C_{(6^1)}$. Since no other tri-*O*-methyl glucoses were found, which would be the case if other tri-*O*-tosyl sucroses were present, the preparation is probably purer than the above figure. The chromatography solvent used (*n*-butanol : ethanol : water, 3 : 1 : 1) resolved 2,3,4-tri-*O*-methyl-D-glucose (R_f 0.62) from 2,3,6-tri-*O*-methyl- (R_f 0.59) and 3,4,6-tri-*O*-methyl-D-glucose (R_f 0.58). Complete separation from 2,4,6-tri-*O*-methyl-D-glucose (R_f 0.61) was not obtained but since tosylation at $C_{(3)}$ of sucrose is unlikely (9) it is probable that this methylated sugar was not present.

Reduction of 6,1^1,6^1-tri-*O*-tosyl sucrose with lithium aluminum hydride gave 6,6^1-dideoxy sucrose (cf. 6), which was cleaved by invertase to 6-deoxy-D-glucose and D-rhamnoketose.

EXPERIMENTAL

Paper chromatograms were developed in the solvent system: *n*-butanol : ethanol : water (3 : 1 : 1). Reducing sugars were detected by *p*-anisidine hydrochloride and a resorcinol spray reagent was used for the specific detection of ketoses (10). Melting points are uncorrected and were determined on a Kofler microheating stage.

Tri-O-tosyl Sucrose

This was prepared by Hockett and Zief's method (1) and had $[\alpha]_D^{17}$ +41.3° (*c*, 2.06 in chloroform). Anal. Calc. for $C_{33}H_{40}O_{17}S_3$: S, 11.9%. Found: S, 11.5%.

Methylation of Tri-O-tosyl Sucrose

Tri-*O*-tosyl sucrose (7.3 g), dried over phosphoric oxide, was dissolved in dimethylformamide (120 ml), which had been distilled from barium oxide, and methyl iodide (45 ml). Silver oxide (45 g) was added portionwise with vigorous stirring, the temperature was not permitted to rise above 35°. After 7 hours, the mixture was filtered, the precipitate was washed with dimethylformamide (2×50 ml), and then chloroform (50 ml), and the combined liquids were poured into 1% aqueous sodium cyanide (500 ml). The aqueous layer was shaken with chloroform, which was then added to the chloroform layer and the combined solutions were washed well with water, dried (sodium carbonate), and concentrated to a sirup (5.33 g) $[\alpha]_D^{24}$ +49.5° (*c*, 4.05 in chloroform). The product showed no hydroxyl peaks in its infrared spectrum. Anal. Calc. for $C_{38}H_{60}O_{17}S_3$: OMe, 17.8%. Found: OMe, 20.7%. The high value for methoxyl suggests contamination of the product with dimethylformamide.

Detosylation of the Methylated Sucrose

The sirup (5.2 g) in 85% aqueous methanol (200 ml) was stirred with 4% sodium amalgam (125 g) for 18 hours. After filtration and neutralization with solid carbon

dioxide, the solution was concentrated to a solid which was extracted with boiling chloroform (3×150 ml). The extract afforded a sirup (2.6 g) which on concentration did not give a solution in water or 50% aqueous ethanol sufficiently clear for optical rotation measurements.

Hydrolysis and Separation of the Methyl Sugars

The methylated sucrose (2.6 g) was hydrolyzed with 0.01 *N* sulphuric acid (150 ml) at 100° for 1½ hours. After neutralization the resulting mixture (2.4 g) was examined on paper chromatograms. With *p*-anisidine, tri-*O*-methyl glucose (R_f 0.62), di-*O*-methyl fructose (R_f 0.52), and di-*O*-methyl glucose (R_f 0.48) were detected. The resorcinol spray showed the presence of a small amount of a further component, tri-*O*-methyl fructose, having an identical R_f value to the tri-*O*-methyl glucose which previously masked it.

The mixture of sugars was fractionated on a cellulose column (30×3 cm) using methyl ethyl ketone : water azeotrope as solvent (7). A complete separation of the component sugars was not obtained so the fractions were combined to give a tri-*O*-methyl hexose fraction (0.75 g) and a di-*O*-methyl hexose fraction (1.2 g).

The tri-*O*-methyl hexose fraction was dissolved in 0.35% methanolic hydrogen chloride (25 ml) and the rotation was followed until equilibrium was reached (22 hours). After neutralization with silver oxide and removal of the silver ions with hydrogen sulphide, tri-*O*-methyl glucose (R_f 0.65) was separated on sheet paper chromatograms from a small amount of tri-*O*-methyl methyl fructofuranoside. The di-*O*-methyl hexose fraction was similarly fractionated into di-*O*-methyl glucose (R_f 0.49) and di-*O*-methyl methyl fructofuranoside (R_f 0.66).

Characterization of the Methyl Sugars

Tri-*O*-methyl hexose (280 mg) was refluxed with redistilled aniline (110 mg) in ethanol (10 ml). Removal of the ethanol under reduced pressure initiated crystallization. After recrystallization from ether – light petroleum (60–80°), the colorless needles had m.p. and mixed m.p. 144°–146° with authentic 2,3,4-tri-*O*-methyl-*N*-phenyl-D-glucosylamine. Anal. Calc. for $C_{15}H_{23}O_5N$: OMe, 31.3%. Found: OMe, 30.9%.

The di-*O*-methyl hexose (202 mg), having $[\alpha]_D$ +54° (*c*, 2.0 in water), was refluxed for 3 hours with *p*-nitroaniline (164 mg) in ethanol (5.5 ml) and acetic acid (5 drops). The reaction mixture was concentrated to a smaller volume and cooled to 5°. The light-brown precipitate was washed with ethanol and recrystallized as pale yellow crystals from ethyl acetate, m.p. 251°, $[\alpha]_D^{24}$ −250° (*c*, 0.38 in pyridine). Anal. Calc. for $C_{14}H_{20}O_7N_2$: OMe, 18.9%. Found: OMe, 19.9%. 2,4-Di-*O*-methyl-*N*-*p*-nitrophenyl-D-glucosylamine has m.p. 250°–251° $[\alpha]_D$ −252° (pyridine) (11).

The di-*O*-methyl methyl fructofuranoside was hydrolyzed (0.05 *N* H_2SO_4; 2 hours; 100°) to yield di-*O*-methyl-D-fructose (0.57 g), $[\alpha]_D$ −45° (*c*, 2.64 in water). Anal. Calc. for $C_8H_{16}O_6$: OMe, 29.7%. Found: OMe, 28.3%. Di-*O*-methyl fructose (160 mg) in 1.15 *M* periodic acid (5 ml) was kept at 25° for 3 days. The solution was freed from iodine by extraction with carbon tetrachloride. Barium chloride (0.5 g) and excess barium carbonate were added, and after filtration, enough bromine was added to give a saturated solution. After 2 days, excess bromine was removed by aeration, hydrobromic acid by lead carbonate, and lead ions with hydrogen sulphide. The solution was filtered and the filtrate was concentrated to a solid which was then refluxed overnight with 4% methanolic hydrogen chloride. Excess hydrogen chloride was removed with lead carbonate, as above, and the filtrate was concentrated to a solid. Chloroform extraction of the solid and

subsequent evaporation of the solvent yielded a sirup (40 mg) which was dissolved in methanolic ammonia (3 ml) and kept at 0°. After 6 days, white crystals (15 mg) of (−)-D-di-methoxysuccinamide were deposited, $[\alpha]_D$ −94° (*c*, 0.60 in water), m.p. and mixed m.p. 275° (capillary tube) with authentic (−)-D-dimethoxysuccinamide. The compound showed maxima in the infrared at 3330 (s), 3150 (s), 2910 (w), 1637 (s), 1425 (s), 1341 (m), 1314 (w), 1210 (m), 1193 (m), 1139 (m), 1100 (s), 1023 (m), 881 (m), 825 (w), 805 (m), 705 (m) cm^{-1} and gave an identical infrared spectrum to authentic (−)-D-dimethoxysuccinamide.

Reaction of Sodium Iodide with Tri-O-tosyl Sucrose

Tri-*O*-tosyl sucrose pentaacetate (2.0 g) was heated at 110° for 2 hours with sodium iodide (5 g) in acetone (5 ml). The reaction mixture was poured into chloroform and after filtration was washed well with water containing sodium thiosulphate (5%) and sodium hydrogen carbonate (5%). After drying ($CaCl_2$), concentration of the chloroform extract gave sirupy mono-*O*-tosyl-di-iodo-di-deoxy sucrose pentaacetate (1.7 g) $[\alpha]_D^{19}$ +40° (*c*, 3.8 in chloroform). Anal. Calc. for $C_{39}H_{36}O_{16}I_2S$: I, 26.5%. Found: I, 24.9%.

Reduction of Tri-O-tosyl Sucrose

Tri-*O*-tosyl sucrose was reduced (10 hours) with $LiAlH_4$ at the boiling point of tetrahydrofuran. Following destruction of excess hydride with moist ethyl acetate and deionization of the solution with ion-exchange resin, 6,6¹-dideoxy sucrose was isolated as a chromatographically homogeneous, crisp solid (R_f 0.32), $[\alpha]_D^{19}$ +49.7° (*c*, 1.27 in water). Anal. Calc. for $C_{12}H_{22}O_9$: CMe, 9.7%. Found: CMe, 9.2%.

Dideoxy sucrose was completely hydrolyzed by invertase (48 hours) to give two compounds which cochromatographed with authentic rhamnoketose and 6-deoxy glucose.

ACKNOWLEDGMENT

The authors wish to thank the Sugar Research Foundation, Inc., for a grant.

REFERENCES

1. HOCKETT, R. C. and ZIEF, M. J. Am. Chem. Soc. **72**, 1839 (1950).
2. TIPSON, R. S. *In* Advances in carbohydrate chemistry. Vol. 8. Academic Press, Inc., New York. 1953.
3. KUHN, R., LOW, I., and TRISCHMANN, H. Ber. **88**, 1492 (1955).
4. HIRST, E. L., MITCHELL, W. E. A., PERCIVAL, E. E., and PERCIVAL, E. G. V. J. Chem. Soc. 3170 (1953).
5. ARNI, P. C. and PERCIVAL, E. G. V. J. Chem. Soc. 1822 (1951).
6. LEMIEUX, R. U. and BARRETTE, J. P. J. Am. Chem. Soc. **80**, 2243 (1958).
7. MCKEOWN, G. G., SERENIUS, R. S. E., and HAYWARD, L. D. Can. J. Chem. **35**, 28 (1957).
8. FINKELSTEIN, F. Ber. **43**, 1528 (1910).
9. SUGIHARA, J. M. *In* Advances in carbohydrate chemistry. Vol. 8. Academic Press, Inc., New York. 1953.
10. HOUGH, L., JONES, J. K. N., and WADMAN, W. H. J. Chem. Soc. 796 (1952).
11. VAN CLEVE, J. W. and SCHAFFER, W. C. J. Am. Chem. Soc. **77**, 5341 (1955).

MASS SPECTROMETRIC STUDY OF THE REACTIONS OF SOME HYDROCARBONS WITH ACTIVE NITROGEN[1]

JOHN T. HERRON, J. L. FRANKLIN,[2] AND PAUL BRADT

ABSTRACT

The reactions of active nitrogen with acetylene, ethylene, and propylene have been studied in a flow system using a mass spectrometer to analyze the products continuously. Certain features of the mass spectra of the products can be explained on the basis of cyano radical replacement reactions.

Winkler and his co-workers have studied the reactions of active nitrogen with acetylene (1), ethylene (2), and propylene (3), in addition to a large number of other compounds (4). The major product containing nitrogen, aside from small amounts of cyanogen, was HCN. In the case of the acetylene reaction an additional product was found in the form of a polymer, containing about 32% nitrogen.

We have made a mass spectrometric study of these reactions, using a flow system. The nitrogen atoms were produced by passing a stream of nitrogen gas at from 1 to 5 mm pressure through a 2450 Mc electrodeless discharge. The atom concentration as measured by gas titration with NO (5) was of the order of 2 mole %. The reactor was made of 10-mm i.d. glass tubing. Hydrocarbons were added to the system through an inlet located about 20 cm ahead of a small glass leak through which the gas stream was continuously sampled and analyzed by a mass spectrometer. With linear flow rates of the order of 1 meter/second, the time for the gas to pass from the hydrocarbon gas inlet to the sampling leak was about 0.02 second.

This type of experimental arrangement does not permit observation of any but very long-lived free radicals. Since the reaction flames themselves extended only a few centimeters from the reactant inlet, it seems reasonably certain that our analytical results refer only to stable products.

In general our results are very similar to those of Winkler and co-workers. However, several new features were observed. For acetylene we found the major product to be HCN, along with smaller amounts of $(CN)_2$, as indicated by their peaks at m/e 27 and

TABLE I

Observed mass spectra

Reactant, m/e	C_2H_2	C_3H_4	C_2H_4	C_3H_6
50	22	100	30	100
51	100	380	100	270
53	—	—	100	370
62	—	—	—	—
63	—	34	—	40
64	—	74	—	70
65	—	100	—	70
66	—	—	—	40
67	—	—	—	100

[1]*Manuscript received November 10, 1958.*

Contribution from the Mass Spectrometry Section, National Bureau of Standards, U.S. Department of Commerce, Washington, D.C. This research was performed under the National Bureau of Standards' Free Radical Research Program, supported by the Department of the Army.

[2]*Guest Scientist on leave from Humble Oil and Refining Company. Present address: Humble Oil and Refining Company, Baytown, Texas.*

52 respectively. In addition, however, there were peaks at m/e 50 and 51, but no peaks at higher masses. Similarly, for methyl acetylene, there were peaks at m/e 50, 51, and m/e 63, 64, 65, but again none at higher masses. The relative magnitudes of the ion currents are shown in Table I. The m/e 52 peak has been omitted.

In the case of the acetylene reaction, the absence of peaks at masses greater than m/e 52 (C_2N_2) makes it difficult to conceive of the m/e 51 peak being due to anything other than C_3HN which we feel certain is cyanoacetylene. The mass 50 peak is probably C_2CN^+ from C_2HCN. It is not diacetylene, since other peaks from the mass spectrum of diacetylene were absent.

Similarly the mass 65 peak probably corresponds to the methyl cyanoacetylene ion, $CH_3C_2CN^+$, the ions of mass 64 and 63 would represent the loss of one and two hydrogens from the parent molecule. Of course, the peaks at 63, 64, 65 could also be attributed to propargyl cyanide, though we think this less likely.

It is difficult to account for these products other than through direct replacement of a hydrogen by a cyano radical. Since diacetylene is not found in either reaction, it seems certain that the C_2H radical does not play an important part. Hence we cannot account for the cyanoacetylene as resulting from the reaction

$$CN + C_2H \rightarrow C_3HCN.$$

Furthermore, the methylacetylene reaction leads to the formation of considerably more cyanoacetylene than methyl cyanoacetylene as is shown in Table II. The absence of a peak at m/e 78 in the products of reaction with methylacetylene shows that the C_3H_3 radical probably plays very little part in the reaction and thus suggests that recombination of this radical with CN is not responsible for the C_3H_3CN observed.

TABLE II

Per cent of N in products for typical experiments

Product reactant	NH_3	HCN	C_3HN	C_2N_2	C_3H_3N	C_4H_3N	C_4H_5N
C_2H_2	13	62	7	18			
C_3H_4	6	75	6	12	?	1	
C_2H_4	<1	97	<1	2	<1		
C_3H_6	?	>78	<4	12	5		1

We consider the most plausible set of reactions to be:

$$CN + C_2H_2 \rightarrow C_2HCN + H \qquad \Delta H^* = -12$$
$$CN + CH_3C_2H \rightarrow C_2HCN + CH_3 \qquad \Delta H = -22$$
$$\rightarrow CH_3C_2CN + H \qquad \Delta H = -12$$
$$\rightarrow CH_2CNC_2H + H \qquad \Delta H = -7$$

Table II gives the per cent of the total nitrogen in each product. The actual numerical values are necessarily somewhat crude, inasmuch as we had no way of determining the relative sensitivities of the various products. In addition the formation of brown deposits on the walls of the reactor largely negates any attempt at exact analyses.

Nevertheless, it can be seen that the proportion of products containing the cyano radical is quite high, i.e. of the order of 25%. This would seem to argue that the cyano radical plays a rather important part in these reactions. It is interesting to note that

*Kcal/mole, estimated from group equivalent values (ref. 6).

in the case of the acetylene reaction, as the flow rate of acetylene is increased, the amount of cyanogen increases quite steeply, and then falls off again as conditions approach complete consumption of the active nitrogen (1). The cyanogen is presumably produced by the recombination of CN radicals.

With the olefins studied, the major product containing nitrogen was again HCN, which accounted for 97% of the nitrogen in the ethylene reaction, and more than 78% in the propylene reaction. The later reaction also yielded appreciable amounts of cyanogen.

Although the mass spectra over the range of masses 50–70 show several interesting features, it would be unwise to draw overly firm conclusions from them, since the peaks are quite small. The spectra are shown in Table I.

With ethylene the largest peaks were at masses 51, 52, and 53 with a series of smaller peaks extending to mass 56. The peak at mass 52 can be attributed at least in part to cyanogen, while that at mass 53 can be attributed to C_3H_3N, which could be cyanoethylene. The peaks at 50, 51 may be due in part to cyanoacetylene, since acetylene is a product of this reaction (2). As can be seen from Table II the proportion of nitrogen in products other than HCN is very small.

In the case of propylene, however, this may not be the case. Propylene gave a series of peaks from masses 50 to 58, and from 63 to 67, the two largest being at 52 and 53. The series at 63 to 67 is probably due to C_4H_5N, which may be either propenyl cyanide, isopropenyl cyanide, allyl cyanide, or a mixture of them. The peak at mass 53 may be cyanoethylene.

By analogy with the corresponding acetylene reactions, the following reactions can be written to describe the olefin reactions:

$$\begin{aligned}
CN + C_2H_4 &\rightarrow C_2H_3CN + H && \Delta H \text{ (ref. 6)} = -10\\
CN + CH_3C_2H_3 &\rightarrow C_2H_3CN + CH_3 && \Delta H = -22\\
&\rightarrow CH_3C(CN)CH_2 + H && \Delta H = -11\\
&\rightarrow CH_3C_2H_2CN + H && \Delta H = -8\\
&\rightarrow CH_2(CN)CHCH_2 + H && \Delta H = -7
\end{aligned}$$

Unfortunately, we were unable to obtain samples of pure cyanoacetylene or methyl cyanoacetylene in order to compare mass spectra. We have obtained the mass spectra of the three possible C_4H_5N products. They are very similar, and have approximately the spectra m/e 67:66:65:64:63; 100:35:6:20:7. In view of the presence of a large m/e 53 peak, the discrepancy in the spectra from m/e 65 to 63 may be due to the presence of a C_3H_4 component.

It is of interest that ammonia was produced in the reactions with both acetylenes and with ethylene,* although it was not detected in the propylene reaction (Table II). Very approximately, the amount of ammonia produced increased with the proportion of cyano containing products. We are unable to propose a mechanism for this formation of ammonia. It might come about by successive recombination of N atoms, which are relatively abundant, with H atoms, but this is purely speculative.

The complete mechanism for the reaction of N atoms with the lower acetylenes and olefins is certainly very complex and we have made no effort to determine it. We do think that the evidence points to the importance of the CN radical in the reaction and strongly suggests that it forms several important products by displacement reactions at one of the carbons of the double or triple bond.

**In agreement with an earlier observation on the ethylene reaction by J. T. Herron and H. I. Schiff (1955, unpublished).*

REFERENCES

1. VERSTEEG, J. and WINKLER, C. A. Can. J. Chem. **31**, 129 (1953).
2. VERSTEEG, J. and WINKLER, C. A. Can. J. Chem. **31**, 1 (1953).
3. TRICK, G. S. and WINKLER, C. A. Can. J. Chem. **30**, 915 (1952).
4. EVANS, H. G. V., FREEMAN, G. R., and WINKLER, C. A. Can. J. Chem. **34**, 1271 (1956).
5. HERRON, J. T., FRANKLIN, J. L., DIBELER, V. H., and BRADT, P. J. Chem. Phys. **29**, 230 (1958).
6. FRANKLIN, J. L. Ind. Eng. Chem. **41**, 1070 (1949).

THE METAL-CATALYZED DECOMPOSITION OF NITROUS OXIDE (I). DECOMPOSITION ON PURE SILVER, SILVER–GOLD, AND SILVER–CALCIUM ALLOYS[1]

KENNETH E. HAYES[2]

ABSTRACT

The decomposition of nitrous oxide on silver, a silver – 1.14% gold alloy, and a series of silver–calcium alloys has been studied. On all of these catalysts the *initial rate* of decomposition is proportional to the nitrous oxide pressure. The activation energy for pure metals, including platinum and gold, is proportional to the work function. For the silver–calcium alloys the activation energy falls rapidly with increasing calcium content, suggesting that the work function of these alloys falls with increasing calcium content.

INTRODUCTION

This investigation was undertaken as part of a larger program concerned with the silver-catalyzed oxidation of ethylene. For many years this laboratory has been interested in the direct oxidation of ethylene to ethylene oxide using silver–calcium alloys as catalysts (1, 2). However, although a great amount of work has been reported in this field, certain ambiguities remain. It was hoped that the investigation of a comparatively simple reaction, such as the decomposition of nitrous oxide, would prove fruitful in establishing an unequivocal mechanism of the silver-catalyzed oxidation of ethylene.

Although the catalytic decomposition of nitrous oxide by semiconductors has claimed the attention of many workers, comparatively little has been done with metallic catalysts. To date the only metals to have been investigated are platinum (3), gold (4), silver (5), and nickel (6), and even for these, activation energies have been reported only for the first two.

The investigation of Suhrmann (7) on the effect of nitrous oxide on the resistance of transparent nickel films (8) and on the photoelectric emission of platinum surfaces (9) shows that nitrous oxide is probably chemisorbed on metals as N_2O^-, the rate determining step in the decomposition then being the adsorption of nitrous oxide, followed by a fast thermal dissociation of nitrogen from the adsorption complex. If this is correct, then the activation energy for the decomposition should be proportional to the work function of the catalyst.

EXPERIMENTAL

Apparatus

The apparatus used was a conventional high-vacuum system. The reactor was a wire wound Pyrex glass tube, 35 mm O.D. and approximately 30 cm long. At one end of this tube was a 29/42 female standard taper joint, for ease in changing catalysts; the matching male joint had a 6-mm thermocouple well running through the center, this tube ending in the center of the reactor, and bent at such an angle so as to be within the catalyst mass when the catalyst was installed. An all-glass centrifugal circulating pump, a 1-liter ballast flask, and a mercury manometer completed the reactor circuit. U-tubes filled with silver turnings were inserted between the reactor and the manometer, and also

[1]*Manuscript received September 15, 1958.*
Contribution from the Division of Applied Chemistry, National Research Council, Ottawa, Canada.
Issued as N.R.C. No. 5060.
[2]*National Research Council Postdoctoral Fellow 1954–56. Assistant Research Officer 1956–58. Present address: Chemistry Department, Dalhousie University, Halifax, N.S.*

between the reactor and inlet to the vacuum system, to prevent contamination of the catalysts by mercury. The temperature of the reactor was held to within ±2° C by a Bristol controller. Catalyst powders were contained in a Pyrex glass boat placed in the center of the reactor. When foils were used as catalysts these were wrapped around the center thermocouple well.

Nitrous Oxide

The nitrous oxide was supplied by the Matheson Company and had a nominal purity of 98%. It was purified in the conventional manner by a triple sublimation/distillation, always discarding the first and last fractions.

The Catalyst

1. The pure silver catalyst was prepared as a foil (10 feet×0.625 in.×0.002 in.) from a vacuum melted, chill cast ingot, the silver had been purified by a triple-electrolysis of Mint-Grade silver, and had a purity of 99.998% as found by spectrographic analysis. This catalyst weighed 37.000 g.

2. The silver–gold alloy foil was prepared in a similar manner to the pure silver foil, i.e. the metals were melted together in a small induction furnace, chill cast under vacuum, and rolled. The gold, which again had been purified by repeated electrolysis, analyzed as 99.9995% Au. The foil contained 1.14% Au. The catalyst was of the same thickness and width as for No. 1, two lengths were used in the experiments to give weights of 28.500 and 40.000 g.

3. The silver–calcium alloys were prepared from an 8.5% calcium in silver master alloy. Some 50–60 g of 60–200 mesh alloy were held in steam at from 200–350° C for from 1–8 hours. After cooling, the alloy was then subjected to the following leaching schedule: (*a*) soak in cold 20% acetic acid for 10 minutes, (*b*) wash well in distilled water, (*c*) repeat (*a*), (*d*) repeat (*b*), (*e*) boil in 20% acetic acid for 30 minutes, (*f*) repeat (*b*), (*g*) boil in 20% acetic acid for 60 minutes, (*h*) repeat (*b*), (*i*) boil in distilled water for 30 minutes, (*j*) drain and dry, resieve the catalyst, retaining only the 60–200 mesh size, and send sample to analysis. By varying the temperature of the steam, and/or the steaming time, a series of catalysts was prepared with residual calcium contents varying from 0.11% to 1.70%.

Experimental Technique

A sample of the catalyst powder was weighed out accurately and put into the reactor as described, the reactor was closed, using a sulphur-free mass-spectrometer wax[3] to seal the 29/42 joint together, the necessary glass blowing was then done, and the catalyst evacuated, by mercury pump, at 500° C for 19–20 hours. This treatment was sufficient to remove any adsorbed gases, such as water, oxygen, or carbon dioxide that had been picked up during storage. Experiments were always performed to check on the reaction kinetics before the activation energy runs, by making observations at constant temperature and different initial pressures. Activation energy runs were always made using the bracketing technique.

RESULTS AND DISCUSSION

For all of the catalysts studied, the *initial rate* law is given by:

$$[1] \qquad \frac{-dP_{N_2O}}{dt} = kP_{N_2O}.$$

[3]*Manufactured by Robert R. Austin, Box 374E, Pasadena 8, California, U.S.A.*

This is illustrated in Fig. 1, which gives typical results for a plot of initial rate (cm/min) against initial nitrous oxide pressure. Steacie and Folkins (5) have shown that, on silver catalysts, the over-all rate of the decomposition is given by:

$$[2] \qquad \frac{-dP_{N_2O}}{dt} = \frac{kP_{N_2O}}{1+bP_{O_2}},$$

the integrated form of [2] is:

$$[3] \qquad k = \frac{(1+ab)}{t} \ln [a/(a-x)] - \frac{bx}{t},$$

where a is the initial nitrous oxide pressure and x is the amount of nitrous oxide that has reacted after time t. Following Steacie and Folkins we may write

$$\frac{1}{t} \ln \frac{a}{(a-x)} = K_m,$$

and $x/t = V$. A plot of K_m against V will then give a straight line if equation [2] is correct. Although this investigation deals in the main with initial rates, an indication that equation [2] is correct is illustrated in Figs. 2 and 3, which give the raw data for the decomposition on pure silver foil at 793° K and the K_m–V plot for the same data. The fall from linearity of the last points for the low pressure experiment is probably due to the reaction becoming diffusion controlled, the extent of reaction having taken place exceeding 95%.

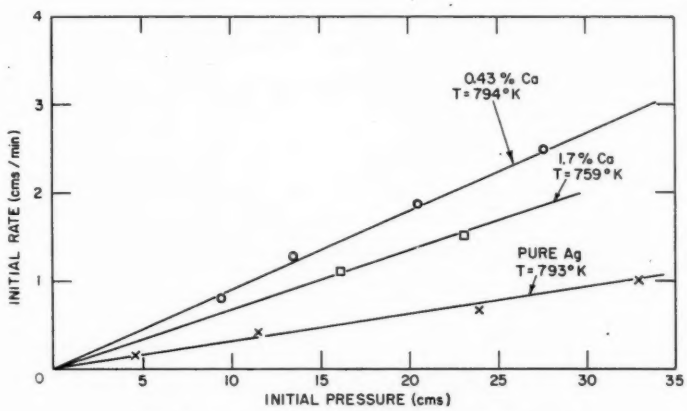

FIG. 1. Dependence of initial rate on N_2O pressure.

In Fig. 4 a plot of $-\log k$ against $1/T$ is given (where k is the initial rate constant per gram of catalyst) for most of the catalysts that were used. Not all of the results are shown for the sake of clarity. The values of the activation energies were obtained by the method of Least Mean Squares, which gave at the same time the values of the logarithm of the pre-exponential factor, A.

In Fig. 5, a composite plot of activation energy against work function, and activation energy against calcium content in silver, is shown. The activation energies obtained by Hinschelwood and Pritchard for platinum and gold are included for completeness. The point for Ag – 1.14% Au is placed on the E–ϕ line quite arbitrarily, being defined solely by the value of E.

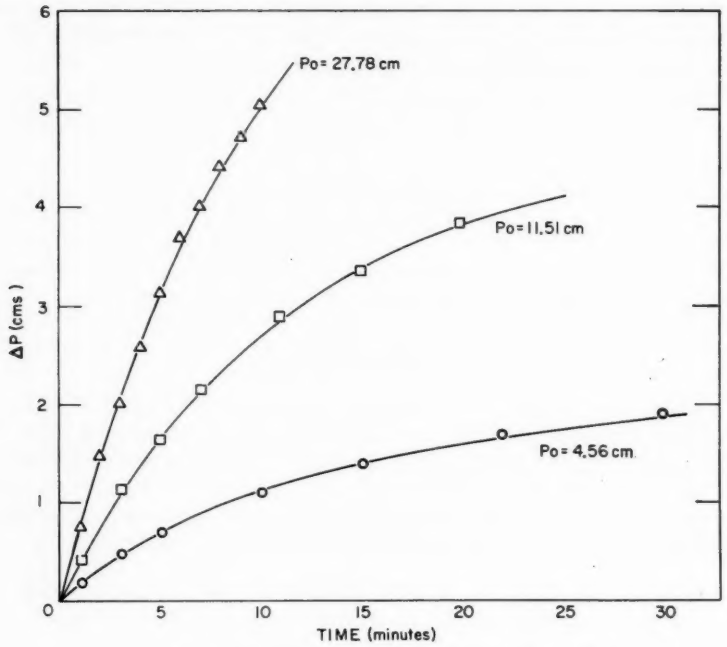

FIG. 2. Decomposition of N_2O on pure Ag at 793° K.

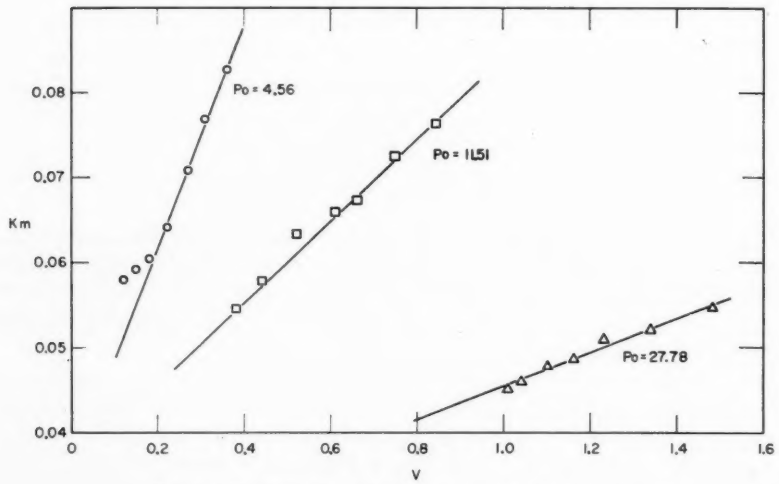

FIG. 3. The data of Fig. 2, plotted according to equation [3].

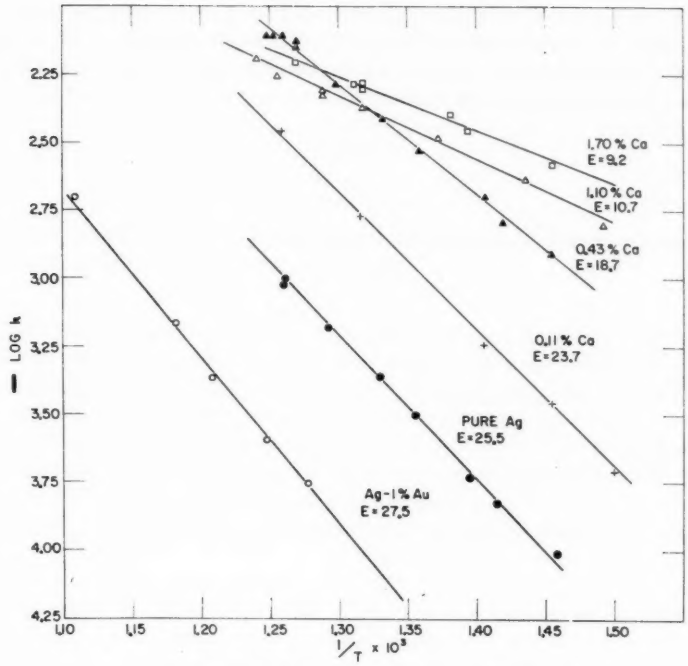

FIG. 4. Arrhenius plot for the various catalysts.

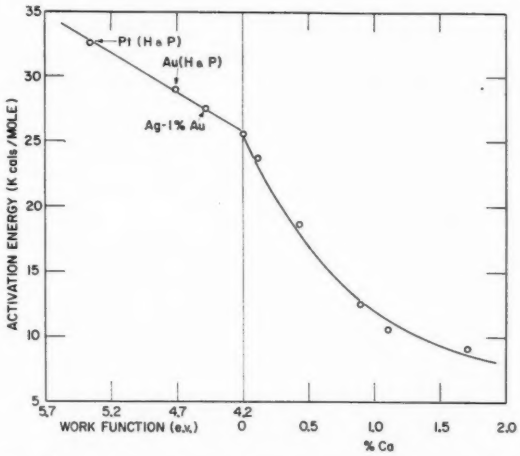

FIG. 5. The relationship between activation energy and work function for pure metals, and between activation energy and calcium content for Ca–Ag alloys.

From the linear relationship between E and ϕ it may be concluded that the rate determining step in the decomposition involves an electron transfer from the catalyst to the adsorbed gas. In this case, there are two possible mechanisms: (1) that the rate determining step is the adsorption of N_2O as N_2O^-,

$$N_2O + e \overset{\text{r.d.s.}}{\rightleftharpoons} N_2O^- \qquad [4a]$$

$$N_2O^- \underset{\text{fast}}{\longrightarrow} N_2 + O^- \qquad [4b]$$

or (2) that the r.d.s. is the dissociative chemisorption of nitrous oxide

$$e + N_2O \overset{\text{r.d.s.}}{\longrightarrow} N_2 + O^-. \qquad [5]$$

Although the present work is unable to distinguish between these two mechanisms, it is clear that the removal of adsorbed oxygen, either by the reaction between two adsorbed O^- ions, or between O^- and gaseous N_2O, cannot be the rate determining step, as either of these two reactions involves the donation of electrons back to the catalyst. Such a requirement would lead to the expectation of finding that the activation energy decreased with increasing work function, in opposition to the observed facts. It is hoped that a projected study of the adsorption characteristics of nitrous oxide on these catalysts, together with a detailed examination of the over-all reaction rate will be able to settle the mechanism of the reaction more definitely.

From Fig. 4 and the right-hand side of Fig. 5, it is seen that residual calcium has a marked effect both on the specific activity of the catalysts and on the activation energy. On the basic postulate that the activation energy is proportional to the work function, it is apparent from Fig. 5 that the role of calcium in the Ca–Ag alloys is to lower the work function, and hence enhance the N_2O decomposition. In view of the well-known role of alkaline earths in governing emission from oxide covered cathodes (10), this result is not surprising.

Figure 6 shows the compensation effect that was obtained with the Ag–Ca alloys. A possible explanation for this effect is that these alloys are truly heterogeneous, even on the macroscale. The values of Ca % of Fig. 5 refer to catalyst samples of 60–200 mesh, and for several samples of the same catalyst the Ca analysis was reproducible to 1% or better. However, an analysis of various mesh sizes for the same catalyst showed that the calcium content was strongly dependent on the degree of subdivision of the catalyst.

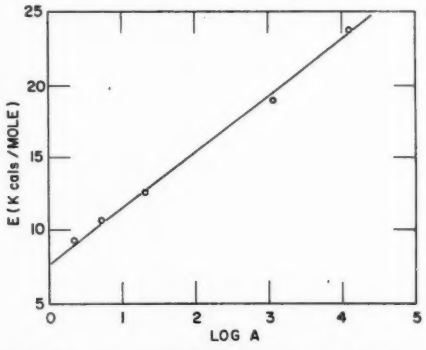

FIG. 6. The compensation effect for Ca–Ag alloys.

Three samples of one catalyst gave the following result: (1) average mesh size 80, Ca % = 0.69; (2) A.M.S. 100, Ca % = 0.53; (3) A.M.S. 150, Ca % = 0.22. It therefore follows that the activation energies found for the Ag–Ca alloys are probably only approximations, good over only a small temperature range; more detailed and accurate values of k extending over a much larger temperature range might be expected to produce $\log k - 1/T$ plots with definite curvatures.

ACKNOWLEDGMENTS

The author is indebted to Drs. W. A. Alexander and W. G. Henry of the Metallurgy Section for assistance in the catalyst preparation.

REFERENCES

1. CAMBRON, A. and MCKIM, F. L. W. U. S. Patent No. 2,562,857 (1951); Can. Patent No. 475,366 (1951).
2. ORZECHOWSKI, A. and MACCORMACK, K. E. Can. J. Chem. **32**, 388, 415, 432, 443 (1954).
3. HINSHELWOOD, C. N. and PRICHARD, C. R. J. Chem. Soc. **127**, 327 (1925).
4. HINSHELWOOD, C. N. and PRICHARD, C. R. Proc. Roy. Soc. (London), A, **108**, 211 (1925).
5. STEACIE, E. W. R. and FOLKINS, H. O. Can. J. Research, B, **15**, 237 (1937).
6. HEDVALL, J. A., HEDIN, R., and PERSSON, O. Z. physik. Chem. B, **27**, 196 (1934).
7. ADVANCES IN CATALYSIS. Vol. VII. Academic Press Inc., New York. 1955. p. 303 ff.
8. SUHRMANN, R. and SCHULZ, K. Z. physik. Chem. (N.F.) **1**, 69 (1954).
9. SUHRMANN, R. and SACHTLOS, W. Z. Naturforsch. **9a**, 14 (1954).
10. BOER, J. H. DE. Electron emission and adsorption phenomena. Cambridge University Press, London. 1935. p. 339 ff.

THE BROMINATION OF URACIL AND THYMINE DERIVATIVES[1]

A. M. MOORE[2] AND SHENA M. ANDERSON[2]

ABSTRACT

The bromination of 1,3-dimethyluracil, uracil, and thymine and of the nucleosides and nucleotides of the latter two compounds has been followed potentiometrically and spectrophotometrically. The results indicate that all the compounds except uracil react initially with 1 mole of bromine to form 5-bromo-6-hydroxy-hydropyrimidine derivatives. If the resulting compound still has a hydrogen at position 5 it may undergo dehydration on heating or with acid catalysis to form the corresponding 5-bromopyrimidine, which is then capable of further reaction with bromine. Uracil itself appears first to undergo substitution to 5-bromouracil, and then both the uracil and 5-bromouracil are brominated together to yield ultimately 5,5-dibromo-6-hydroxyhydrouracil.

INTRODUCTION

The study of the chemical changes induced by ultraviolet light in the uracil and cytosine components of nucleic acids has led to the recognition that the initial products of reaction in aqueous systems belong to the class of 6-hydroxy-hydropyrimidines (8, 9, 10, 12). This finding has led, in turn, to new interest in the 5-bromo-6-hydroxyhydrouracils and related compounds both as intermediates in the synthesis of the irradiation products and as chemical analogues of such products.

A recent report by Wang (11) has shed a good deal of light on the bromination reactions of uracil and 1,3-dimethyluracil. Our own studies reported here have included these compounds but have also been extended to the nucleosides and nucleotides of uracil and thymine.

EXPERIMENTAL

The spectrophotometric measurements were made with a Beckman Model DK2 Recording Spectrophotometer. Except where otherwise noted the spectroscopic changes during bromination were determined by adding 10^{-2} *M* bromine water a few microliters at a time to 10^{-4} *M* pyrimidine solutions. The small dilution involved has been neglected.

For the potentiometric titrations a platinum and a saturated calomel electrode were used in conjunction with a Leeds and Northrup Student Potentiometer in the earlier experiments, and with a Radiometer Titrator in the later ones. A small beaker equipped with a magnetic stirrer and held at room temperature (22–24° C) was charged with a measured volume of 10^{-2} *M* solution of the pyrimidine compound in acetate buffer and, with continuous rapid stirring, the potential was measured after successive additions of standard bromine water (approximately 10^{-2} *M*). The bromine was dispensed from a small automatic burette with blackened reservoir. To minimize the effect of a rather rapid initial drift in potential the measurements were all made 1 minute after each addition of bromine. Corresponding measurements using the same volume of buffer in place of the pyrimidine solution were used to determine a blank correction.

The uracil, uridine, uridylic acid, and thymine were obtained from Nutritional Biochemicals Corp., the thymidine from California Biochemical Research Corp. The uracil was recrystallized twice from water and dried at room temperature *in vacuo*. 1,3-Dimethyluracil was prepared from it by the method of Davidson and Baudisch (2) and was

[1]*Manuscript received December 5, 1958.*
Contribution from Atomic Energy of Canada Limited, Chalk River, Ontario.
Issued as A.E.C.L. No. 761.
[2]*Biology Division, Atomic Energy of Canada Limited.*

recrystallized from 95% ethanol (m.p. 122° C; $\epsilon = 8600$ at 266 mμ). The rest of the compounds were used as received after checking that the molecular extinctions and other characteristics of their absorption spectra were in satisfactory agreement with published values (1).

RESULTS

1,3-Dimethyluracil

Potentiometric titration (Fig. 1) indicated that any excess bromine beyond 1 mole per mole of dimethyluracil remained in solution as free bromine. This finding was supported by the spectrophotometric measurements (Fig. 2) which demonstrated that 1 mole of bromine was sufficient to eliminate completely the absorption band at 266 mμ. The absorption curves throughout the reaction exhibited isosbestic points at 215 and 245 mμ, thus pointing to a quantitative conversion of 1,3-dimethyluracil to 5-bromo-6-hydroxy-1,3-dimethyluracil. If, after the addition of 1 mole of bromine, the solution was heated at 100° C or if it was acidified to pH 1 (HCl) the spectrum underwent further progressive change, with a new isosbestic point at 254 mμ, to yield finally and quantitatively 5-bromo-1,3-dimethyluracil ($\epsilon_{max} = 8000$ at 283 mμ; $\epsilon_{min} = 1290$ at 245 mμ; m.p. 181° C) (cf. curve 5, Fig. 2).

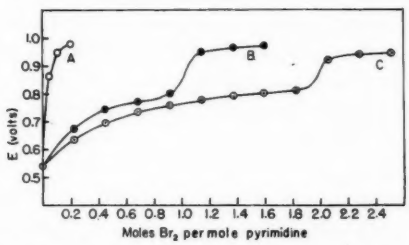

FIG. 1. Potentiometric titrations with bromine water (0.01 *M*). The pyrimidines (0.01 *M*) were dissolved in 0.1 *M* acetate buffer, pH 4.76. A—Buffer blank; B—1,3-dimethyluracil; C—uracil.

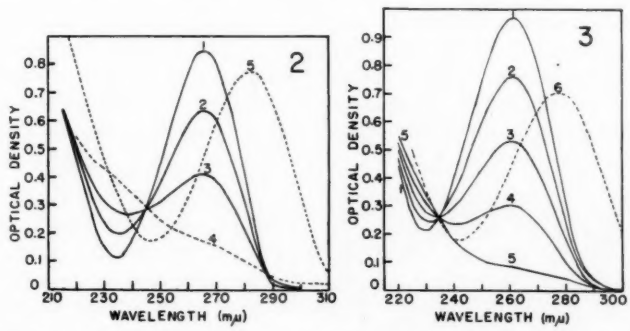

FIG. 2. Bromination of 1,3-dimethyluracil (10^{-4} *M*; in water). Curves 1–4 respectively represent spectra obtained after adding zero, 0.27, 0.54, and 0.98 moles of Br_2 per mole of 1,3-dimethyluracil. Curve 5 is the spectrum obtained upon adding 1 molecular equivalent of bromine and heating for 15 minutes at 100° C after acidification to pH 1 with concentrated HCl.

FIG. 3. Bromination of uridylic acid (10^{-4} *M*; in water). Curves 1–5 respectively represent spectra obtained after adding zero, 0.25, 0.50, 0.75, and 1.0 mole of Br_2 per mole of uridylic acid. Curve 6 shows the result of adding 1 molecular equivalent of Br_2 and then heating for 10 minutes at 100° C before reading the spectrum.

Uridine and Uridylic Acid

These behaved similarly and will be considered together. Both compounds lost their 262 mμ absorption band on addition of 1 molecular equivalent of bromine, the transformation exhibiting isosbestic points at 234 and 291 mμ in both cases. An experiment with uridylic acid is illustrated in Fig. 3.

To follow the titration of these compounds with bromine two procedures were employed. At a concentration of 10^{-4} *M* the optical density at 260 mμ was found to decrease linearly with the amount of added bromine to a limiting value corresponding to the absorbance of the product; thereafter the density remained constant. The limiting density was reached in the case of uridine at 0.97 and in the case of uridylic acid at 0.99 moles of bromine per mole of pyrimidine.

In the second procedure, by using concentrations of the order of 10^{-3} *M* for both the bromine and the pyrimidines it was possible to observe the appearance of the absorption band at 390 mμ due to free bromine when the end point was reached. At this wavelength the optical density was constant (nearly zero) up to the end point and then rose rapidly as extra bromine was added. The end point occurred for uridine at 1.01 and for uridylic acid at 0.95 moles bromine per mole of pyrimidine.

In the case of uridylic acid an argentimetric titration (potentiometric) of the free bromide ion at the end point verified that 1 mole of bromine while eliminating the absorption band at 262 mμ yielded 1 equivalent of bromine.

When the brominated solution of uridylic acid was heated at 100° C the spectrum developed a new maximum at 278 mμ and minimum at 242 mμ as dehydration gave rise to 5-bromouridylic acid. (Compare ϵ_{max} 279 mμ, ϵ_{min} 244 mμ for the deoxyribonucleotide of 5-bromouracil in 0.1 *N* HCl (3).)

Uracil

The spectral changes accompanying the reaction of bromine with uracil in 0.1 molar acetate buffer (pH 4.7) are illustrated in Fig. 4. Two moles of bromine were required to eliminate the absorption maximum at 259 mμ. Although, at that wavelength the absorbance decreased progressively as bromine was added, the situation was quite

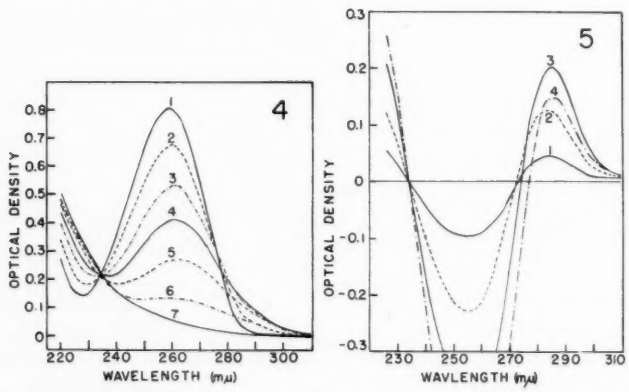

FIG. 4. Bromination of uracil (10^{-4} *M*; in 0.1 *M* acetate buffer, pH 4.7). Curves 1–7 respectively show the spectra obtained upon adding zero, 0.32, 0.64, 0.96, 1.28, 1.60, and 1.92 moles of Br_2 per mole of uracil.

FIG. 5. Differential spectra obtained by placing 10^{-4} *M* uracil in both the sample and reference cuvettes of the spectrophotometer and then recording the spectrum after successive additions of Br_2 to the sample cuvette. Curves 1–4 respectively represent 0.41, 0.84, 1.44, and 1.85 moles of Br_2 per mole of uracil.

different at 280 mμ. Here the absorbance first increased to a maximum and then decreased again as more bromine was added. The changes during the first part of the reaction can be more clearly understood by examining the differential spectra (Fig. 5).

The form of the absorption curves suggested that 5-bromouracil (λ_{max} = 276 mμ) was being produced as an intermediate and that it reacted eventually with more bromine to yield 5,5-dibromo-6-hydroxyhydrouracil. In such an event presumably the 5-bromouracil would increase in amount initially to the point at which it would be reacting with bromine at the same rate as the residual uracil and then, as the uracil was used up, the reaction of the 5-bromouracil would predominate. If this were true one might expect that if one added 5-bromouracil to the uracil initially, in sufficient quantity, the absorption curves during the bromination would not exhibit the preliminary increase in the region of 280 mμ. A series of mixtures of the two compounds was studied in this way and this was indeed the finding. Figure 6 gives one example in which 5-bromouracil was added initially to the sample to a concentration of 0.55×10^{-4} *M*. The same amount of 5-bromouracil was added to the reference cell so that its contribution to the absorption curve was cancelled out. The changes during bromination thus appeared as the simple removal of uracil and its conversion to 5,5-dibromo-6-hydroxyhydrouracil, the known final product.

The results of the potentiometric titration with bromine, included in Fig. 2, were in agreement with the spectrophotometric measurements in indicating no end point until 2 moles of bromine had been added per mole of uracil.

Thymine

The family of absorption curves obtained for the bromination of thymine exhibited 2 isosbestic points (at 223 and 233.5 mμ) corresponding to a mole for mole conversion of thymine to 5-bromo-6-hydroxyhydrothymine. The elimination of the absorption band required approximately 1 mole of bromine. As the thymine was found chromatographically to contain several per cent of uracil as impurity quantitative study was not pursued further in this case.

Thymidine

The spectral changes during the bromination of thymidine resembled those for thymine but with isosbestic points at 225.5 and 236 mμ (Fig. 8). The absorption band at 265 mμ was eliminated by 1.07 moles of bromine per mole of thymidine. The rate of reaction was lower than in the case of the uracil derivatives so that some minutes were required for it to go to completion. A 10-minute reaction time was employed in the experiments reported here. The effect of heating the brominated thymidine solution is shown in the final curve of Fig. 8.

Reaction of Uracil with 5,5-Dibromo-6-hydroxyhydrouracil

As an aid in interpreting the results of the uracil bromination experiments the following reaction has been investigated: 0.112 g uracil (0.001 mole) and 0.288 g of 5,5-dibromo-6-hydroxyhydrouracil (0.001 mole) were dissolved in 10 ml of 1 *N* HCl at 100° C and the solution was kept in the steam bath at 100° C. Samples were withdrawn from time to time and the absorption spectra recorded after diluting 1:1000 with water. The results are illustrated in Fig. 7. It should be pointed out that, after about 30 minutes, 5-bromouracil began to crystallize from the solution, so that its concentration remained constant from then on. At the times the samples were taken aliquots were also removed for chromatography on paper along with markers of uracil, 5-bromouracil, and 5,5-dibromo-6-hydroxyhydrouracil. The paper chromatogram was developed with *n*-butanol saturated

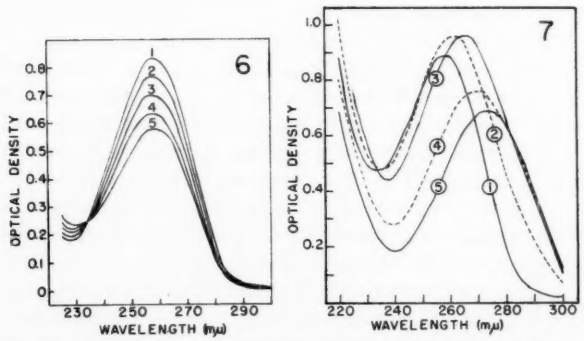

FIG. 6. Bromination of a mixture of uracil (10^{-4} *M*) and 5-bromouracil (0.55×10^{-4} *M*). Curves 1–4 correspond respectively to zero, 0.125, 0.25, 0.375, and 0.50 moles of Br_2 per mole of pyrimidine. A solution of 5-bromouracil (0.55×10^{-4} *M*) was used as a reference in the spectrophotometer.

FIG. 7. Bromination of uracil by means of 5,5-dibromo-6-hydroxyhydrouracil. Curves 1–5 show the spectra obtained for samples withdrawn at 3 minutes, 1 hour, 2 hours, 4 hours, and 24 hours respectively.

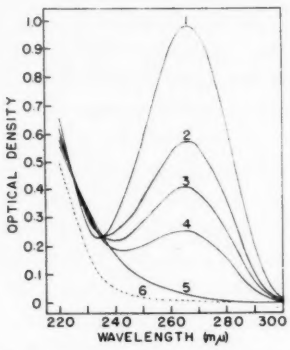

FIG. 8. Bromination of thymidine (10^{-4} *M*). Curves 1–5 respectively correspond to addition of zero 0.47, 0.65, 0.84, and 1.21 moles of Br_2 per mole of thymidine. Curve 6 shows the effect of heating at 100° C for 10 minutes after adding 1.21 molecular equivalents of Br_2.

with water and the spots located by the ultraviolet print method. The formation of 5-bromouracil (R_f 0.48) and the disappearance of both uracil (R_f 0.31) and 5,5-dibromo-6-hydroxyhydrouracil (R_f 0.62) during the reaction was clearly evident (Fig. 9).

DISCUSSION

The results of these studies lead to the conclusion that the reaction of dilute solutions ($\leqslant10^{-2}$ *M*) of uridine, uridylic acid, and 1,3-dimethyluracil with bromine water may be summarized:

[1] 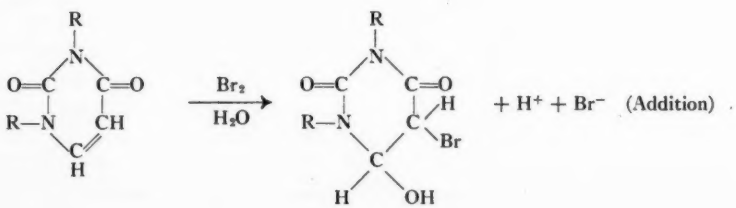 (Addition)

[2] 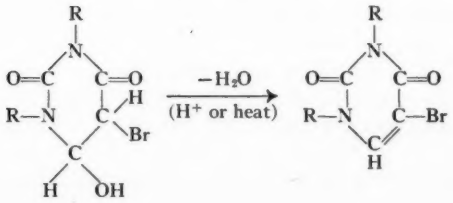

(Dehydration)

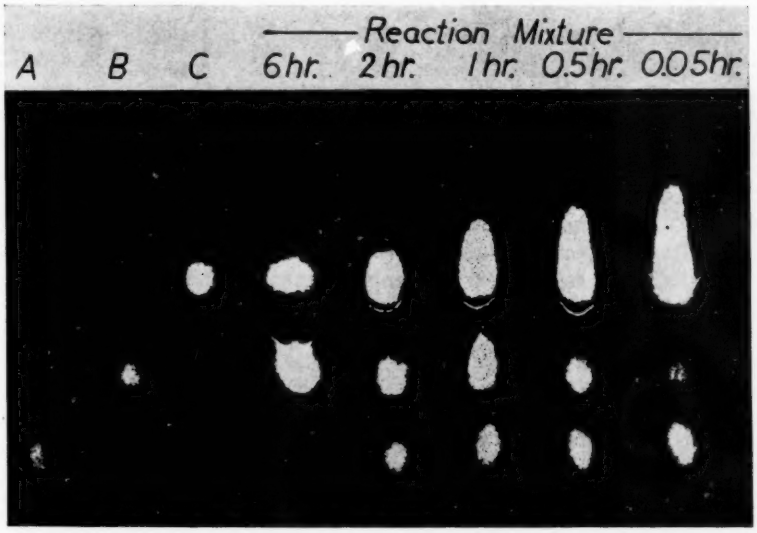

FIG. 9. Paper chromatogram showing reaction of uracil with 5,5-dibromo-6-hydroxyhydrouracil. Origin at top. Lanes A, B, and C represent markers (0.01 ml) of 5,5-dibromo-6-hydroxyhydrouracil (0.1 *M*), 5-bromouracil (10^{-2} *M*), and uracil (10^{-2} *M*) respectively. Solvent: *n*-butanol saturated with water. The narrow arc preceding some of the uracil spots is due to the presence of HCl in the reaction mixture.

The products of reaction [1], all 5-monobromo-6-hydroxyhydrouracil derivatives, are moderately stable compounds which, however, lose water on heating or, with acid catalysis, at room temperature to yield nearly quantitatively the corresponding 5-bromouracil derivative. Both reactions are readily observed spectrophotometrically, the first leading to elimination of the original absorption band in the 260–265 mμ region, the second producing a new band in the vicinity of 280 mμ. Unless reaction [2] is promoted the uptake of bromine stops when 1 mole has reacted. In the case of uridylic acid it was shown that 1 equivalent of bromide ion was produced at this stage.

Thymine and thymidine undergo the first of the foregoing reactions but the products, lacking any hydrogen on position 5, are not capable of the subsequent dehydration. Instead, on heating in weakly acid solution they react in a manner that leads to a marked decrease in ultraviolet absorption at all wavelengths <280 mμ. This change is probably attributable to opening of the pyrimidine ring but we have made no attempt to isolate the products.

The foregoing interpretation is in general agreement with the conclusions of Wang (11) based on his study of the bromination of 1,3-dimethyluracil.

The case of uracil itself we have found to be rather more complicated than Wang's interpretation would indicate. The potentiometric titration gave no end point until 2 moles of bromine had been added per mole of uracil (Fig. 1) and 2 moles of bromine were required to eliminate the absorption band at 259 mμ (Fig. 4). The picture is further complicated by the transient appearance of what appears to be 5-bromouracil during the bromination.

This is the behavior that one would expect of a reaction proceeding as follows:

[3] 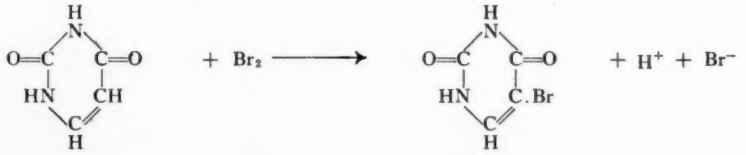

[4] 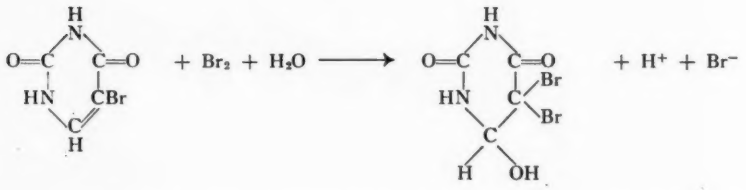

If we represent the instantaneous concentrations of bromine, uracil, 5-bromouracil, and 5,5-dibromo-6-hydroxyhydrouracil at time t by s, x, y, and z respectively then we may write for these reactions the following equations in which the subscript zero implies initial concentration:

$$[5] \qquad -dx/dt = k_1xs,$$

$$[6] \qquad dy/dt = k_1xs - k_2ys,$$

$$[7] \qquad dz/dt = k_2ys,$$

$$[8] \qquad -ds/dt = k_1xs + k_2ys,$$

$$[9] \qquad x_0 = x + y + z,$$

$$[10] \qquad s_0 = s + y + 2z.$$

An analytical solution of these equations does not yield the values of y and z in a convenient explicit form, but it has been possible, with the aid of a Datatron electronic digital computer, to calculate the final concentrations of x, y, and z for values of s_0 from zero to $2x_0$ and for values of $\kappa = k_2/k_1$ ranging from 0.5 to 2.0. Using these concentrations together with the known molecular extinctions of the three organic compounds the corresponding absorption spectra have been calculated for $\kappa = 2$ and are plotted in Fig. 10 for comparison with the experimental curves (Fig. 4). The general agreement is very good. The variation of the curves is not sufficiently sensitive to κ to make this a good way of estimating this constant, but an estimate may be obtained from the experimental results. From equation [6] it is evident that when uracil and 5-bromouracil are both reacting with bromine in such a way that $dy/dt = 0$, $k_1xs = k_2ys$ and $\kappa = k_2/k_1 = x/y$. Thus by brominating various initial mixtures of uracil and 5-bromouracil and determining the ratio at which $dy/dt = 0$ one may estimate κ. This is easily done, since,

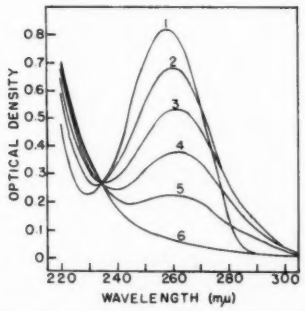

FIG. 10. Calculated curves for the bromination of uracil (10^{-4} M) by mechanism proposed in text, assuming $\kappa = 2$, and amounts of Br_2 ranging from zero to 2 molecular equivalents in 5 equal steps.

of the various components of the reaction mixture, only the 5-bromouracil contributes appreciably to the optical density at 282 mμ. The initial density change, ΔD_{282}, for a fixed amount of added bromine (0.1 mole) is nearly a linear function of the initial uracil:bromouracil ratio, and interpolation to $\Delta D_{282} = 0$ yields $\kappa = 1.7$. The reactions [3] and [4] are so rapid that direct estimation of k_1 and k_2 was not feasible.

The foregoing is not the only possible mechanism for the bromination of uracil that might be considered. An alternative would be the route suggested by reactions [1] and [2] followed by reaction of the 5-bromouracil thus formed with a second mole of bromine. Qualitatively this would explain the formation of 5-bromouracil and the over-all consumption of 2 moles of bromine.

Unfortunately for this hypothesis the dehydration of the 5-bromo-6-hydroxyhydrouracils is quite a slow reaction at room temperature and near neutral pH's, whereas the over-all bromination (2 moles) as observed during the present experiments is very rapid—too fast to measure by our technique. For all the uracil derivatives which we have investigated, the dehydration of the 5-bromo-6-hydroxyhydrouracil derivative is markedly slower than the dehydration of the corresponding 6-hydroxyhydrouracil derivative. Now the dehydration of 6-hydroxyhydrouracil itself at pH 5 and 20° C has a half life of about 19 hours (7) so that one would expect 5-bromo-6-hydroxyhydrouracil to have a half life of at least this magnitude under these conditions.

We must conclude that this can not be the mechanism by which the 5-bromouracil is formed and that, in contrast with the 1-substituted uracils which react by the mechanism cited in reactions [1] and [2], uracil itself first undergoes substitution at position 5 and only then enters into reactions [1] and [2].

One further point deserves comment here. It has been stated in the literature that uracil solutions treated with 1 molecular equivalent of bromine and subsequently heated give quantitative yields of 5-bromouracil (11). Our findings indicate that, before heating, such solutions contain 5,5-dibromo-6-hydroxyhydrouracil, 5-bromouracil, and uracil in roughly comparable amounts. How then can one explain the reported high yield of 5-bromouracil?

We suggest that the explanation lies in the fact that one of the two bromine atoms of 5,5-dibromo-6-hydroxyhydrouracil is capable of acting as a brominating agent. Hilbert and Jansen (4) observed that warm aqueous solutions of the compound liberated iodine from potassium iodide, and Johnson *et al.* (5, 6) showed that under similar conditions it oxidized thiourea and brominated malonic acid. In each case the dibromo-compound

itself was reduced to 5-bromouracil. In the present instance the residual uracil is presumably brominated on heating, at the expense of the 5,5-dibromo-6-hydroxyhydrouracil so that 5-bromouracil is the sole product.

In the usual preparation of 5-bromouracil, one evaporates to dryness a brominated solution of uracil which is strongly acid (HBr). Our study of the reaction between uracil and 5,5-dibromo-6-hydroxyhydrouracil under similar conditions of acidity and temperature showed that 5-bromouracil is formed in good yield at the expense of both reagents. With an initial concentration of 10^{-4} M for each compound the reaction was too slow to follow conveniently but at 0.1 M concentration, as reported here, the reaction proceeded at an easily measurable rate. Evaporation of a reaction mixture would provide ideal conditions for complete reaction. We believe that this mechanism provides the solution of the apparent discrepancy between our findings and those of Wang (11). On the other hand, this reaction is evidently much too slow to necessitate its inclusion along with reactions [3] and [4] in describing the kinetics of bromination of dilute (10^{-4} M) solutions of uracil at room temperature.

ACKNOWLEDGMENT

The authors gratefully acknowledge their indebtedness to Dr. J. M. Kennedy of the Theoretical Physics Branch, Atomic Energy of Canada Limited, for programming and carrying out the computations, the results of which are reported in the foregoing pages.

REFERENCES

1. CHARGAFF, E. and DAVIDSON, J. N. The nucleic acids. Vol. 1. Academic Press, Inc., New York. 1955. p. 502 ff.
2. DAVIDSON, D. and BAUDISCH, O. J. Am. Chem. Soc. **48**, 2379 (1926).
3. DUNN, D. B. and SMITH, J. D. Biochem. J. **67**, 494 (1957).
4. HILBERT, G. E. and JANSEN, E. F. J. Am. Chem. Soc. **56**, 134 (1934).
5. JOHNSON, T. B. J. Am. Chem. Soc. **62**, 2269 (1940).
6. JOHNSON, T. B. and WINTON, M. G. J. Am. Chem. Soc. **63**, 2379 (1941).
7. MOORE, A. M. and THOMSON, C. H. *In* Progress in radiobiology. *Edited by* Mitchell, J. J., Holmes, B. E., and Smith, C. L. Oliver and Boyd, Edinburgh. 1956. p. 75 ff.
8. MOORE, A. M. and THOMSON, C. H. Can. J. Chem. **35**, 163 (1957).
9. MOORE, A. M. Can. J. Chem. **36**, 281 (1958).
10. WANG, S. Y., APICELLA, M., and STONE, B. R. J. Am. Chem. Soc. **78**, 4180 (1956).
11. WANG, S. Y. Nature, **180**, 91 (1957).
12. WIERZCHOWSKI, K. L. and SHUGAR, D. Biochim. et Biophys. Acta, **25**, 355 (1957).

PRESSURE AND TEMPERATURE EFFECTS ON THE KINETICS OF THE ALKALINE FADING OF ORGANIC DYES IN AQUEOUS SOLUTION[1]

DAVID T. Y. CHEN AND KEITH J. LAIDLER

ABSTRACT

The rates of the alkaline fading of bromphenol blue, phenolphthalein, crystal violet, and malachite green have been studied from atmospheric pressure to 16,000 pounds per square inch. The rates for phenolphthalein and malachite green were also measured over a range of temperatures in order to determine the activation energies and entropies. The reactions went essentially to completion with the exception of the fading of phenolphthalein, for which the effects of temperature and pressure on the back reaction and equilibrium constant were also studied. No effect of pressure was found for the fading of crystal violet, but the reactions of the other three dyes were accelerated by pressure, so that there are negative volumes of activation. These are correlated with the entropies of activation and are interpreted in terms of the reaction mechanisms.

INTRODUCTION

Previous work (1, 2, 3, 4) has shown that for a number of reactions in aqueous solution the effects of pressure may be interpreted in terms of the electrostriction of the solvent around ions and dipoles. The present investigation consists of a study of reactions involving the attack by a hydroxide ion on large organic dye molecules. These reactions are of such a nature that electrostriction effects are not as powerful as in many of the previous reactions studied, so that structural effects are expected to play a part in determining the influence of pressure. Since the reactions chosen are structurally similar to one another, but are quite different electrically, they provide a useful means of separating the two effects. The dyes used were bromphenol blue, phenolphthalein, crystal violet, and malachite green, and of these the first two are negatively charged and the second two positively charged.

The kinetics of the alkaline fading of bromphenol blue were first studied under atmospheric pressure by Panepinto and Kilpatrick (5) and by Amis and La Mer (6). The results of these workers led to the following proposed mechanism, which was suggested by Amis and La Mer:

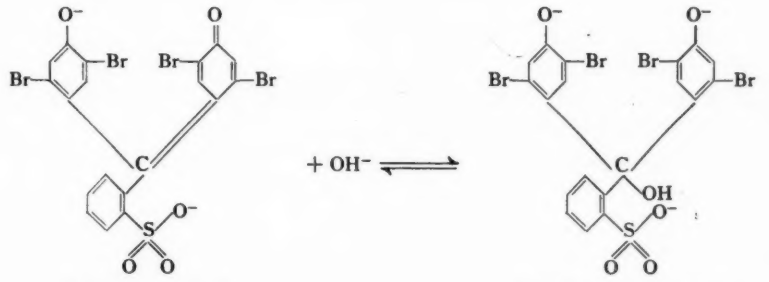

Quinoid form (blue) Carbinol form (colorless)

The reaction went to completion.

The alkaline fading of phenolphthalein was studied by Kober and Marshall (7), Biddle

[1]*Manuscript received November 20, 1958.*
Contribution from the Department of Chemistry, University of Ottawa, Ottawa, Canada.

and Porter (8), Lund (9), Wygaerts and Eeckhout (10), and by Barnes and La Mer (11). The mechanism of the reaction can be represented by the following equations:

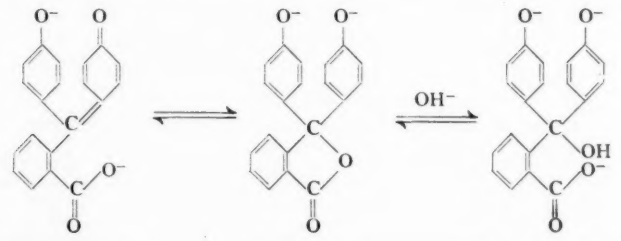

Quinoid form (red) Lactone form Carbinol form (colorless)

The reaction does not go to completion, and in our investigation the kinetics have been investigated in both directions over a range of temperatures and pressures.

The kinetics at atmospheric pressure of the fading of crystal violet in alkaline solution was studied by Biddle and Porter (8), Hockberg and La Mer (12), Goldacre and Phillips (13), and in great detail by Turgeon and La Mer (14). The reaction goes essentially to completion, and again involves the formation of a carbinol, as indicated below:

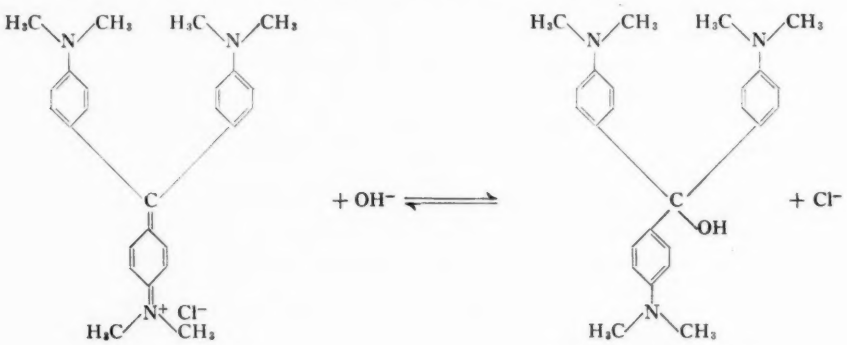

Quinoid form (violet) Carbinol form (colorless)

Very little work has previously been done on the fading of malachite green, which proceeds according to the equation:

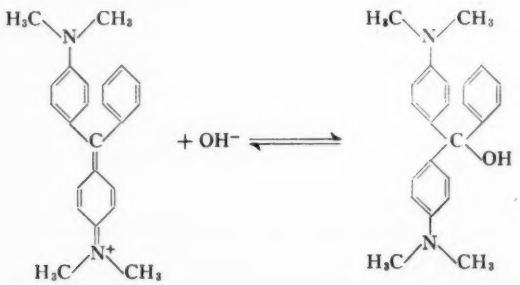

Quinoid form (green) Carbinol form (colorless)

In 1909 Sidgwick and Moore (15) made a few rate measurements, and Goldacre and Phillips (13) later made some studies in buffered solutions of pH 7.9.

It is to be seen that the four reactions may be represented schematically by the following equations:

$$(\text{B.P.B.})^{=} + \text{OH}^{-} \leftrightarrows (\text{B.P.B.})^{=}\text{OH}$$

$$(\text{P.P.})^{=} + \text{OH}^{-} \leftrightarrows (\text{P.P.})^{=}\text{OH}$$

$$(\text{C.V.})^{+} + \text{OH}^{-} \leftrightarrows (\text{C.V.})\text{OH}$$

$$(\text{M.G.})^{+} + \text{OH}^{-} \rightleftarrows (\text{M.G.})\text{OH}$$

The first two are reactions between ions of the same sign, the last two between ions of opposite sign. If electrostatic effects alone were important the first two reactions would therefore be expected to involve a decrease in volume during the activation process, and to be accelerated by pressure. The last two reactions, on the other hand, should involve an increase in volume and should be retarded by pressure. The results below show that these anticipations are realized in the first two cases, but that the third reaction is unaffected by pressure. The fourth reaction is accelerated by pressure. These results may be due to the fact that the charges do not approach very closely in the formation of the activated complex, and that structural effects are important.

EXPERIMENTAL PROCEDURE

Materials

The bromphenol blue used in the investigation was an Eastman Organics product. A stock solution was prepared by dissolving the dye in absolute ethanol, adding 0.01 *M* sodium hydroxide to convert it to the monosodium salt, evaporating the resulting solution in vacuum to dryness, and diluting with water to 1 liter. The phenolphthalein used was a C.P. grade Fisher product, and it was recrystallized three times from absolute methanol. The crystal violet used was an Anachemia Chemicals Ltd. product, and was purified by precipitating it as the carbinol, dissolving in hydrochloric acid, and recrystallizing the chloride twice; the crystals were dried in a vacuum desiccator. The malachite green used was a Fisher Scientific Company product (M-73), and was found by analysis to have the composition $2[C_{23}H_{25}N_2]C_2H_2O_4 + C_2H_2O_4$ (mol. wt. 926.90). It was purified by recrystallizing it twice from water.

High-pressure Technique

The high-pressure technique used has been described in detail in a previous paper (4) in which a diagram of the apparatus is shown. In brief, the pressure vessel is designed so that the solutions are separated by mercury from the oil used in the rest of the apparatus, and so that samples can be introduced and withdrawn within a short period of time.

Kinetic Procedure

Since the sodium hydroxide was in all cases in excess of the dye, the reactions in the case of bromphenol blue, crystal violet, and malachite green were simple first-order reactions. The phenolphthalein reaction, on the other hand, had to be treated as consisting of opposing first-order reactions.

The first-order rate constants for the bromphenol blue reaction were obtained by plotting the logarithm of the photometric density L against the time and determining the slopes. The kinetic runs were carried out using a mixture that was 2×10^{-5} *M* in bromphenol blue and 0.2 *M* in sodium hydroxide. Five-milliliter samples were taken at

intervals of about 1500 seconds and delivered into a colorimeter tube containing 5 ml of water. The photometric densities of the solution were determined in an Evelyn photoelectric colorimeter using filter 565; the Lambert–Beer law was found to be obeyed by the dye solutions.

Since the phenolphthalein fading is reversible the mechanism must be represented as

$$(\text{P.P.})^{=} + \text{OH}^{-} \underset{k_{-1}}{\overset{k_1}{\rightleftharpoons}} (\text{P.P.})^{=}\text{OH}.$$

The rate of disappearance of the dye is therefore given by

$$[1] \qquad -\frac{d[(\text{P.P.})^{=}]}{dt} = k_1[(\text{P.P.})^{=}][\text{OH}^{-}] - k_{-1}[(\text{P.P.})^{=}\text{OH}],$$

where k_1 is the second-order rate constant for the forward reaction and k_{-1} is the first-order rate constant for the reverse reaction. Since $[\text{OH}^{-}]$ is practically constant we can combine it with k_1 to form a pseudo-first-order constant k_1', the resulting equation being

$$[2] \qquad -\frac{d[(\text{P.P.})^{=}]}{dt} = k_1'[(\text{P.P.})^{=}] - k_{-1}[(\text{P.P.})^{=}\text{OH}].$$

The behavior is therefore that of reversible first-order reactions, which obey the kinetic law

$$[3] \qquad k_1' + k_{-1} = \frac{2.303}{t} \log \frac{c_e}{c_e - c}.$$

Here c_e is the equilibrium concentration of the carbinol form of phenolphthalein, and c is the concentration of the carbinol form at any time t. Let c_τ be the total concentration of phenolphthalein, c_e' the equilibrium concentration of the pink form of phenolphthalein, and c' the concentration of the pink form at any time t. Then since

$$[4] \qquad c_e = c_\tau - c_e'$$

and

$$[5] \qquad c = c_\tau - c',$$

equation [3] becomes

$$[6] \qquad k_1' + k_{-1} = \frac{2.303}{t} \log \frac{c_\tau - c_e'}{c' - c_e'}.$$

The absorption of light by the substance was found to obey the Lambert–Beer law, and the concentration of the colored substance is therefore directly proportional to the photometric density L according to the expression

$$[7] \qquad c' = L/K_1.$$

Here K_1 is the calibration constant whose value depends on the nature of the colored substance and the characteristics of the filter used. L is the photometric density, equal to $\log (I_0/I)$, where I_0 is the intensity of the incident light and I that of the transmitted light. Equation [6] therefore becomes

$$[8] \qquad k_1' + k_{-1} = \frac{2.303}{t} \log \frac{L_\tau - L_e}{L - L_e},$$

where L_e is the photometric density of the solution at equilibrium, L_r is the photometric density of the solution when all its phenolphthalein is in the pink form, and L that at any time t. L_r and L_e are constants. From equation [8] it can be seen that a plot of $\log (L-L_e)$ against the time should result in a straight line with a slope equal to

$$-\frac{k_1'+k_{-1}}{2.303},$$

so that the value of the combined rate constant $(k_1'+k_{-1})$ can be calculated. The individual rate constants k_1 and k_{-1} can be found from the equilibrium constant K, which is equal to k_1/k_{-1}. If $(k_1'+k_{-1})$ is called k_c then

[9] $$k_1 = \frac{k_1'}{[OH^-]} = \frac{k_c-k_{-1}}{[OH^-]} = \frac{k_c-k_1/K}{[OH^-]}.$$

From this

[10] $$k_1 = \frac{k_c}{[OH^-]+(1/K)}$$

so that

[11] $$k_{-1} = k_c-k_1'.$$

The kinetic runs with phenolphthalein were carried out using a solution that was 1.00×10^{-5} M in phenolphthalein and 0.01 M in sodium hydroxide. Ten-milliliter samples were taken at about 2000-second intervals and the photometric densities of the samples were determined in the Evelyn photoelectric colorimeter using filter 540 (the absorption maximum is at 550 μ). The photometric density at equilibrium was determined in each case by allowing the reaction mixture to remain under the experimental conditions for at least 24 hours. The value of the combined rate constant k_c was determined by plotting $\log (L-L_e)$ against the time.

The procedure with crystal violet was similar to that with bromphenol blue. The dye shows an adsorption maximum at 590 μ and the best filter was No. 565. The Lambert–Beer law was again obeyed. The kinetic runs were carried out in a mixture that was 5.0×10^{-6} M in dye and 2.0×10^{-3} M in sodium hydroxide. Samples were withdrawn at intervals of about 900 seconds and the photometric densities L determined using the colorimeter. The values of $\log L$ were plotted against the time, and straight lines obtained in each case. The apparent first-order rate constants were calculated from the slopes of the lines.

The kinetic procedure with malachite green was similar to that with crystal violet. The solutions used were 0.0004 N in NaOH and 0.00002 M in malachite green. Owing to the much lower concentration of NaOH used the solutions were protected from CO_2 with a soda-lime tube. For runs under pressure, 40 ml each of the reacting solution were mixed and introduced into the pressure vessel. Ten-milliliter samples were taken at about 1000-second intervals and the photometric density measured as before using filter No. 565. In each case the logarithms of the photometric densities were plotted against the time.

EXPERIMENTAL RESULTS

Bromphenol Blue

Rate constants for the bromphenol blue reaction were determined at a temperature of 25.0° C and at pressures varying from atmospheric to 16,000 pounds per square inch. Typical plots of $\log L$ against time are shown in Fig. 1, and the rate constants,

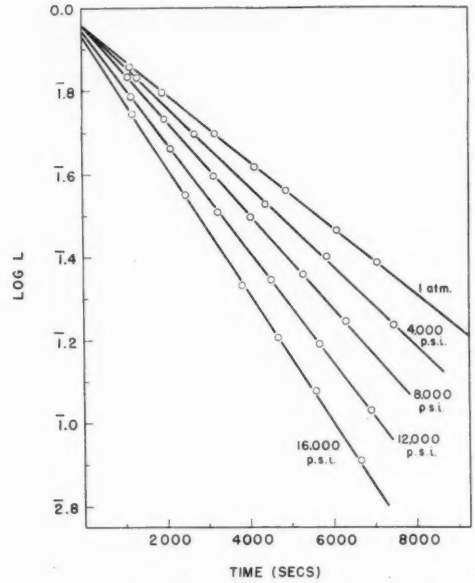

FIG. 1. Plots of log L against time for the fading of bromphenol blue at various pressures.

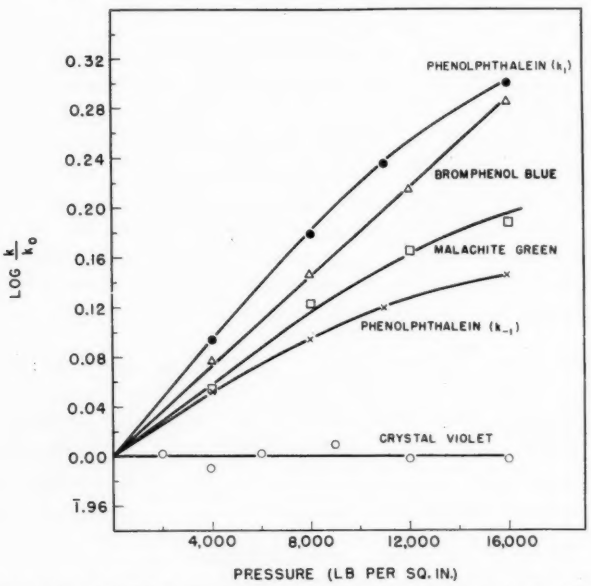

FIG. 2. Van't Hoff plots of the logarithms of k/k_0 against the hydrostatic pressure.

obtained from the slopes, are listed in Table I; k_1' represents the apparent first-order rate constant and k_1 the second-order rate constant. Figure 2 includes a plot of log k/k_0 against the pressure for this reaction. The relationship is seen to be quite linear, and the

slope of the line corresponds to a volume of activation of -14.9 cc per mole. The energy of activation for the reaction was determined by Amis and La Mer (6), and the results at zero ionic strength are

$$\Delta S^* = -13.34 \text{ calories per degree per mole},$$
$$E = 12.2 \text{ kcal per mole},$$
$$A = 2.04 \times 10^{10} \text{ liters per mole per second}.$$

TABLE I

Summary of results for the alkaline fading of bromphenol blue ($T = 25.0°$ C)

P (lb/in.^{2})	k_1' (sec^{-1})	k_1 (M^{-1} sec^{-1})	k/k_0	log k/k_0
14.7	0.0001860	0.0009298	1	0
4000	0.0002226	0.001113	1.197	0.0781
8000	0.0002609	0.001305	1.404	0.1473
12000	0.0003056	0.001528	1.643	0.2156
16000	0.0003588	0.001794	1.929	0.2853

$\Delta V^* = -14.90$ cc/mole.

Phenolphthalein

Since an activation energy for the phenolphthalein reaction had not previously been determined, the rates of the reaction in both directions were measured over a range of temperatures. From the slopes of plots of log $(L-L_e)$ against time, the values of $k_1'+k_{-1}$ can be calculated, and the results are included in Table II. By allowing the mixtures to

TABLE II

Rate and equilibrium constants for the fading of phenolphthalein at various temperatures

Temperature (° C)	$k_1'+k_{-1}$ (sec^{-1})	K (M^{-1})	k_1' (sec^{-1})	k_1 (M^{-1} sec^{-1})	k_{-1} (sec^{-1})
9.7	0.0000412	74.0	0.0000262	0.00262	0.0000151
20.0	0.0000960	86.9	0.0000446	0.00446	0.0000513
25.0	0.000143	66.7	0.0000572	0.00572	0.0000858
34.6	0.000311	41.8	0.0000917	0.00917	0.000219

$\Delta H = -9.97$ kcal/mole. $\Delta F = -2.49$ kcal/mole.
$E_1 = 8.59$ kcal/mole. $\Delta S_1^* = -41.94$ cal/deg-mole. $A_1 = 1.14 \times 10^4$ M^{-1} sec^{-1}.
$E_{-1} = 18.47$ kcal/mole. $\Delta S_{-1}^* = -17.12$ cal/deg-mole. $A_{-1} = 3.06 \times 10^9$ sec^{-1}.

stand for over 24 hours at the four temperatures the equilibrium constants were determined, and are also shown in the table. The separated values of k_1' and k_{-1} are also shown and from k_1' the values of k_1 are calculated, and are shown in the table. Figure 3 shows a van't Hoff plot of the logarithm of the equilibrium constant against the reciprocal of the absolute temperature, and it is seen that a straight line is obtained. The thermodynamical values obtained from this plot are as follows:

$$\Delta H = -9.97 \text{ kcal per mole},$$
$$\Delta F = -2.49 \text{ kcal per mole},$$
$$\Delta S = -25.1 \text{ cal mole}^{-1} \text{ deg}^{-1}.$$

Figures 4 and 5 show plots of log k_1 against $1/T$ and of log k_{-1} against $1/T$. The Arrhenius law is seen to be obeyed accurately, and the frequency factors and energies and entropies of activation obtained are:

$$E_1 = 8.59 \text{ kcal per mole},$$
$$A_1 = 1.14 \times 10^4 \text{ liters mole}^{-1} \text{ sec}^{-1},$$
$$\Delta S_1^* = -41.49 \text{ cal mole}^{-1} \text{ deg}^{-1},$$
$$E_{-1} = 18.47 \text{ kcal per mole},$$
$$A_{-1} = 3.06 \times 10^9 \text{ sec}^{-1},$$
$$\Delta S_{-1}^* = -17.12 \text{ cal mole}^{-1} \text{ deg}^{-1}.$$

Table III shows the results obtained at 25.0° C and at the various pressures employed. Figure 6 shows a plot of the logarithm of the equilibrium constant against the pressure and from the slope of the straight line a value of ΔV of 8.7 cc per mole was calculated. The plots of the logarithms of k_1 and k_{-1} against the pressure are included in Fig. 2, and from the initial slopes values of −19.7 and −11.0 cc per mole are calculated for the volumes of activation for the forward and reverse reactions.

TABLE III

Rate and equilibrium constants for the fading of phenolphthalein, at various pressures (T = 25.0° C)

P (p.s.i.)	$k_1'+k_{-1}$ (sec^{-1})	K (liters mole^{-1})	k_1' (sec^{-1})	k_1 (liters mole^{-1} sec^{-1})	k_{-1} (sec^{-1})	k_1/k_0	k_{-1}/k_0
14.7	0.000143	66.7	0.0000572	0.00572	0.0000858	1	1
4000	0.000168	73.6	0.0000712	0.00712	0.0000967	1.245	1.127
8000	0.000193	81.2	0.0000865	0.00865	0.000107	1.512	1.241
11000	0.000212	87.3	0.0000986	0.00986	0.000113	1.724	1.317
16000	0.000232	98.0	0.000115	0.0115	0.000120	1.993	1.398

$\Delta V_1^* = -19.66$ cc/mole.
$\Delta V_{-1}^* = -10.98$ cc/mole.
$\Delta V = -8.68$ cc/mole.

Crystal Violet

Rate constants for the fading of crystal violet were measured at a temperature of 25.0° C and at pressures varying from atmospheric to 16,000 lb per sq. in. The results are summarized in Table IV, which shows the apparent first-order constants k_1' and the true second-order constants k_1 obtained by dividing k_1' by the concentration of hydroxide ions.

TABLE IV

Summary of results for the alkaline fading of crystal violet (T = 25.0° C)

P (p.s.i.)	k_1' (sec^{-1})	k_1 (liters mole^{-1} sec^{-1})	k_1/k_0	log k_1/k_0
14.7	0.000520	0.260	1	0
2000	0.000522	0.261	1.004	0.0017
4000	0.000509	0.255	0.981	$\bar{1}$.9917
6000	0.000522	0.261	1.004	0.0017
9000	0.000532	0.266	1.023	0.0098
12000	0.000518	0.259	0.996	$\bar{1}$.9983
16000	0.000518	0.259	0.996	$\bar{1}$.9983

$\Delta V^* = 0$.

Pressure is seen to have essentially no effect on the rates, a conclusion that is verified by the plot shown in Fig. 2.

The results obtained by Turgeon and La Mer (14) at atmospheric pressure are, at an ionic strength of 0.0011 M,

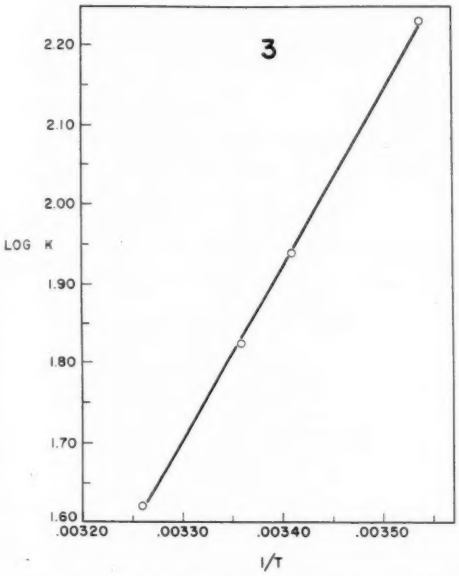

FIG. 3. Plot of the logarithm of the equilibrium constant against $1/T$, for the fading of phenolphthalein.

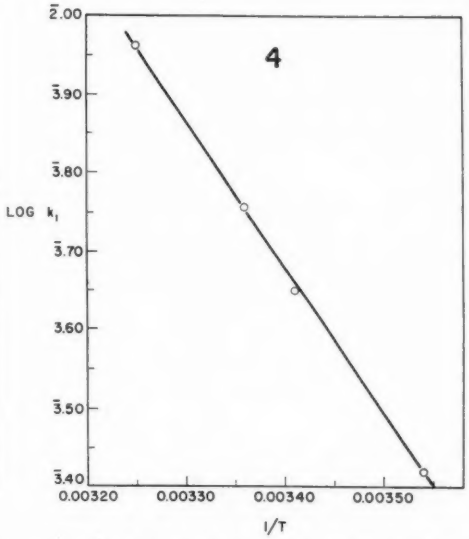

FIG. 4. Plot of log k_1 against $1/T$, for the fading of phenolphthalein.

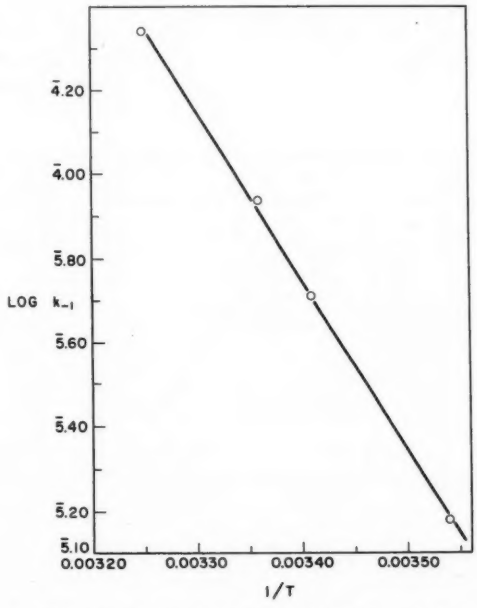

FIG. 5. Plot of log k_{-1} against $1/T$, for the fading of phenolphthalein.

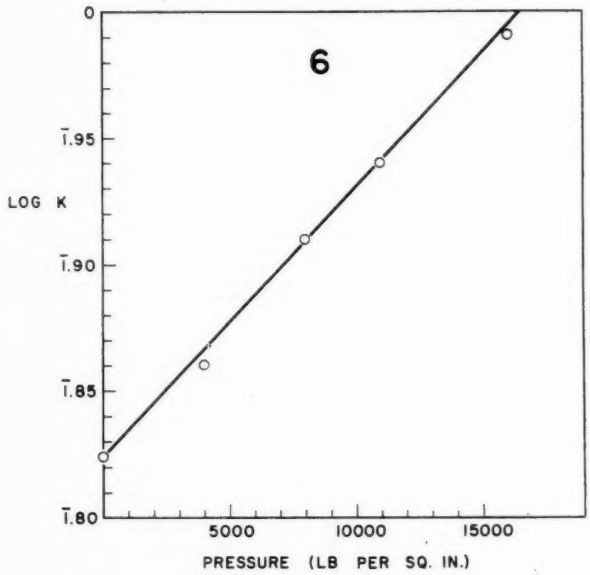

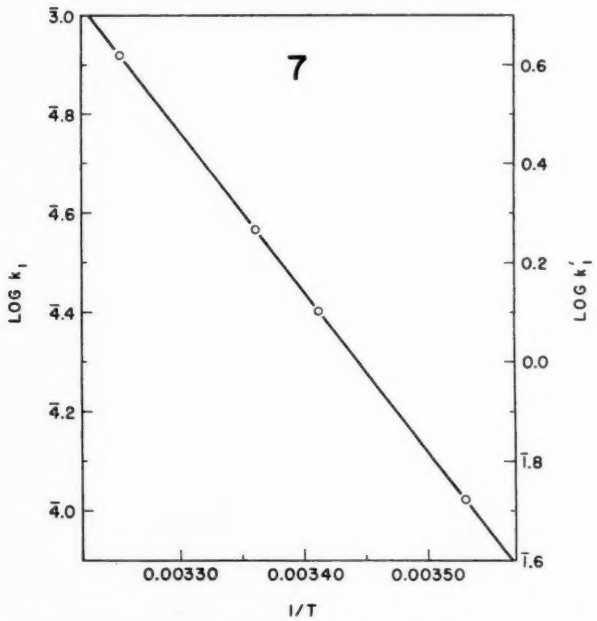

FIG. 6. Plot of log K against the pressure, for the fading of phenolphthalein.
FIG. 7. Plot of log k_1 against $1/T$ for the fading of malachite green.

$$E = 15.1 \text{ kcal mole}^{-1},$$
$$A = 3.13 \times 10^{10}\ M^{-1} \text{ sec}^{-1},$$
$$\Delta S^* = -12.3 \text{ cal deg}^{-1} \text{ mole}^{-1}.$$

Malachite Green

Rate constants under atmospheric pressure and at the various temperatures employed are summarized in Table V, in which k_1' represents the apparent first-order rate constant

TABLE V

Summary of results for the alkaline fading of malachite green under atmospheric pressure

Temperature (° C)	k_1' (sec^{-1})	k_1 ($M^{-1}\,\text{sec}^{-1}$)
10.2	0.0001053	0.5265
20.0	0.0002533	1.267
25.0	0.0003684	1.842
34.9	0.0008291	4.146

E = 14.65 kcal/mole.
$A = 1.023 \times 10^{11}\ M^{-1}\,\text{sec}^{-1}$.
$\Delta S^* = -10.15$ e.u.

and k_1 the true second-order rate constant. The corresponding Arrhenius plot is shown in Fig. 7. The energy of activation, frequency factor, and entropy of activation obtained are:

$$E = 14.65 \text{ kcal mole}^{-1},$$
$$A = 1.023 \times 10^{11}\ M^{-1} \text{ sec}^{-1},$$
$$\Delta S^* = -10.15 \text{ e.u.}$$

Table VI shows the rate constants obtained at 25.0° C and under various pressures. The corresponding van't Hoff plot is included in Fig. 2; the curve is seen to be not linear. From the slope at the lower pressures we calculate a volume of activation of −12.0 cc per mole.

TABLE VI

Summary of results for the alkaline fading of malachite green (T = 25.0° C)

P (p.s.i.)	k_1' (sec^{-1})	k_1 ($M^{-1}\,\text{sec}^{-1}$)	k_1/k_0
14.7	0.0004789	2.395	1
4000	0.0005422	2.711	1.132
8000	0.0006358	3.179	1.327
12000	0.0007014	3.507	1.464
16000	0.0007384	3.692	1.542

$\Delta V^* = -12.0$ cc/mole.

DISCUSSION

Comparison with Previous Work

It is difficult to compare the rate constants obtained in the present investigation with those obtained by previous workers, owing to the different conditions employed. The following comparisons may, however, be of interest.

For bromphenol blue the value of the rate constant obtained at 25.0° C and 1 atm pressure was 0.000932 $M^{-1}\,\text{sec}^{-1}$. Extrapolation of Amis and La Mer's (6) results to the same ionic strength (0.2 M) gives 0.000854 $M^{-1}\,\text{sec}^{-1}$.

For the fading of phenolphthalein the present values of K, k_1, and k_{-1} at 25° C and 1 atm pressure are as shown below:

$$K = 65.25\ M^{-1},$$
$$k_1 = 0.00572\ M^{-1}\ \text{sec}^{-1},$$
$$k_{-1} = 0.0000858\ \text{sec}^{-1}.$$

The values obtained by Barnes and La Mer (11) under the same conditions are:

$$K = 66.70\ M^{-1},$$
$$k_1 = 0.00634\ M^{-1}\ \text{sec}^{-1},$$
$$k_{-1} = 0.0000972\ \text{sec}^{-1}.$$

For crystal violet the value of k_1 obtained in the present work was 0.260 M^{-1} sec^{-1} at 25.0° C. The value of Turgeon and La Mer (14), corrected to the same ionic strength, was 0.256 M^{-1} sec^{-1}. It was found that for this reaction there was some catalysis by the mercury in contact with the solution in the case of the work done in the high pressure vessel; the rate constant in the absence of mercury was 0.207 M^{-1} sec^{-1}.

On the whole the agreement between the results of the present work and those of the previous workers is quite satisfactory.

Significance of the ΔV^* Values

The ΔV^* values obtained in the present investigation are listed in the last column of Table VII, which also gives the values of E, A, and ΔS^*. Also included in this table are the data for a number of other reactions; the last four are in solvents other than pure water.

TABLE VII

Summary of data for reactions in aqueous solution

Reaction	E (kcal)	A	ΔS^* (e.u.)	ΔV^* (cc per mole)	Ref.
Bromphenol blue + OH^-	12.2	2.0×10^{10}	−13.3	−14.9	Present work
Phenolphthalein + OH^- (k_1)	8.6	1.1×10^{4}	−41.9	−19.7	Present work
Phenolphthalein + OH^- (k_{-1})	18.5	3.1×10^{9}	−17.1	−10.6	Present work
Crystal violet + OH^-	15.1	3.1×10^{10}	−12.3	0.0	Present work
Malachite green + OH^-	14.7	1.0×10^{11}	−10.2	−12.0	Present work
Methyl acetate + OH^-	12.0	9.3×10^{7}	−24.1	− 9.9	4
Ethyl acetate + OH^-	11.6	3.2×10^{7}	−26.2	− 8.8	4
Acetamide + OH^-	14.2	9.5×10^{5}	−33.5	−14.2	4
Propionamide + OH^-	14.6	1.5×10^{6}	−32.6	−16.9	4
$CH_2BrCOO^- + S_2O_3^=$	13.3	1.6×10^{9}	−17.0	− 4.8	2
$CH_2ClCOO^- + OH^-$	22.7	5.7×10^{10}	−11.6	− 6.1	16, 17, 18
$CH_2BrCOOCH_3 + S_2O_3^=$	17.2	1.0×10^{14}	− 5.7	+ 3.2	2
$Co(NH_3)_5Br^{++} + OH^-$	23.6	5.0×10^{17}	21.7	8.5	2
$(CH_3)(C_2H_5)(C_6H_5)(C_6H_5CH_2)N^+Br^- \rightarrow$ $(CH_3)(C_6H_5)(C_6H_5CH_2)N + C_2H_5Br$	29.7	3.1×10^{16}	14.9	3.3	17, 18
$C_2H_5O^- + C_2H_5I \rightarrow C_2H_5OC_2H_5 + I^-$	20.7	2.1×10^{11}	− 9.7	− 4.1	16, 18, 19
$C_6H_5CCl_3 \rightarrow C_6H_5CCl_2^+ + Cl^-$	15.0	3.5×10^{5}	−35.0	−14.5	1, 2
$C_5H_5N + C_2H_5I \rightarrow C_5H_5N^+(C_2H_5)I^-$	14.4	3.6×10^{5}	−35.4	−15.8	18, 19

Figure 8 shows a plot of ΔV^* against ΔS^* for all of the reactions listed in Table VII. As previously shown (4), there is a fairly good correlation between the values, although the reactions studied in the present work show greater deviations than do the other reactions. This is presumably due to the fact that structural factors are playing a more important role. When electrostatic interactions are predominant a correlation is expected, for reasons discussed in a previous paper (3), but structural effects may introduce deviations.

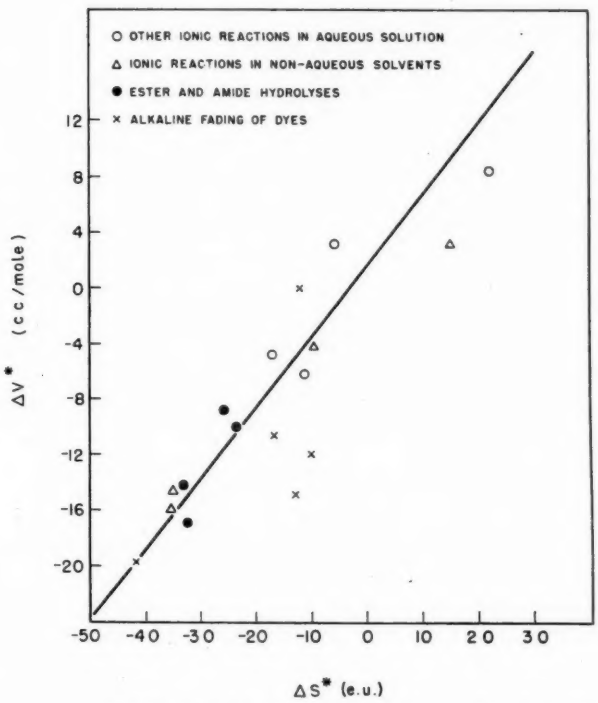

FIG. 8. Plot of ΔV^* against ΔS^* for a number of reactions.

The values of ΔV^* obtained in the present investigation will now be discussed with reference to the mechanisms. The negative volumes of activation obtained for the fading of bromphenol blue and of phenolphthalein are consistent with the fact that there is an approach of charges of the same sign. However, since the hydroxide ion approaches the uncharged central carbon atom, a strong electrostatic effect is not to be expected. It therefore seems likely that structural effects contribute, and some evidence with regard to this is referred to below.

With crystal violet there is no volume of activation in spite of the approach of ions of opposite sign. The hydroxide ion, however, attacks the central carbon atom which is separated by several Ångstroms from the three nitrogen atoms which share the positive charge. Electrostriction effects are therefore unimportant, and the zero value of ΔV^* suggests that there is no volume change due to structural effects.

This conclusion gives the clue to the negative volumes of activation found with the other three fading reactions. The crystal violet ion is the only one of the four investigated in which the three benzene rings lie in a plane. This arises because the resonance involving the quinoid forms of the rings can occur with all three rings.* In the case of bromphenol blue, phenolphthalein, and malachite green only two of the three rings can be involved

*Spectroscopic results (20) have in fact indicated that, owing to repulsion between hydrogen atoms on neighboring rings, the crystal violet ion is not quite planar but that the three rings are twisted slightly out of the plane. This is not found with malachite green and other molecules in which one ring does not enter into the resonance and is therefore out of the plane of the other two rings.

in such resonance. The third ring may therefore be twisted out of the plane of the rest of the molecule, and the molecule may occupy a somewhat greater volume relative to the carbinol form.

The suggestion is therefore that in the bromphenol blue, phenolphthalein, and malachite green reactions the quinoid forms of the dyes may structurally be somewhat larger (relative to the carbinol forms) than in crystal violet, so that the fading reaction involves a decrease in volume. In the bromphenol blue and phenolphthalein reactions there may also be small contributions from electrostriction effects; these, however, will be unimportant for malachite green for the same reason as for crystal violet.

REFERENCES

1. BUCHANAN, J. and HAMANN, S. D. Trans. Faraday Soc. **49**, 1425 (1953).
2. BURRIS, C. T. and LAIDLER, K. J. Trans. Faraday Soc. **51**, 1497 (1955).
3. LAIDLER, K. J. Discussions Faraday Soc. **22**, 88 (1956).
4. LAIDLER, K. J. and CHEN, D. T. Y. Trans. Faraday Soc. **54**, 1026 (1958).
5. PANEPINTO, F. W. and KILPATRICK, M. J. Am. Chem. Soc. **59**, 1871 (1937).
6. AMIS, E. S. and LA MER, V. K. J. Am. Chem. Soc. **61**, 905 (1939).
7. KOBER, P. A. and MARSHALL, J. T. J. Am. Chem. Soc. **33**, 59 (1911).
8. BIDDLE, H. C. and PORTER, C. W. J. Am. Chem. Soc. **37**, 1571 (1915).
9. LUND, H. J. Chem. Soc. 1844 (1930).
10. WYGAERTS, M. and EECKHOUT, J. Natuurw. Tijdschr. **17**, 163 (1935).
11. BARNES, M. D. and LA MER, V. K. J. Am. Chem. Soc. **64**, 2312 (1942).
12. HOCKBERG, S. and LA MER, V. K. J. Am. Chem. Soc. **63**, 3110 (1941).
13. GOLDACRE, R. S. and PHILLIPS, J. N. J. Chem. Soc. 1724 (1949).
14. TURGEON, J. C. and LA MER, V. K. J. Am. Chem. Soc. **74**, 9588 (1952).
15. SIDGWICK, N. V. and MOORE, T. S. J. Chem. Soc. **95**, 889 (1909).
16. PERRIN, M. W. Trans. Faraday Soc. **34**, 144 (1938).
17. WILLIAMS, E. W., PERRIN, M. W., and GIBSON, R. C. Proc. Roy. Soc. A, **154**, 684 (1936).
18. MOELWYN-HUGHES, E. A. The kinetics of reactions in solution. Clarendon Press, Oxford. 1947. p. 324.
19. GIBSON, R. C., FAWCETT, E. W., and PERRIN, M. W. Proc. Roy. Soc. A, **150**, 223 (1935).
20. LEWIS, G. N., MAGEL, T. T., and LIPKIN, D. J. Am. Chem. Soc. **64**, 1774 (1942).

SOME OBSERVATIONS ON THE THEORY OF DIELECTRIC RELAXATION IN ASSOCIATED LIQUIDS[1]

B. E. CONWAY

ABSTRACT

The theory of absolute reaction rates is examined for the case of relaxation in associated polar liquids where the activation process is probably an excitation of a librational motion to one of complete rotation over a rotational potential energy barrier. The rotational barriers in water are calculated using the point-charge model of the water quadrupole and the effect of thermal bond bending is examined. The experimental heats of activation for dielectric relaxation in water and deuterium oxide are discussed and their temperature dependence examined; the heat capacity change for rotational activation is derived. Isotopic effects in the heats of activation, the relaxation times, and frequency factors are discussed. A qualitative explanation is sought for the homogeneity of relaxation times in water; rotation of water molecules in the fields of the hydroxonium and hydroxide ions present in water may account for the narrow distribution of relaxation times observed experimentally. This mechanism is shown to be consistent with other theoretically derived quantities and with the mechanism of proton mobility in water. A different mechanism is indicated in ice, where the proton concentration is lower, but in ice containing extra protons, the mechanism probably reverts to that existing in water.

INTRODUCTION

Although it appears that a number of substances, e.g. H_2S, hydrogen halides, N_2, O_2, CH_4, and certain ammonium salts exhibit rotation–libration transitions (1) as indicated by changes of the specific heat (2, 3) and dielectric constant (4, 5) over a relatively narrow range of temperatures, a free rotation model for treatment of dielectric relaxation behavior is in general inapplicable to more polar associated condensed phases, e.g. water and the alcohols. In such systems the molecules execute librational oscillations rather than rotational motion except upon activation when a temporary libration–rotation transition is indicated, the frequency of which is inversely related to the relaxation time as determined from dielectric dispersion or absorption conductance studies. In the theory of absolute reaction rates as applied to ordinary chemical reactions, the passage of the reacting particle over the potential-energy barrier has been regarded as a transition of one vibrational mode into a linear translational one along the reaction co-ordinate. Extraction of the partition function for this motion from the total partition function for the activated state, followed by multiplication by the classical average linear velocity of the particle along the reaction co-ordinate, leads to the familiar rate expression for the rate constant of the process. It has usually been assumed (6, 7) without proof that the same expression holds for a libration–rotation activation in dielectric relaxation. It is of interest to show that a formal treatment of rotational instead of the translational activation leads to the same absolute rate equation.

For an activation of, for example, a diatomic molecule A from librational to complete rotational motion we may write the equilibrium constant $K^{\ddagger}$ for the quasi-equilibrium between activated and initial states as

$$K^{\ddagger} = (F_A{}^{\ddagger}/F_A)\, e^{-E_0/RT}.$$

Extracting the partition function for the rotational motion arising from the activation gives

$$K^{\ddagger} = (F_A{}^{\ddagger\prime}/F_A)(1/\sigma)(8\pi^3 IkT/h^2)^{\frac{1}{2}}\, e^{-E_0/RT}, \qquad [1]$$

[1]*Manuscript received June 4, 1958.*
Contribution from the Department of Chemistry, University of Ottawa, Ottawa, Canada.

where $F^{\ddagger}$ is the total partition function for the activated state and F_A that for the initial state; E_0 is the energy of activation at 0° K and $F^{\ddagger\prime}$ differs from $F_A{}^{\ddagger}$ since one librational mode has been converted to one of free rotation in the activated state; σ is the Ehrenfest symmetry factor. If the molecule has a moment of inertia I, its classical rotational kinetic energy in one degree of freedom is $\frac{1}{2}I\omega^2$ if ω is the angular velocity. The average angular velocity $\bar{\omega}$ is hence $(kT/2\pi I)^{\frac{1}{2}}$, whence the corresponding average effective circular frequency $\bar{\nu}$ for σ-fold symmetry is

$$\bar{\nu} = \sigma\bar{\omega}/2\pi = \sigma(kT/8\pi^3 I)^{\frac{1}{2}}. \qquad [2]$$

By analogy with the procedure for activation in a linear vibrating bond, we now multiply $K^{\ddagger}$ by $\bar{\nu}$ to obtain the rate constant $\mathbf{k}$. Then from [1] and [2]

$$\mathbf{k} = 1/\tau = (kT/h)(F_A{}^{\ddagger\prime}/F_A)\, e^{-E_0/RT} \qquad [3]$$

where τ is the relaxation time. The expression is thus of the same form as for bond-stretching activation in ordinary chemical reactions.

HEAT OF ACTIVATION AND ITS TEMPERATURE DEPENDENCE

Heats of activation for dielectric relaxation processes may be obtained by determination of the temperature dependence of the critical wavelength at which dispersion of the dielectric constant occurs. In water and deuterium oxide, the heat of activation determined in this way shows a marked apparent dependence upon temperature. The plot of the logarithm of the experimental relaxation times (τ)* against $1/T$ is non-linear and apparent heats of activation, $\Delta H^{\circ\ddagger}$, derived by taking tangents at various temperatures on this plot, decrease with increasing temperature. Arrhenius plots based on the data for water collected by Smyth (8) and on the measurements of Collie, Hasted, and Ritson (9) for water and heavy water are shown in Fig. 1. The temperature dependence of the heat of activation found in the dielectric relaxation measurements parallels that

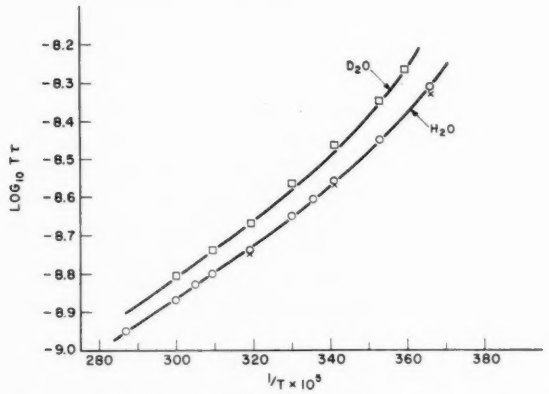

FIG. 1. Arrhenius plots for dielectric relaxation times for water and deuterium oxide.
○ Data for H_2O based on values of Smyth (8).
× Data for H_2O based on individual values of Collie, Hasted, and Ritson (9).
□ Data for D_2O based on values of Collie, Hasted, and Ritson (9).

**From the form of the rate equation, it is clear that it is the log of $T\tau$ which should be plotted in order to obtain the heat of activation. Although log τ itself is often plotted (11, 12), the data for water appear to be of sufficient accuracy to justify plotting log $T\tau$. This has been done in Fig. 1.*

found for the viscosity of water and for proton mobility in aqueous acid solutions, which process has a rate controlled by the frequency of rotation of water molecules (10). The non-linearity of the Arrhenius plots could arise from a temperature dependence of $\Delta H^{\circ\ddagger}$ and of the entropy of activation, $\Delta S^{\circ\ddagger}$, usually regarded as constant. If $\Delta H^{\circ\ddagger}$ varies with temperature, it is because there is a finite difference of heat capacity, $\Delta C_p^{\ddagger}$, between molecules in the activated state and those in the initial state of the relaxation process. $\Delta C_p^{\ddagger}$ can be evaluated as follows and hence the true dependence of $\Delta H^{\circ\ddagger}$ and $\Delta S^{\circ\ddagger}$ upon temperature, calculated. We may write [3] in the form

$$\mathbf{k} = 1/\tau = (kT/h)\, e^{-\Delta G^{\circ\ddagger}/RT}, \qquad [4]$$

where $\Delta G^{\circ\ddagger}$ is the standard free energy of activation corresponding to $\Delta H^{\circ\ddagger}$ and $\Delta S^{\circ\ddagger}$. With $K^{\ddagger}$ as defined above, it follows from equation [4] that

$$K^{\ddagger} = (1/\tau)(h/kT).$$

Following the treatment of Everett and Wynne-Jones (13), we may obtain $\Delta C_p^{\ddagger}$ from knowledge of pairs of $K^{\ddagger}$ values at various pairs of temperatures, since by applying the treatment of Everett and Wynne-Jones to the activation equilibrium constant $K^{\ddagger}$, it may be shown in general that for pairs of results 1,2 at different temperatures

$$\frac{\Delta_{1,2}(T \ln K^{\ddagger})}{\Delta_{1,2}T} = \frac{\Delta C_p^{\ddagger}}{R}.\frac{\Delta_{1,2}(T \ln T)}{\Delta_{1,2}T} + B, \qquad [5]$$

where $B = (\Delta S_0^{\circ\ddagger} - \Delta C_p^{\ddagger})/R$. The slope of the line obtained by plotting $\Delta_{1,2}(T \ln K^{\ddagger})/\Delta_{1,2}(T)$ versus $\Delta_{1,2}(T \ln T)/\Delta_{1,2}(T)$ then gives $\Delta C_p^{\ddagger}/R$. $K^{\ddagger}$ values are calculated from the data given by Smyth (8) and Collie, Hasted, and Ritson (9), and terms in the equation [5] are plotted in Fig. 2 from which $\Delta C_p^{\ddagger}$ for water and deuterium oxide may be calculated as -33.2 cal ° C^{-1} mole^{-1}. Isotopic differences in $\Delta C_p^{\ddagger}$ cannot be detected within the accuracy of the derivation of $\Delta C_p^{\ddagger}$, since the calculation requires high accuracy in the initial data, because a second derivative of the relaxation times with respect to temperature is, in effect, being calculated. The results shown in Figs. 2 and 3 speak well for the accuracy of the data on the relaxation times, since satisfactory lines are obtained in the $\Delta C_p^{\ddagger}$ plot (Fig. 2) and there is very little spread amongst the points through which the lines in Fig. 3 have been drawn.

If $\Delta C_p^{\ddagger}$ is independent of temperature,

$$\ln K^{\ddagger} = \frac{A}{T} + \frac{\Delta C_p^{\ddagger}}{R} \ln T + B, \qquad [6]$$

where $A = \Delta H_0^{\circ\ddagger}/R$ and B is another constant. $\Delta H_0^{\circ\ddagger}$, the heat of activation at the absolute zero (if water remained a liquid down to this temperature), can be derived from Fig. 3 using equation [6]. The values of $\Delta H_0^{\circ\ddagger}$ calculated from slopes of the two lines in Fig. 3 are significantly different, viz. 13.7 kcal g mole^{-1} for water and 14.0 kcal g mole^{-1} for deuterium oxide. Values of $\Delta H^{\circ\ddagger}$ at other temperatures can be derived together with $\Delta G^{\circ\ddagger}$ and $\Delta S^{\circ\ddagger}$ using equation [4] and the data for the relaxation times (8, 9). The thermodynamic data for the activation process are summarized in Table I for one temperature and several results of interest may be pointed out. Firstly the value of $\Delta C_p^{\ddagger}$ is surprising as it is large and negative and similar to that found, for example, in the ionization of acids. $\Delta S^{\circ\ddagger}$ on the other hand is positive but it follows from the data given that it becomes less positive as the temperature is raised. Qualitatively, this is as

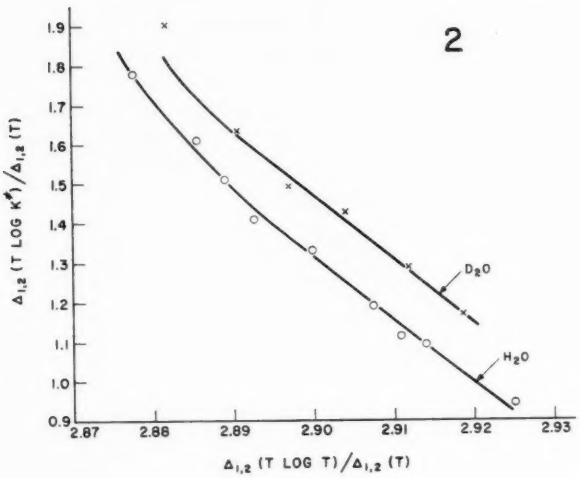

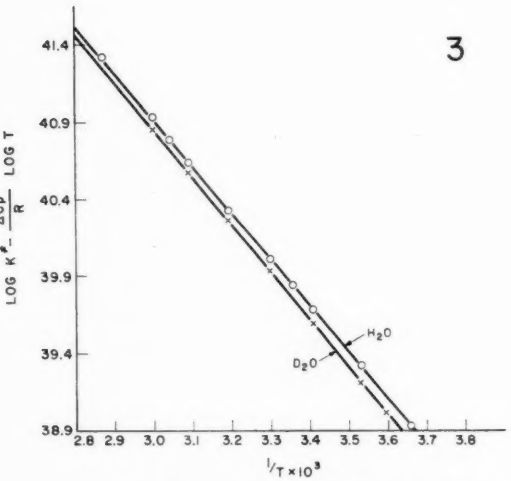

FIG. 2. Wynne-Jones plots for $\Delta C_p^{\ddagger}$ for H_2O and D_2O.
FIG. 3. Wynne-Jones plots for $\Delta H_0^{\circ\ddagger}$ for H_2O and D_2O.

expected, for reasons which are discussed below. However, the difference of sign between $\Delta C_p^{\ddagger}$ and $\Delta S^{\circ\ddagger}$ is difficult to account for but may be connected with long-range structure breaking (29) in the water. Similar anomalous differences between the signs of ΔC_p and ΔS° values for ionization of bases in water are known (13) and are connected with structure breaking (32).

$\Delta H^{\circ\ddagger}$ diminishes with increasing temperature since $\Delta C_p^{\ddagger}$ is negative. It has been considered (14, 15) that increase of temperature causes increasing breakage of H bonds in water. If this were so, the decrease of $\Delta H^{\circ\ddagger}$ with increase of temperature would be readily accounted for, since with increasing breakage of H bonds, fewer would have to

be broken in the activation step. However, thermodynamic considerations (cf. 16) preclude the possibility that any significant proportion of H bonds are broken even near the boiling point. This is confirmed by the fact that the latent heat of vaporization of water at the boiling point is still close to the energy required to break four half-hydrogen bonds per molecule, each having the usually accepted (16, 17) dissociation energy of about 5–6 kcal mole^{-1}. The structural change in water which occurs through the melting point and at higher temperatures is best regarded as resulting from the "bending" (16) of the O—H---O bonds rather than from their dissociation; on the basis of such a model the temperature dependence of the dielectric constant has been quantitatively deduced (16) and the change of radial distribution function with temperature accounted for. It is of interest to apply this model in order to examine the effect of bond-bending upon the activation energy for rotation of a water molecule in water.

TABLE I

Thermodynamic data for the activation process in dielectric relaxation in water and deuterium oxide

	$\Delta H_0°‡$ kcal mole^{-1}	$\Delta S°‡$ (10° C) cal ° C^{-1} mole^{-1}	$\Delta G°‡$ (10° C) kcal mole^{-1}	$\Delta C_p‡$ cal °C^{-1} mole^{-1}
Water	13.7	6.6	2.42	−33
Deuterium oxide	14.0	7.4	2.54	−33

THE ROTATIONAL POTENTIAL ENERGY BARRIER

The H bond in water can be regarded (16) to a satisfactory approximation as arising from the sum of a number of electrostatic interactions between point charges in each OH bond dipole and the two partially hybridized unshared pairs of electrons on the oxygen atoms of neighboring water molecules. Due to hybridization, these unshared pairs have a strong directional character (16, 18) and act as localized centers of negative charge. The electrostatic model for the hydrogen bond has been shown to be adequate (19) except for extreme vibrational excursions of the H atom or for very short bonds where covalent canonical forms become important. For water, the electrostatic model provides a satisfactory basis for calculation of bulk dielectric properties of the substance (16, 20). It will therefore be applied here in order to examine the features of the potential energy barrier for a water molecule rotating in the field of its nearest neighbors whose orientations have been thermally perturbed from the average orientations existing in ice. As a basis for the calculation, an idealized 4-co-ordinated structure is assumed such as exists to a first approximation in ice and to an important extent (21) in liquid water near the melting point. The rotational potential barriers for motions about the bond XY and the dipole axis of the water molecule shown in Fig. 4 in a thermally unperturbed structure have already been calculated by Conway *et al.* (10). The method used may be adapted for calculation of the rotational barrier when one or more bonds are bent and there is thermal perturbation of the ideal structure. Reference is made to Fig. 5 where XYZ is the water molecule undergoing rotation, for example about the axis XY. The choice of the mode of rotation is somewhat arbitrary but the one assumed here and in the previous calculations, (10), involves least breakage of hydrogen bonds and may therefore be the preferred motion; other modes, e.g., the axial spin mode previously examined in connection with proton mobility (10), cannot lead to a change of dielectric polarization of the water upon application of a field and is hence not considered here.

In the hydrogen bond YZW, point charges are assumed to be localized as in the model

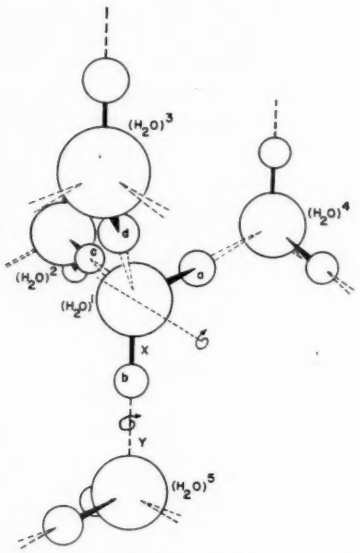

FIG. 4. The situation of a water molecule H_2O^1 amongst tetrahedrally co-ordinated neighbors showing the possible modes of rotation about H bond XY through H atom b, or axially; the latter mode involves breaking of all four bonds through H atoms a, b, c, and d.

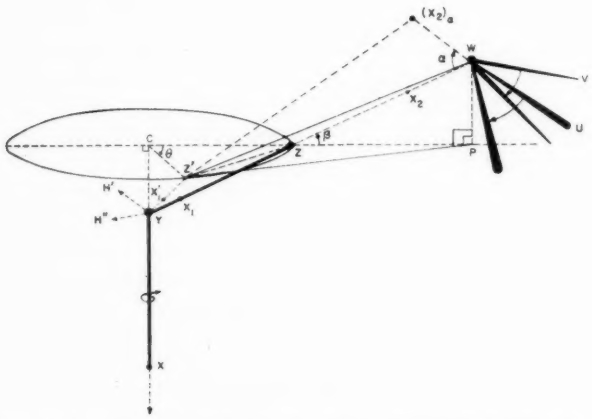

FIG. 5. Model for calculation (cf. 10) of the rotational potential energy barrier for a water molecule in water as a function of the angle of rotation, θ, and the angle α, of disorientation or bond bending of bonds with nearest neighbors.

given by Lennard-Jones and Pople (16). The energy of the hydrogen bond YZW is then calculated as a function of the angle, θ, of rotation of the bond YZ from its equilibrium position, as previously carried out (10) but now for various degrees of bond-bending determined, for example, by the degree of disorientation, α, of the directed lone pair of electrons X_2 in the hydrogen bond YZW, or of the OH bond. For any position of Z (e.g. at Z'), the distance WZ' or X_2Z' may be computed and the energy of electrostatic

interaction between the two electronic charges at W and X_2, and the one at the proton at Z' (16), can be calculated (16). The other four electrostatic interactions (16) leading to the total interaction energy in the bond are calculated similarly for various values of θ. It can be shown (10) that

$$(WZ')^2 = 4(CZ')\ (\sin^2\theta/2)\ [CZ'+ZW\cos\beta]+(ZW)^2 \qquad [7]$$

and similar expressions may be obtained for the other distances required, e.g., WX_1', X_2Z', X_2X_1'. As the molecule XYZ is rotated, lone-pair electrons directed towards other hydrogen atoms H′ and H″ (not shown in Fig. 5) also suffer rotation. The energy of the two hydrogen bonds involving these orbitals are calculated as a function of θ by equations similar in form to that of [7].

When the orbital directed from W to X_2 is oriented by an angle, α, from the colinear configuration YX_1ZX_2W, X_2Z' and other similar distances may be calculated trigonometrically, since it may be shown that

$$(X_2Z')^2 = (ZW)^2+(WX_2)^2-2(ZW).(WX_2)\cos\alpha+4(CZ')\sin^2\theta/2.[CZ'+ZW\cos\beta]. \qquad [8]$$

The form of this equation is general, so that other distances may be calculated, e.g. X_2X_1' as a function of θ and α; alternatively the molecule XYZ in Fig. 5, and hence the bond YZ may be considered oriented and the barrier for rotation of the molecule UVW about UW or VW calculated.

In order to examine the *form* of the dependence of the height of the rotational barrier for a given water molecule upon the angle α, calculations have been carried out for four values of α from 0° to 90° and for six values of θ from 0° to 100°. It must be emphasized that only a very small fraction of molecules will be thermally disoriented to angles as large as 90°. A greater number will be thermally disoriented at lower values of α. However, a rotation of a given molecule will involve bending or temporary breaking of bonds with neighbors and this will also facilitate the rotation of the neighbors themselves. Thus, those molecules which do rotate, would preferentially tend to do so at regions of the liquid where there is already a transient thermal disorientation. The process of activation is therefore probably best regarded as a somewhat co-operative one involving the participation of other molecules as well as the one which actually "rotates".

Each H bond has six component coulombic interactions and the resulting 144 interactions for the range of angles considered enables the electrostatic potential energy of the representative water molecule to be calculated as a function of θ and α for various assumed conformations of the structure; for example one, two, three, or four bonds to nearest neighbors may be considered to be disoriented. The total energy of the representative water molecule is calculated by summing the relevant individual partial coulombic interactions as described previously (10). Examples of the effect of bond bending on the rotational barrier are shown in Figs. 6 and 7. As a given molecule rotates in an ideal ice-like structure the molecule successively passes through the configurations shown as projections in Fig. 8. Unless the structure is perturbed, it is clear that any rotation must always lead to states of higher energy, since repulsive interactions will occur either between pairs of OH bonds or between the unshared-pair orbitals as they come into opposition as shown in Fig. 8. This leads to maxima at 120° and 240° in the rotational barrier as shown in Fig. 6. The energy of repulsion which arises when two OH bonds are in opposition is diminished if there is some bending of the H bonds, as shown by the result in Fig. 6; one of the most important qualitative effects of thermal bending is seen to be the diminution of the energy of this repulsive interaction. That such an

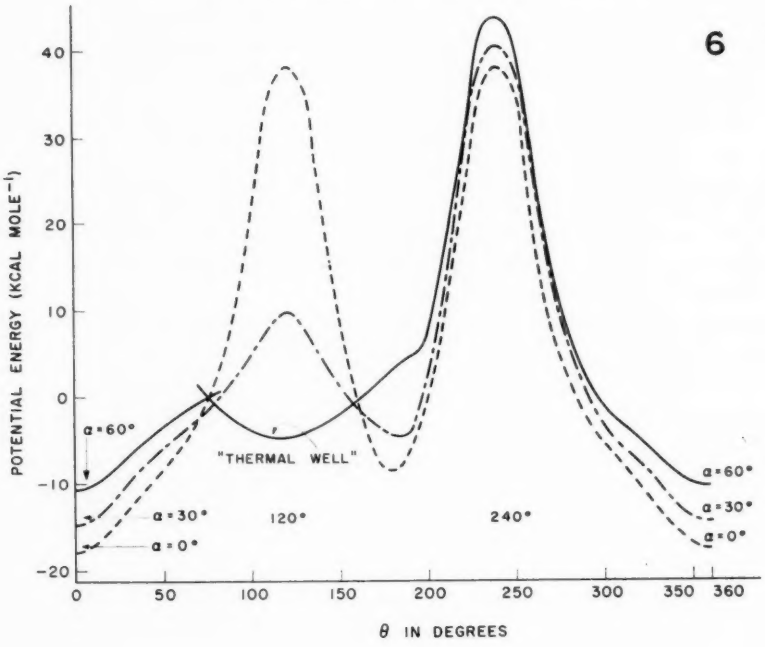

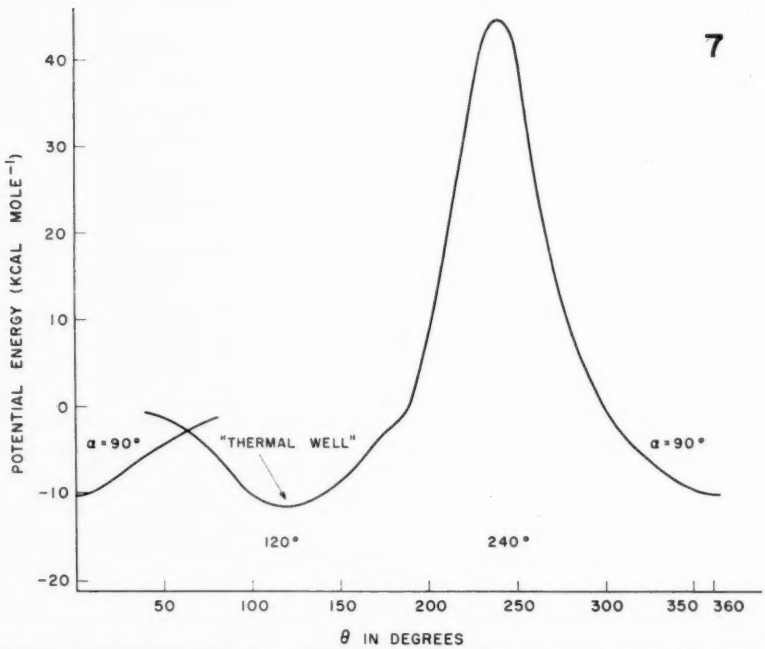

FIG. 6. The electrostatic potential energy barriers for rotation of a water molecule in water as a function of θ and α (α = 0, 30, and 60°).
FIG. 7. The potential energy barrier as in Fig. 6, but for α = 90°.

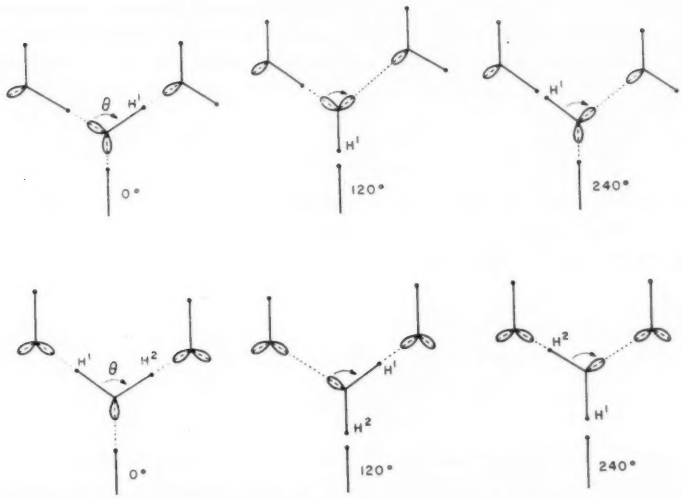

FIG. 8. Projections of configurations passed through by a water molecule rotating about one OH....O bond in water.

(i) Upper series: rotation about OH....O
(ii) Lower series: rotation about O....HO

H^1 and H^2 are H atoms in the representative H_2O molecule undergoing rotation.

interaction may be of importance in the experimental relaxation behavior in ice is indicated by the fact that the heat of activation for relaxation in ice is 13.2 kcal mole^{-1}, i.e., significantly larger than the energy necessary (viz. the heat of sublimation) completely to break all four "half"-hydrogen bonds per water molecule in ice. In liquid water, where $\Delta H^{\circ\ddagger}$ is between 2 and 5 kcal mole^{-1} over the temperature range 0–75° C, this effect must be almost absent, Figs. 6 and 7 show that if the degree of bending is sufficient, the repulsive interaction, for example at 120° of rotation, is eliminated and in fact replaced by one of attraction. Under these conditions a new potential energy minimum occurs other than that at the initial state (0°) and at the intermediate state (180°) of the rotation. We may identify minima of this kind with the transient "thermal wells" postulated by Garton (22) to explain the dielectric behavior of polar liquids. We have, of course, only considered some special cases where one bond to a nearest neighbor water molecule is bent or disoriented. Qualitatively similar effects arise if two or more bonds are simultaneously bent; however, such a situation will be statistically less probable than that in which fewer bonds to a given water molecule are bent.

From Figs. 6 and 7, it is clear that the barrier for rotation of a given water molecule can be considerably lowered by thermal bending of bonds or "disorientation" of neighboring molecules and hence the dependence of $\Delta H^{\ddagger}$ upon temperature qualitatively explained. In so far as disorientation of molecules other than the given one is involved, the rotation process is a co-operative one.

An alternative explanation for the temperature dependence of the thermodynamic parameters for dielectric relaxation in water may be sought in terms of the hole-theory of liquids (23); thus Schellman (24) has suggested that defects (missing bonds) in the ice structure are propagated in the rotational process, and a similar effect could occur in water. Rotation at defect sites will certainly require less energy of activation and this may be demonstrated by calculating the rotational barrier for such sites, as shown in

Fig. 9. This approach is equivalent to assuming that a significant number of hydrogen bonds are completely dissociated in water and ice; whilst this is thermodynamically unlikely (16), metastable crystal imperfections in ice may, however, provide the necessary sites for rotation in that case (33).

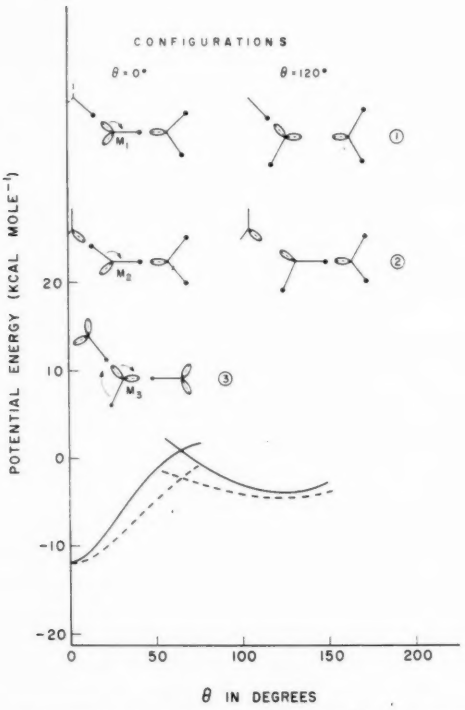

FIG. 9. The rotational potential energy barrier from 0 to 120° for a water molecule M in ice at a bond vacancy site where there are only three H bonds to the representative molecule. Projections of three situations are shown: (1) rotation about the OH. . . . O bond (dotted line); (2) rotation about the O. . . . HO bond (solid line). The configurations at $\theta = 0°$ (initial state) and $\theta = 120°$ (final state) are indicated; (3) rotation in this configuration can only lead to OH bonds in opposition with a resultant increase of potential energy with no minimum as in Fig. 6 for $\alpha = 0$.

FREQUENCY FACTORS

Since $\Delta H_0^{\circ\ddagger}$ has been evaluated for relaxation in water and deuterium oxide, we can use equation [3] as a basis for comparison of experimental and theoretical frequency factors.

If the potential energy function for libration is of the form $V = V_0 \cos \theta$, and three modes of restricted rotation are possible in the initial state, F_A in equation [3] may be written (27)

$$F_A = \frac{8\pi^2(8\pi^3 I_1 I_2 I_3 k^3 T^3)^{\frac{1}{2}}}{h^3} \frac{\sinh(V_0/kT)}{V_0/kT} F_v \cdot F_t, \qquad [9]$$

where F_v is the product of partition functions for the internal vibrations in the bonds of the molecule and F_t the total translational partition function. The cosine potential function will only be applicable if the internal field is uniform. This, however, is unlikely

for the short range interactions considered above. Inspection of the minima near $\theta = 0$ in the rotational potential energy diagrams indicates (Fig. 6) that the potential function near the minima is more accurately represented by $V = \frac{1}{2}K\theta^2$, where K is the force constant for the restricted rotation, so that (cf. 28) F_A is then given by

$$F_A = \left[1-\exp\left(\frac{-h\nu_1}{kT}\right)\right]^{-1}\cdot\left[1-\exp\left(\frac{-h\nu_2}{kT}\right)\right]^{-1}\cdot\left[1-\exp\left(\frac{-h\nu_3}{kT}\right)\right]^{-1}\cdot F_v\cdot F_t, \qquad [10]$$

where ν_1, ν_2, and ν_3 are the three frequencies of restricted rotation corresponding to the normal modes of rotation of an unhindered non-linear triatomic molecule. In equation [1], $F_A^{\ddagger\prime}$ differs from F_A only on account of the conversion of one mode of libration to one of (temporary) free rotation.
Hence*

$$\mathbf{k} = \frac{kT}{h}\cdot\frac{1}{\left[1-\exp\left(\frac{-h\nu_3}{kT}\right)\right]^{-1}}\cdot e^{-E_0/RT} \qquad [11]$$

if the librational mode designated as 3 is the one which becomes a free rotational motion in the activation step. The frequency ν_3 may be estimated from the rotational potential energy function. Figure 10 shows the dependence of the energy of a water molecule in water (in the thermally unperturbed structure) upon θ^2 in degrees. The slope of the line in Fig. 10 calculated in terms of erg molecule^{-1} and radians gives $K = 2.1\times10^{-12}$. Now for the simple harmonic libration of type 3,

$$\nu_3 = 1/2\pi(K_3/I_3)^{\frac{1}{2}} \qquad [12]$$

and taking I_3 as 1.9×10^{-40} g cm^2 (37), gives $\bar{\nu}_3 = 550$ cm^{-1}. This is in satisfactory agreement with the value of the frequency of hindered rotation ($\bar{\nu} = 570$ cm^{-1}) calculated by a different method from Morse functions by Cross *et al.* (14). The value falls in the

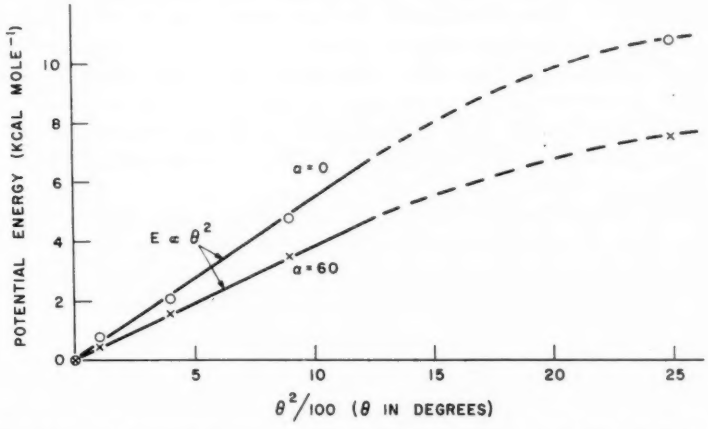

FIG. 10. Plot of potential energy vs. square of angle, θ, of rotation for low values of θ, and two values of α, showing the effect of bond bending on the force constant K.

**This involves the assumption that the other two librational modes maintain the same frequencies during the rotational motion. Whilst this is probably true only as a first approximation, the results which follow for the ratio of frequency factors for relaxation in H_2O and D_2O ice confirm the general correctness of the assumption, at least in the case of ice.*

middle of the infrared band in water ascribed to "hindered rotation" (14). The above calculation is based on the rotational potential energy function for the unperturbed structure, i.e., with no bond-bending; this is justified by the fact that the majority of the molecules observed spectroscopically will be in states corresponding to a relatively unperturbed structure, since perturbed molecules will be distributed as $e^{-E/RT}$, where E is the energy involved in causing a perturbation. Lower values of $\bar{\nu}_3$ result when perturbed structures (i.e. α in Fig. 5 differs from zero) are considered, since then K_3 is less, as shown for example in Fig. 10. We may now evaluate the apparent frequency factor in equation [11], whereupon

$$\mathbf{k} = (kT/h)\ (0.93)\ e^{-E_0/RT} = 5.8\times10^{12}\ e^{-E_0/RT}. \qquad [13]$$

Direct comparison of this frequency factor with those obtained experimentally near room temperature is complicated by the large temperature dependence of the experimental heat of activation found at room temperature for relaxation in water.

In a condensed phase, E_0 and $\Delta H_0^{\circ\ddagger}$ are almost identical (35) but differ from the experimentally measured activation energy, $E^{\ddagger}$, according to

$$E^{\ddagger} = E_0+\Delta C_p{}^{\ddagger}T+RT. \qquad [14]$$

The experimental behavior is represented by

$$1/\tau = Ae^{-E^{\ddagger}/RT} = [(ekT/h)\ e^{\Delta S_0{}^{\ddagger}/R}]\ e^{-E^{\ddagger}/RT}. \qquad [15]$$

In order to compare the experimental frequency factor in [15] with that arising theoretically in [13], we convert [13] into a form comparable with [15] by eliminating E_0 in [13] using equation [14], so that both equations involve $E^{\ddagger}$. Hence

$$k = 5.8\times10^{12}e.\ e^{\Delta C_p{}^{\ddagger}/R}\ e^{-E^{\ddagger}/RT} \qquad [16]$$

and the frequency factor A is then $5.8\times10^{12}\ e.\ e^{\Delta C_p{}^{\ddagger}/R}$. At 20° C, A is 3×10^{14} sec^{-1}, whilst the apparent frequency factor from [16], to be compared with the experimental value, is 6×10^{5} sec^{-1} using the value of $\Delta C_p{}^{\ddagger}$ derived above. It is clear that the simple model in which a loose libration becomes a complete rotation does not account adequately for the experimental frequency factor which is much higher than that deduced theoretically with the above model; accordingly an alternative mechanism must be sought (see below). Further insight into the molecular processes occurring in the activation step may be obtained by considering isotopic effects in water and ice.

ISOTOPIC EFFECTS

In ice, the ratio of frequency factors for the relaxation rates, $1/\tau$, in H_2O and D_2O is (29) 1.45. The libration frequencies for any pair of corresponding modes of libration in ordinary and heavy ice will be in the ratio (see equation 12)

$$\nu_{H_2O}/\nu_{D_2O} = (2)^{\frac{1}{2}},$$

since the force constants for the libration of the isotopic molecules are approximately the same. The $\sqrt{2}$ factor is also confirmed by the experimental infrared data for water (14). Equation [11] then gives the ratio of frequency factors for the relaxation in ice and D_2O ice as 1.1 if the libration frequencies are such that $h\nu_3 > kT$. The experimental ratio is close to $\sqrt{2}$. This suggests that the libration which becomes a rotation in the relaxation process is a looser one than those predominating in the normal ice structure, since then, if $h\nu_3 < kT$, equation [11] indicates that the isotopic ratio of frequency factors becomes

$\sqrt{2}$. This value could be accounted for if the relaxation process in ice only occurs at sites where there is a considerable perturbation of the structure, e.g. at crystal defects or imperfections (33) or holes, where one or more of the normal four hydrogen bonds is absent or where two H atoms are in opposition in a given bond. The librational potential energy well for a molecule at a bond-vacancy site will then be less deep (Fig. 9) and the librational frequency of the molecule would be correspondingly less. Sufficiently loose librations ($\nu_3 < kT/h$) to account for the isotopic factor of $\sqrt{2}$ must have frequencies less than about 210 cm^{-1}. Such a mode of motion is, in fact, known in ice (14) near this frequency.

In liquid water the situation is different. From the data in Table I, the entropy of activation, e.g., at 30° C for D_2O is 5.1 and that for H_2O at the same temperature is 4.4 cal $^\circ C^{-1}$ $mole^{-1}$. The ratio of experimental frequency factors for H_2O and D_2O at 30° C is hence $\exp[-0.7/R] \doteqdot 1/\sqrt{2}$, i.e. in the *opposite direction* to that found with ice. Qualitatively the higher positive entropy of activation found for the relaxation rate in D_2O than in H_2O follows from the greater degree of order which exists in liquid D_2O (14) than in water owing to the greater apparent* strength of "deuterium-bonds" than that of hydrogen bonds. In the rotation of the D_2O molecule from its initial state of libration more entropy is gained than in water, since the initial state is more regular in D_2O. The apparent strength of the "deuterium bond" in D_2O is some 0.23 kcal $mole^{-1}$ greater than that of the hydrogen bond in water, as may be deduced from the heats of sublimation of D_2O and H_2O (12,631 and 12,170 cal $mole^{-1}$ respectively (30)); hence in D_2O there will be less thermal perturbation of the structure by bond-bending than in H_2O. The origin of this isotopic difference in the heats of sublimation has been explained by Eucken (31). The greater interaction energy between D_2O molecules in heavy water than between H_2O molecules in ordinary water also accounts for the consistently higher value (about 0.3 kcal) of $\Delta H^{\circ\ddagger}$ (Table I) for the relaxation rate in D_2O than in H_2O, since more energy is required rotationally to displace a D_2O molecule than an H_2O molecule. The higher value of $\Delta H^{\circ\ddagger}$ leads to an isotopic effect on the relaxation rate opposite in direction to that arising from the difference in frequency factors. Thus at 30° C, the ratio of the terms containing the heats of activation for rotation of H_2O and D_2O is $(e^{-3650/RT})/(e^{-3970/RT})$, i.e. 1.71. The ratio of the relaxation rates is hence

$$(1/\tau_{H_2O})/(1/\tau_{D_2O}) = 0.7 \times 1.71, \text{ i.e. } 1.20.$$

At 30° C, comparison of the actual values of τ (8) for D_2O and H_2O gives $\tau_{D_2O}/\tau_{H_2O} = 1.22$.

Positive values of $\Delta S^{\circ\ddagger}$ which are found (Table I) for the relaxation process in water may be contrasted with the negative ones found for more complex molecules, e.g., permitol (36). However, it is not difficult to see that the rotation of large and complex molecules such as the chlorinated diphenyls may well require more co-operative (and hence less probable) reorientation by neighboring molecules than is the case for rotation of a water molecule in water. Furthermore, an important qualitative difference between these cases is that the water is already a relatively highly ordered structure (21), whilst there is no evidence that a similar structure exists in permitol. Any thermal perturbations, such as those involved in the reorientation of a molecule, may not unreasonably be supposed to lead locally to more disordered configurations in the quasi-crystalline water structure. That this is likely is indicated by the positive values of $\Delta S^{\ddagger}$ which become more positive with decreasing temperature (see the data in Table I). Such a

*This effect arises (34) from the lower zero-point librational energies of the deuterium analogue than those of water.

trend of the $\Delta S^{\ddagger}$ values would not be unexpected in the case of water, since the degree of quasi-crystalline structure in the liquid increases with decrease of temperature so that the initial state of the relaxation process can become relatively more ordered, i.e., have a lower entropy. A more quantitative evaluation of the frequency factors for the rotation process in liquid water and deuterium oxide must await a more detailed knowledge of the structure of water and how it depends on temperature.

PROTON MOBILITY IN WATER AND ICE, AND THE ROTATION MECHANISM

We have shown previously (10, 26) in calculations of the proton mobility in aqueous solutions, that above a certain critical concentration of about 10^{-6} M in H_3O^+ ions, there is a sufficient flux of protons that virtually all rotations of solvent molecules which occur do so in the fields of each newly produced H_3O^+ ion as the latter is formed from an antecedent H_3O^+ ion by rapid proton tunneling (10) to an adjacent water molecule already reoriented in the immediately preceding proton jump event. Whilst the actual concentration of H_3O^+ and OH^- ions is small (10^{-7} g ion $l.^{-1}$ at 25° C, of each ion), they can indirectly affect a large number of water molecules.

The rotation rate, which is observed in dielectric dispersion experiments, may therefore correspond to rotation of water molecules in the fields of the H_3O^+ (and/or OH^-) ions, as the protons arrive at various sites during their motion throughout the liquid. Such a mechanism is consistent with a number of aspects of the relaxation behavior.

Rotation of water molecules adjacent to the H_3O^+ ions may account for the apparent lack of any significant distribution of relaxation times in water; thus, it has consistently been observed that the dispersion behavior can be treated in terms of a single* relaxation time, which suggests that the rotations occur in a relatively reproducible environment, e.g. adjacent to and in the strong orienting fields of the ions. On the other hand, random thermal bond bending in "non-ionic" environments in the bulk water structure might be expected to lead to a distribution of heats of activation for rotation, and hence of the corresponding relaxation times.

In support of these views, it may be noted that the heat of activation for rotation in water (3–5 kcal $mole^{-1}$) is considerably less than that required to break four hydrogen bonds even in a partially thermally perturbed structure of water. The rotation process in the field of the new H_3O^+ ion upon arrival of a proton at a given water molecule will have a lower heat of activation (cf. 10) than that for rotation in the bulk of the solvent, since the energy of interaction (*ca.* 15 kcal $mole^{-1}$) of the water dipole with the ion assists the rotation process. When molecules are rotated near the ion out of their normal average orientations in the 4-co-ordinated water structure, a multiplicative effect can originate, since rotation of one molecule causes temporary opposition of OH bonds between nearest neighbors (i.e., there are "bonds" doubly occupied by H atoms as shown in Fig. 8); this facilitates rotation of a neighboring molecule by repulsion in the doubly occupied "bonds". This effect will enhance the probability of rotation and could account for the experimentally observed greater probability of rotation than that calculated for simple thermal reorientation on the basis of librational partition functions as from equations [13] and [16].

In ice, the different isotopic effects from those in water and the much greater heat of activation suggest a different mechanism for the rotational process. We have shown previously (26) that on account of the lower proton concentration in ice, the proton

**Some heterogeneity may still be present but not apparent in the Cole and Cole plot. This, for example, is shown with mixtures (36) in certain ranges of concentration.*

mobility in ice is no longer limited in its rate (as it is in water) by the rotation of water molecules in the fields of H_3O^+ ions, the rotation process occurring predominantly amongst neighboring water molecules in the absence of ionic fields. The observed heat of activation for the relaxation is then about 13 kcal mole^{-1} (29, 33) as expected (see Figs. 6, 9) for thermal reorientation.

The self-consistency of the proposed change of mechanism may be checked by calculating the relative probabilities of relaxation by the field-induced mechanism, (I), and the thermal reorientation mechanism, (II). Process I can be regarded as a pseudo-unimolecular reaction involving H_3O^+ and H_2O while II is to be regarded as unimolecular involving only H_2O. $\Delta H^{\circ\ddagger}$ for I is 3.9 kcal mole^{-1} at 25° C (see Table I) and $\Delta H^{\circ\ddagger}$ for II is 13.3 kcal mole^{-1} (29). The relative probability R that rotations will occur in unit volume and time by process I or by II is given approximately by

$$R = 3\times10^{14}\, a_{H_3O^+}\times 4\, \exp[-3900/RT]/1.8\times10^{-15}\times55.5\, \exp[-13300/RT] \quad [17]$$

and is unity when $a_{H_3O^+}$ is about 10^{-5} g ion l.$^{-1}$. In equation [17], the figures 3×10^{14} and 1.8×10^{15} are the experimental frequency factors for rotation in water and ice, respectively, and the factor 4 allows for the fact that each H_3O^+ ion influences the orientation of four nearest neighbor water molecules. The mechanism of rotation would hence tend to become predominantly II as C_{H^+} is decreased much below about 10^{-5} g ion l.$^{-1}$ (as in ice) and mainly I in more acidic solutions ($a_{H_3O^+} > 10^{-5}$ g ion l.$^{-1}$). Comparable contributions from both mechanisms would occur at proton concentrations of the order of magnitude of 10^{-5} g ion l.$^{-1}$. This concentration, at which a change of mechanism for rotation is predicted, is of a similar order of magnitude as that for which the change of mechanism for proton mobility is indicated (26).

Upon addition of extra protons to the ice by the formation of solid solutions with an acid we should expect a change of mechanism of proton mobility back to that (viz. rate-determining rotation of water molecules in the field of H_3O^+ ions) which occurs in water (10), and a corresponding drop of the heat of activation for rotation of the water molecule as discussed above. In ice containing traces of HF this is actually found (33) and the experimentally observed heat of activation for relaxation drops from 13 kcal mole^{-1} in pure ice to about 5 kcal mole^{-1} in HF–ice, a value very close to that for liquid water at 0° C (Table I). It therefore appears that the mechanisms for relaxation in pure ice and water differ on account of the different orders of concentration of ions in these phases, the critical concentration of H_3O^+ or OH^- ions for the change of mechanisms both of proton mobility (26) and dielectric relaxation, being about 10^{-6} to 10^{-7} mole l.$^{-1}$. Although protons are present in ice, it appears that they do not participate significantly in the relaxation process unless they are present above the critical concentration (10, 26). Below this concentration the rotation of the molecules can occur at non-ionic defect sites. This conclusion is supported by the work of Gränicher *et al.* (33). The proton polarization mechanism of Latimer (25) appears to be applicable only when the ice contains extra protons (33).

In pure liquid methanol where the proton concentration is very much lower than in ice or water, it is experimentally found (12, 36) that the frequency factor for relaxation is about 2.5×10^{12} (36) and $\Delta C_p^{\ddagger}$ is very small or zero within the experimental accuracy of the results (12). Theoretically, using [13], a value of the order 10^{13} is expected if the mechanism is one of rotation amongst other methanol molecules and not in the fields of ions. These values are in much better agreement than in the case of water considered above and give a further indication that in liquid water a simple rotation process amongst

other water molecules is unlikely to be the mechanism of relaxation. The isotopic ratio of relaxation frequencies in MeOH and MeOD appears to be about $(2)^{\frac{1}{2}}$ (12), within the experimental uncertainties, as expected from [13] if the librational mode becoming a rotation upon activation, is a loose one, and is consistent with a non-ionic mechanism. This is also the ratio found for ice, for which the non-ionic mechanism is indicated.

ACKNOWLEDGMENT

The author is indebted to Dr. D. W. Davidson for making available some results on the relaxation behavior of MeOH and MeOD prior to their publication.

REFERENCES

1. PAULING, L. Phys. Rev. **36**, 430 (1930).
2. GIAUQUE, W. F. and WIEBE, R. J. Am. Chem. Soc. **50**, 101, 2193 (1928); **51**, 1441 (1929).
3. CLUSIUS, K. Z. Elektrochem. **39**, 528 (1933).
4. SMYTH, C. P. and HITCHCOCK, C. S. J. Am. Chem. Soc. **56**, 1084 (1934).
5. CONE, R. M., DENISON, G. H., and KEMP, J. D. J. Am. Chem. Soc. **53**, 1278 (1931).
6. STEARN, A. E. and EYRING, H. J. Chem. Phys. **7**, 113 (1937).
7. KAUZMANN, W. Revs. Mod. Phys. **14**, 12 (1942).
8. SMYTH, C. P. Dielectric behavior and molecular structure. McGraw-Hill Book Co., Inc., New York. 1955.
9. COLLIE, C. H., HASTED, J. B., and RITSON, D. M. Proc. Phys. Soc. (London), **60**, 145 (1948).
10. CONWAY, B. E., BOCKRIS, J. O'M., and LINTON, H. J. Chem. Phys. **24**, 834 (1956).
11. HENNELLEY, E. J., HESTON, W. M., and SMYTH, C. P. J. Am. Chem. Soc. **70**, 4102 (1948).
12. DAVIDSON, D. W. Can. J. Chem. **35**, 458 (1957).
13. EVERETT, D. H. and WYNNE-JONES, W. F. K. Trans. Faraday Soc. **35**, 1380 (1939).
14. CROSS, P. C., BURNHAM, J., and LEIGHTON, P. A. J. Am. Chem. Soc. **59**, 1134 (1957).
15. EWELL, R. H. and EYRING, H. J. Chem. Phys. **5**, 726 (1937).
16. LENNARD-JONES, J. and POPLE, J. A. Proc. Roy. Soc. (London), A, **205**, 155, 163 (1951).
17. COULSON, C. A. Valence. Oxford University Press, London. 1953.
18. SCHNEIDER, W. G. J. Chem. Phys. **23**, 26 (1955).
19. COULSON, C. A. and DANIELSSON, U. Arkiv Fysik, **8**, 239, 245 (1954).
20. POWLES, J. G. J. Chem. Phys. **20**, 1302 (1952).
21. BERNAL, J. D. and FOWLER, R. H. J. Chem. Phys. **1**, 515 (1933).
22. GARTON, C. G. Trans. Faraday Soc. A, **42**, 56 (1946).
23. FRENKEL, J. Kinetic theory of liquids. Oxford University Press, London. 1946.
24. SCHELLMAN, J. A. Ph.D. Thesis, Princeton University. 1951.
25. LATIMER, W. M. Chem. Revs. **44**, 59 (1949).
26. CONWAY, B. E. and BOCKRIS, J. O'M. J. Chem. Phys. **28**, 354 (1958).
27. FOWLER, R. H. Statistical mechanics. Cambridge University Press, London. 1936.
28. ELEY, D. D. and EVANS, M. G. Trans. Faraday Soc. **34**, 1093 (1938).
29. AUTY, R. P. and COLE, R. H. J. Chem. Phys. **20**, 1309 (1952).
30. BARTHOLEMÉ, E. and CLUSIUS, K. Z. physik. Chem. B, **28**, 167 (1935).
31. EUCKEN, A. Nachr. Akad. Wiss. Göttingen, Math-phys. Kl. Biol. physiol. chem. Abt. 1 (1949).
32. FRANK, H. C. and WEN, W. Y. Discussions Faraday Soc. Preprint No. 11 (1958) (In press).
33. GRÄNICHER, H., JACCARD, C., SCHERRER, P., and STEINMANN, A. Discussions Faraday Soc. **23**, 50 (1957).
34. WHALLEY, E. Trans. Faraday Soc. **53**, 1578 (1957).
35. GLASSTONE, S., LAIDLER, K. J., and EYRING, H. The theory of rate processes. McGraw-Hill Book Co., Inc., New York. 1941.
36. DENNEY, D. J. and COLE, R. H. J. Chem. Phys. **23**, 1767 (1955).
37. MOELWYN HUGHES, E. A. Physical chemistry. Cambridge University Press, London. 1947.

PREPARATION AND CHEMISTRY OF TRANS 1-CYANO-4-CHLORO-2-BUTENE

CL. DAESSLE, E. J. TARLTON, AND A. F. MCKAY

Trans 1-cyano-4-chloro-2-butene (III) and 1-cyano-2-chloro-3-butene (II) were prepared by the addition of butadiene to a complex of aluminum chloride and cyanogen chloride in nitromethane. Cowen (1) previously used this complex to add cyanogen

$$\underset{\text{I}}{CH_2{=}CH{-}CH{=}CH_2} + CNCl \xrightarrow{AlCl_3} \underset{\text{II}}{CH_2{=}CH{-}CHClCH_2CN} + \underset{\text{III}}{CH_2ClCH{=}CHCH_2CN}$$

chloride to monoolefins. Both 1-cyano-4-chloro-2-butene (III) and 1-cyano-2-chloro-3-butene (II) were converted in liquid ammonia into 1-cyano-1,3-butadiene. The former compound also gave 1-cyano-1,3-butadiene on treatment with hexamethylenetetramine. The known 1,4-dicyano-2-butene (2, 3, 4) was prepared by the reaction of sodium cyanide with 1-cyano-4-chloro-2-butene in the presence of cuprous chloride.

3-Carbethoxy-7-cyano-5-hepten-2-one was prepared by condensation of ethyl acetoacetate with 1-cyano-4-chloro-2-butene in the presence of sodium ethylate. Similar reaction with diethyl malonate gave ethyl 2-carbethoxy-6-cyano-4-hexenoate (12.6% yield), identified by its conversion to pimelic acid through subsequent hydrogenation, hydrolysis, and decarboxylation (5).

The main bands of the infrared absorption spectra of these nitrile derivatives are listed in Table I. The assignments agree with those reported by Bellamy (6). 1-Cyano-4-chloro-2-butene, 1,4-dicyano-2-butene, and 3-carbethoxy-7-cyano-5-hepten-2-one display a strong absorption band at 968–972 cm^{-1} characteristic of CH out-of-plane

TABLE I

Infrared absorption bands of nitrile derivatives

	C—H stretching	C≡N stretching	C—H in-plane deformations	C—H out-of-plane deformations	Other bands
$CNCH_2CH{=}CHCH_2Cl$	3040, 2960, 2930, 2850	2270 (m)	1412, 1441	968 (s), 936 (w), 909 (w)	688
$CNCH_2CH{=}CH{-}CH_2CN$		2265 (m) 2230 (sh)	1416 (s)	972 (s), 912 (m)	
$CN{-}CH{=}CH{-}CH{=}CH_2$	3120, 3080, 3000, 2950, 2925, 2860	2235 (s)		1004 (m), 966 (sh), 958 (sh), 933 (m)	1623 (C=C) (m) 1593 (m), 1530
$CNCH_2CHClCH{=}CH_2$	3080, 2965, 2930, 2875	2270 (m)	1414	986 (s), 955 (sh), 938 (s), 909 (sh)	700 (s), 1530
$CH_3C(O)CH(COOEt)$-$CH_2CH{=}CHCH_2CN$	2970, 2930 (sh)	2270 (m→w)	1418, 1460	970 (m→s), 926 (vw), 906 (vw)	677 (s), 1733 (ester) (s), 1719 (carbonyl) (s), 1623 (C=C) (m)

s, Strong; m, medium; w, weak; and vw, very weak absorption bands; sh, shoulder on stronger absorption bands.

deformation for a trans —CH=CH— group. 1-Cyano-1,3-butadiene and 1-cyano-2-chloro-2-butene have absorption bands at 1004 cm^{-1} and 986 cm^{-1}, respectively, which are associated with the CH out-of-plane deformations of the vinyl group. 1-Cyano-1,3-butadiene also has an absorption band at 966 cm^{-1}, since it also contains the —CH=CH— grouping. The absorption spectrum of 1,4-dicyano-2-butene was determined in Nujol mull so the C—H stretching vibrations are not recorded in Table I.

EXPERIMENTAL[1]

Cyanogen Chloride

Cyanogen chloride was prepared as a clear, colorless liquid in 70% yield by the method of Barnett *et al.* (7).

Addition of Cyanogen Chloride to Butadiene

Cyanogen chloride (52 ml, 1.0 mole) was vaporized into a mixture of anhydrous aluminum chloride (133.5 g, 1.0 mole) in nitromethane (100 ml) cooled to −5° C. Butadiene (27 l., 1.1 mole) was led in under the surface of this reaction mixture over a period of 3 hours. Strong cooling was required to maintain the temperature between 0 and 5° C. After the addition of the butadiene, the reaction mixture was poured into ice and water, and acidified with dilute hydrochloric acid solution. This acidified mixture was extracted with ether, the ether was removed by evaporation, and the residue was distilled *in vacuo*. The following fractions were obtained: (1) liquid b.p. 90–95° C at 15 mm, yield 25 g; (2) yellow liquid b.p. 100–105° C at 15 mm, yield 12.5 g; and (3) liquid b.p. 100–150° C at 2–3 mm, yield 3.5 g. Redistillation *in vacuo* using a Vigreux column gave 16.5 g (14.3%) of 1-cyano-2-chloro-3-butene (b.p. 74–76° C at 13 mm, n_D^{25} 1.45837) and 19 g (16.4%) of 1-cyano-4-chloro-2-butene (b.p. 105–107° C at 13 mm, 67–68° C at 1.5 mm, n_D^{25} 1.47330, d_4^{25} 1.087, M_R calc. 29.44, found 29.85). 1-Cyano-2-chloro-3-butene, anal. calc. for C_5H_6ClN: C, 52.05; H, 5.23; Cl, 30.70; N, 12.12%. Found: C, 51.94; H, 5.27; Cl, 30.02; N, 12.54%. 1-Cyano-4-chloro-2-butene, anal. calc. for C_5H_6ClN: C, 52.05; H, 5.23; Cl, 30.70; N, 12.12%. Found: C, 51.86; H, 5.41; Cl, 30.34; N, 12.41%. The physical constants reported by Prichard and Whitman (8) for 1-cyano-4-chloro-2-butene are b.p. 44–46° C at 0.3 mm and n_D^{25} 1.4735.

In other experiments where the amount of aluminum chloride was reduced to 0.1 mole or replaced by antimony pentachloride, only resinous products were obtained. In the presence of zinc chloride (ethereal solution), cyanogen chloride and butadiene failed to react.

1-Cyano-1,3-butadiene

Method A.—1-Cyano-4-chloro-2-butene (4.8 g, 0.042 mole) was dissolved in liquid ammonia (80 ml) and the solution was allowed to stand for 3 hours. After the ammonia had evaporated from the reaction mixture, the residue was extracted with ether. The liquid residue from the ether extract was fractionally distilled *in vacuo*. The main fraction (b.p. 56–58° C at 42 mm; n_D^{25} 1.4892) was 1-cyano-1,3-butadiene, yield 2.4 g (75%). Anal. Calc. for C_5H_5N: C, 75.91; H, 6.37; N, 17.70%. Found: C, 75.61; H, 6.37; N, 18.18%. The physical constants of 1-cyano-1,3-butadiene are reported by Snyder and Poos (9) to be b.p. 49.5–53° C at 31 mm, n_D^{20} 1.4852–1.4895.

Method B.—1-Cyano-2-chloro-3-butene (4.8 g, 0.042 mole) on treatment with liquid

[1]*All melting points and boiling points are uncorrected. Microanalyses by Micro-Tech Laboratories, Skokie, Ill.*

ammonia under the conditions described in method A gave a 72% yield of 1-cyano-1,3-butadiene (b.p. 56–58° C at 43 mm). This product was identified by its infrared spectrum and analysis.

Method C.—1-Cyano-4-chloro-2-butene (5.6 g, 0.05 mole) was added to hexamethylenetetramine (7 g, 0.05 mole) in chloroform (50 ml) and the reaction mixture was heated under reflux for 18 hours. After the reaction mixture cooled to room temperature, the precipitated hexamethylenetetramine hydrochloride was removed by filtration. The filtrate was evaporated to remove chloroform and the residue was filtered free from solid. Fractional distillation of the filtrate gave 1.5 g (45%) of 1-cyano-1,3-butadiene (b.p. 75° C at 70 mm). This product was identified by a comparison of its infrared spectrum and physical properties with 1-cyano-1,3-butadiene prepared by method B.

1,4-Dicyano-2-butene

1-Cyano-4-chloro-2-butene (3.42 g, 0.03 mole) was added over a period of 1 hour to a refluxing suspension of sodium cyanide (1.5 g, 0.03 mole) and cuprous chloride (0.12 g) in acetonitrile (8.4 g) under an atmosphere of nitrogen. The reaction mixture was refluxed for a further period of 48 hours after which the hot mixture was filtered and the filter cake was washed with hot acetonitrile. The combined filtrate and washings were evaporated and the crystalline residue was dissolved in methanol. This methanol solution on cooling deposited crystals (m.p. 74–76° C), yield 1.2 g (35%). The reported melting points of 1,4-dicyano-2-butene are 75–77° C (4) and 74° C (2).

3-Carbethoxy-7-cyano-5-hepten-2-one

A solution of ethyl acetoacetate (6.3 g, 0.045 mole) and sodium metal (1.05 g, 0.045 mole) in ethanol (23 ml) was treated dropwise (cooling) with 1-cyano-4-chloro-2-butene (5.2 g, 0.045 mole), and the reaction was allowed to proceed at room temperature overnight. The precipitated sodium chloride was removed by filtration and the filtrate was evaporated *in vacuo*. Dilution of the residue with water (20 ml) followed by ether extraction gave a crude oil, which was distilled *in vacuo* to give 2.5 g (26.6%) of 3-carbethoxy-7-cyano-5-hepten-2-one (b.p. 134–136° C at 0.6 mm, n_D^{25} 1.4592, d_4^{25} 1.078). Anal. Calc. for $C_{11}H_{15}NO_3$: C, 63.11; H, 7.22; N, 6.69%. Found: C, 63.27; H, 7.12; N, 7.06%.

ACKNOWLEDGMENT

The infrared absorption spectra were determined by Dr. C. Sandorfy of the Department of Chemistry, University of Montreal, Montreal, Quebec.

1. COWEN, F. M. J. Org. Chem. **20**, 287 (1955).
2. KURTZ, P. Ann. **572**, 23 (1951).
3. CASS, O. W. and ROGERS, A. O. U.S. Patent No. 2,342,101; Chem. Abstr. **38**, 4622 (1944).
4. IMPERIAL CHEMICAL INDUSTRIES LTD. Brit. Patent No. 647,420; Chem. Abstr. **45**, 7139 (1951).
5. CHARLISH, J. L., DAVIS, W. H., and ROSE, J. D. J. Chem. Soc. 232 (1948).
6. BELLAMY, L. J. The infrared spectra of complex molecules. Methuen & Co., London. 1954.
7. BARNETT, H. W., DAVIS, R. G., and GRAHAM, R. P. Can. J. Research, B, **25**, 289 (1947).
8. PRICHARD, W. W. and WHITMAN, G. M. U.S. Patent No. 2,524,833; Chem. Abstr. **45**, 1618 (1951).
9. SNYDER, H. R. and POOS, G. I. J. Am. Chem. Soc. **71**, 1055 (1949).

RECEIVED SEPTEMBER 9, 1958.
REPORT NO. 23,
L. G. RYAN RESEARCH LABORATORIES,
MONSANTO CANADA LIMITED,
VILLE LASALLE, QUEBEC.

INFRARED SPECTRUM OF CRYSTALLINE H_2S_2

NUMAN ZENGIN[1] AND PAUL A. GIGUÈRE

Wilson and Badger (1) have measured the infrared spectrum of gaseous hydrogen persulphide, H_2S_2, while Fehér and his co-workers (2, 3) have studied the Raman spectrum of the liquid. However, no structural investigation of the crystal, either by X-ray diffraction or spectroscopy, has been reported yet. The infrared spectrum of that solid is of some interest in view of the close analogy of the molecule with hydrogen peroxide, on the one hand, and the absence of hydrogen bonding, on the other hand.

The sample of H_2S_2 used for the present work was prepared after the method of Butler and Maass (4). Three successive fractional distillations were sufficient to yield a clear, colorless liquid, free from higher polysulphides. All traces of water were removed by collecting the distillate over P_2O_5. The final product seemed very stable when kept at dry-ice temperature in a Pyrex flask previously treated with gaseous HCl. No analyses were carried out since the purity of the persulphide was confirmed by the absence from its spectra of any absorption due to H_2S. As a further precaution the measurements were always made on freshly distilled samples. Clear, transparent films of the solid were easily obtained by deposition of the vapor on disks of NaCl or CsI cooled to liquid-air temperature in a conventional absorption cell. From the amount of liquid used and the surface of the salt disk and its metal support, the thickness of the crystalline films was estimated of the order of 10 microns. The infrared absorption was measured over the range 290 to 5000 cm^{-1} with a Perkin–Elmer, Model 12-C spectrometer using prisms of NaCl, KBr, and CsBr.

The various bands observed are shown in Fig. 1 and the frequency of the maxima are listed in Table I along with those of the gas and the Raman shifts of the liquid. As could be expected from the weakness of the intermolecular forces, the vibrational frequencies of the free molecule change very little in the condensed phases. For the same

TABLE I

Frequency of the bands in the infrared spectra of crystalline H_2S_2

Gas, cm^{-1}	Liquid, cm^{-1}	Solid, cm^{-1}	Intensity	Assignment
	509	501	w.	ν_3
		518	v.w.	
		814	w.	$\nu_6 - \nu_T$
		857	v.w.	
		868	v.s.	ν_2 or ν_6
875		881	v.w.	
897	882	890	v.s.	ν_6
		940	v.w.	$\nu_6 + \nu_T$
		1070	m.	$\nu_6 + \nu_4$?
		2380	v.w.	$\nu_5 - \nu_R$
2557		2480	v.s.	ν_5
	2509	2495	s.	ν_1 ?
		2590	w.	$\nu_5 + \nu_R$
		2930	v.w.	
3065		2960	w.	$\nu_3 + \nu_5$
		2995	v.w.	
3400		3345	m.	$\nu_5 + \nu_6$
5007		4840	v.w.	$\nu_1 + \nu_5$

[1]*Postdoctorate Fellow of the National Research Council, Ottawa, Canada. Present address: University of Ankara, Faculty of Science, Ankara, Turkey.*

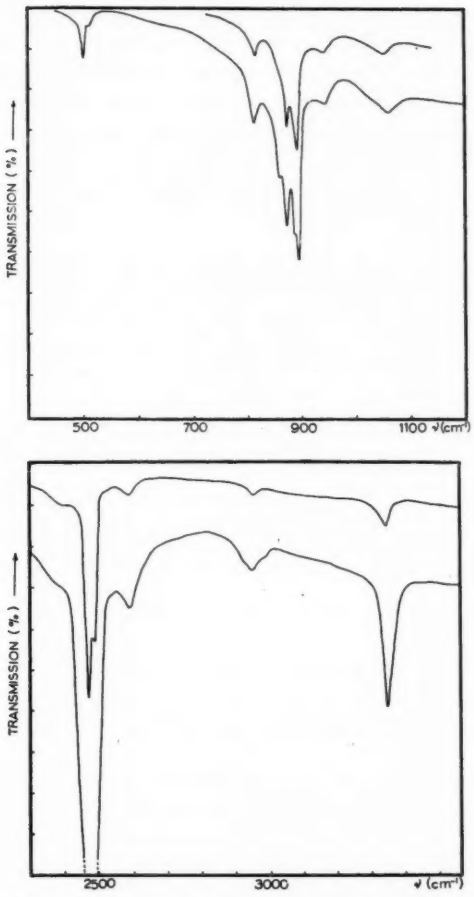

FIG. 1. Infrared absorption spectra of crystalline H_2S_2, for two films of different thickness.

reason the H_2S_2 bands are much sharper than those of its oxygen analogue, H_2O_2 (5). Apart from ν_3, the S–S stretching vibration at 501 cm^{-1}, the S–H stretching and bending fundamentals give rise to regions of strong absorption near 2500 and 880 cm^{-1} respectively. Because the crystal structure of H_2S_2 is unknown the various peaks in these two bands cannot be assigned unambiguously. Tentatively the pair of strong lines at 890 and 868 cm^{-1} may be ascribed to the asymmetric (ν_6) and the symmetric (ν_2) bending modes although they could also be two components of the former mode. The very weak shoulders at 10 cm^{-1} on the low-frequency side of the two main peaks, visible only in the thickest samples, might conceivably belong to the isotopic molecules $HS^{32}S^{34}H$ (natural abundance about 4%). They show roughly the same relative intensity as some of the isotopic bands of SO_2 (6). Sum–difference combinations of the bending frequencies with a lattice vibration of some 65–70 cm^{-1} give rise to the weak satellites at 814 and 940 cm^{-1}. Another combination band at 1070 cm^{-1} involves, no doubt, ν_6 and a frequency of the order of 200 cm^{-1}. This is of the right magnitude for ν_4, the torsional frequency,

which has not been detected yet. It must be added, however, that it could also fit one of the libration frequencies of the H_2S_2 molecule, namely that about the S–S axis. As in the case of H_2O_2 (7) these two frequencies are expected to lie fairly close together. Naturally the corresponding frequencies are very much higher in solid H_2O_2 (about 650 cm^{-1}) on account of the strong hydrogen bonds. The strongest lines at 2480 and 2495 cm^{-1} also show sum–difference combinations with a lattice frequency of about 110–120 cm^{-1}. Finally the overtone bands at 2960, 3345, and 4840 cm^{-1} are assigned after the corresponding vapor bands (1).

1. WILSON, M. K. and BADGER, R. M. J. Chem. Phys. **17**, 1232 (1949).
2. FEHÉR, F. and BAUDLER, M. Z. Elektrochem. **47**, 844 (1941).
3. FEHÉR, F., LANE, W., and WINKHAUS, G. Z. anorg. Chem. **288**, 113 (1956).
4. BUTLER, K. H. and MAASS, O. J. Am. Chem. Soc. **52**, 2184 (1930).
5. BAIN, O. and GIGUÈRE, P. A. Can. J. Chem. **33**, 527 (1955).
6. REDING, F. P. and HORNIG, D. F. J. Chem. Phys. **27**, 1024 (1957).
7. GIGUÈRE, P. A. and HARVEY, K. B. J. Mol. Spectroscopy. In press.

RECEIVED NOVEMBER 26, 1958.
DEPARTMENT OF CHEMISTRY,
LAVAL UNIVERSITY,
QUEBEC, QUE.

ELECTRON SPIN RESONANCE ABSORPTION SPECTRUM OF PUMMERER'S OXYGEN RADICAL

J. B. FARMER, Y. MATSUNAGA,* AND C. A. MCDOWELL

Though dehydro-hydroxy-binaphthylene-oxide (I) was prepared as early as 1914 by Pummerer and Frankfurter and reported to dissociate nearly completely into free radicals in dilute benzene solution (1), no magnetic measurements have been done on this compound.

The electron spin resonance absorption spectra of dehydro-oxy-binaphthylene-oxide (I), and binaphthyl-bis-peroxy-binaphthylene-oxide (II) in benzene and pyridine solutions, were examined at room temperature at a frequency of 9 k Mc/s, in a high-resolution high-sensitivity electron spin resonance spectrometer constructed in this department (7). The resonance spectrum shown in Fig. 1 was found in both cases and attributed to the existence of the free radical (III). The reddish-violet solution of this free radical is somewhat sensitive toward oxygen, but for these measurements it was unnecessary to handle it in vacuum or in an inert atmosphere.

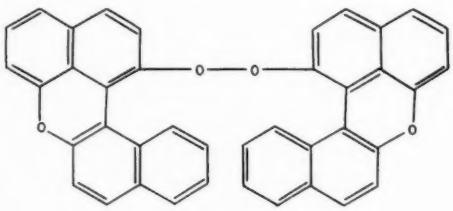

(I)

*N.R.C. Postdoctoral Fellow 1957–.

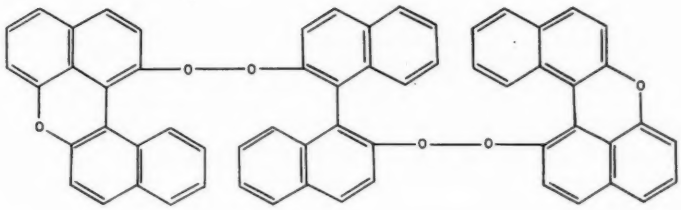

(II)

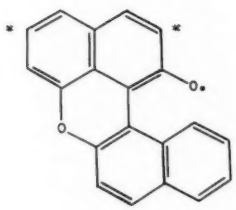

(III)

Dehydro-hydroxy-binaphthylene-oxide (I) and binaphthyl-bis-peroxy-binaphthylene-oxide (II) were prepared by the methods given in refs. 1 and 2, respectively.

The spectra of the two compounds in benzene or pyridine consist of three equally-spaced lines with a separation of 2.5 oersteds. The center of spectrum of Pummerer's radical is located 0.50 oersted lower in field than that of diphenyl-picryl-hydrazyl. If we take the *g*-value of the latter as 2.0036 (3), the value for Pummerer's radical is approximately 2.0039.

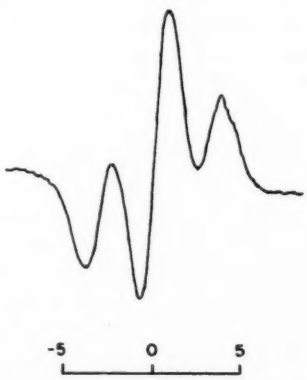

FIG. 1. Electron spin resonance absorption spectrum of Pummerer's oxygen radical.

As the compounds (I) and (II) give the same resonance spectrum, it appears that the middle part of the compound (II) does not form a biradical in the process of dissociation, or the lifetime of the radical formed is too short to be detected.

The number of lines in Fig. 1 shows that only two protons among eleven in Pummerer's radical can interact with the unpaired electron. It is suggested that the radical is highly distorted by steric hindrance and the distribution of the unpaired electron is restricted to the naphthalene nucleus to which the peroxide oxygen atom is attached. By the simple LCAO-MO method, the density of the frontier electrons, i.e., the electrons in the highest occupied energy level, in β-substituted naphthalene was calculated by Fukui *et al.* (4). Based on their result, the protons which contribute to the hyperfine splitting can be assigned to those attached to the starred carbon atoms in (III). The same conclusion can be obtained by consideration of the following resonance structures:

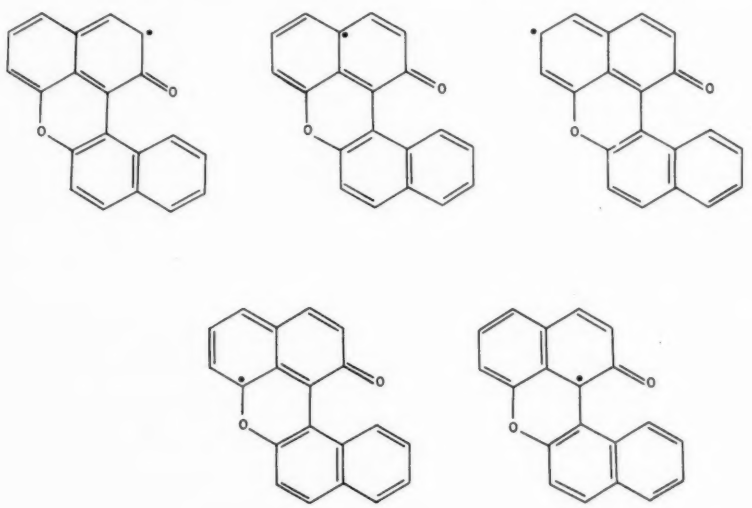

If we assume that the unpaired electron density on each carbon atom in Pummerer's radical is given by one half of the frontier-electron density in β-substituted naphthalene, the constant Q in the relation $a_j = Q \cdot \rho_j$ (5) is about 42 in the present case. This value seems to be of the correct order.

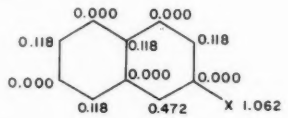

FIG. 2. Density of frontier electrons after Fukui *et al.* (Assumed $\alpha_x = \alpha_c$, $\beta_{cx} = \beta_{ar}$.)

The anomalous stability of Pummerer's radical may be due, in part, to conjugation between the naphthalene nucleus and the attached oxygen atom. However, the main reason is probably that the bulky substituent protects the oxygen atom from any reaction, as in the case of 2,4,6-tri-tert-butyl-1-phenoxyl (6).

We wish to thank the National Research Council and the Defence Research Board for grants in aid of this work.

1. PUMMERER, R. and FRANKFURTER, F. Ber. **47**, 1472 (1914).
2. PUMMERER, R. and RIECHE, A. Ber. **59**, 2161 (1926).
3. HOLDEN, A. N., YAGER, W. A., and MERRITT, F. R. J. Chem. Phys. **19**, 1319 (1951).
4. FUKUI, K., YONEZAWA, T., NAGATA, C., and SHINGU, H. J. Chem. Phys. **22**, 1433 (1954).
5. MCCONNELL, H. M. J. Chem. Phys. **24**, 632 (1956).
6. MÜLLER, E. and LEY, K. Chem. Ber. **87**, 922 (1954).
7. CORFIELD, W., FARMER, J. B., HORSFIELD, A., and MCDOWELL, C. A. To be published.

RECEIVED NOVEMBER 24, 1958.
DEPARTMENT OF CHEMISTRY,
UNIVERSITY OF BRITISH COLUMBIA,
VANCOUVER 8, BRITISH COLUMBIA.

THE ADSORPTION OF SULPHUR DIOXIDE BY GRAPHITE*

H. L. MCDERMOT AND B. E. LAWTON

INTRODUCTION

The adsorption of sulphur dioxide by a number of carbon blacks and graphite has been studied by Beebe and Dell (1). The carbon blacks used were Spheron 6 and a number of samples of Spheron 6 which had been deoxygenated at successively higher temperatures. A very pure graphite whose properties have already been described (4) was used. It was found that the untreated Spheron 6 with about 4% of oxygen on its surface adsorbed about seven times more sulphur dioxide than the samples from which virtually all the oxygen had been removed. It was also found that Spheron 6 which had been deoxygenated and graphitized at 2700° C displayed a similar isotherm to that of pure graphite. Thus it was concluded that the adsorption of sulphur dioxide provided a sensitive method for the detection of chemisorbed oxygen. It is likely that this conclusion can be extended to all polar groups on the surface. In the work reported here the adsorption of sulphur dioxide by artificial graphites was undertaken as a part of the program to study these carbons. Isotherms were measured to test for the presence of chemisorbed oxygen and to ascertain whether the hysteresis effects reported with non-polar gases on these graphites also existed for sulphur dioxide. Finally, isotherms were measured at a number of temperatures to study the temperature dependence of the branches of the hysteresis loop.

EXPERIMENTAL AND RESULTS

The graphites used in these experiments were two Acheson graphites designated by us as GF-3 and GF-5. Their properties have been given before (3, 5).

The sulphur dioxide was obtained from the Matheson Company and used without further purification.

Isotherms were measured at four temperatures for each graphite: at 236.6°, 244.5°, 256.8°, and 273.2° K for GF-3; and at 244.3°, 253.8°, 261.5°, and 273.2° K for GF-5. Adsorption was measured by means of a simple volumetric adsorption apparatus. A Dewar flask full of cracked ice and water was used for the isotherms at 273.2° K. For the lower temperatures, the bath was cooled by pumping liquid nitrogen through a copper coil. Two bath fluids were used: a 50:50 mixture of water and ethylene glycol, and a 65:35 mixture of chloroform and carbon tetrachloride. The bath was agitated by an electric stirrer and regulated by a sulphur dioxide vapor pressure thermometer. Before each isotherm, the sample was evacuated for at least 12 hours at 200° C.

**Issued as D.R.C.L. Report No. 297.*

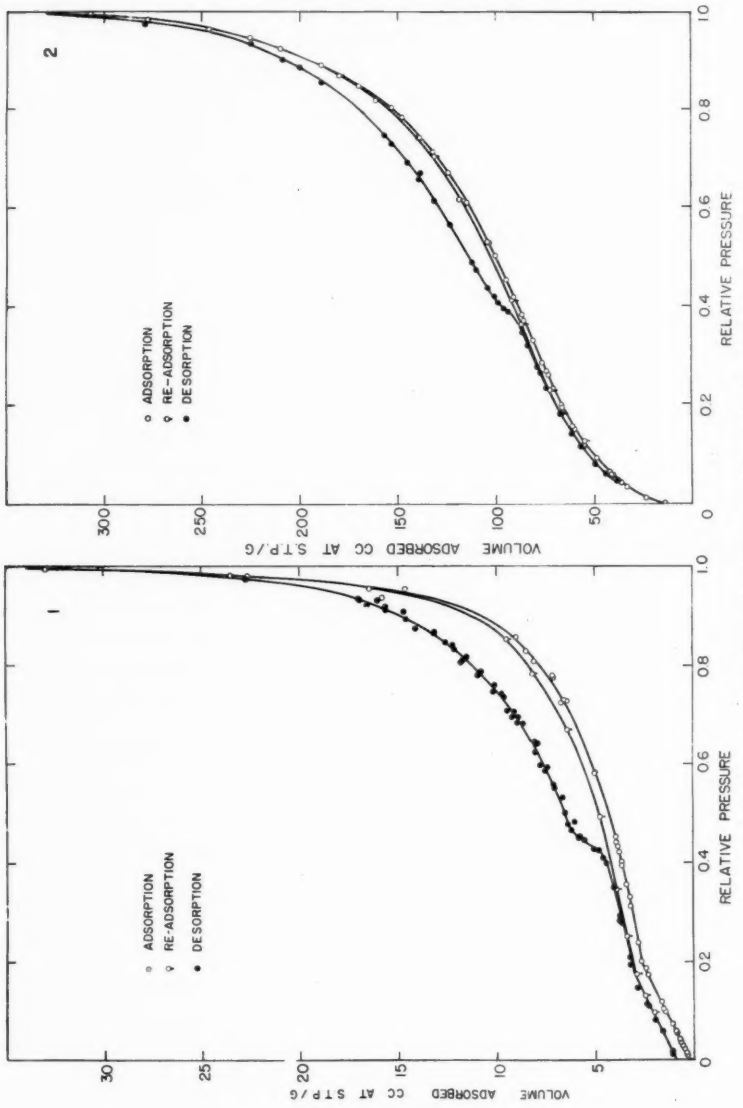

FIG. 1. The adsorption of sulphur dioxide by GF-3 at 256.8° K.
FIG. 2. The adsorption of sulphur dioxide by GF-5 at 253.8° K.

Two typical isotherms are presented in Figs. 1 and 2. Figure 1 shows the isotherm of sulphur dioxide adsorbed on GF-3 at 256.8° K. Figure 2 depicts the isotherm for GF-5 at 253.8° K. It is interesting to note that the isotherm in Fig. 1 shows a sharp break at a relative pressure of about 0.2. This break, which was characteristic of the isotherms measured with GF-3, was absent in those measured with GF-5.

DISCUSSION

The low adsorption of sulphur dioxide by these graphites is indicative of their lack of chemisorbed oxygen. This point is illustrated by Fig. 3, which compares the adsorption of sulphur dioxide by GF-3 and GF-5 with the data of Beebe and Dell (1) for a deoxygenated carbon black and a very pure graphite. All four carbons adsorb sulphur dioxide to about the same degree. It has been demonstrated that smooth isotherms such as have been observed with these graphites for the adsorption of nitrogen and argon are indicative of heterogeneous surfaces (2). The graphites contain little ash and the data given here show the absence of chemisorbed oxygen, hence the heterogeneity must be of the topographic type.

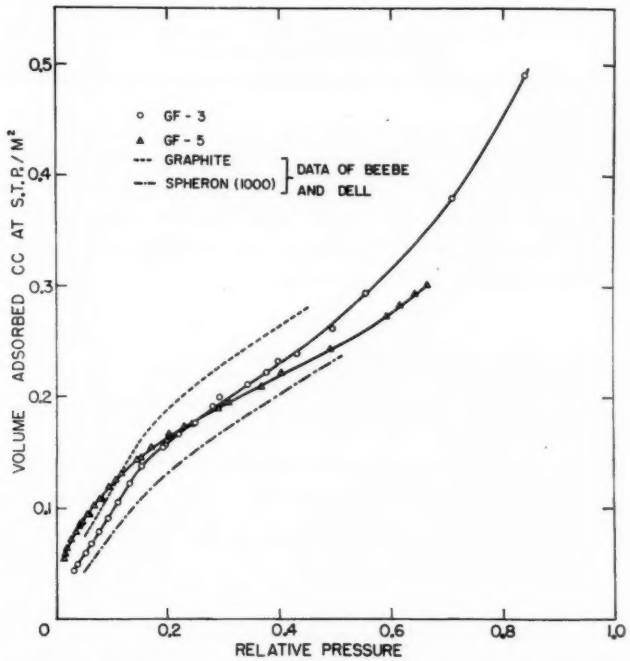

FIG. 3. A comparison of the adsorption of sulphur dioxide by three graphites and a deoxygenated carbon black.

Figures 1 and 2 show that isotherms of both of these graphites give evidence of what we have called "swelling" type hysteresis as well as the normal hysteresis caused by the presence of pores. The "swelling" type hysteresis manifests itself as a second curve just above the initial adsorption curve extending from low to high relative pressures. Isosteric heats have been calculated from both of these curves using data from all four

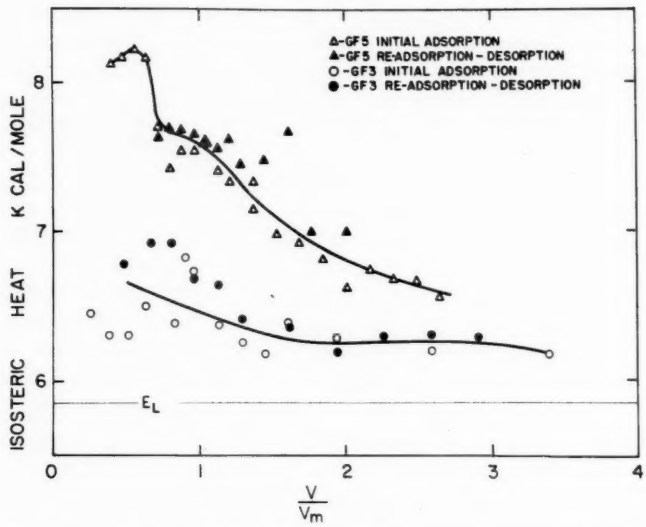

FIG. 4. Isosteric heats for the adsorption of sulphur dioxide by GF-3 and GF-5.

temperatures. These heats presented in Fig. 4 show values well above the heat of liquefaction of sulphur dioxide. Within the experimental error, no difference could be discerned between heats calculated from the initial adsorption curves and those calculated from the desorption and readsorption curves. Thus no heat effect can be detected in this way which could be attributed to swelling of the graphite crystallites. Possibly the method is too rough to measure the heats involved.

REFERENCES

1. BEEBE, R. A. and DELL, R. M. J. Phys. Chem. **59**, 746 (1955).
2. BEEBE, R. A. and YOUNG, D. M. J. Phys. Chem. **58**, 93 (1954).
3. MCDERMOT, H. L. and LAWTON, B. E. Can. J. Chem. **34**, 769 (1956).
4. PIERCE, C., SMITH, R. N., WILEY, J. W., and CORDES, H. J. Am. Chem. Soc. **73**, 4551 (1951).
5. WILSON, L. G. and MCDERMOT, H. L. Can. J. Chem. **35**, 15 (1957).

RECEIVED SEPTEMBER 12, 1958.
DEFENCE RESEARCH CHEMICAL LABORATORIES,
DEFENCE RESEARCH BOARD,
OTTAWA, CANADA.

NOTES TO CONTRIBUTORS

Canadian Journal of Chemistry

MANUSCRIPTS

General.—Manuscripts, in English or French, should be typewritten, double spaced, on paper 8½×11 in. **The original and one copy are to be submitted.** Tables and captions for the figures should be placed at the end of the manuscript. Every sheet of the manuscript should be numbered. Style, arrangement, spelling, and abbreviations should conform to the usage of recent numbers of this journal. Greek letters or unusual signs should be written plainly or explained by marginal notes. Characters to be set in bold face type should be indicated by a wavy line below the characters. Superscripts and subscripts must be legible and carefully placed. Manuscripts and illustrations should be carefully checked before they are submitted. Authors will be charged for unnecessary deviations from the usual format and for changes made in the proof that are considered excessive or unnecessary.

Abstract.—An abstract of not more than about 200 words, indicating the scope of the work and the principal findings, is required, except in Notes.

References.—These should be designated in the text by a key number and listed at the end of the paper, with the number, in the order in which they are cited. The form of the citations should be that used in this journal; in references to papers in periodicals, titles should not be given and only initial page numbers are required. The names of periodicals should be abbreviated in the form given in the most recent *List of Periodicals Abstracted by Chemical Abstracts*. All citations should be checked with the original articles and each one referred to in the text by the key number.

Tables.—Tables should be numbered in roman numerals and each table referred to in the text. Titles should always be given but should be brief; column headings should be brief and descriptive matter in the tables confined to a minimum. Vertical rules should not be used. Numerous small tables should be avoided.

ILLUSTRATIONS

General.—All figures (including each figure of the plates) should be numbered consecutively from 1 up, in arabic figures, and each figure referred to in the text. The author's name, title of the paper, and figure number should be written in the lower left corner of the sheets on which the illustrations appear. Captions should not be written on the illustrations.

Line drawings.—Drawings should be carefully made with India ink on white drawing paper, blue tracing paper, or co-ordinate paper ruled in blue only; any co-ordinate lines that are to appear in the reproduction should be ruled in black ink. Paper ruled in green, yellow, or red should not be used. All lines must be of sufficient thickness to reproduce well. Decimal points, periods, and stippled dots must be solid black circles large enough to be reduced if necessary. Letters and numerals should be neatly made, preferably with a stencil (**do NOT use typewriting**), and be of such size that the smallest lettering will not be less than 1 mm high when the figure is reduced to a suitable size. Many drawings are made too large; originals should not be more than 2 or 3 times the size of the desired reproduction. Wherever possible two or more drawings should be grouped to reduce the number of cuts required. In such groups of drawings, or in large drawings, full use of the space available should be made; the ratio of height to width should conform to that of a journal page (5½×7¾ in.) but allowance must be made for the captions. **The original drawings and one set of clear copies (e.g. small photographs) are to be submitted.**

Photographs.—Prints should be made on glossy paper, with strong contrasts. They should be trimmed so that essential features only are shown and mounted carefully, with rubber cement, on white cardboard, with no space between those arranged in groups. In mounting, full use of the space available should be made. **Photographs are to be submitted in duplicate;** if they are to be reproduced in groups one set should be mounted, the duplicate set unmounted.

REPRINTS

A total of 50 reprints of each paper, without covers, are supplied free. Additional reprints, with or without covers, may be purchased at the time of publication.

Charges for reprints are based on the number of printed pages, which may be calculated approximately by multiplying by 0.5 the number of manuscript pages (double-space typewritten sheets, 8½×11 in.) and including the space occupied by illustrations. Prices and instructions for ordering reprints are sent out with the galley proof.

Contents

Printed in Canada *by* University of Toronto Press